ADVANCES IN WIRELESS COMMUNICATIONS: MULTI-USER CONSTELLATION DESIGN AND SEMANTIC INFORMATION CODING

ADVANCES IN WIRELESS COMMUNICATIONS: MULTI-USER CONSTELLATION DESIGN AND SEMANTIC INFORMATION CODING

BY

PEIYAO CHEN, B.Eng., M.Sc.,

A THESIS

SUBMITTED TO THE DEPARTMENT OF ELECTRICAL & COMPUTER ENGINEERING

AND THE SCHOOL OF GRADUATE STUDIES

OF MCMASTER UNIVERSITY

IN PARTIAL FULFILMENT OF THE REQUIREMENTS

FOR THE DEGREE OF

DOCTOR OF PHILOSOPHY

Doctor of Philosophy (2023)	McMaster University
(Electrical & Computer Engineering)	Hamilton, Ontario, Canada

TITLE:	Advances in Wireless Communications: Multi-user Constellation Design and Semantic Information Coding
AUTHOR:	Peiyao Chen M.Sc. (Information and Communication Engineering), Xidian University, Xi'an, China B.Eng. (Communication Engineering), Xidian University, Xi'an, China
SUPERVISOR:	Dr. Jun Chen Dr. Tim Davidson Dr. Jian-Kang Zhang (Dec.)
NUMBER OF PAGES:	xix, 218

Lay Abstract

The proliferation of smart phones and electronic devices has spurred explosive growth in high-speed multimedia services over the next generation of wireless cellular networks. Indeed, high data rates and large-scale connectivity with seamless coverage are the dominant themes of wireless communication system design. Moreover, beyond the accurate representation and successful transmission of information, the interpretation of its meaning is being paid more attention nowadays, which requires the development of approaches to semantic communication.

The goal of this thesis is to contribute to the development of both conventional and semantic communication systems. Two advanced transmission technologies, namely, multiple access and relay-assisted communications are considered. By taking advantage of the special structures of digital communication signals, new approaches to multiple access and relay-assisted communications are developed. These designs enable high data rates, while simultaneously facilitating low-latency detection. Since there has been very limited analysis of the source coding of a vector source subject to semantic information constraints, we also study the rate distortion to trade-off for vector sources in both the case of centralized encoding and the case of distributed encoding, and we establish some insights that will guide the future development of semantic communication systems.

Abstract

The realization of high data rate wireless communication and large-scale connectivity with seamless coverage has been enabled by the introduction of various advanced transmission technologies, such as multiple access (MAC) technology and relay-assisted communications. However, beyond the accurate representation and successful transmission of information, in many applications it is the semantic aspect of that information that is really of interest.

This thesis makes contributions to both the technology of conventional wireless communications and the theory of semantic communication. The main work is summarized as follows:

- We first consider an uplink system with K single-antenna users and one base station equipped with a single antenna, where each user utilizes a binary constellation to carry data. By maximizing the minimum Euclidean distance of the received sum constellation, the optimal user constellations and sum constellation are obtained for $K = 3$ users. Using the principle of lattice coding, that design is extended to the K-user case. In both settings, the sum constellation belongs to additively uniquely decomposable constellation group (AUDCG).

That property enables us to reduce the maximum likelihood multi-user detector to a single-user quantization based receiver. The symbol error probability (SEP) formula is derived, showing that our proposed non-orthogonal multiple access (NOMA) scheme outperforms the existing time division multiple access (TDMA) designs for the same system. Our design also sheds light on the general complex constellation designs for the MAC channel with arbitrary user constellation size. Specifically, K-user constellations with any 2^{M_k} size can be obtained using combinations of the proposed binary constellations.

- Next we concentrate on a multi-hop relay network with two time slots, consisting of single-antenna source and amplify-and-forward relay nodes and a destination node with M antennas. We develop a novel uniquely-factorable constellation set (UFCS) based on a PSK constellation for such system to allow the source and relay nodes to transmit their own information concurrently at the symbol level. By taking advantage of the uniquely-factorable property, the optimal maximum likelihood (ML) detection was equivalently reduced to a symbol-by-symbol detection based on phase quantization. In addition, the SEP formula was given, while enable us to show that the diversity gain of the system is one.

- For semantic communication, a new source model is considered, which consists of an intrinsic state part and an extrinsic observation part. The intrinsic state corresponds to the semantic feature of the source. It is not observable, and can only be inferred from the extrinsic observation. As an instance of the general model, the case of Gaussian distributed extrinsic observations is studied, where we assume a linear relationship between the intrinsic and extrinsic parts. We derive the rate-distortion function (in both centralized encoding and distributed encoding) of semantic-aware source coding under quadratic distortion structure by converting the semantic distortion constraint of the source to a surrogate distortion constraint on the observations.

With proposed AUDCG and UFCS-based designs, high data rates as well as low detection latency can be achieved. Our modulation division method will be one of the promising technologies for the next generation communication and the analysis of the source coding with semantic information constraints also provides some insights that will guide the future development of semantic communication systems.

To my family, for their love and support.

Acknowledgements

I would like to take this opportunity to express my sincere gratitude to those extraordinary people.

First and foremost, I would like to acknowledge my gratitude to my supervisor, Dr. Jian-Kang Zhang (Dec), a respectable, responsible and earnest scholar. Dr. Zhang has influenced me in many ways, not only for his profound knowledge and well-equipped mathematical abilities, but also for his encouragement, impressive patience and genuine concern with people. What impressed me most was that Dr. Zhang always had the courage to guess and prove open problems, and did not stop at one solution, but kept thinking and seeking the solutions or proof having nice mathematical structures. I feel extremely fortunate and proud of being his student, and I deeply regret the loss of such a knowledgeable as well as kindness supervisor. In my future life, I will do my best to pass his generosity and spirits to other people.

Furthermore, I would like to express my gratitude to my supervisor, Dr. Jun Chen, for his insightful guidance and assistance, as well as spiritual and financial supports, especially for accepting me as his Ph.D. student when I needed it most. As an expert in information theory, he attaches great importance to guiding and cultivating our divergent and innovative thinking. His insightful suggestions can always give me some enlightenment. Dr. Chen is the most knowledgeable, intelligent and hardworking scholar I have ever met. During the epidemic, he still insisted on working on campus. His earnest attitude has always inspired me to emulate him and work hard.

My sincere appreciation also goes to my supervisor, Dr. Timothy Davidson, for his continuous encouragement, support and invaluable guidance. Dr. Davidson was very busy during his tenure as chair, but he took time out of his busy schedule every week to give me one-on-one guidance. Moreover, as an expert in wireless communication, he is very modest and patient. It is always a pleasure to discuss with Dr. Davidson and he acts both as a knowledgeable mentor and a close friend.

I would like to thank my supervisory committee members, Dr. Sorina Dumitrescu and Dr. Shiva Kumar, for their valuable comment and feedback on my research works.

My gratitude also goes to my friends and fellow collaborators, especially to Xiaoxuan Chu, Jingxin Wang, Xiaohong Liu, Huan Liu, Siyao Zhou, Jingjing Qian, Kangdi Shi, for their assistance and friendship.

Last but not least, I would like to thank my family, especially my mother, Xiaoqin Liu, for their endless love and unwavering support in my life. I would also like to thank my husband, Runchen Liang, who gives me all his love and encouragement for the past three years.

Contents

List of Figures

List of Tables

Abbreviations

Abbreviations

AF	Amplify and Forward
AI	Artificial Intelligence
AUDCG	Additively Uniquely Decomposable Constellation Group
BDM	Bit Division Multiplexing
BS	Base Station
CDMA	Code Division Multiple Access
CIR	Channel Impulse Responses
DF	Decode and Forward
eMBB	Enhanced Mobile Broadband
FDMA	Frequency Division Multiple Access
FFT	Fast Fourier Transform

LDS	Low-Density Signature
MAC	Multiple Access
MBB	Mobile Broadband
MC-CDMA	Multi-Carrier Code Division Multiple Access
MIMO	Multiple-Input Multiple-Output
ML	Maximum Likelihood
MMSE	Minimum Mean Square Error
mMTC	Massive Machine-Type Communication
mmWave	Millimeter-Wave
MPA	Message Passing Algorithm
MUD	Multiuser Detection
MUSA	Multiuser Shared Access
NOMA	Nonorthogonal Multiple Access
OFDMA	Orthogonal Frequency Division Multiple Access
OMA	Orthogonal Multiple Access
PAM	Pulse Amplitude Modulation
PDF	Probability Density Function
PDMA	Pattern Division Multiple Access

PSK	Phase Shift Keying
QAM	Quadrature Amplitude Modulation (QAM)
SCMA	Sparse Code Multiple Access
SDMA	Spatial Division Multiple Access
SNR	Signal-to-Noise Ratio
SIC	Successive Interference Cancellation
SISO	Single-Input Single-Output
TDMA	Time Division Multiple Access
3D	Three-Dimensional
3GPP	Third Generation Partnership Project
UFCS	Uniquely-Factorable Constellation Set
URLLC	Ultra-Reliable and Low-Latency Communication
VR	Virtual Reality

Chapter 1

Introduction

1.1 Conventional Wireless Communication

By using the characteristics of electromagnetic waves signal to transport information through free space, wireless communications systems have fundamentally transformed our daily lives and have created a connected society. Over the past decades, high data rates and large-scale connectivity with seamless coverage have been the dominant themes of wireless communication system design. The realization of these objectives has been enabled by the introduction of various advanced transmission technologies, including multiple-input multiple-output (MIMO), multi-carrier transmission, channel-adaptive transmission, etc [19, 109]. In 2016, the expectations for 5G were established by the 3rd Generation Partnership Project (3GPP) [1, 2], where three main usage scenarios are considered: enhanced mobile broadband (eMBB), massive machine-type communication (mMTC), and ultra-reliable and low-latency communication (URLLC). The distinguishing feature of the envisioned eMBB scenario is a peak data rate of 20 Gb/s and the distinguishing features of mMTC and

URLLC are a device density of $10^6/\text{km}^2$ and a latency less than 1 ms with a probability of outage of less than 10^{-5}, respectively [63]. To meet these goals, several new techniques, such as new frequency bands (e.g., millimeter-wave (mmWave) [75] and optical spectra [15]), advanced spectrum usage/management, and the integration of licensed and unlicensed bands, have been developed in the various "releases" of the 5G standard [37].

Compared with the 4G LTE system, the 5G communication systems have significant improvements. However, they will not be able to fulfill the demands of future intelligent and automation systems. With the remarkably rapid development of various emerging applications, such as artificial intelligence (AI), virtual reality (VR), and three-dimensional (3D) media, the demands for extremely high-data-rate services and mass-offering of mobile broadband (MBB) access are predicted to eventually exceed the capabilities of the 5G systems. Therefore, innovative technologies will be needed to address the challenges of the next generation (Beyond 5G or 6G), to effectively deliver ultra-high data rates, while providing massive connectivity and accommodating dramatically different quality of service requirements [22, 50].

The goal of this thesis is to contribute to the development of such systems. This is done in two phases. In the first phase, new approaches to multiple access and relay-assisted communications are developed. These approaches take advantage of some of the special structures of digital communication signals. In the second phase, we reconsider the nature of the information that should be communicated and develop insights into the fundamental limits on how the meaning conveyed by the information can be represented.

1.1.1 Multiple Access Technology

The development of effective wireless access technologies is a key step towards meeting the requirements of future wireless communication system. Since the available physical resources, such as bandwidth and time, are inherently limited, they must be shared among the devices that are seeking to communicate. That sharing process is known as multiple access.

At a fundamental level, multiple access schemes can be categorized as orthogonal multiple access (OMA) [3, 34, 35, 77, 78] and non-orthogonal multiple access (NOMA) [76, 20, 98]. In OMA, each user is allocated to one dedicated orthogonal radio resource block, such as a specific time slot, frequency band, or code. In this way, the multiple access scheme explicitly avoids interference between the users. Doing so enables the receiver to separate the signals from different users using simple linear processing. Well-known conventional OMA techniques include frequency division multiple access (FDMA), time division multiple access (TDMA), synchronous code division multiple access (CDMA), and orthogonal frequency division multiple access (OFDMA), which dominate 1G $\sim$ 4G wireless communication systems, respectively. The principles that underlie the FDMA, TDMA, and CDMA techniques are illustrated in Fig.1.1. For FDMA, the system bandwidth is divided into several bands without overlapping frequencies, and all users can transmit simutaneously, but in their own specific frequency band. For TDMA, the data frame is split into non-overlapping time slots and all users can transmit in the same frequency band, but in their own specific time slots. In synchronous CDMA, users can transmit simultaneously in the same frequency band via (orthogonal) spread-spectrum codes. The

OFDMA system is an advanced version of FDMA, in which transmissions are synchronized. That enables the use of fast Fourier transform (FFT) operations at both the transmitter and the receiver to produce orthogonal signals that partially overlap in frequency. (OFDMA can be viewed as a form of synchronous CDMA, in which the codes are generated by the FFT; e.g., [92])

In contrast to OMA, in NOMA, users are allowed to utilize non-orthogonal resources concurrently with the receiver mitigating the resulting interference, typically using non-linear processing, and sometimes in coordination with the transmitter. Although the users suffer from interference (due to simultaneous transmission) in NOMA system, there is the potential for improved performance [94, 95]. Indeed, the capacity achieving input distribution for the (Gaussian) multiple access channel involves non-orthogonal transmission [18]. While the NOMA principle has been known for decades, specific NOMA schemes have recently attracted significant attention in both academia and industry. The recent NOMA schemes can be classified into two categories: power-domain NOMA and code-domain NOMA. In power-domain NOMA, each user is assigned a unique power level according to the channel gains of all the users. All users use their assigned power to transmit signals and share the same time-frequency-code resources. In particular, all signals are superimposed and sent simultaneously from the transmitter. At the receiver, a successive interference cancellation (SIC) scheme with a particular detection order is employed to detect the signals from each individual user [76]. For code-domain NOMA, multiple access is achieved by employing a specific code or spreading sequence for each user, which has sparse, low-density and low inter-correlation properties. This is somewhat similar to orthogonal CDMA, but in this case the codes are not constrained to be

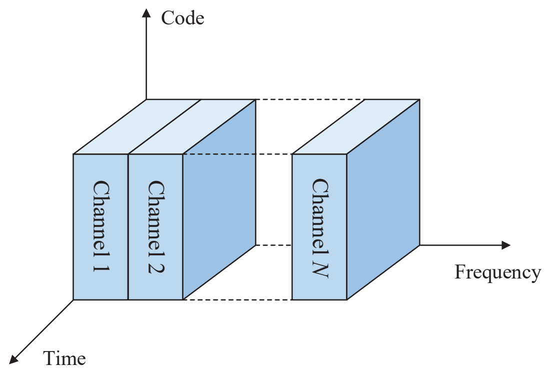

(a) FDMA

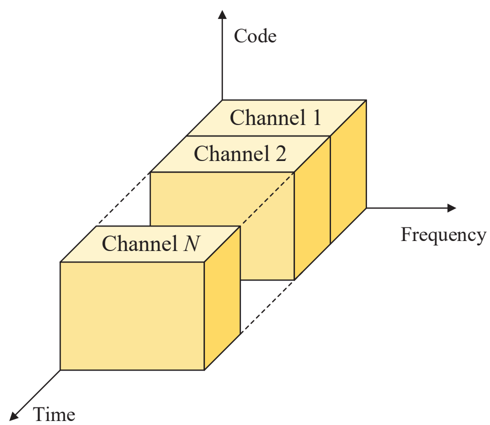

(b) TDMA

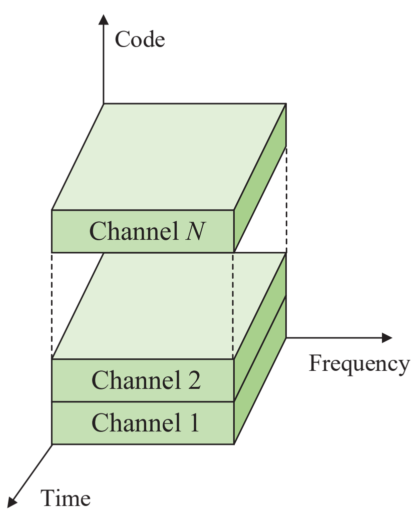

(c) CDMA

Figure 1.1: Illustration of FDMA/TDMA/CDMA techniques.

orthogonal. The common code-domain NOMA schemes are multiuser shared access (MUSA) [107], low-density signature (LDS) [42, 84], and sparse code multiple access (SCMA) [65, 81]. In the MUSA scheme, the data of each user are spread with a short spreading sequence, and signals from multiple users are superposed at the receiver, where SIC is used to cancel interference between users. Both LDS and SCMA are motivated by multi-carrier code division multiple access (MC-CDMA) by introducing sparse codebooks. Unlike SIC-based multiuser detection (MUD), message passing algorithm (MPA) is used to detect the transmitted signals. The MPA takes advantage of the sparse structure of the codewords. In addition, there are other NOMA schemes such as pattern division multiple access (PDMA) [21] and spatial division multiple access (SDMA) [44] schemes. PDMA can be realized in various domains, but SIC-based MUD is always required. Rather than using specific spreading sequences, SDMA distinguishes different users by using specific channel impulse responses (CIRs), thus there is a challenge of CIR estimation for a large number of users.

Compared with code-domain NOMA, power-domain NOMA has a simple implementation and does not require additional bandwidth to improve spectral efficiency [20]. Thus, the primary focus of Chapter 2 of this thesis is on the design of a new approach to multiple access that fits within the framework of power-domain NOMA. The proposed NOMA scheme is based around the notion of uniquely decomposable sum constellations, and results in the maximum likelihood (ML) detector having a simple structure. As a result, it can provide lower detection latency than conventional SIC based PD-NOMA schemes.

1.1.2 Relay-Assisted Technology

Improving the throughput and coverage of wireless networks is a key step in the evolution of future communication systems. Relay-assisted communication is a promising approach to this problem, especially in non-line-of-sight or long-distance communication, where a set of relay nodes are placed between the base station (BS) and the end terminal in order to facilitate a better received signal-to-noise ratio for end-to-end transmission. In addition to extending the coverage of link services, the introduction of relay nodes on existing transmission links can also mitigate signal attenuation and end-user power consumption, and improve the performance of cellular edge users.

Two popular types of relaying strategy are decode and forward (DF) and amplify and forward (AF). In DF systems, the relay first fully decodes the received signal from the previous node, then re-encodes it and forwards the newly encoded signal to the next node. In AF systems, the relay simply amplifies the signal that it receives from the previous node, and then forwards it to the next node, without any kind of decoding. Considerable comparative performance analysis has been presented for DF and AF systems [43, 53, 106]. Although it is known that DF systems with one relay outperform the corresponding AF system under Rayleigh fading conditions [30, 59], DF may suffer from the error propagation caused by incorrectly decoding at relay, resulting in inferior performance for multi-hop relays. Furthermore, DF systems are more complicated to implement and incur greater latency due to the re-encoding and decoding processes.

One particular application in which relay-assisted communication has attracted attention is high-speed train (HST) communication with studies on, performance analysis [48, 54, 108], relay selections [31, 36], and handover scheme [70, 73]. In particular, relay-assistance is a promising scheme for 5G HST communication with mmWave band, because the path loss induced by train shell and the doppler shift are more serious at mmWave frequencies [80]. In Chapter 3 of thesis, we propose a new signalling scheme for a multi-hop relay-assisted HST system, in which AF relaying model is applied. Different from the existing work, each relay can simultaneously forward the previous signal and transmit its own signal, resulting in the potential for high efficiency and low detection latency. While the multiple access system proposed in Chapter 2 is based on the notion of additively uniquely decomposable constellations, the relay system proposed in Chapter 3 is based on the notion of uniquely factorizable constellations.

1.2 Semantic Communication

Semantic communication, the concept of which was introduced by Weaver in 1949 [93], is regarded as a higher level of communication beyond the traditional technical level. The traditional communication problems, categorized by Shannon and Weaver, are mainly concerned with the accurate representation and successful transmission of information regardless of its meaning [79, 93]. In contrast, semantic communication problems are concerned with the representation and successful transmission of semantic information conveyed by the sender; that is, the information that is implicit in the interpretation of meaning by the receiver.

Since the concerns are different, the system model for conventional communication cannot be simply applied to semantic communication. Thus, many efforts have been made to extend the Shannon's information theory to a semantic information theory [9, 32, 33] and explore a generic model [4, 45, 57]. In [9], rather than the statistical probabilities used in classic information theory, a logical probability measure was introduced to analyze the semantic information carried by sentences in a given language system. The authors in both [4] and [45] observed that background knowledge as well as common understanding plays a key role in semantic communication, which may lead to different truth evaluations and, hence, semantic mismatches.

The information source in [57] was modeled as a tuple of an extrinsic observation and an intrinsic state, in which the former is subject to lossy source coding and the latter, corresponding to the semantic information feature, is not directly observable. The task of (scalar) source coding in [57] is to efficiently encode the extrinsic observation so that the decoder can infer both the intrinsic state and the extrinsic observation, subject to their fidelity criteria, simultaneously. Two instances of this model are video coding for machines (VCM) and coding of speech signals [58]. Based on this intrinsic-state extrinsic-observation model, with or without side information, there are several analyses of the information-theoretic characterization of the performance of this system, i.e., the rate-distortion function [57, 58, 101]. However, as far as we are aware, there has been very limited analysis of the source coding of a vector source subject to semantic information constraints. We study the rate-distortion trade-off with semantic distortion constraints for vector sources in both the case of centralized encoding and the case of distributed encoding.

1.3 Contributions and Thesis Organization

The thesis is organized in the format of a sandwich thesis as outlined in the terms and regulations of McMaster University. It consists of three articles that address multiple access, multi-hop relay, and semantic source coding problems, respectively. The contributions to each article are described in the abstract of each chapter and are summarized below.

- Chapter 2 develops a new NOMA signalling scheme for the general K-user (synchronous) multiple access channel (MAC). The scheme exploits the structure of practical digital communication signals, and is based on the notion of a uniquely decomposable constellation. That constellation structure enables fast detection to be applied rather than conventional SIC, and this results in low detection latency. The free parameters of the design are optimized to maximize the minimum distance of the constellation, and that optimization reveals lattice structures that enable efficient implementation. An analysis of symbol error probability demonstrate that the proposed NOMA scheme performs strictly better than OMA schemes.

  Peiyao Chen, Jian-Kang Zhang, Timothy N. Davidson, and Jun Chen, "Constellation design for uplink NOMA", to be submitted to *IEEE Transactions on Communication*.

- Chapter 3 develops a new signalling strategy for a multi-hop relay-assisted system that has applications to high speed trains. In this system, each relay can transmit its own information, as well as forwarding the signal that it receives. By employing the notion of a uniquely factorizable constellation, we design a system that enables fast multiuser detection by finding maximum eigenvalue of received symbol matrix.

  Peiyao Chen, Jian-Kang Zhang, Timothy N. Davidson, and Jun Chen, "Non-coherent multiuser code design for multi-hop relay channels", to be submitted to *IEEE Transactions on Vehicular Technology*.

- Chapter 4 provides the analysis of the rate-distortion function for semantic-aware Gaussian source coding in both centralized and distributed scenarios. This analysis sheds light on potential practical encoding and decoding strategies. **Peiyao Chen**, Jun Chen, Yuxuan Shi, Shuo Shao, Yongpeng Wu, Timothy N. Davidson, "Gaussian semantic source coding", to be submitted to *IEEE Transactions on Information Theory*.

Chapter 2

Constellation Design for Uplink NOMA

Abstract

This chapter develops a new approach to non-orthogonal multiple access (NOMA) for the K-user single-antenna uplink channel. Using knowledge of the users' channels, the access point jointly designs the constellation for each user so that the free distance of the received sum constellation is maximized, subject to individual power constraints. Beyond the inherent performance advantages, this has the additional advantage that the received sum constellation is uniquely decomposable, and hence that the maximum likelihood multiuser detector can be reduced to a simple single-user quantization-based detector for the sum constellation. Closed form expressions for the optimal constellations are obtained for the case of 3 users with binary signalling. Observations regarding the structure of the corresponding sum constellation enable a lattice-based extension that generates good solution for the K-user case.

A simplification of that extension leads to sum constellation carved from either the ring of Gaussian integers or from the Eisenstein integer ring. These constellations are analytically shown to be superior to the corresponding orthogonal multiple access (OMA) systems, using closed-form expressions for the minimum distance and the error probability. Finally, we develop a strategy to extend the design approach to systems in which each user employs a high-order constellation.

2.1 Introduction

It has long been understood (e.g., [18]) that the implementation simplicity of orthogonal multiple access (OMA) schemes, such as time-division multiple access (TDMA) and frequency-division multiple access (FDMA), comes at the cost of a reduction of the achievable spectral efficiency and other measures of communication performance. As a result there has been considerable interest in developing a variety of non-orthogonal multiple access (NOMA) schemes that seek to provide better communication performance than orthogonal schemes, while only incurring a modest increase in implementation complexity [21, 23]. Several of these schemes have emerged as promising candidates for 5G and subsequent generations of mobile/wireless communication standards. The core principle of spectrally-efficient multiple access is to allow superposition of the transmitted signals and to employ some form of multiple user detection, often in the form of successive interference cancellation, at the receiver [18]. Some of the popular instantiations of this principle include power domain NOMA, and sparse code multiple access (SCMA) [21], each of which explore different trade-offs between achievable rates, bandwidth and implementation complexity.

In this chapter, we will develop a new approach to NOMA signalling in which the access point designs the constellations to be employed by each user. Our approach is related to power-domain NOMA, in the sense that it acts on the transmitted symbols themselves, without the bandwidth expansion of code-based NOMA schemes. However, the proposed approach has more degrees of design freedom because it adapts each user's constellation to the scenario, rather than simply adapting the power. (In the case of binary signalling we design both the power and the rotation of each user's constellation.) Indeed, our approach can be viewed as an uplink "constellation-domain" NOMA scheme. (A downlink constellation-domain NOMA scheme was developed in [10].)

To provide more context for that characterization of our approach, we observe that, up until now, many power domain NOMA designs have been developed under the assumption that Gaussian input signals, based on insights from the fundamental limits of multiple access channels [18]. However, in practical communication systems, it is often unaffordable to directly implement accurate approximations of Gaussian input signals, due to the prohibitively large storage capacity, high computational complexity, the need to use power-efficient (non-linear) amplifiers, and long decoding delay [27]. In practice, finite-alphabet constellations such as phase shift keying (PSK), pulse amplitude modulation (PAM), and quadrature amplitude modulation (QAM), are typically used to carry the information to be transmitted. It has been demonstrated in [60] that a significant performance loss will be incurred if we directly apply systems designed for Gaussian inputs to systems that employs finite-alphabet inputs.

Motivated by this fact, the design of NOMA systems with finite-alphabet inputs has attracted some attention [27, 40, 41, 55, 56, 64]. The underlying principle of these works was inspired by the work in [46], where the codebooks of the two users are carefully designed to ensure that each codeword can be uniquely decoded from the sum signal at the receiver. That principle has been extended to uniquely decomposable constellations for two-user multiple access systems [27, 40]. Design criteria for optimizing such constellations for the two-user case have included the mutual information, (i.e., the constellation constrained capacity) [40, 41], and the minimum distance between points of the sum constellation at the receiver [27, 55, 56, 64], with the design variables being the rotation of each user's constellation [40], the power allocation to each user [41], or both [27, 55, 56, 64]. In related work, an explicit two-user constellation for the two-way relay channel was developed in [49].

Since the previous work on finite constellation design for the Gaussian MAC has been limited to the case of two users, in this chapter we develop finite constellation design techniques for the K-user MAC.

- Our first key contribution is for the case of $K = 3$ users, each of which employs binary signalling. We derive a closed-form expression for the set of user constellations that maximizes the minimum distance between the points of the received sum constellation under individual power constraints on each user. Along the way we also derive also obtain a closed-form parameterization of the family of optimal user constellations in the case of $K = 2$ users.

- Next, we develop an efficient design technique for an arbitrary number of users K. This design is based on viewing a carefully rescaled version of the three-user sum constellation as the generator for a two-dimensional lattice constellation.

- Beyond the inherent performance advantages, the proposed sum constellation is uniquely decomposable. This enables fast detection, in the sense that maximum likelihood (ML) multiuser detection reduces to simple (single-user) quantization-based detection over the sum constellation.

- A further simplification of our lattice-based constellation for $K > 3$ users yields a sum constellation that can be viewed as being carved from the Eisenstein integer ring and a different simplification results in the sum constellation being carved from the Gaussian integer ring. Both rings have appealing geometric structures that enables a simple representation of the decision regions employed by the simplified ML detector. Furthermore, those simple decision regions enable analytic computation of the symbol error probability (SEP), which can be represented by using the SEP expressions of M-ary PSK ($M = 2, 3, 6$) constellations.

- We then analytically show that all of our proposed sum constellations provide a larger minimum distance than the corresponding orthogonal scheme with the same transmitted power that employs conventional QAM signaling.

- Finally, we develop a constellation construction technique that enables us to extend the principles of our design approach to a system in which the k-th user employs a constellation with 2^{M_k} points. Numerical results show that the resulting scheme provides better performance than the scheme in [27], which was based on insights from Farey sequences.

2.2 System Model and Problem Statement

Inspired by the previous work on finite constellation design for the two-user multiple access channel [27, 40, 49, 74], our goal is to design an optimized constellation for the K user case. We consider a narrow band, symbol synchronous system with a single antenna at each node. At an arbitrary symbol instance, the baseband received signal at the base station can be written as

$$y = \sum_{k=1}^{K} h_k x_k + \xi, \tag{2.2.1}$$

where h_k is the channel gain between user k and the base station, and the additive noise ξ is modeled as being Gaussian and white; i.e., $\xi \sim \mathcal{CN}(0, 2\sigma^2)$. The term x_k denotes the symbol transmitted by user k, which is chosen in a random, independent and equally likely manner from a constellation $\mathcal{X}_k$. Our goal is to jointly design these constellations. It is assumed that the base station operates coherently, and hence has perfect channel state information (CSI). We will also assume that the base station has a control channel over which it can inform each user of the constellation it will employ. For equally-likely symbol transmission, the detector that minimizes the symbol error probability (SEP) for jointly detecting the transmitted symbols $\{x_k\}_{k=1}^{K}$ is the maximum likelihood (ML) detector. In the case of the coherent multiple access channel with white Gaussian noise, that receiver solves the following optimization problem:

$$\{\hat{x}_1, \ldots, \hat{x}_K\} = \arg \min_{x_k \in \mathcal{X}_k} \Big| y - \sum_{k=1}^{K} h_k x_k \Big|. \tag{2.2.2}$$

In the relatively high SNR regime, the error performance of the ML detector is dominated by the free distance, d_{free}, which is the minimum distance between any two distinct received signal points, i.e.,

$$d_{\text{free}} = \min_{(x_1,\ldots,x_K)\neq(\tilde{x}_1,\ldots,\tilde{x}_K),x_k,\tilde{x}_k\in\mathcal{X}_k} \Big|\sum_{k=1}^{K} h_k(x_k - \tilde{x}_k)\Big|.$$

The primary goal of this chapter is to seek for a solution to the following optimization problem:

Problem 2.1 *For given channel coefficients h_k, $k = 1,\ldots,K$, find K user constellations $\mathcal{X}_k$ such that the minimum Euclidean distance of any two distinct received constellation points is maximized, i.e.,*

$$\begin{aligned} &\max_{\{\mathcal{X}_k\}} \; d_{\text{free}} \\ &\quad \text{s.t. } \mathbb{E}[|x_k|^2] \leq Q_k,\; k = 1,\ldots,K, \end{aligned}$$

where Q_k is the average transmitted power budget for user k.

In order to simplify the objective function of Problem 2.1, we define a scaled and rotated version of the user constellation by absorbing the (complex-valued) channel gain, i.e., $\mathcal{S}_k = h_k\mathcal{X}_k$ for $k = 1,\ldots,K$. Then, Problem 2.1 can be reformulated into the following equivalent optimization problem:

Problem 2.2 *Find K user constellations $\mathcal{S}_k$ such that the minimum Euclidean distance of any two distinct received signal constellation points is maximized, i.e.,*

$$\begin{aligned} &\max_{\mathcal{S}_k} \min_{(s_1,\ldots,s_K)\neq(\tilde{s}_1,\ldots,\tilde{s}_K),s_k,\tilde{s}_k\in\mathcal{S}_k} \Big|\sum_{k=1}^{K}(s_k - \tilde{s}_k)\Big| \\ &\text{s.t. } \mathbb{E}[|s_k|^2] \leq P_k,\; k = 1,\ldots,K, \end{aligned} \tag{2.2.3}$$

where $P_k = |h_k|^2 Q_k$.

Without loss of generality, we will index the users so that $P_1 \leq \ldots \leq P_K$. We observe that if the user constellations $\{\mathcal{S}_k\}_{k=1}^K$ are such that the objective in (2.2.3) is greater than zero, then the sum constellation $\{z = \sum_{k=1}^K s_k, s_k \in \mathcal{S}_k\}$ is uniquely decomposable in the sense that we will define in the next section.

2.3 Uniquely Decomposable Sum Constellations

The methodology that underlies our approach to solving Problem 2.2 is based on insights from the notion of an additively uniquely decomposable constellation group (AUDCG); see [40, 46]. Such a group is defined as follows:

Definition 2.1 (AUDCG) *Define a sum constellation* $\mathcal{S} = \{z_m\}_{m=1}^M$ *formed from group of constellations* $\mathcal{S}_k$ *as* $\{z_m = \sum_{k=1}^K s_{k,m}, s_{k,m} \in \mathcal{S}_k\} = \mathcal{S}_1 \biguplus \mathcal{S}_2 \biguplus \ldots \biguplus \mathcal{S}_K = \biguplus_{k=1}^K \mathcal{S}_k$. *We observe that* $M = |\mathcal{S}| = \prod_{k=1}^K |\mathcal{S}_k|$. *We will say that* $\mathcal{S}$ *is an additively uniquely decomposable constellation group (AUDCG) if the assumption that there exists two sets* $\{s_k \in \mathcal{S}_k\}_{k=1}^K$ *and* $\{\tilde{s}_k \in \mathcal{S}_k\}_{k=1}^K$, *such that* $\sum_{k=1}^K s_k = \sum_{k=1}^K \tilde{s}_k$, *implies that we have* $s_k = \tilde{s}_k$ *for all* $1 \leq k \leq K$.

In our application, the AUDCG $\mathcal{S}$ will be the sum constellation received by the base station, and $\mathcal{S}_k$ will be the received constellation of the k-th user. The concept of an AUDCG can be considered as an extension of uniquely decodable code (UDC) over the binary field [14, 46, 47] to the complex number domain for K-users.

The first key contribution of this chapter will be to design a family of AUDCGs for the case of binary signalling for each user, i.e., $\mathcal{S}_k = \{s_{k1}, s_{k2}\}$ with $|\mathcal{S}_k| = 2$ for each $1 \leq k \leq K$. Then, in Sect 2.5, we will extend that design to a K-user multiple access system in which the K-th user employs a constellation of size $|\mathcal{S}_k| \geq 2^{M_k}$ with $M_k \geq 1$. A result on the case of binary signalling that will assist in our development is as follows:

Lemma 2.1 *Consider an AUDCG $\bar{\mathcal{S}} = \biguplus_{k=1}^{K} \bar{\mathcal{S}}_k$ with $\bar{\mathcal{S}}_k = \{0, s_k\}$, and also consider the symmetrized user constellations $\mathcal{S}_k = \{-s_k/2, s_k/2\}$. Then the sum constellation $\mathcal{S} = \biguplus_{k=1}^{K} \mathcal{S}_k$ is also an AUDCG with the same minimum Euclidean distance, each user constellation $\mathcal{S}_k$ has half the average energy of $\bar{\mathcal{S}}_k$.*

Proof Since $\mathcal{S}$ can be obtained by shifting $\mathcal{S}$ by $\sum_{k=1}^{K} s_k/2$, and since the shifting doesn't change any relative distance, the sum constellation $\mathcal{S}$ is an AUDCG with the same minimum Euclidean distance as $\bar{\mathcal{S}}$. Moreover, the average energy of $\mathcal{S}_k$ is $|s_k|^2/4$, which is half of that of $\bar{\mathcal{S}}_k$. $\square$

2.4 Constellation Design for Multiple-access Channel with Binary Signalling

In this section, we will derive solutions to the constellation design in Problem 2. In Sect 2.4.2, we state the solution for two user case when the users employ binary signalling and relate that result to previous designs. In Sect 2.4.3, we derive the first of the key results in the chapter, namely, the family of optimal solutions to the case of $K = 3$ users. In Sect 2.4.4, we extend that result to generate good designs for K-user uplink system with $K > 3$. In Sect 2.4.7, we show that the proposed sum constellation design achieves a larger minimum distance than the corresponding orthogonal scheme with (square/rectangular/cross) QAM, resulting in a superior performance.

In Sect 2.4.5, we define a fast ML detection method, in which the maximum likelihood multiuser detection is reduced to a single-user quantization-based detection. In Sect 2.4.6, sum constellation with a simplified lattice structure are introduced, and the numerical results show that they can achieve similar performance to our original design.

2.4.1 Problem Formulation

For the case of binary signalling, each user constellation[1] takes the form $\mathcal{S}_k = \{-s_k/2, s_k/2\}$ with $s_k = |s_k|e^{j\theta_k}$ and $|s_k| \leq 2\sqrt{P_k}$ for $1 \leq k \leq K$. In order to simplify some of the proofs, we will also consider its unipolar form, which is given by $\bar{\mathcal{S}}_k = \{0, s_k\}$. It will also help to simplify the proofs if we define $\mathcal{D}$ to the smallest subset of all the pairwise distances in the (unipolar) sum constellation $\bar{\mathcal{S}} = \biguplus_{k=1}^{K} \bar{\mathcal{S}}_k$ that is guaranteed to include the minimum pairwise distance in (2.2.3). We will call this set the simplest minimum Euclidean distance set. This definition enables us to simplify the inner minimization in (2.2.3) to $\min\limits_{d \in \mathcal{D}} d = \min \mathcal{D}$, and hence the instance of Problem 2.2 with binary signalling can be written as

$$\max_{\substack{s_k, |s_k| \leq 2\sqrt{P_k}, \\ k=1,\ldots,K}} \min \mathcal{D} \tag{2.4.1}$$

Since we have assumed that $P_1 \leq \ldots \leq P_K$, without loss of generality we can focus on the case where $|s_1| \leq \ldots \leq |s_K|$. Furthermore, since $\{\theta_k\}$ can be regarded as the directions of basis vectors on which the constellations are constructed, there are equivalence classes of constellations generated by (common) rotations of the basis vectors. We will choose case of $\theta_1 = 0$ as the representative of the equivalence class.

[1]Given the nature of the constraints, each user constellation should be symmetric.

Furthermore, given the symmetry of antipodal constellations, we can restrict attention to $0 \leq \theta_2 \leq \frac{\pi}{2}$.

2.4.2 Optimal Constellation for Two-User MAC

To set the context for our key results, we first address the case of two users.

Theorem 2.1 *A class of the optimal user constellations for the two-user case is*

$$\begin{cases} \mathcal{S}_1 = \{-d/2, d/2\}, \\ \mathcal{S}_2 = \{-d/2 \exp(j\theta_2), d/2 \exp(j\theta_2)\} \end{cases} \tag{2.4.2}$$

where $d = 2\sqrt{P_1}$ *and* $\frac{\pi}{3} \leq \theta_2 \leq \frac{\pi}{2}$.

Proof Consider the unipolar form $\bar{\mathcal{S}}_k = \{0, s_k\}$ with $s_k = |s_k|e^{j\theta_k}$ $(k = 1, 2)$ for each user constellation. As discussed above, by symmetry it is sufficient to restrict θ_2 so that $0 \leq \theta_2 \leq \frac{\pi}{2}$. For such θ_2, $|s_2 + s_1| \geq |s_2 - s_1|$ and hence, the simplest minimum Euclidean distance set is $\mathcal{D} = \{|s_1|, |s_2 - s_1|\}$. According to (2.4.1), the optimal constellation can be found by solving

$$\max_{\substack{|s_1|\leq|s_2|, 0\leq\theta_2\leq\frac{\pi}{2}, \\ |s_k|\leq 2\sqrt{P_k}(k=1,2)}} \min \mathcal{D} = \max_{\substack{|s_1|\leq|s_2|, 0\leq\theta_2\leq\frac{\pi}{2}, \\ |s_k|\leq 2\sqrt{P_k}(k=1,2)}} \min\{|s_1|, |s_2 - s_1|\}. \tag{2.4.3}$$

An upper bound of (2.4.3) is $\max\limits_{|s_1|\leq 2\sqrt{P_k}} |s_1| = 2\sqrt{P_k}$. Furthermore, this bound is tight and can be achieved when $|s_2 - s_1| \geq |s_1|$. As illustrated in Fig. 2.1, since $|s_2| \geq |s_1|$, this happens when $\frac{\pi}{3} \leq \theta_2 \leq \frac{\pi}{2}$.

Therefore, we have $\max\limits_{\substack{|s_1|\leq|s_2|, 0\leq\theta_2\leq\frac{\pi}{2}, \\ |s_k|\leq 2\sqrt{P_k}(k=1,2)}} \min \mathcal{D} = \max\limits_{|s_1|\leq 2\sqrt{P_k}} |s_1| = 2\sqrt{P_1}$ with $\frac{\pi}{3} \leq \theta_2 \leq \frac{\pi}{2}$. Since $|s_2| \geq |s_1|$, and s_2 must satisfy the constraint $|s_2| \leq 2\sqrt{P_2}$, any $|s_2| \in$

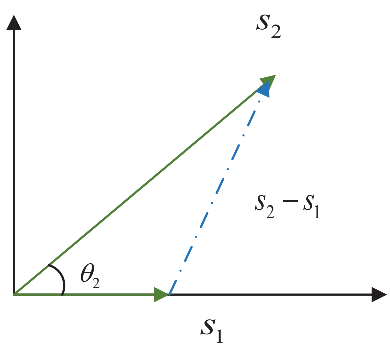

Figure 2.1: Illustration of $|s_2 - s_1| \geq |s_1|$.

$[2\sqrt{P_1}, 2\sqrt{P_2}]$ would solve (2.4.1). In order to save energy, it is desirable to choose s_2 so that $|s_2| = 2\sqrt{P_1}$. □

As outlined in the proof of Theorem 2.1, the optimal Euclidean distance can be achieved, as long as the user with smaller power constraint uses its maximum allowable power, and the other user uses at least that amount. If $P_2 > P_1$, that user still has some transmitted power left, which can be used for the other communication purposes. Note that although there is no difference among the solutions in Theorem 2.1 with $\frac{\pi}{3} \leq \theta_2 \leq \frac{\pi}{2}$ in the sense of the minimum Euclidean distance, the kissing numbers may be different, and the decision regions are different, and hence the constellation may have different probability of error. In Fig. 2.2(b), we have provided three examples of optimal two-user based sum constellations, one with $\theta_2 = \frac{\pi}{3}$ (in blue), one with $\theta_2 = \frac{\pi}{2}$ (in red), and one with $\theta_2 = \frac{5\pi}{12}$ (in green), and Fig. 2.2(a) shows the corresponding user constellations.

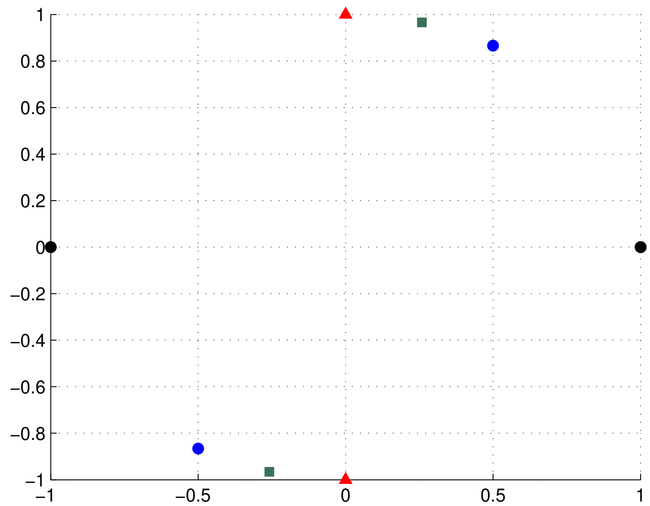

(a) User constellations: $\mathcal{S}_1$(black circle) and three optimal choices for $\mathcal{S}_2$ with $\theta_2 = \frac{\pi}{3}$ (blue circle), $\theta_2 = \frac{\pi}{2}$ (red triangle), and $\theta_2 = \frac{5\pi}{12}$ (green square).

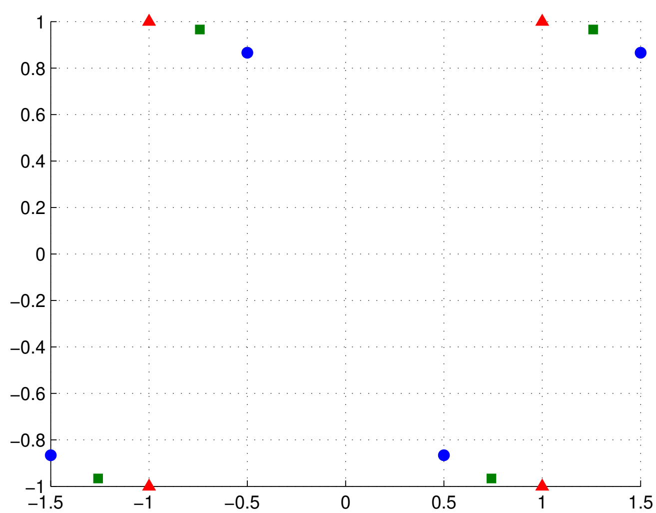

(b) The three sum constellations $\mathcal{S}$, corresponding to the choices of θ_2 in part (a).

Figure 2.2: Three examples of optimal two-user constellations.

2.4.3 Optimal Constellation for Three-User MAC

In this subsection, we derive the first key result of this chapter, a closed form expression for the optimal constellations for the three-user case with binary signalling.

For later notational convenience, let us once again consider the unipolar form $\bar{\mathcal{S}}_k = \{0, s_k\}$ with $s_k = |s_k|e^{j\theta_k}$ and $|s_k| \leq 2\sqrt{P_k}$ $(1 \leq k \leq 3)$. Due to the fact that $e^{j\theta} = \cos\theta + j\sin\theta$, $e^{-j(\theta+\pi)} = e^{-j\pi}e^{-j\theta} = -\cos\theta + j\sin\theta$, it is sufficient for us to focus on the case where $\theta_1 = 0$ and $-\frac{\pi}{2} \leq \theta_3 \leq \frac{\pi}{2}$. We will find it convenient to reparametrize the problem in terms of the relative angle of θ_3 with respect to θ_2, $\alpha = \theta_2 - \theta_3$, where $0 \leq \alpha \leq \pi$, as illustrated in Fig. 2.3. By comparing the distance between any two points in the sum constellation $\bar{\mathcal{S}} = \{0, s_1, s_2, s_3, s_1+s_2, s_1+s_3, s_2+s_3, s_1+s_2+s_3\}$, the simplest minimum Euclidean distance set can be shown to be $\mathcal{D} = \{|s_1|, |s_2-s_1|, |s_3-s_1|, |s_3+s_2|, |s_3-s_2|, |s_1+s_2-s_3|, |s_1+s_3-s_2|, |s_2+s_3-s_1|\}$. Therefore, for the three-user case with binary signalling, we can rewrite Problem 2.2 as $\max\limits_{\Theta,\mathcal{A}} \min \mathcal{D}$, where the design variables are $\Theta = \{(\theta_2, \alpha) : 0 \leq \theta_2 \leq \frac{\pi}{2}, 0 \leq \alpha \leq \pi\}$ and $\mathcal{A} = \{(|s_1|, |s_2|, |s_3|) : |s_1| \leq |s_2| \leq |s_3|, |s_1| \leq \sqrt{\bar{P}_1}, |s_2| \leq \sqrt{\bar{P}_2}, |s_3| \leq \sqrt{\bar{P}_3}\}$, where $\bar{P}_k = 4P_k$. A closed-form expression for the optimal solution is provided in the following theorem.

Theorem 2.2 *A class of sum constellation and the corresponding user constellations are:*

$$\mathcal{S} = \frac{d}{2}\big\{-3, -1+2e^{j2\theta_2}, -1, -1-2e^{j2\theta_2}, 1+2e^{j2\theta_2}, 1, 1-2e^{j2\theta_2}, 3\big\} \tag{2.4.4}$$

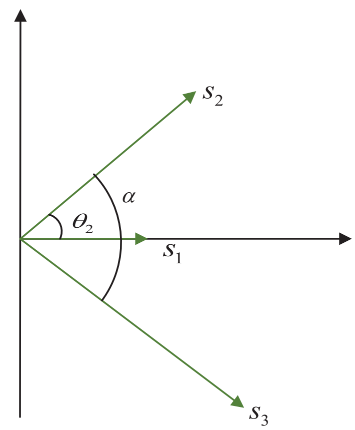

Figure 2.3: Illustration of a generic arrangements of s_1, s_2 and s_3, where $|s_k| \leq \sqrt{\bar{P}_k}$ and $P_1 \leq P_2 \leq P_3$.

$$\begin{cases} \mathcal{S}_1 = \{-d/2, d/2\}, \\ \mathcal{S}_2 = \{-d\cos\theta_2 \exp(j\theta_2), d\cos\theta_2 \exp(j\theta_2)\} \\ \mathcal{S}_3 = \{-d\sin\theta_2 \exp(j(\theta_2 - \pi/2)), d\sin\theta_2 \exp(j(\theta_2 - \pi/2))\} \end{cases}, \tag{2.4.5}$$

with the minimum Euclidean distance $d = \min\{2\sqrt{P_1}, \frac{\sqrt{P_2}}{\cos\theta_2}\}$ *and*

$$\theta_2 = \begin{cases} \arctan\sqrt{\frac{P_3}{P_2}}, & \textit{if } \sqrt{\frac{P_3}{3}} < \sqrt{P_2} \leq \sqrt{P_3}, \\ \frac{\pi}{3}, & \textit{if } \sqrt{P_2} \leq \sqrt{\frac{P_3}{3}}. \end{cases} \tag{2.4.6}$$

Some examples of the optimal constellations for $\bar{P}_1 = 1$ and different values of $\bar{P}_2$ and $\bar{P}_3$ are given in Fig. 2.4.

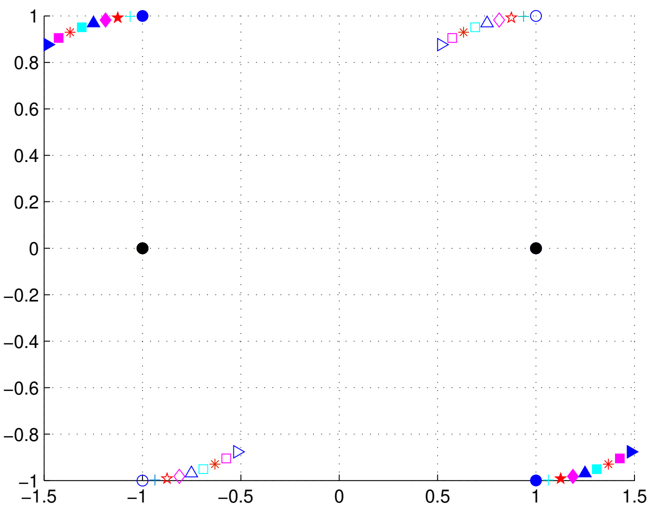

(a) User constellations: $\mathcal{S}_1$ (black circle), $\mathcal{S}_2$ (open symbols), $\mathcal{S}_1$ (filled symbols).

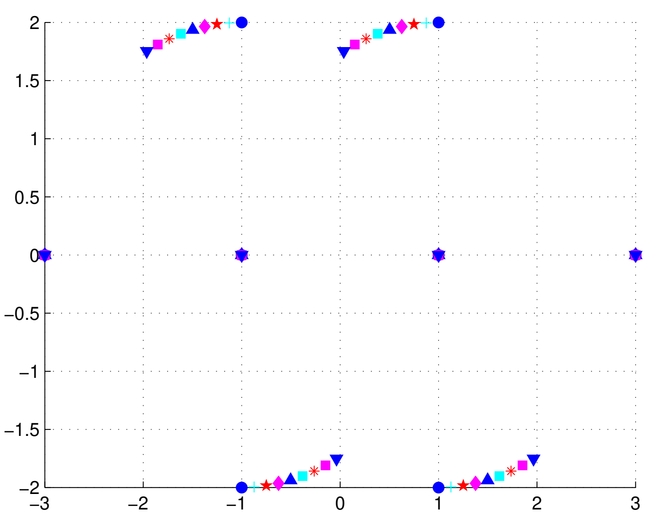

(b) Sum constellation

Figure 2.4: Structure of 9 examples of optimal sum constellations in the three-user case. Each different symbol corresponds to a different case of $\bar{P}_1 = 1$, $\bar{P}_2$ and $\bar{P}_3$. The pairs $(\bar{P}_2, \bar{P}_3)$ are $(2, 2)$ (blue circle), $(1.8744, 2.1256)$ (cyan plus), $(1.7493, 2.2507)$ (red star), $(1.6252, 2.3748)$ (magenta rhombus), $(1.5026, 2.4974)$ (blue triangle), $(1.382, 2.6180)$ (cyan square), $(1.2638, 2.7362)$ (red multiple sign), $(1.1484, 2.8516)$ (magenta square), and $(1.0365, 2.9635)$ (blue inverted triangle).

Proof Guided by the results in Lemma 2.3 in Appendix 2.B, we first consider the scenario in which $\sqrt{|s_2|^2+|s_3|^2} < 2|s_1|$. Let

$$f(|s_1|,|s_2|,|s_3|) = \frac{2}{3}\left(|s_1|^2 - \sqrt{|s_1|^4 + 9|s_2|^2|\bar{s}_3|^2}\cos\gamma\right),$$

where

$$\gamma = \frac{1}{3}\arccos\frac{2|s_1|^6 + 27|s_2|^2|s_3|^4 + 27|s_2|^4|s_3|^2 - 81|s_1|^2|s_2|^2|s_3|^2}{2(|s_1|^4 + 9|\bar{s}_2|^2|s_3|^2)^{3/2}} + \frac{4\pi}{3}.$$

By taking the derivative, we can show that $f(|s_1|,|s_2|,|s_3|)$ is an increasing function of $|s_2| > 0$ and $|s_3| > 0$, and when $|s_1| > \frac{\sqrt{|s_2|^2+|s_3|^2}}{2}$, it is a decreasing function of $|s_1|$. Now, let us consider the following two cases, one in which $\bar{P}_2 + \bar{P}_3 < 4\bar{P}_1$ and the other in which $\bar{P}_2 + \bar{P}_3 \geq 4\bar{P}_1$.

- For the case where $\bar{P}_2 + \bar{P}_3 < 4\bar{P}_1$, the upper bound on $f(|s_1|,|s_2|,|s_3|)$ occurs when $|s_1| = \frac{\sqrt{\bar{P}_2+\bar{P}_3}}{2}$, $|s_2| = \sqrt{\bar{P}_2}$ and $|s_3| = \sqrt{\bar{P}_3}$. The value of that upper bound is $\frac{\sqrt{\bar{P}_2+\bar{P}_3}}{2}$. Using that observation and the constellation structure illustrated in Fig. 2.3, it can be shown that the upper bound on $f(|s_1|,|s_2|,|s_3|)$ can be achieved by setting $\alpha^* = \frac{\pi}{2}$ and $\theta_2^* = \arctan\sqrt{\frac{\bar{P}_3}{\bar{P}_2}}$. We note that with these definitions, the upper bound can be written as $\sqrt{\frac{\bar{P}_2+\bar{P}_3}{2}} = \frac{\sqrt{\bar{P}_2}}{2\cos\theta_2^*} = \frac{\sqrt{\bar{P}_3}}{2\sin\theta_2^*}$. Furthermore, we observe that since the users are ordered such that $\bar{P}_3 \geq \bar{P}_2 \geq \bar{P}_1$, the fact that $4\bar{P}_1 > \bar{P}_2 + \bar{P}_3$ implies that $\bar{P}_2 > \frac{\bar{P}_3}{3}$, and then we have that $\frac{\pi}{4} \leq \theta_2^* = \arctan\sqrt{\frac{\bar{P}_3}{\bar{P}_2}} < \frac{\pi}{3}$.

- For the case where $\bar{P}_2 + \bar{P}_3 \geq 4\bar{P}_1$, according to the lemmas in Appendices 2.A and 2.B, we note that an upper bound on $f(|s_1|,|s_2|,|s_3|)$ occurs when $|s_1| = \sqrt{\bar{P}_1}$, $|s_2| = 2\cos\theta_2\sqrt{\bar{P}_1}$ and $|s_3| = 2\sin\theta_2\sqrt{\bar{P}_1}$. The value of that upper bound is $\sqrt{\bar{P}_1}$ and it can be achieved by setting $\alpha^* = \frac{\pi}{2}$ and

$$\theta_2^* = \begin{cases} \arctan\sqrt{\frac{P_3}{P_2}}, & \text{if } \sqrt{\frac{P_3}{3}} < \sqrt{P_2} \le \sqrt{P_3}, \\ \frac{\pi}{3}, & \text{if } \sqrt{P_2} \le \sqrt{\frac{P_3}{3}}. \end{cases} \tag{2.4.7}$$

Based on the above, we have that $\max\limits_{\mathcal{A},\Theta} \min \mathcal{D} = \min\{\sqrt{\bar{P}_1}, \frac{\sqrt{\bar{P}_2}}{2\cos\theta_2^*}\}$.

Now, we consider the remaining scenario, in which $\sqrt{|s_2|^2 + |s_3|^2} \ge 2|s_1|$. In that case, according to the lemma in Appendix 2.B, we know that $\max\limits_{\mathcal{A},\Theta} \min \mathcal{D} = \max\limits_{\mathcal{A},\Theta} |s_1|$. Since $|s_1| \le \min\{\sqrt{\bar{P}_1}, \frac{\sqrt{\bar{P}_2+\bar{P}_3}}{2}\}$, we have $\max\limits_{\mathcal{A},\Theta} \min \mathcal{D} = \min\{\sqrt{\bar{P}_1}, \frac{\sqrt{\bar{P}_2+\bar{P}_3}}{2}\}$. As in the first scenario, we can divide our analysis into two cases.

- For the case where $\bar{P}_2 + \bar{P}_3 < 4\bar{P}_1$, we know that $\max\limits_{\mathcal{A},\Theta} \min \mathcal{D} = \frac{\sqrt{\bar{P}_2+\bar{P}_3}}{2}$, and it can be achieved by letting $|s_1| = \frac{\sqrt{\bar{P}_2+\bar{P}_3}}{2}$, $|s_2| = \sqrt{\bar{P}_2}$, $|s_3| = \sqrt{\bar{P}_3}$, $\alpha^* = \frac{\pi}{2}$ and $\theta_2^* = \arctan\sqrt{\frac{\bar{P}_3}{\bar{P}_2}}$. Moreover, we also have $\frac{\sqrt{\bar{P}_2+\bar{P}_3}}{2} = \frac{\sqrt{\bar{P}_2}}{2\cos\theta_2^*}$, i.e., $\max\limits_{\mathcal{A},\Theta} \min \mathcal{D} = \frac{\sqrt{\bar{P}_2}}{2\cos\theta_2^*}$.

- For the case where $\bar{P}_2 + \bar{P}_3 \ge 4\bar{P}_1$, we know that $\max\limits_{\mathcal{A},\Theta} \min \mathcal{D} = \sqrt{\bar{P}_1}$, and it can be achieved by letting $|s_1| = \sqrt{\bar{P}_1}$, $|s_2| = 2\cos\theta_2\sqrt{\bar{P}_1}$, $|s_3| = 2\sin\theta_2\sqrt{\bar{P}_1}$, $\alpha^* = \frac{\pi}{2}$ and

$$\theta_2^* = \begin{cases} \arctan\sqrt{\frac{P_3}{P_2}}, & \text{if } \sqrt{\frac{P_3}{3}} < \sqrt{P_2} \le \sqrt{P_3}, \\ \frac{\pi}{3}, & \text{if } \sqrt{P_2} \le \sqrt{\frac{P_3}{3}}. \end{cases} \tag{2.4.8}$$

By combining the analyses for the two scenario above, we have that $\max\limits_{\mathcal{A},\Theta} \min \mathcal{D} = \min\{\sqrt{\bar{P}_1}, \frac{\sqrt{\bar{P}_2}}{2\cos\theta_2^*}\}$. Since $\bar{P}_k = 4P_k$, we let $d = \max\limits_{\mathcal{A},\Theta} \min \mathcal{D} = \min\{2\sqrt{P_1}, \frac{\sqrt{P_2}}{\cos\theta_2}\}$. By shifting $\bar{\mathcal{S}}_k = \{0, s_k\}$ ($|s_k| \le \sqrt{\bar{P}_k}$) to $\mathcal{S}_k = \{-s_k/2, s_k/2\}$, and observing that in both cases the optimal value $\alpha^* = \frac{\pi}{2}$, we obtain the optimal user constellations in (2.4.5). By using Euler's formula, we obtain the optimal sum constellation in (2.4.4). $\square$

2.4.4 Extension for the K-User MAC

Theorem 2.2 provides a closed-form expression for a globally optimal solution to the problem of finding user constellations that maximize the minimum distance of the received sum constellation at the base station for binary signalling with $K = 3$ users. While a corresponding expression for the optimal user constellations K-user case with binary signal appears to be beyond our grasp, in this section we will use the results of Theorem 2.2 to develop an efficient technique for generating good constellations for the K-user case.

The basic principle of our approach uses Theorem 2.2 to design optimal constellations for a specially-selected subset of three users. We then use scaled versions of those constellations for the other users. More specifically, given the power constraints of the users, $\bar{P}_1 \leq \bar{P}_2 \leq \cdots \leq \bar{P}_K$, the subset of three users is chosen to be user 1, a representative of the even indexed users and a representative of the odd indexed users. (We will describe the selection of the representatives below.) Once Theorem 2.2 has been used to design the optimal constellations for that triple (with appropriately scaled power constraints), those constellations are assigned to users 1, 2, and 3. The remaining constellations for the even indexed users are obtained by iteratively scaling the constellation assigned to user 2 by a factor of 2. Since we have binary signalling, this ensures that the minimum distance of the (K-user) sum constellation is the same as that of the underlying three-user design. The remaining constellations for the odd indexed users are generated in an analogous way from the constellation for user 3. In order for this process to yield user constellations that satisfy the power constraints, the representative users from the sets of even and odd indexed users must be chosen so that the iterative doubling of the powers does not violate the constraint. For the even indexed users, that means that we should choose the representative to be the one that has the minimum value of $\left\{\frac{\bar{P}_{2\ell}}{4^{(\ell-1)}}\right\}_{\ell\geq 1}$. Analogously, the representative for the odd indexed users should be the one that minimizes $\left\{\frac{\bar{P}_{2\ell+1}}{4^{(\ell-1)}}\right\}_{\ell\geq 1}$. With the user constellations generated in this way, the sum constellation at the receiver takes the form of an offset lattice constellation, where the lattice structure arises from the scaling of the constellations for user 2 and 3 in the underlying three-user constellation, and the offset comes from the constellation assigned to user 1.

Having outlined those principles, we now formally state the construction procedure in Algorithm 1.

2.4.5 Efficient ML Detection

Given our channel model in (2.2.1) and the transformation $\mathcal{S}_k = h_k\mathcal{X}_k$ that was used to obtain Problem 2.2 from Problem 2.1, the maximum likelihood multiuser detector can be written as

$$\{\hat{s}_1, \cdots, \hat{s}_K\} = \arg \min_{\{s_k \in \mathcal{S}_k\}_{k=1}^K} |y - \sum_{k=1}^{K} s_k|. \tag{2.4.9}$$

However, the way in which we have designed the user constellations $\{\mathcal{S}_k\}_{k=1}^K$ ensures that the sum constellation $\mathcal{S}$ is an additive uniquely decomposable constellation group (AUDCG); see Section 2.3. That is, given a point $\hat{s} \in \mathcal{S}$ we can uniquely determine the set $\{\hat{s}_k\}_{k=1}^K$ such that $\hat{s} = \sum_{k=1}^K \hat{s}_k$. That means that for the purposes of detection, we can treat the received signal as if it was generated by a transmission from a single user that employs the sum constellation $\mathcal{S}$. That is, for the purpose of

Algorithm 1: Construction of a good solution to Problem 2 for $K \geq 3$ users with binary signalling

Input: $K \geq 3$, $P_1 \leq P_2 \leq \ldots \leq P_K$;
Output: $\mathcal{S}_k$ $(1 \leq k \leq K)$, $\mathcal{S}$;
if K is even **then**
  Set $\tilde{P}_{even} \leftarrow \min\left\{\frac{P_{2\ell}}{4^{(\ell-1)}}, 1 \leq \ell \leq K/2\right\}$, $\tilde{P}_{odd} \leftarrow \min\left\{\frac{P_{2\ell+1}}{4^{(\ell-1)}}, 1 \leq \ell \leq K/2-1\right\}$;
else
  Set $\tilde{P}_{even} \leftarrow \min\left\{\frac{P_{2\ell}}{4^{(\ell-1)}}, 1 \leq \ell \leq (K-1)/2\right\}$,
  $\tilde{P}_{odd} \leftarrow \min\left\{\frac{P_{2\ell+1}}{4^{(\ell-1)}}, 1 \leq \ell \leq (K-1)/2\right\}$;
end if
if $\sqrt{\tilde{P}_{even}} \leq \sqrt{\frac{\tilde{P}_{odd}}{3}}$ **then**
  • Set $\theta_2 \leftarrow \frac{\pi}{3}$;
else
  • Set $\theta_2 \leftarrow \arctan\sqrt{\frac{\tilde{P}_{odd}}{\tilde{P}_{even}}}$;
end if
Set $d \leftarrow \min\{2\sqrt{P_1}, \frac{\sqrt{P_{even}}}{\cos\theta_2}\}$, $\mathcal{S}_1 \leftarrow \{-d/2, d/2\}$,
$\mathcal{S}_2 \leftarrow \{-d\cos\theta_2\exp(j\theta_2), d\cos\theta_2\exp(j\theta_2)\}$,
$\mathcal{S}_3 \leftarrow \{-d\sin\theta_2\exp(j(\theta_2-\pi/2)), d\sin\theta_2\exp(j(\theta_2-\pi/2))\}$;
if K is even **then**
  for $t = 2$ *to* $K/2$ **do**
    • Set $\lambda_t \leftarrow 2^{t-1}$, $\mu_t \leftarrow 2^{t-1}$, $\mathcal{S}_{2t} \leftarrow \lambda_t\mathcal{S}_2$, $\mathcal{S}_{2t-1} \leftarrow \mu_{t-1}\mathcal{S}_3$,
  end for
else
  for $t = 2$ *to* $(K-1)/2$ **do**
    • Set $\lambda_t \leftarrow 2^{t-1}$, $\mu_t \leftarrow 2^{t-1}$, $\mathcal{S}_{2t} \leftarrow \lambda_t\mathcal{S}_2$, $\mathcal{S}_{2t+1} \leftarrow \mu_t\mathcal{S}_3$,
  end for
  Set $\mathcal{S} \leftarrow \biguplus_{k=1}^{K}\mathcal{S}_k$.
end if

detection we can use the channel model

$$y = s + \xi, \tag{2.4.10}$$

where $s \in \mathcal{S}$. With that model in mind we can develop an equivalent maximum likelihood detector to that in (2.4.9) that consists of the following two steps:

1. Using the sum constellation $\mathcal{S}$ generated by Algorithm 1, determine

$$\hat{s} = \arg\min_{s\in\mathcal{S}} |y - s|. \tag{2.4.11}$$

2. Given $\hat{s}$, determine $\{\hat{s}_k \in \mathcal{S}_k\}_{k=1}^{K}$ such that $\sum_{k=1}^{K} \hat{s}_k = \hat{s}$.

In this form, the (worst-case) computational cost of (2.4.11) is the same as that of (2.4.9). However, the expression in (2.4.11) reveals that if we determine the decision regions, or Voronoi cells, of the designed sum constellation $\mathcal{S}$, then maximum likelihood detection of the sum constellation point reduces to a simple quantization-style detector for a single-user system; and hence can be efficiently implemented. Fig. 2.5(a) shows an example of the detection regions for a sum constellation carved from the Eisenstein integer ring. If the received point is in the detection range $\mathbf{D}_i$, the user points can be easily found by looking up the table in Fig. 2.5(b).

2.4.6 Structured sum constellations

For the case of $K = 3$ users the optimal value of the constellation parameter θ_2 depends on the ratio of the power constraints for users 2 and 3 (recall $P_1 \le P_2 \le P_3$). Indeed $\theta_2 \in \left[\frac{\pi}{4}, \frac{\pi}{3}\right]$, with $\theta_2 = \frac{\pi}{4}$ when $P_3 = P_2$, and if P_2 is fixed, θ_2 increases as P_3

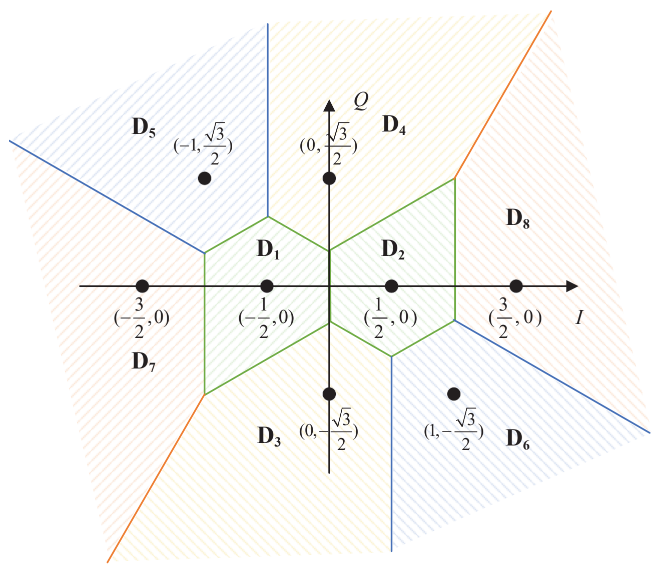

(a) Detection regions for quantization-based detection of sum constellation points.

$\mathcal{S}$	$\mathcal{S}_1$	$\mathcal{S}_2$	$\mathcal{S}_3$
$-\frac{3}{2}$	$-\frac{1}{2}$	$-\frac{1+\sqrt{3}j}{4}$	$-\frac{3-\sqrt{3}j}{4}$
$-1+\frac{\sqrt{3}}{2}j$	$-\frac{1}{2}$	$\frac{1+\sqrt{3}j}{4}$	$-\frac{3-\sqrt{3}j}{4}$
$-\frac{1}{2}$	$\frac{1}{2}$	$-\frac{1+\sqrt{3}j}{4}$	$-\frac{3-\sqrt{3}j}{4}$
$-\frac{\sqrt{3}}{2}j$	$-\frac{1}{2}$	$-\frac{1+\sqrt{3}j}{4}$	$\frac{3-\sqrt{3}j}{4}$
$\frac{\sqrt{3}}{2}j$	$\frac{1}{2}$	$\frac{1+\sqrt{3}j}{4}$	$-\frac{3-\sqrt{3}j}{4}$
$\frac{1}{2}$	$-\frac{1}{2}$	$\frac{1+\sqrt{3}j}{4}$	$\frac{3-\sqrt{3}j}{4}$
$1-\frac{\sqrt{3}}{2}j$	$\frac{1}{2}$	$-\frac{1+\sqrt{3}j}{4}$	$\frac{3-\sqrt{3}j}{4}$
$\frac{3}{2}$	$\frac{1}{2}$	$\frac{1+\sqrt{3}j}{4}$	$\frac{3-\sqrt{3}j}{4}$

(b) Decomposing the sum constellation

Figure 2.5: Example of fast detection for $K = 3$.

increases, with $\theta_2 = \frac{\pi}{3}$ for all $P_3 \geq 3P_2$. For the case of $K > 3$ users, the value of θ_2 used in the construction of good constellations in Algorithm 1 depends on a ratio of power constraints in an analogous way.

While those designs are indeed good, the implementation can be simplified if the constellation has more structure. Therefore, in this section we will consider a modified version of Algorithm 1 in which θ_2 is fixed to either $\frac{\pi}{4}$ or $\frac{\pi}{3}$ and the calculation of d_{min} is adjusted so that the users' power constraints are satisfied; see Algorithm 2 below.

When $\theta_2 = \frac{\pi}{4}$, the sum constellation is carved from (a scaled version of) the Gaussian integer ring, which is the set of complex numbers for which both the real and imaginary parts are integers; i.e., $\mathcal{S} \subset \{\alpha(a + jb) | a, b \in \mathbb{Z}\}$. As such, when $\theta_2 = \frac{\pi}{4}$ the points in the sum constellation are carved from a "square" lattice in the complex plane. When $\theta_2 = \frac{\pi}{3}$, the sum constellation is carved from (a scaled version of) the Eisenstein integer ring, which is the set of complex numbers of the form $Z = \left((2a-1) + jb\sqrt{3}\right)/2$ where a and b are integers. As a result, when $\theta_2 = \frac{\pi}{3}$ the points in the sum constellation are carved from a "triangular" (or "hexagonal") lattice in the complex plane.

In the case that the number of users, K, is even, it can be shown that our constellation based on the Eisenstein ring ($\theta_2 = \frac{\pi}{3}$) always yields a larger minimum distance than that based on the Gaussian ring. However, in the case that K is odd, the relationships between the power constraints of the users will determine which construction has the larger minimum distance.

The design procedure for the K user constellations is stated in Algorithm 2. Given the values of d_{min} (i.e., d, d^G or d^E) obtained in the algorithm, the sum constellations produced by those designs can be written as follows.

Algorithm 2: Construction of a simplified solution to Problem 2 for $K \geq 3$ users with binary signalling

Input: $K \geq 3$, $P_1 \leq P_2 \leq \ldots \leq P_K$;
Output: $\mathcal{S}_k$ $(1 \leq k \leq K)$, $\mathcal{S}$;
if K is even **then**
  • Set $\theta_2 \leftarrow \frac{\pi}{3}$, $d \leftarrow \min\{2\sqrt{P_1}, 2\sqrt{P_2}, 2\sqrt{\frac{P_3}{3}}\}$;
  for $k = 4$ *to* K **do**
    • Set $i \leftarrow \lfloor k/2 \rfloor$, $t \leftarrow k - 2(i-1)$;
    • Set $d \leftarrow \min\{d, \sqrt{\frac{P_k}{4^{i-2}3^{t-2}}}\}$;
  end for
  • Set $\mathcal{S}_1 \leftarrow \{-d/2, d/2\}$, $\mathcal{S}_2 \leftarrow \{-\frac{(1+\sqrt{3}j)d}{2}, \frac{(1+\sqrt{3}j)d}{2}\}$,
  $\mathcal{S}_3 \leftarrow \{-\frac{(3-\sqrt{3}j)d}{2}, \frac{(3-\sqrt{3}j)d}{2}\}$;
else
  • Set $\theta_2^G \leftarrow \frac{\pi}{4}$, $\theta_2^E \leftarrow \frac{\pi}{3}$, $d^G \leftarrow \min\{2\sqrt{P_1}, 2\sqrt{\frac{P_2}{2}}, 2\sqrt{\frac{P_3}{2}}\}$,
  $d^E \leftarrow \min\{2\sqrt{P_1}, 2\sqrt{P_2}, 2\sqrt{\frac{P_3}{3}}\}$;
  for $k = 4$ *to* K **do**
    • Set $i \leftarrow \lfloor k/2 \rfloor$, $t \leftarrow k - 2(i-1)$;
    • Set $d^G \leftarrow \min\{d^G, \sqrt{\frac{P_K}{4^{i-2}2}}\}$, $d^E \leftarrow \min\{d^E, \sqrt{\frac{P_K}{4^{i-2}3^{t-2}}}\}$;
  end for
  if $d^G \geq d^E$ **then**
    • Set $\mathcal{S}_1 \leftarrow \{-d^G/2, d^G/2\}$, $\mathcal{S}_2 \leftarrow \{-(1+j)d^G, (1+j)d^G\}$,
    $\mathcal{S}_3 \leftarrow \{-(1-j)d^G, (1-j)d^G\}$;
  else
    • Set $\mathcal{S}_1 \leftarrow \{-d^E/2, d^E/2\}$, $\mathcal{S}_2 \leftarrow \{-\frac{(1+\sqrt{3}j)d^E}{2}, \frac{(1+\sqrt{3}j)d^E}{2}\}$,
    $\mathcal{S}_3 \leftarrow \{-\frac{(3-\sqrt{3}j)d^E}{2}, \frac{(3-\sqrt{3}j)d^E}{2}\}$;
  end if
end if
for $k = 4$ *to* K **do**
  • Set $i \leftarrow \lfloor k/2 \rfloor$, $t \leftarrow k - 2(i-1)$, $\mathcal{S}_k \leftarrow 2^{i-1}\mathcal{S}_t$
end for

If $K \geq 3$ is even, the sum constellation is chosen from *Eisenstein integers* and determined by

$$\mathcal{S}^E = \frac{d_{\min}}{2}\left\{ a+\sqrt{3}bj : \begin{array}{l} a \in \{2n-m+b+1, 0 \leq n \leq m-1\}, \text{if } 0 \leq |b| \leq \frac{m}{4}; \\ a \in \{2n-m+b+1, 0 \leq n \leq \frac{3m}{2}-2b-1\}, \\ \quad \text{if } \frac{m}{4}+1 \leq b \leq \frac{3m}{4}-1; \\ a \in \{-(2n-m+b+1), 0 \leq n \leq \frac{3m}{2}-2|b|-1\}, \\ \quad \text{if } -\frac{3m}{4}+1 \leq b \leq -\frac{m}{4}-1; \end{array} \right\} \tag{2.4.12}$$

where $m = 2^{K/2}$.

If $K \geq 3$ is odd, the sum constellation is further determined as follows:

1. If Algorithm 2 yields $d^G > d^E$, the sum constellation is chosen from the *Gaussian integers* and is determined by

$$\mathcal{S}^G = \frac{d_{\min}}{2}\left\{ a+2bj : \begin{array}{l} a \in \{2n-m+2|b|+1, 0 \leq n \leq m-1-2|b|\}, \\ 0 \leq |b| \leq \frac{m}{2}-1 \end{array} \right\} \tag{2.4.13}$$

2. Otherwise, the sum constellation is chosen from the *Eisenstein integers* and is determined by

$$\mathcal{S}^E = \frac{d_{\min}}{2}\left\{ a+\sqrt{3}bj : \begin{array}{l} a \in \{2n-m+|b|+1, 0 \leq n \leq m-1-2|b|\}, \\ 0 \leq |b| \leq \frac{m}{2}-1 \end{array} \right\} \tag{2.4.14}$$

where $m = 2^{(K+1)/2}$.

Fig. 2.6 shows the sum constellation from Eisenstein integers for even K users. Fig. 2.7 and Fig. 2.8 show the sum constellation from Gaussian and Eisenstein integers for odd K users.

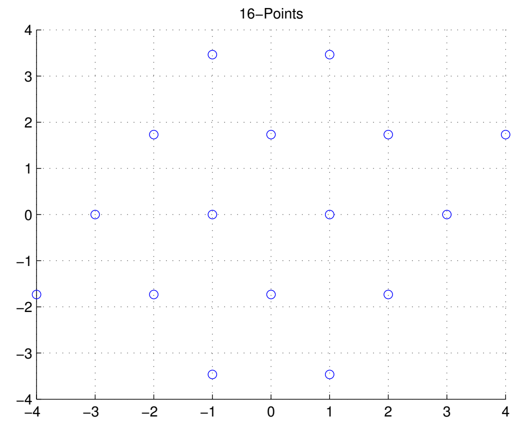

(a) $K = 4$

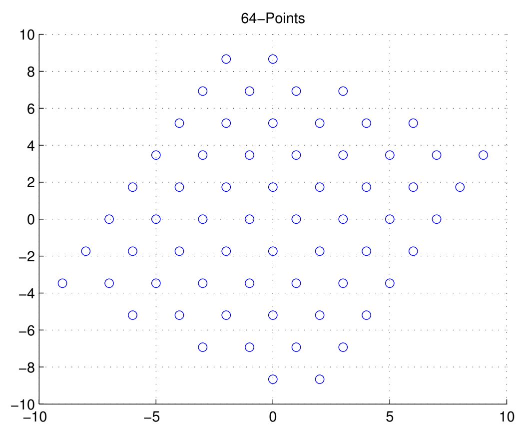

(b) $K = 6$

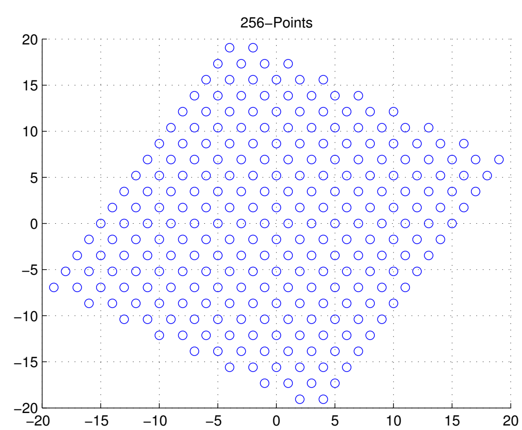

(c) $K = 8$

Figure 2.6: Sum constellations from Eisenstein integers for even number of users, K.

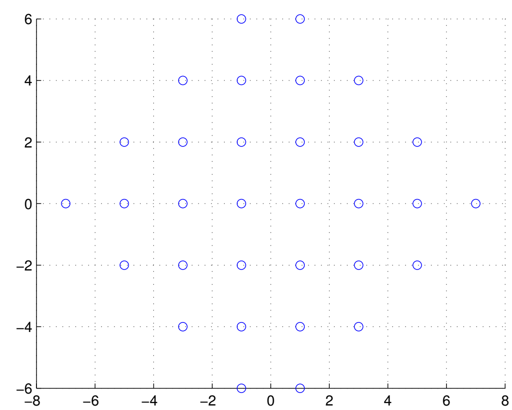

(a) $K = 5$

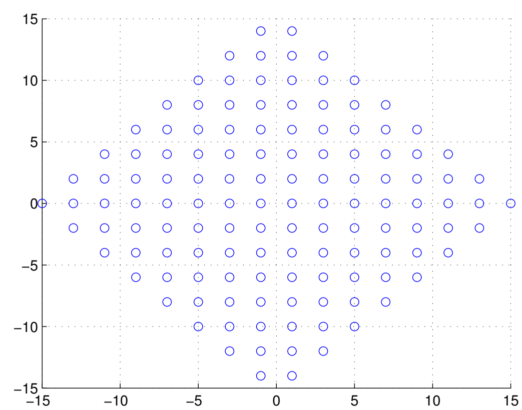

(b) $K = 7$

Figure 2.7: Sum constellations from Gaussian integers for odd numbers of users, K.

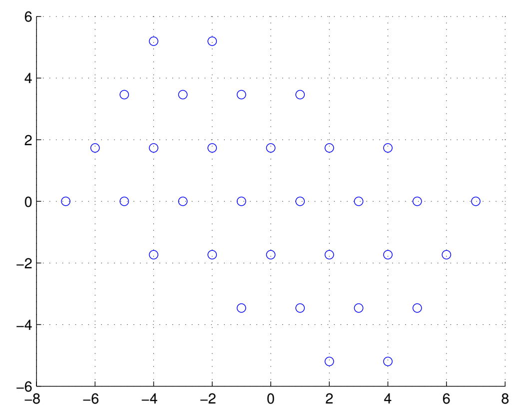

(a) $K = 5$

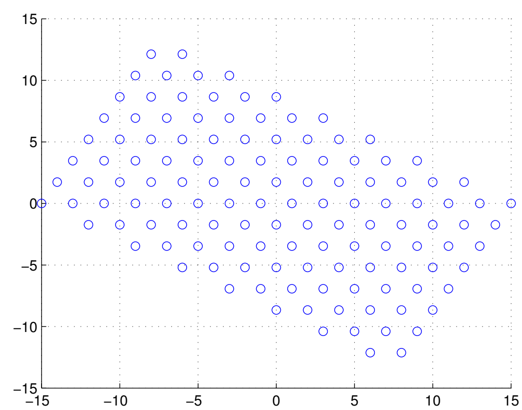

(b) $K = 7$

Figure 2.8: Sum constellations from Eisenstein integers for odd numbers of users, K.

2.4.7 The Superiority of Our Proposed NOMA Scheme over TDMA

In this section, we will show, analytically, that the minimum distance of the proposed NOMA schemes described in Algorithm 1 and Algorithm 2 achieve a larger minimum distance than the corresponding TDMA scheme, respectively. In the proposed scheme, each of the K users transmits one bit in each channel use, subject to a per-channel-use power constraint P_k, $k = 1, 2, \ldots, K$, that captures the physical limitation of the amplifiers at each user. In the corresponding TDMA scheme, there are K channel uses, and each user transmits K bits in its assigned channel use, subject to the same per-channel-use power constraint. When K is even, the TDMA scheme will use a square QAM constellation, and when K is odd, we will consider both rectangular QAM and cross QAM constellations.

For the proposed NOMA scheme, the minimum distance is a function of the power constraints of all the users. In particular, for the scheme proposed in Algorithm 1,

$$d_{\min,\text{NOMA}} = \min_{1 \leq \ell \leq \lceil (K-1)/2 \rceil} \left\{ 2\sqrt{P_1}, \frac{\sqrt{\frac{P_{2\ell}}{4^{\ell-1}}}}{\cos\theta_2} \right\}, \tag{2.4.15}$$

where, as shown in steps 8–12 of Algorithm 1, θ_2 is a function of $\{P_2, P_3, \ldots, P_K\}$. Furthermore, $d_{\min,\text{NOMA}}$ is a non-decreasing function of each P_k, $1 \leq k \leq K$. That means that an increase in the available transmission power for one user may improve the minimum distance of the whole system and hence may improve the error performance of all users in the system. The minimum distance of the NOMA scheme is related to the probability that the system as a whole makes no errors in detecting the symbols sent by all the users. The corresponding notion of minimum distance in the

TDMA scheme is

$$d_{\min,\mathrm{TDMA}} = \min_{1\le k\le K}\{d_{\min,\mathrm{XQAM}}(P_k)\}, \tag{2.4.16}$$

where $d_{\min,\mathrm{XQAM}}(P)$ is the minimum distance of the QAM constellation that is used and X $\in$ {S,R,C} denotes whether a square, rectangular or cross constellation is used. Since $d_{\min,\mathrm{XQAM}}(P)$ is an increasing function of P, and the users are indexed so that $P_1 \le P_2 \le \ldots \le P_K$,

$$d_{\min,\mathrm{TDMA}} = d_{\min,\mathrm{XQAM}}(P_1). \tag{2.4.17}$$

Expressions for $d_{\min}$ for square and cross QAM are derived in [16] and an expression for rectangular QAM is derived in Appendix 2.E. These expressions are

$$\begin{aligned} d_{\min,\mathrm{SQAM}}(P_1) &= \sqrt{\frac{6P_1}{2^K-1}}, \text{ for even } K,\\ d_{\min,\mathrm{RQAM}}(P_1) &= \sqrt{\frac{6P_1}{\frac{5}{4}2^K-1}}, \text{ for odd } K,\\ d_{\min,\mathrm{CQAM}}(P_1) &= \sqrt{\frac{6P_1}{\frac{31}{32}2^K-1}}, \text{ for odd } K. \end{aligned} \tag{2.4.18}$$

In the case of $K=2$, according to Theorem 2.1, it is straight forward to show that the minimum distance of the proposed design $2\sqrt{P_1} > d_{\min,\mathrm{SQAM}}(P_1) = \sqrt{2P_1}$. The main result of this section concerns the case of $K \ge 3$ and it is summarized in the following theorem.

Theorem 2.3 *The minimum Euclidean distance of the NOMA scheme proposed in Algorithm 1 is strictly larger than that of the corresponding QAM-based TDMA scheme.*

Proof The proof can be found in Appendix 2.C. □

For the structured sum constellation-based NOMA for $K \ge 3$ users that was proposed in Algorithm 2, the minimum distance can be written as

$$d_{\min,\text{NOMA}} = \min_{1\leq\ell\leq K/2, 1\leq\tilde{\ell}\leq K/2-1} \left\{2\sqrt{P_1}, 2\sqrt{\frac{P_{2\ell}}{4^{\ell-1}}}, 2\sqrt{\frac{P_{2\tilde{\ell}}}{4^{\tilde{\ell}-1}3}}\right\}, \tag{2.4.19}$$

when K is even, and

$$d_{\min,\text{NOMA}} = \max\left\{\min_{1\leq\ell\leq(K-1)/2}\left\{2\sqrt{P_1}, 2\sqrt{\frac{P_{2\ell}}{4^{\ell-1}2}}\right\}, \min_{1\leq\ell\leq(K-1)/2}\left\{2\sqrt{P_1}, 2\sqrt{\frac{P_{2\ell}}{4^{\ell-1}}}, 2\sqrt{\frac{P_{2\ell}}{4^{\ell-1}3}}\right\}\right\}, \tag{2.4.20}$$

when K is odd. Then, we also have the following theorem.

Theorem 2.4 *The minimum Euclidean distance of the structured sum constellation-based NOMA scheme proposed in Algorithm 2 is also strictly larger than that of the corresponding QAM-based TDMA scheme.*

Proof The proof can be found in Appendix 2.D. □

Even though our constellation design approach was developed for the multiple access channel, the sum constellation that we obtain is a candidate constellation for the single-user channel. We now make some observations regarding that connection.

Remark 2.1 *The relationship between the average energy of the proposed sum constellation in Algorithm 1 and its minimum distance is derived in Appendix 2.E. That enables us to show that when K is odd, it can provide larger minimum Euclidean distance $d_{\min}$ than the 2^K-ary rectangular QAM constellation with same average energy.*

Remark 2.2 *For the structured sum constellation, when K is even, it can be shown that $E_{even}(\mathcal{S}) = \frac{(2^K-1)+2^{K-1}}{12}d_{\min}^2 = \frac{(7M-4)d_{\min}^2}{48}$. When $K \geq 4$, this is smaller than the* *energy of the corresponding square QAM constellation* $E_{SQAM} = \frac{d_{\min}^2(M-1)}{6}$*. Equivalently, for the same energy, the structured sum constellation provides a larger minimum Euclidean distance than square QAM. Actually, in the single-user case, this structured sum constellation is well-known as hexagonal QAM.*

2.4.8 Symbol Error Probability for Structured Sum Constellations

One of the advantages of the user constellations designed using Algorithm 2 is that the sum constellation has a nice regular geometrical structure. Indeed, the sum constellation is carved from either a square lattice (in the case of Gaussian integers) or an equilateral triangular lattice (in the case of Eisenstein integers). As a result, the decision regions for the ML detector also have a regular geometric structure, which significantly reduces the storage requirements of the receiver. As we show in Theorem 2.5 below, this regular structure also enables us to obtain closed-form expressions for the symbol error probability (SEP). There expressions are based on the closed-form expressions for the SEP of the M-ary PSK constellations with $M = 2, 3, 6$.

Theorem 2.5 *If we let* $d_{\min} = d$*, the SEP for the sum constellations arising from Algorithm 2 are given as follows*

- *When $K \geq 3$ is even, the SEP is*

$$\begin{aligned}P_e =&\Big(2^{-K/2+1} - 3 \cdot 2^{-K+1}\Big) P_{\text{2PSK}}\Big(\frac{\sqrt{3}d}{2\sigma}\Big) - \Big(6 + 3 \cdot 2^{-K+1} - 2^{-K/2+4}\Big) P_{\text{2PSK}}\Big(\frac{d}{\sigma}\Big)\\ &+ 6\Big(1 - 2^{-K/2+1} + 2^{-K}\Big) P_{\text{3PSK}}\Big(\frac{\sqrt{3}d}{3\sigma}\Big) - \Big(2^{-K/2} - 2^{-K+1}\Big) P_{\text{3PSK}}\Big(\frac{d}{\sigma}\Big)\\ &+ 2^{-K} P_{\text{6PSK}}\Big(\frac{\sqrt{3}d}{\sigma}\Big) + \Big(2^{-K/2+1} - 2^{-K+2}\Big) P_{\text{6PSK}}\Big(\frac{d}{\sigma}\Big)\end{aligned} \tag{2.4.21}$$

- *When $K \geq 3$ is odd, and the sum constellation is carved from the Eisenstein integer ring, the SEP is*

$$\begin{aligned}P_e =&\Big(2^{-(K-1)/2} - 3 \cdot 2^{-K}\Big) P_{\text{2PSK}}\Big(\frac{\sqrt{3}d}{2\sigma}\Big) - \Big(6 + 2^{-K+1} - 2^{-(K-3)/2}\Big) P_{\text{2PSK}}\Big(\frac{d}{\sigma}\Big)\\ &+ 6\Big(1 - 3 \cdot 2^{-(K+1)/2} + 2^{-K}\Big) P_{\text{3PSK}}\Big(\frac{\sqrt{3}d}{3\sigma}\Big) - \Big(2^{-(K-1)/2} - 2^{-K+1}\Big) P_{\text{3PSK}}\Big(\frac{d}{\sigma}\Big)\\ &+ 2^{-K} P_{\text{6PSK}}\Big(\frac{\sqrt{3}d}{\sigma}\Big) + \Big(2^{-(K-3)/2} - 2^{-K+2}\Big) P_{\text{6PSK}}\Big(\frac{d}{\sigma}\Big)\end{aligned} \tag{2.4.22}$$

- *When $K \geq 3$ is odd and the sum constellation is carved from the Gaussian integer ring, the SEP is*

$$\begin{aligned}P_e =&\Big(4 - 2^{-(K-5)/2} + 2^{-K+1}\Big) Q\Big(\frac{d}{2\sigma}\Big) + \Big(2^{-(K-3)/2} - 2^{-K+2}\Big) Q\Big(\frac{\sqrt{2}d}{2\sigma}\Big)\\ &- \Big(4 - 2^{-(K-5)/2}\Big) Q^2\Big(\frac{d}{2\sigma}\Big)\end{aligned} \tag{2.4.23}$$

where $P_{\text{MPSK}}(u) = \frac{1}{\pi}\int_0^{\frac{\pi(M-1)}{M}} \exp(-\frac{u^2 \sin^2 \frac{\pi}{M}}{2\sin^2\theta}) d\theta$ *and* $Q(u) = \frac{1}{\sqrt{2\pi}}\int_u^{\infty} \exp(-\frac{t^2}{2}) dt = \frac{1}{\pi}\int_0^{\frac{\pi}{2}} \exp(-\frac{x^2}{2\sin^2\theta}) d\theta$ *with* $x \geq 0$.

Proof The proof is provided in Appendix 2.F. □

Fig. 2.9 shows the simulated and theoretical SEP performance comparison, where both the Eisenstein integer ring and the Gaussian integer ring are considered when K is odd. As claimed in the theorem, the results match exactly.

2.4.9 Numerical Results

In this section, we carry out computer simulations to compare the error performance of our proposed NOMA scheme with that of the corresponding TDMA scheme in various channel conditions. Both three-user and six-user multi-access channels are considered. We consider the scenario in which each user has the same power constraint with $Q_k = 1, k \geq 1$, and the receiver noise variance is $2\sigma^2$. Hence we can define a system wide (transmitted) signal to (receiver) noise ratio (SNR) as $\eta = \frac{1}{2\sigma^2}$. The channel coefficients h_k are modelled using a Rayleigh distribution, $h_k \sim \mathcal{CN}(0, 2\delta_k^2)$. For simplicity, we denote a vector consisting of variances of channel coefficients δ_k^2 by Δ. Recall that $P_k = |h_k|^2 Q_k$ and hence for each channel realization we may need to re-index the users during the constellation design process.

For the proposed NOMA schemes we consider both the design in Algorithm 1, which is optimal in the three user case and will be called the “Proposed scheme”, and the simplified designs in Algorithm 2, which we will call the “Proposed simplified scheme”. In our comparisons, two cases are considered for the TDMA schemes, too. In the first case, each user uses all of its available power. This is denoted by “full power” in the figures. In the second case, the power for each user is constrained to be the same as that used in the proposed scheme. This is denoted by “TDMA with power allocation”. When K is even, each TDMA user employs a square constellation of 2^K points so that the data rates of the proposed NOMA scheme and TDMA are the same. When K is odd, we consider both rectangular and cross QAM constellations

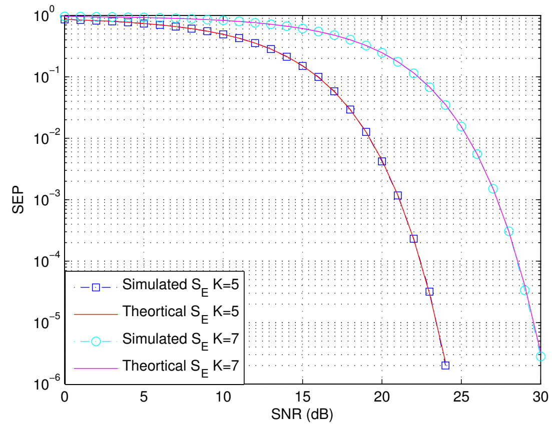

(a) K is odd and constellation from Eisenstein integer ring.

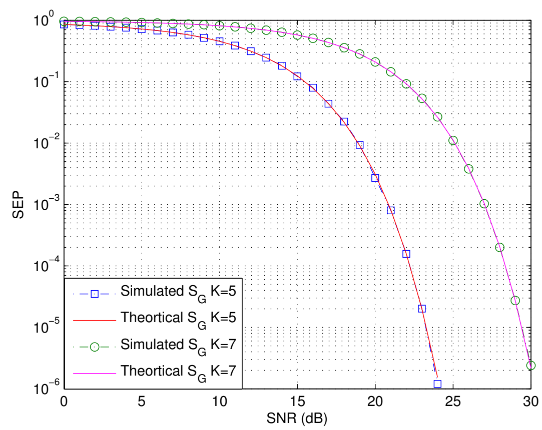

(b) K is odd and constellation from Gaussian integer ring.

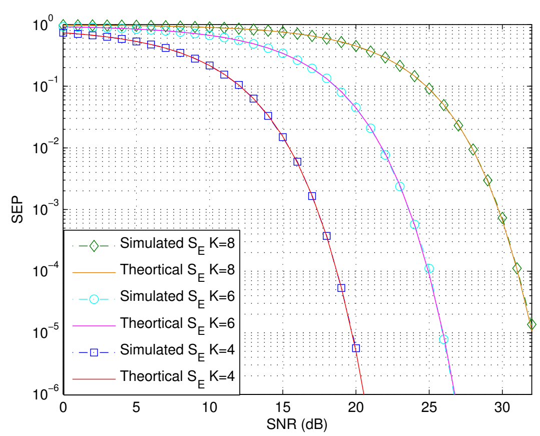

(c) K is even.

Figure 2.9: Simulated and theoretical SEP performance comparison.

of size 2^K. Figs. 2.10, 2.11 and 2.12 show the SEP performance with three users, five users and six users, respectively, where in Fig. 2.10, RQAM is applied to TDMA scheme, but in Fig. 2.11 both RQAM and cross-QAM are considered.

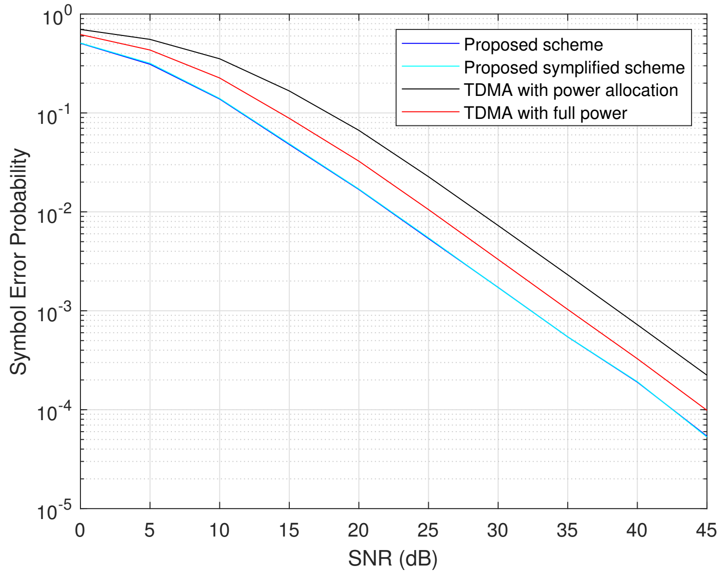

Figure 2.10: Performance comparison between the proposed-NOMA and TDMA schemes with $K = 3$ and $\Delta = (1, 1, 1)$

It can be seen that our proposed NOMA scheme outperforms the QAM based TDMA schemes. In particular, our proposed scheme can provide up to 3 dB gain for the three user-MAC and 8 dB gain for the six user-MAC with respect to the TDMA with full power scheme at SEP=10^{-3}. Moreover, we observe that the SEP performance of our simplified lattice-based designs in Algorithm 2 is nearly indistinguishable from the performance of the original lattice-based design in Algorithm 1 at the scale of the figures.

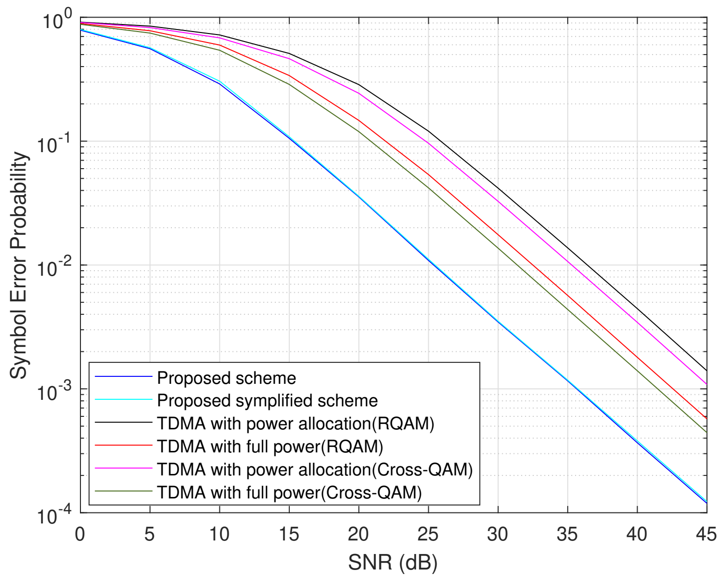

Figure 2.11: Performance comparison between the proposed-NOMA and TDMA schemes with $K = 5$ users and $\Delta = (1, 1, 1, 1, 1)$

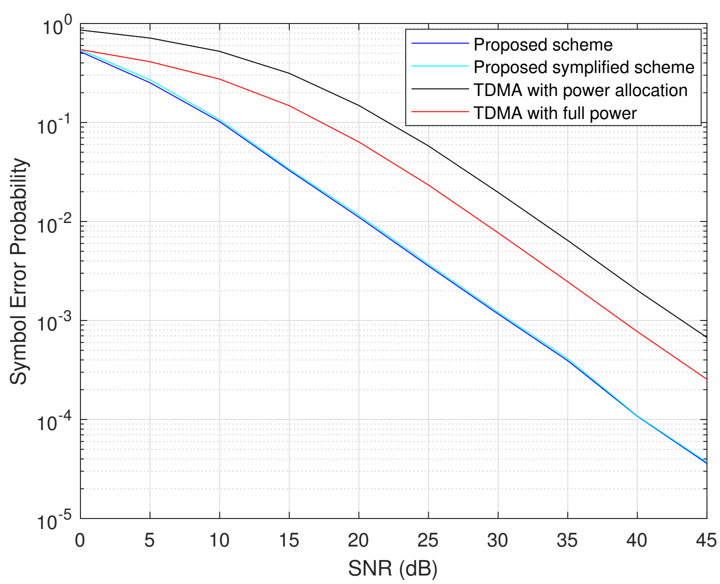

Figure 2.12: Performance comparison between the proposed-NOMA and TDMA schemes with $K = 6$ users and $\Delta = (1, 1, 1, 1, 1, 1)$.

2.5 Extension for K-user-case with Any 2^{M_k} Size Constellation

In the previous sections, our goal has been to design constellations for the users of a multiple access channel in such a way that the minimum Euclidean distance of the received sum constellation is maximized. The design techniques (for our NOMA scheme) take into account the different power constraints on the user's transmission, and their different channels to the receiver. However, all these design techniques are restricted to the case in which each user transmits a binary signal.

In this section, we will use insights from the binary case to develop a technique for designing effective constellation for the K-user case in which the k-th user transmits M_k bits per channel use. The key principle is to observe that our previous approaches were based on designing the user constellations. By construction, the resulting sum constellation is an additive uniquely decomposable constellation (AUDC). An alternative approach would have been to design an AUDC and then decompose it into binary constellations for each user. We will adapt the latter strategy to the case of higher-order constellations for each user. In particular, for a system with K users, the k-th of which seeks to transmit M_k bits per channel use subject to a (scaled) power constraint P_k (cf., (2.2.3)), we first design a normalized AUDC sum constellation of size 2^M, where $M = \sum_{k=1}^{K} M_k$, using the insights from the previous section. Then, we decompose the sum constellation into the K user constellations of sizes $\{2^{M_k}\}_{k=1}^{K}$ based on the users' power constraints. The decomposition is akin to a set partitioning process, but since the target partitions are of size $\{2^{M_k}\}$, and the decomposition metric is controlled by the users' power constraints (which may be different), it is a somewhat different partitioning process from that used in coded-modulation [83]. For simplicity, we will restrict attention to the sum constellations that are carved from the Eisenstein and Gaussian integers, as outlined in Algorithm 2.

2.5.1 Constellation Decomposition

As outlined above, we consider a system with K users, the k-th of which seeks to transmit M_k bits per channel use, subject to a (scaled) power constraint P_k. The starting point for the construction is a sum constellation of 2^M points, $M = \sum_{k=1}^{K} M_k$, designed for M (virtual) users with binary signalling, normalized channels (cf., Problem 2.2) and a minimum distance $d_{\min} = 1$. We will denote that (normalized) sum constellation by $\bar{\mathcal{S}}$ and its constituent binary constellations for the M virtual users by $\{\bar{\mathcal{S}}_j\}_{j=1}^{M}$. Based on the insights that led to Algorithm 2, if M is even, $\bar{\mathcal{S}}$ will be carved from the Eisenstein integers, and if M is odd, we will perform two constructions, one based on $\bar{\mathcal{S}} = \bar{\mathcal{S}}_E$ carved from Eisenstein integers, and one based on $\bar{\mathcal{S}} = \bar{\mathcal{S}}_G$ carved from Gaussian integers, and then we will select the design that leads to the larger minimum distance. Explicit expressions for each $\bar{\mathcal{S}}_j$ are also available in Algorithm 2.

Given the constituent scaled binary constellations $\{\bar{\mathcal{S}}_j\}_{j=1}^{M}$, the number of ways that they can be partitioned, in a non-overlapping manner, into K sets of sizes $\{M_k\}_{k=1}^{M}$ is $T = \underbrace{\binom{M}{M_1} \times \binom{M-M_1}{M_2} \cdots \times \binom{M-\sum_{k=1}^{K-2} M_k}{M_{K-1}}}_{K-1} = \frac{M!}{M_1! \cdots M_K!}$. To index these partitions, let $\{\mathcal{A}_k\}_{k=1}^{K}$ denote a (non-overlapping) partition of the index set $\{1, \ldots, M\}$ in which $|\mathcal{A}_k| = M_k$. There are T such partitions, and we will index those partitions by t, i.e., the t-th partition is $\{\mathcal{A}_{k,t}\}_{k=1}^{K}$. Our construction process involves examining each partition of the normalized sum constellation and determining which are enables the largest minimum distance subject to the users' power constraints being satisfied.

That is, for each t, we determine $d_t = \min_{1\le k\le K}\{\sqrt{\frac{P_k}{\sum_{j\in\mathcal{A}_{k,t}} E_{s_j}}}\}$, where E_{s_j} is the (average) energy of the binary constellation $\bar{\mathcal{S}}_j$ of the normalized sum constellation $\bar{\mathcal{S}}$. This average energy can be explicitly computed from the expressions for $\bar{\mathcal{S}}_j$ in Algorithm 2. The final design problem is to find t^* such that $t^* = \arg\max_{1\le t\le T} d_t$. Once that has been determined, the constellation to be employed by user k is $\mathcal{Q}_k = \biguplus_{j\in\mathcal{A}_{k,t^*}} d_{t^*}\bar{\mathcal{S}}_j$ and the minimum distance of the sum constellation at the receiver is d_{t^*}. This result is summarized in the following algorithm.

Algorithm 3: Construction processing for 2^M-point sum constellation $\mathcal{Q}$ and 2^{M_k}-point user constellations $\mathcal{Q}_k$

1. If M is even, $\bar{\mathcal{S}}$ is carved from the Eisenstein integers with $d_{min} = 1$, see (2.4.12). Let $t^* = \arg\max_{1\le t\le T} d_t$. Then $\mathcal{Q}_k = \biguplus_{j\in\mathcal{A}_{k,t^*}} d_{t^*}\bar{\mathcal{S}}_j$ and $\mathcal{Q} = d_{t^*}\bar{\mathcal{S}}$.
2. If M is odd, let t_G^* and t_E^* represent $\arg\max_{1\le t\le T} d_t$ when $\bar{\mathcal{S}}$ is the sum constellation with $d_{min} = 1$ chosen from the Gaussian integers and the Eisenstein integers, respectively.
   - If $d_{t_G^*} \ge d_{t_E^*}$, $\bar{\mathcal{S}}$ is carved from the Gaussian integers with $d_{min} = 1$, see (2.4.13). Then $\mathcal{Q}_k = \biguplus_{j\in\mathcal{A}_{k,t_G^*}} d_{t_G^*}\bar{\mathcal{S}}_j^G$ and $\mathcal{Q} = d_{t_G^*}\bar{\mathcal{S}}^G$.
   - If $d_{t_G^*} < d_{t_E^*}$, $\bar{\mathcal{S}}$ is carved from the Eisenstein integers with $d_{min} = 1$, see (2.4.14). Then $\mathcal{Q}_k = \biguplus_{j\in\mathcal{A}_{k,t_E^*}} d_{t_E^*}\bar{\mathcal{S}}_j^E$ and $\mathcal{Q} = d_{t_E^*}\bar{\mathcal{S}}^E$.

Specifically, for a classical two-user MAC, the sum constellation and its corresponding user constellations can be determined by Algorithm 4. In Algorithm 4, the superscript E and G represents the constellation carved from Eisenstein integer ring and Gaussian integer ring, respectively.

Algorithm 4: Constellation Splitting for Two-user MAC

Input: M, M_1, $\bar{\mathcal{S}}_1, \ldots, \bar{\mathcal{S}}_M$, and $\bar{\mathcal{S}}$
Output: $\mathcal{Q}_1, \mathcal{Q}_2$ and $\mathcal{Q}$

$\theta_2 \leftarrow \frac{\pi}{3}$, $d_{\min} \leftarrow 0$, $d_E \leftarrow 0$, $d_G \leftarrow 0$.
for $i = 0$ *to* $2^M - 1$ **do**
  • Convert the integer i to an M-length binary sequence, i.e., $\mathbf{b}_i = (b_{i,1}, \ldots, b_{i,M})$ with $b_{i,j} \in \{0, 1\}$.
  if $\sum_{j=1}^{M} b_{i,j} = M_1$ **then**
    $E_1^E \leftarrow \sum_{j=1}^{M} b_{i,j} E_{s_j}^E$, $d_E \leftarrow \min\{\sqrt{\frac{P_1}{E_1^E}}, \sqrt{\frac{P_2}{E^E - E_1^E}}\}$.
    if $M \mod 2 = 1$ **then**
      $E_1^G \leftarrow \sum_{j=1}^{M} b_{i,j} E_{s_j}^G$, $d_G \leftarrow \min\{\sqrt{\frac{P_1}{E_1^G}}, \sqrt{\frac{P_2}{E^G - E_1^G}}\}$
    $d_{\min} \leftarrow \max\{d_{\min}, d_E, d_G\}$.
    if $d_{\min} = d_E$ **then**
      $\mathcal{Q}_1 \leftarrow \biguplus_{j=1}^{M} b_{i,j} d_{\min} \bar{\mathcal{S}}_j^E, \mathcal{Q}_2 \leftarrow \biguplus_{j=1}^{M} (1 - b_{i,j}) d_{\min} \bar{\mathcal{S}}_j^E, \mathcal{Q} \leftarrow d_{\min} \bar{\mathcal{S}}^E$
    if $d_{\min} = d_G$ **then**
      $\theta_2 \leftarrow \frac{\pi}{4}$.
      $\mathcal{Q}_1 \leftarrow \biguplus_{j=1}^{M} b_{i,j} d_{\min} \bar{\mathcal{S}}_j^G, \mathcal{Q}_2 \leftarrow \biguplus_{j=1}^{M} (1 - b_{i,j}) d_{\min} \bar{\mathcal{S}}_j^G, \mathcal{Q} \leftarrow d_{\min} \bar{\mathcal{S}}^G$.

2.5.2 Numerical Results

In this subsection, we compare the performance of our proposed NOMA scheme with the Farey-NOMA scheme proposed in [27] and TDMA.

It can be seen that our proposed NOMA scheme has a significant SNR gain over both Farey-NOMA and TDMA schemes. Specifically, when SER is at the level of 10^{-3}, our scheme has about 8 dB SNR gain over the TDMA scheme, and about 3 dB SNR gain over the Farey-NOMA scheme.

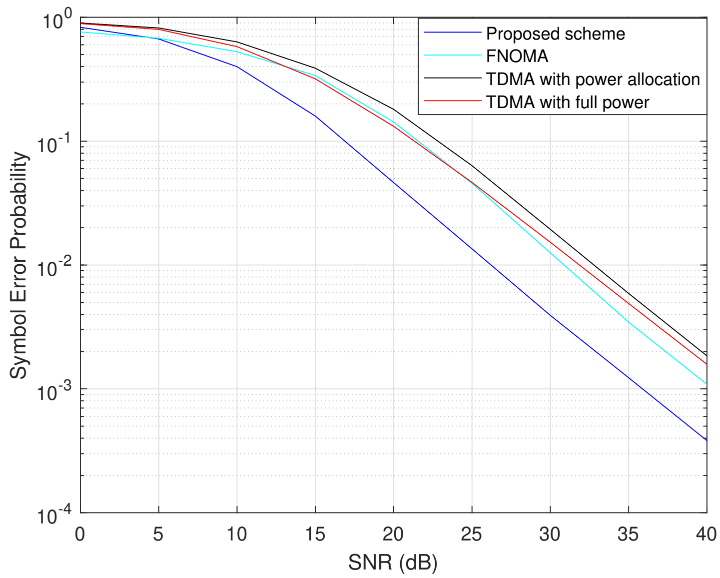

Figure 2.13: Performance comparison between the proposed-NOMA and TDMA schemes with $K = 2$ users, with $M_1 = 2, M_2 = 4$, and channel parameters $\Delta = (1, 1)$.

2.6 Conclusions

In this paper, we have considered an uplink system with K single-antenna users and one base station equipped with a single antenna, in which each user utilizes a binary constellation to carry data. By maximizing the minimum Euclidean distance of the received sum constellation, a closed-form optimal solution to the user constellations and the corresponding optimal sum constellation were attained for $K \leq 3$. The insight from those designs was then combined with lattice coding principles to extend the technique, so that it yields efficient designs for $K \geq 4$. These constellation designs have the advantage that the maximum likelihood receiver reduces to a simple quantization-based detector. A further simplification of the technique yielded designs that led to the sum constellation being carved from a square or equilateral triangular (hexagonal) lattice. In those cases the storage requirement of the receiver is significantly reduced, and closed form expressions for the symbol error probability were obtained. Furthermore, we were able to show, analytically, that the proposed NOMA design yields a larger minimum distance than the corresponding TDMA-based design. Computer simulations verified that this advantage results in a significant decrease with symbol error probability. We also showed how insights from our design for the case of binary signalling could be expanded to the case of high-order constellations by using (generalized) set partitioning techniques. The resulting "constellation domain" NOMA systems provided significantly lower symbol error probability than the TDMA counterparts, and also provided better performance than a related scheme based on constellations designed using Farey sequences [26].

2.A Appendix: Lemma for fixed $|\bar{s}_1|$

Lemma 2.2 *Given $|\bar{s}_1|$, $\min\mathcal{D} = |\bar{s}_1|$ if and only if $\sqrt{|s_2|^2+|s_3|^2}$ is no less than $2|\bar{s}_1|$, and $|s_2|$ and $|s_3|$ are no less than $2|\bar{s}_1|\cos\theta_2$ and $2|\bar{s}_1|\sin\theta_2$, where $\frac{\pi}{4} \leq \theta_2 \leq \frac{\pi}{3}$, respectively.*

Proof **Sufficiency:** Since $\min\mathcal{D} = |\bar{s}_1|$, then $|s_2 - s_1| \geq |\bar{s}_1|$, resulting in $|s_2| \geq 2|s_1|\cos\theta_2$. Let $\mathcal{A}^* = \{\theta_2, \alpha, |s_3| : |\theta_2 - \alpha| \leq \frac{\pi}{2}, |s_3| \geq |s_2|\}$.

- If $\frac{\pi}{3} \leq \theta_2 \leq \frac{\pi}{2}$, then $|s_2| \geq |\bar{s}_1| \geq 2|\bar{s}_1|\cos\theta_2$. Let $|s_2| = |\bar{s}_1|$. We'd like to find the minimum $|s_3|$ to achieve $\min\mathcal{D} = |\bar{s}_1|$.
  - If $0 \leq \alpha \leq \frac{\pi}{2}$, then we know that $|\theta_2-\alpha| \leq \theta_2$, resulting in $|s_3|\cos(\theta_2-\alpha) \geq |s_2|\cos\theta_2$, $|s_1+s_3-s_2| \geq |s_1+s_2-s_3|$ and $|s_3-s_2| \leq |s_3+s_2|$. Also, if $|s_2-s_1| \geq |\bar{s}_1|$ and $|s_3-s_1| \geq |\bar{s}_1|$, it is guaranteed that $|s_2+s_3-s_1| \geq |\bar{s}_1|$. Thus, if $\min\mathcal{D} = |\bar{s}_1|$, we have $|\bar{s}_1| \leq \min\{|s_3-s_1|, |s_3-s_2|, |s_1+s_2-s_3|\}$.

* If $|s_3 - s_2| \le |s_1 + s_2 - s_3|$, we have $|s_3| \le \frac{1+2\cos\theta_2}{2\cos(\theta_2-\alpha)}|\bar{s}_1|$ with $|s_2| = |\bar{s}_1|$. Since $\min \mathcal{D} = |\bar{s}_1| \le \min\{|s_3 - s_1|, |s_3 - s_2|\}$, we know that $|s_3| \ge \max\{2\cos(\theta_2 - \alpha)|\bar{s}_1|, 2\cos\alpha|\bar{s}_1|\}$. Then, the optimal solution for

$$\begin{aligned} &\min_{\frac{\pi}{3}\le\theta_2\le\frac{\pi}{2}, 0\le\alpha\le\frac{\pi}{2}, \mathcal{A}^*} |s_3| \\ &s.t., \frac{1+2\cos\theta_2}{2\cos(\theta_2-\alpha)} \ge \max\{2\cos(\theta_2-\alpha), 2\cos\alpha\} \end{aligned} \tag{2.A.1}$$

is that $|s_3| = 2\cos\frac{\pi}{12}|\bar{s}_1|$ with $\theta_2 = \frac{\pi}{2}$ and $\alpha = \frac{\pi}{12}$, where $|\bar{s}_1| = |s_3 - s_1| < \min\{|s_2 - s_1|, |s_3 - s_2|\}$.

* If $|s_1 + s_2 - s_3| < |s_3 - s_2|$, we have $|s_3| > \frac{1+2\cos\theta_2}{2\cos(\theta_2-\alpha)}|\bar{s}_1|$ with $|s_2| = |\bar{s}_1|$. Since $\min \mathcal{D} = |\bar{s}_1| \le \min\{|s_3 - s_1|, |s_1 + s_2 - s_3|\}$, then we know that $|s_3| \ge 2\cos(\theta_2 - \alpha)|\bar{s}_1|$ and $|s_3|^2 - 2(\cos(\theta_2 - \alpha) + \cos\alpha)|\bar{s}_1||s_3| + (1 + 2\cos\theta_2)|\bar{s}_1|^2 \ge 0$. Then, the optimal solution for

$$\min_{\frac{\pi}{3}\le\theta_2\le\frac{\pi}{2}, 0\le\alpha\le\frac{\pi}{2}, \mathcal{A}^*} |s_3| \tag{2.A.2}$$

is that $|s_3| = \sqrt{3}|\bar{s}_1|$ with $\theta_2 = \frac{\pi}{3}$ and $\alpha = \frac{\pi}{2}$, where $|\bar{s}_1| = |s_3 - s_1| = |s_2 - s_1| < |s_1 + s_2 - s_3|$.

– If $\frac{\pi}{2} \le \alpha \le \pi$, then we know that $|s_3 + s_2| \le |s_3 - s_2|$, $|s_1 + s_2 - s_3| \ge |s_3 - s_1|$ and $|s_1 + s_3 - s_2| \ge |s_2 - s_1|$. Thus, if $\min \mathcal{D} = |\bar{s}_1|$, we have $|\bar{s}_1| \le \min\{|s_3 - s_1|, |s_3 + s_2|, |s_2 + s_3 - s_1|\}$.

* If $|s_2 + s_3 - s_1| \le |s_3 + s_2|$, we have $|s_3| > \frac{1+2\cos\theta_2}{2\cos(\theta_2-\alpha)}|\bar{s}_1|$ with $|s_2| = |\bar{s}_1|$. Since $\min \mathcal{D} = |\bar{s}_1| \le \min\{|s_3 - s_1|, |s_2 + s_3 - s_1|\}$, then we know that $|s_3| \ge 2\cos(\theta_2 - \alpha)|\bar{s}_1|$ and $|s_3|^2 + 2(\cos\alpha - \cos(\theta_2 - \alpha))|\bar{s}_1||s_3| + (1 -$

$2\cos\theta_2)|\bar{s}_1|^2 \geq 0$. Then, the optimal solution for

$$\min_{\frac{\pi}{3}\leq\theta_2\leq\frac{\pi}{2},\frac{\pi}{2}\leq\alpha\leq\pi,\mathcal{A}^*} |s_3| \tag{2.A.3}$$

is that $|s_3| = \sqrt{3}|\bar{s}_1|$ with $\theta_2 = \frac{\pi}{3}$ and $\alpha = \frac{\pi}{2}$, where $|\bar{s}_1| = |s_3 - s_1| = |s_2 - s_1| = |s_2 + s_3 - s_1| < |s_3 + s_2|$.

* If $|s_3+s_2| \leq |s_2+s_3-s_1|$, we have $|s_3| \leq \frac{1-2\cos\theta_2}{2\cos(\theta_2-\alpha)}|\bar{s}_1|$ with $|s_2| = |\bar{s}_1|$. Since $\min\mathcal{D} = |\bar{s}_1| \leq \min\{|s_3 - s_1|, |s_3 + s_2|\}$, we know that $|s_3| \geq \min\{2\cos(\theta_2 - \alpha)|\bar{s}_1|, -2\cos\alpha|\bar{s}_1|\}$. Then, the optimal solution for

$$\begin{aligned} &\min_{\frac{\pi}{3}\leq\theta_2\leq\frac{\pi}{2},\frac{\pi}{2}\leq\alpha\leq\pi,\mathcal{A}^*} |s_3| \\ &s.t., \frac{1-2\cos\theta_2}{2\cos(\theta_2-\alpha)} \geq \max\{2\cos(\theta_2-\alpha), -2\cos\alpha\} \end{aligned} \tag{2.A.4}$$

is that $|s_3| = \sqrt{3}|\bar{s}_1|$ with $\theta_2 = \frac{\pi}{3}$ and $\alpha = \frac{5\pi}{6}$, where $|\bar{s}_1| = |s_2 - s_1| = |s_3 + s_2| = |s_2 + s_3 - s_1| < |s_3 - s_1|$.

- If $0 \leq \theta_2 \leq \frac{\pi}{3}$, then $|s_2| \geq 2|\bar{s}_1|\cos\theta_2 \geq |\bar{s}_1|$. Let $|s_2| = 2|\bar{s}_1|\cos\theta_2$. We'd like to find the minimum $|s_3|$ and $|s_2|$ to achieve $\min\mathcal{D} = |\bar{s}_1|$ (since $|s_2| = 2|\bar{s}_1|\cos\theta_2$, the minimum $|s_2|$ corresponds to the largest θ_2).

  – If $0 \leq \alpha \leq \frac{\pi}{2}$, then we know that $|s_3-s_2| \leq |s_3+s_2|$. Also, if $|s_2-s_1| \geq |\bar{s}_1|$ and $|s_3 - s_1| \geq |\bar{s}_1|$, we always have $|s_2 + s_3 - s_1| \geq |\bar{s}_1|$. Moreover, due to the fact that $\cos(\theta_2 - \alpha) \geq \cos\theta_2\cos\alpha$, thus if $|s_1 + s_3 - s_2| \leq |s_3 - s_2|$, we always have $|s_1 + s_3 - s_2| \geq |s_3 - s_1|$ with $|s_2| = 2|\bar{s}_1|\cos\theta_2$ and $|s_1 + s_3 - s_2| \leq |s_1 + s_2 - s_3|$. Thus, if $\min\mathcal{D} = |\bar{s}_1|$, we have $|\bar{s}_1| \leq \min\{|s_3 - s_1|, |s_3 - s_2|, |s_1 + s_2 - s_3|\}$.

* If $|s_3 - s_2| \leq |s_1 + s_2 - s_3|$, we have $|s_3| \leq \frac{1+4\cos^2\theta_2}{2\cos(\theta_2-\alpha)}|\bar{s}_1|$ with $|s_2| = 2\cos\theta_2|\bar{s}_1|$. Since $\min\mathcal{D} = |\bar{s}_1| \leq \min\{|s_3 - s_1|, |s_3 - s_2|\}$, we know that $|s_3| \geq \max\{2\cos(\theta_2 - \alpha)|\bar{s}_1|, 2\cos\alpha|\bar{s}_1|\}$. Then, the optimal solution for

$$\min_{0\leq\theta_2\leq\frac{\pi}{3}, 0\leq\alpha\leq\frac{\pi}{2}, \mathcal{A}^*} \{|s_3|, \cos\theta_2\} \tag{2.A.5}$$

is that $|s_3| = 2\sin\theta_2|\bar{s}_1|$ with $\frac{\pi}{4} \leq \theta_2 \leq \phi^*$ and $\alpha = \frac{\pi}{2}$, where $|\bar{s}_1| = |s_3 - s_1| = |s_2 - s_1| < |s_3 - s_2|$, and ϕ^* is the root of the equation $\phi + \arccos\frac{\sqrt{4\cos^2\phi+1}}{2} - \frac{\pi}{2} = 0$. (We observe that $\phi^* \approx \frac{\pi}{3.4457}$.)

* If $|s_1 + s_2 - s_3| \leq |s_3 - s_2|$, we have $|s_3| \geq \frac{1+4\cos^2\theta_2}{2\cos(\theta_2-\alpha)}|\bar{s}_1|$ with $|s_2| = 2\cos\theta_2|\bar{s}_1|$. Since $\min\mathcal{D} = |\bar{s}_1| \leq \min\{|s_3 - s_1|, |s_1 + s_2 - s_3|\}$, then we know that $|s_3| \geq 2\cos(\theta_2 - \alpha)|\bar{s}_1|$ and $|s_3| \leq \frac{2\cos\theta_2}{\cos\alpha}|\bar{s}_1|$. Then, the optimal solution for

$$\begin{aligned} &\min_{0\leq\theta_2\leq\frac{\pi}{3}, 0\leq\alpha\leq\frac{\pi}{2}, \mathcal{A}^*} \{|s_3|, \cos\theta_2\} \\ &s.t., \frac{2\cos\theta_2}{\cos\alpha} \geq \max\{2\cos(\theta_2 - \alpha), \frac{1+4\cos^2\theta_2}{2\cos(\theta_2-\alpha)}\} \end{aligned} \tag{2.A.6}$$

is that $|s_3| = 2\sin\theta_2|\bar{s}_1|$ with $\phi^* \leq \theta_2 \leq \frac{\pi}{3}$ and $\alpha = \frac{\pi}{2}$, where $|\bar{s}_1| = |s_3 - s_1| = |s_2 - s_1| < |s_1 + s_2 - s_3|$.

– If $\frac{\pi}{2} \leq \alpha \leq \pi$, then we know that $|s_3 + s_2| \leq |s_3 - s_2|$, $|s_1 + s_2 - s_3| \geq |s_3 - s_1|$ and $|s_1 + s_3 - s_2| \geq |s_2 - s_1|$. Since $\cos\theta_2 \geq \frac{1}{2}$, we have $|s_2 + s_3 - s_1| \leq |s_3 + s_2|$ with $|s_2| = 2\cos\theta_2|\bar{s}_1|$. Moreover, since $\min\mathcal{D} = |\bar{s}_1| \leq \min\{|s_3 - s_1|, |s_2 + s_3 - s_1|\}$, then we know that $|s_3| \geq \max\{2\cos(\theta_2 - \alpha)|\bar{s}_1|, -2\cos(\theta_2 +$

$\alpha)|\bar{s}_1|\}$. Then, the optimal solution for

$$\min_{0\le\theta_2\le\frac{\pi}{3},\frac{\pi}{2}\le\alpha\le\pi,\mathcal{A}^*} |s_3| \tag{2.A.7}$$

is that $|s_3| = 2\sin\theta_2|\bar{s}_1|$ with $\frac{\pi}{4} \le \theta_2 \le \frac{\pi}{3}$ and $\alpha = \frac{\pi}{2}$, where $|\bar{s}_1| = |s_3 - s_1| = |s_2 - s_1| = |s_2 + s_3 - s_1|$.

Based on the above, we know that if $\min \mathcal{D} = |\bar{s}_1|$, the condition $|s_2| \ge 2\cos\theta_2|\bar{s}_1|$ and $|s_3| \ge 2\sin\theta_2|\bar{s}_1|$, i.e., $\sqrt{|s_2|^2 + |s_3|^2} \ge 2|\bar{s}_1|$ should be satisfied, where $\frac{\pi}{4} \le \theta_2 \le \frac{\pi}{3}$.

Necessity: If $|s_2| \ge 2\cos\theta_2|\bar{s}_1|$ and $|s_3| \ge 2\sin\theta_2|\bar{s}_1|$, i.e., $\sqrt{|s_2|^2 + |s_3|^2} \ge 2|\bar{s}_1|$, we know that $\{|s_2 - s_1|, |s_3 - s_1|, |s_3 + s_2|, |s_3 - s_2|, |s_1 + s_2 - s_3|, |s_1 + s_3 - s_2|, |s_2 + s_3 - s_1|\} \ge |\bar{s}_1|$, then we have $\min \mathcal{D} = |\bar{s}_1|$.

Thus, the proof is completed. □

2.B Appendix: Lemma for fixed $|\bar{s}_k|, 1 \le k \le 3$

As in Sect. 2.4.3, we will define $\Theta = \{(\theta_2, \alpha)$.

Lemma 2.3 *For fixed $|\bar{s}_1|$, $|\bar{s}_2|$, $|\bar{s}_3|$ with $|\bar{s}_1| \le |\bar{s}_2| \le |\bar{s}_3|$, the optimal θ_2 and α are determined as follows:*

- *If $\sqrt{|\bar{s}_2|^2 + |\bar{s}_3|^2} < 2|\bar{s}_1|$, we have*

$$\max_{\Theta} \min \mathcal{D} = \sqrt{\frac{2}{3}\left(|\bar{s}_1|^2 - \sqrt{|\bar{s}_1|^4 + 9|\bar{s}_2|^2|\bar{s}_3|^2}\cos\gamma\right)}, \tag{2.B.1}$$

with $\theta_2 = \arccos\frac{|\bar{s}_1|^2+3|\bar{s}_2|^2+2\cos\gamma\sqrt{|\bar{s}_1|^4+9|\bar{s}_2|^2|\bar{s}_3|^2}}{6|\bar{s}_1||\bar{s}_2|}$ and $\alpha = \arccos\frac{2|\bar{s}_1|\cos\theta_2-|\bar{s}_2|}{2|\bar{s}_3|}$, where $\gamma = \frac{1}{3}\arccos\frac{2|\bar{s}_1|^6+27|\bar{s}_2|^2|\bar{s}_3|^4+27|\bar{s}_2|^4|\bar{s}_3|^2-81|\bar{s}_1|^2|\bar{s}_2|^2|\bar{s}_3|^2}{2(|\bar{s}_1|^4+9|\bar{s}_2|^2|\bar{s}_3|^2)^{3/2}} + \frac{4\pi}{3}$.

- *If* $\sqrt{|\bar{s}_2|^2 + |\bar{s}_3|^2} \geq 2|\bar{s}_1|$, *we have*

$$\max_{\Theta} \min \mathcal{D} = |\bar{s}_1|, \tag{2.B.2}$$

with

$$\theta_2 = \begin{cases} \arctan \frac{|\bar{s}_3|}{|\bar{s}_2|}, & \textit{if } \frac{\pi}{4} \leq \arctan \frac{|\bar{s}_3|}{|\bar{s}_2|} \leq \frac{\pi}{3}, \\ \frac{\pi}{3}, & \textit{if } \arctan \frac{|\bar{s}_3|}{|\bar{s}_2|} > \frac{\pi}{3}, \end{cases} \tag{2.B.3}$$

and $\alpha = \pi/2$.

Proof We consider the following cases:

- For $\sqrt{|\bar{s}_2|^2 + |\bar{s}_3|^2} < 2|\bar{s}_1|$, according to Lemma 4, we know that $\mathcal{D} < |\bar{s}_1|$. Also, if $|s_1 + s_3 - s_2| \leq \min\{|s_3 - s_2|, |s_1 + s_2 - s_3|\}$, it is guaranteed that $|s_1 + s_3 - s_2| \geq |\bar{s}_1|$. Thus, the minimum Euclidean distance set can be reduced to $\mathcal{D} = \{|s_2 - s_1|, |s_3 - s_1|, |s_3 + s_2|, |s_3 - s_2|, |s_1 + s_2 - s_3|, |s_2 + s_3 - s_1|\}$.
  - if $\min \mathcal{D} = |s_1 + s_2 - s_3|$, which implies that $0 \leq \alpha \leq \frac{\pi}{2}$, we have that $|s_3 + s_2| \geq |s_3 - s_2|$, $|s_2 + s_3 - s_1| \geq \min\{|s_2 - s_1|, |s_3 - s_1|, |s_3 - s_2|\}$, and that $|s_2 - s_1| \geq \min\{|s_3 - s_1|, |s_3 - s_2|\}$. Then, by considering the sub-cases with respect to the order of $\{|s_3 - s_1|, |s_3 - s_2|\}$, we have $\max_{\Theta} |s_1 + s_2 - s_3| = |s_3 - s_1| = \sqrt{|\bar{s}_1|^2 + |\bar{s}_3|^2 - |\bar{s}_1|\sqrt{4|\bar{s}_3|^2 - |\bar{s}_2|^2}}$ with $\theta_2 = \frac{\pi}{2}$ and $\alpha = \arccos \frac{|\bar{s}_2|}{2|\bar{s}_3|}$.
  - if $\min \mathcal{D} = |s_3 - s_2|$, which implies that $0 \leq \alpha \leq \frac{\pi}{2}$, we have that $|s_3 + s_2| \geq |s_3 - s_2|$, and $|s_2 + s_3 - s_1| \geq |s_1 + s_2 - s_3|$. Then, by considering the sub-cases with respect to the order of $\{|s_2 - s_1|, |s_3 - s_1|, |s_3 - s_2|\}$, we have $\max_{\Theta} |s_3 - s_2| = |s_1 + s_2 - s_3| = \sqrt{|\bar{s}_2|^2 + |\bar{s}_3|^2 - |\bar{s}_2|\sqrt{4|\bar{s}_3|^2 - |\bar{s}_1|^2}}$ with $\theta_2 = \frac{\pi}{2}$ and $\alpha = \frac{\pi}{2} - \arccos \frac{|\bar{s}_1|}{2|\bar{s}_3|}$.

– if $\min \mathcal{D} = |s_3+s_2|$, which implies that $\frac{\pi}{2} \le \alpha \le \pi$, we have that $|s_3-s_2| \ge |s_3+s_2|$ and $|s_1+s_2-s_3| \ge |s_3-s_1| \ge |s_2-s_1|$. Then, by considering the sub-cases with respect to the order of $\{|s_2-s_1|, |s_2+s_3-s_1|\}$, we have $\max\limits_{\Theta} |s_3+s_2| = |s_2-s_1| = |s_1+s_2-s_3| = \sqrt{\frac{2}{3}\left(|\bar{s}_2|^2 - \sqrt{|\bar{s}_2|^4+9|\bar{s}_1|^2|\bar{s}_3|^2}\cos\omega\right)}$ with $\theta_2 = \arccos\frac{3|\bar{s}_1|^2+|\bar{s}_2|^2+2\cos\omega\sqrt{|\bar{s}_2|^4+9|\bar{s}_1|^2|\bar{s}_3|^2}}{6|\bar{s}_1||\bar{s}_2|}$ and $\alpha = \theta_2 + \arccos\frac{|\bar{s}_1|-2|\bar{s}_2|\cos\theta_2}{2|\bar{s}_3|}$, where $\omega = \frac{1}{3}\arccos\frac{2|\bar{s}_2|^6+27|\bar{s}_1|^2|\bar{s}_3|^4+27|\bar{s}_1|^4|\bar{s}_3|^2-81|\bar{s}_1|^2|\bar{s}_2|^2|\bar{s}_3|^2}{2(|\bar{s}_2|^4+9|\bar{s}_1|^2|\bar{s}_3|^2)^{3/2}} + \frac{4\pi}{3}$.

– if $\min \mathcal{D} = |s_2-s_1|$, which implies that $|s_3-s_1| \le |s_1+s_2-s_3|$, then by considering the sub-cases with respect to the order of $\{|s_3-s_1|, |s_3-s_2|, |s_3+s_2|, |s_2+s_3-s_1|\}$, we have

$$\max_{\Theta} |s_2-s_1| = |s_3-s_1| = |s_2+s_3-s_1| = \sqrt{\frac{2}{3}\left(|\bar{s}_1|^2 - \sqrt{|\bar{s}_1|^4+9|\bar{s}_2|^2|\bar{s}_3|^2}\cos\gamma\right)}$$

with $\theta_2 = \arccos\frac{|\bar{s}_1|^2+3|\bar{s}_2|^2+2\cos\omega\sqrt{|\bar{s}_1|^4+9|\bar{s}_2|^2|\bar{s}_3|^2}}{6|\bar{s}_1||\bar{s}_2|}$ and $\alpha = \arccos\frac{2|\bar{s}_1|\cos\theta_2-|\bar{s}_2|}{2|\bar{s}_3|}$, where $\gamma = \frac{1}{3}\arccos\frac{2|\bar{s}_1|^6+27|\bar{s}_2|^2|\bar{s}_3|^4+27|\bar{s}_2|^4|\bar{s}_3|^2-81|\bar{s}_1|^2|\bar{s}_2|^2|\bar{s}_3|^2}{2(|\bar{s}_1|^4+9|\bar{s}_2|^2|\bar{s}_3|^2)^{3/2}} + \frac{4\pi}{3}$.

– if $\min \mathcal{D} = |s_3-s_1|$, which implies that $|s_2-s_1| \le \min\{|s_3-s_2|, |s_3+s_2|\}$, then by considering the sub-cases with respect to the order of $\{|s_2-s_1|, |s_2+s_3-s_1|, |s_1+s_2-s_3|\}$, we have

$$\max_{\Theta} |s_3-s_1| = |s_2-s_1| = |s_2+s_3-s_1| = \sqrt{\frac{2}{3}\left(|\bar{s}_1|^2 - \sqrt{|\bar{s}_1|^4+9|\bar{s}_2|^2|\bar{s}_3|^2}\cos\gamma\right)}$$

with $\theta_2 = \arccos\frac{|\bar{s}_1|^2+3|\bar{s}_2|^2+2\cos\gamma\sqrt{|\bar{s}_1|^4+9|\bar{s}_2|^2|\bar{s}_3|^2}}{6|\bar{s}_1||\bar{s}_2|}$ and $\alpha = \arccos\frac{2|\bar{s}_1|\cos\theta_2-|\bar{s}_2|}{2|\bar{s}_3|}$, where $\gamma = \frac{1}{3}\arccos\frac{2|\bar{s}_1|^6+27|\bar{s}_2|^2|\bar{s}_3|^4+27|\bar{s}_2|^4|\bar{s}_3|^2-81|\bar{s}_1|^2|\bar{s}_2|^2|\bar{s}_3|^2}{2(|\bar{s}_1|^4+9|\bar{s}_2|^2|\bar{s}_3|^2)^{3/2}} + \frac{4\pi}{3}$.

– if $\min \mathcal{D} = |s_2+s_3-s_1|$, which implies that $|s_2-s_1| \le \min\{|s_3-s_2|, |s_1+s_2-s_3|\}$, then by considering the sub-cases with respect to the order of $\{|s_3 - s_1|, |s_3 + s_2|, |s_2 + s_3 - s_1|\}$, we have $\max_{\Theta} |s_2 + s_3 - s_1| = |s_2 - s_1| = |s_3 - s_1| = \sqrt{\frac{2}{3}\left(|\bar{s}_1|^2 - \sqrt{|\bar{s}_1|^4 + 9|\bar{s}_2|^2|\bar{s}_3|^2}\cos\gamma\right)}$ with $\theta_2 = \arccos \frac{|\bar{s}_1|^2+3|\bar{s}_2|^2+2\cos\gamma\sqrt{|\bar{s}_1|^4+9|\bar{s}_2|^2|\bar{s}_3|^2}}{6|\bar{s}_1||\bar{s}_2|}$ and $\alpha = \arccos \frac{2|\bar{s}_1|\cos\theta_2 - |\bar{s}_2|}{2|\bar{s}_3|}$, where $\gamma = \frac{1}{3}\arccos \frac{2|\bar{s}_1|^6+27|\bar{s}_2|^2|\bar{s}_3|^4+27|\bar{s}_2|^4|\bar{s}_3|^2-81|\bar{s}_1|^2|\bar{s}_2|^2|\bar{s}_3|^2}{2(|\bar{s}_1|^4+9|\bar{s}_2|^2|\bar{s}_3|^2)^{3/2}} + \frac{4\pi}{3}$.

Based on the above, we have now determined

$$
\begin{aligned}
\max_{\Theta} \min \mathcal{D} = & \max \Big\{ \max_{\Theta} |s_1 + s_2 - s_3|, \max_{\Theta} |s_3 - s_2|, \max_{\Theta} |s_3 + s_2|, \\
& \max_{\Theta} |s_2 - s_1|, \max_{\Theta} |s_3 - s_1|, \max_{\Theta} |s_3 + s_2 - s_1| \Big\} \\
= & \max_{\Theta} |s_2 - s_1| = \max_{\Theta} |s_3 - s_1| = \max_{\Theta} |s_3 + s_2 - s_1| \\
= & \sqrt{\frac{2}{3}\left(|\bar{s}_1|^2 - \sqrt{|\bar{s}_1|^4 + 9|\bar{s}_2|^2|\bar{s}_3|^2}\cos\gamma\right)},
\end{aligned}
\tag{2.B.4}
$$

where $\gamma = \frac{1}{3}\arccos \frac{2|\bar{s}_1|^6+27|\bar{s}_2|^2|\bar{s}_3|^4+27|\bar{s}_2|^4|\bar{s}_3|^2-81|\bar{s}_1|^2|\bar{s}_2|^2|\bar{s}_3|^2}{2(|\bar{s}_1|^4+9|\bar{s}_2|^2|\bar{s}_3|^2)^{3/2}} + \frac{4\pi}{3}$. Thus, we have the claim.

- For $\sqrt{|\bar{s}_2|^2 + |\bar{s}_3|^2} > 2|\bar{s}_1|$, we let

$$
\theta_2 = \begin{cases} \arctan \frac{|\bar{s}_3|}{|\bar{s}_2|}, & \text{if } \frac{\pi}{4} \leq \arctan \frac{|\bar{s}_3|}{|\bar{s}_2|} \leq \frac{\pi}{3}, \\ \frac{\pi}{3}, & \text{if } \arctan \frac{|\bar{s}_3|}{|\bar{s}_2|} > \frac{\pi}{3}. \end{cases}
\tag{2.B.5}
$$

Then, we know that if $|\bar{s}_2| < \frac{\sqrt{3}}{3}|\bar{s}_3|$, we have $\theta_2 = \frac{\pi}{3}$. Since $|\bar{s}_2| \geq |\bar{s}_1|$, we always have $|\bar{s}_2| \geq 2|\bar{s}_1|\cos\theta_2$ and $|\bar{s}_3| \geq 2|\bar{s}_1|\sin\theta_2$. Moreover, if $\frac{\sqrt{3}}{3}|\bar{s}_3| \leq |\bar{s}_2| \leq |\bar{s}_3|$, we have $2|\bar{s}_1|\cos\theta_2 = \frac{2|\bar{s}_1|}{\sqrt{|\bar{s}_2|^2+|\bar{s}_3|^2}}|\bar{s}_2| \leq |\bar{s}_2|$. Similarly, $2|\bar{s}_1|\sin\theta_2 = \frac{2|\bar{s}_1|}{\sqrt{|\bar{s}_2|^2+|\bar{s}_3|^2}}|\bar{s}_3| \leq |\bar{s}_3|$. Then, according to Lemma 2.2, we know that $\min \mathcal{D} = |\bar{s}_1|$ can be achieved by $s_2 = |\bar{s}_2|\exp(j\theta_2)$ and $s_3 = |\bar{s}_3|\exp(j(\theta_2 - \pi/2))$.

□

2.C Appendix: Proof of Theorem 2.3

Proof The expression for the minimum distance of the corresponding QAM scheme is $d_{\text{min,XQAM}}(P_1)$, where the expressions for that minimum distance are given in (2.4.18). In order to compare these expressions with $d_{\text{min,NOMA}}$, we recall that $d_{\text{min,NOMA}}$ in (2.4.16) is a non-decreasing function of each P_k. Hence, we can obtain a lower bound on $d_{\text{min,NOMA}}$ by letting P_k, $k = 2, 3, \ldots, K$ equal to P_1. In that case, it can be shown from the expression in Algorithm 1 that $\theta_2 = \frac{\pi}{4}$, and hence that

$$\begin{aligned} d_{\text{min,NOMA}} &\geq \min\left\{2\sqrt{P_1}, \sqrt{\frac{8P_1}{4^{\lceil (K-1)/2 \rceil}}}\right\}, \\ &= \sqrt{\frac{8P_1}{4^{\lceil (K-1)/2 \rceil}}}, \end{aligned} \tag{2.C.1}$$

where $\lceil(\cdot)\rceil$ denotes rounding up to the nearest integer and $K \geq 3$. To simplify our comparisons, we can rewrite (2.C.1) as

$$d_{\text{min,NOMA}} \geq \begin{cases} \sqrt{\dfrac{16P_1}{2^K}}, & \text{if } K \geq 3 \text{ is odd} \\ \sqrt{\dfrac{8P_1}{2^K}}, & \text{if } K \geq 3 \text{ is even.} \end{cases} \tag{2.C.2}$$

By comparing with the expression in (2.4.18), we obtain the follow results,

- when $K \geq 3$ is even, $d_{\text{min,TDMA}} = \sqrt{\frac{6P_1}{2^K - 1}}$. In that case,

$$\frac{d^2_{\text{min,NOMA}}}{d^2_{\text{min,TDMA}}} \geq \frac{8P_1}{2^K}\frac{(2^K-1)}{6P_1} = \frac{4}{3}\left(1 - 2^{-K}\right) > \frac{5}{4}, \tag{2.C.3}$$

where the last bound arises from the case where $K = 4$. This establishes the result when $K \geq 3$ is even.

- when $K \geq 3$ is odd and cross-QAM constellations are used, $d_{\min,\text{TDMA}} = \sqrt{\frac{6P_1}{\frac{31}{32}2^K - 1}}$. In that case,

$$\frac{d^2_{\min,\text{NOMA}}}{d^2_{\min,\text{TDMA}}} \geq \frac{16P_1}{2^K} \frac{(\frac{31}{32}2^K - 1)}{6P_1} = \frac{8}{3}\Big(\frac{31}{32} - 2^{-K}\Big) > \frac{9}{4}, \tag{2.C.4}$$

where the last bound arises from the case where $K = 3$. This establishes the result when $K \geq 3$ is odd and the cross constellation is used. Since $d_{\min,\text{RQAM}} < d_{\min,\text{CQAM}}$ (cf, (2.4.18)), we have implicitly established the result for rectangular QAM as well. To do that explicitly, we note that when $K \geq 3$ is odd and rectangular QAM constellations are used, $d_{\min,\text{TDMA}} = \sqrt{\frac{6P_1}{\frac{5}{4}2^K - 1}}$, and hence that

$$\frac{d^2_{\min,\text{NOMA}}}{d^2_{\min,\text{TDMA}}} \geq \frac{16P_1}{2^K} \frac{(\frac{5}{4}2^K - 1)}{6P_1} = \frac{8}{3}\Big(\frac{5}{4} - 2^{-K}\Big) > 3, \tag{2.C.5}$$

which completes the proof.

□

2.D Appendix: Proof of Theorem 2.4

Proof Similar to the concept of the proof in Appendix 2.C, we can obtain a lower bound on $d_{\min,\text{NOMA}}$ by letting P_k, $k = 2, 3, \ldots, K$ equal to P_1. When $K \geq 3$ is even, that is

$$\begin{aligned} d_{\mathrm{min,NOMA}} &\geq \min\left\{2\sqrt{P_1}, 2\sqrt{\frac{P_1}{4^{K/2-1}}}, 2\sqrt{\frac{P_1}{4^{(K-1)/2-1}3}}\right\}, \\ &= 2\sqrt{\frac{8P_1}{2^K 3}}, \end{aligned} \tag{2.D.1}$$

and when $K \geq 3$ is odd, we have

$$\begin{aligned} d_{\mathrm{min,NOMA}} &\geq \max\left\{\min\left\{2\sqrt{P_1}, 2\sqrt{\frac{P_1}{4^{(K-1)/2-1}2}}\right\}, \min\left\{2\sqrt{P_1}, 2\sqrt{\frac{P_1}{4^{(K-1)/2-1}}}, 2\sqrt{\frac{P_1}{4^{(K-1)/2-1}3}}\right\}\right\}, \\ &= \max\left\{\min\left\{2\sqrt{P_1}, 2\sqrt{\frac{4P_1}{2^K}}\right\}, \min\left\{2\sqrt{P_1}, 2\sqrt{\frac{8P_1}{2^K}}, 2\sqrt{\frac{8P_1}{2^K 3}}\right\}\right\}, \\ &\geq 2\sqrt{\frac{8P_1}{2^K 3}}. \end{aligned} \tag{2.D.2}$$

Thus, we always have $d_{\mathrm{min,NOMA}} \geq 2\sqrt{\frac{8P_1}{2^K 3}}$.

By comparing with the expression in (2.4.18), we obtain the follow results:

- when $K \geq 3$ is even, $d_{\mathrm{min,TDMA}} = \sqrt{\frac{6P_1}{2^K-1}}$. In that case,

$$\frac{d^2_{\mathrm{min,NOMA}}}{d^2_{\mathrm{min,TDMA}}} \geq \frac{32P_1}{2^K 3}\frac{(2^K-1)}{6P_1} = \frac{16}{9}\left(1-2^{-K}\right) > \frac{5}{3}. \tag{2.D.3}$$

  This establishes the result when $K \geq 3$ is even.

- when $K \geq 3$ is odd and cross-QAM constellations are used, $d_{\mathrm{min,TDMA}} = \sqrt{\frac{6P_1}{\frac{31}{32}2^K-1}}$. In that case,

$$\frac{d^2_{\mathrm{min,NOMA}}}{d^2_{\mathrm{min,TDMA}}} \geq \frac{32P_1}{2^K 3}\frac{(\frac{31}{32}2^K-1)}{6P_1} = \frac{16}{9}\left(\frac{31}{32}-2^{-K}\right) > \frac{3}{2}, \tag{2.D.4}$$

  This establishes the result when $K \geq 3$ is odd and the cross constellation is used. When $K \geq 3$ is odd and rectangular QAM constellations are used,

$d_{\min,\text{TDMA}} = \sqrt{\frac{6P_1}{\frac{5}{4}2^K-1}}$, and hence

$$\frac{d^2_{\min,\text{NOMA}}}{d^2_{\min,\text{TDMA}}} \geq \frac{32P_1}{2^K 3}\frac{(\frac{5}{4}2^K-1)}{6P_1} = \frac{16}{9}\left(\frac{5}{4}-2^{-K}\right) > 2, \tag{2.D.5}$$

which completes the proof.

□

2.E Appendix: Property of Proposed Sum Constellation

Lemma 2.4 *If each user constellation $\mathcal{S}_k$ is central symmetric, the average energy of the sum constellation $\biguplus_{k=1}^{K}\mathcal{S}_k$ $(K \geq 1)$ equals the sum of the average energy of each user constellation $\mathcal{S}_k$.*

Proof Since each user constellation is symmetric, any combination of user constellations is centrally symmetric. Assume that a_t and $-a_t$ $(1 \leq t \leq 2^{K-2})$ is any pair of points in $\biguplus_{k=1}^{K-1}\mathcal{S}_k$ and $\mathcal{S}_K = \{-b, b\}$. Denote the average energy of $\biguplus_{k=1}^{K-1}\mathcal{S}_k$ and $\mathcal{S}_K$ by $E_{S_{K-1}}$ and E_{s_k}, respectively, where $E_{S_{K-1}} = \frac{1}{2^{K-2}}\sum_{t=1}^{2^{K-2}}|a_t|^2$ and $E_{s_k} = |b|^2$. By constructions, both $a-b$ and $a+b$ belong to $\biguplus_{k=1}^{K}\mathcal{S}_k$. Consider the average energy

E_{S_K} of $\biguplus_{k=1}^{K} \mathcal{S}_k$, we have

$$
\begin{aligned}
E_S &= \frac{2}{2^K} \sum_{t=1}^{2^{K-2}} \left(|a_t + b|^2 + |a_t - b|^2\right) = \frac{2}{2^K} \sum_{t=1}^{2^{K-2}} 2(|a_t|^2 + |b|^2) \\
&= \frac{1}{2^{K-2}} \sum_{t=1}^{2^{K-2}} |a_t|^2 + \frac{2}{2^K} \times 2^{K-2}|b|^2 \\
&= \frac{1}{2^{K-2}} \sum_{t=1}^{2^{K-2}} |a_t|^2 + |b|^2 = E_{S_{K-1}} + E_{s_k}.
\end{aligned}
\tag{2.E.1}
$$

Since S_{K-2} is also a centrally symmetric constellation, recursively, we have the claim.

□

According to Lemma 2.4, we have the following properties.

Property 2.1 *When K is odd, the average energy of the proposed sum constellation $\mathcal{S}$ equals*

$$E_{odd}(\mathcal{S}) = (1/4 + (4^{(K-1)/2} - 1)/3)d^2 = \frac{d^2(2M-1)}{12}, \tag{2.E.2}$$

and when K is even, the average energy equals

$$E_{even}(\mathcal{S}) = (1/4 + (4^{K/2-1} - 1)/3 + 4^{K/2-1}\cos\theta_2^2)d^2 = \frac{d^2(M-1)}{12} + 4^{K/2-1}\cos\theta_2^2 d^2, \tag{2.E.3}$$

where θ_2 is given by (2.4.6) and $M = 2^K$.

Property 2.2 *When K is odd, the proposed sum constellation $\mathcal{S}$ can provide arger minimum Euclidean distance $d_{\min}$ than M-ary RQAM with same average energy ($M = 2^K$).*

Proof According to Property 2.1, we know that $E_{\text{odd}}(\mathcal{S}) = \frac{d^2_{\min}(2M-1)}{12}$. For $M = 2^K$-ary RQAM, we know that $2^{(K+1)/2}$ points in one direction and $2^{(K-1)/2}$ points in the other. Therefore, the average energy is given by

$$\begin{aligned} E_{\text{RQAM}} &= \frac{d_{\min}^2}{M}\left(\frac{2^{K+1}-1}{12}\times 2^{(K+1)/2}\times 2^{(K-1)/2}+\frac{2^{K-1}-1}{12}\times 2^{(K-1)/2}\times 2^{(K+1)/2}\right) \\ &= \frac{d_{\min}^2(5M-4)}{24}. \end{aligned} \tag{2.E.4}$$

Then, for constellations with the same minimum distance,

$$E_{\text{RQAM}} - E_{\text{odd}}(\mathcal{S}_G) = E_{\text{RQAM}} - E_{\text{odd}}(\mathcal{S}_E) = \frac{(M-2)}{24}d_{\min}^2 > 0. \tag{2.E.5}$$

which suggests that for same average energy, our proposed constellation can provide larger minimum Euclidean distance. □

2.F Appendix: Proof of Theorem 2.5

Proof First, we notice that the condition probability density function (PDF) for any given sum signal point $s \in \mathcal{S}$ is a Gaussian distribution with mean s and variance $2\sigma^2$, given by

$$f_Y(y|s) = \frac{1}{2\pi\sigma}\exp\Big(-\frac{|y-s|^2}{2\sigma^2}\Big).$$

It is known that the relationship between the rectangular system and the polar system is characterized by

$$y_{\text{re}} = s_{\text{re}} + \rho\cos\theta \text{ and } y_{\text{im}} = s_{\text{im}} + \rho\sin\theta, \tag{2.F.1}$$

where s_{re} and s_{im} are the respective real part and imaginary part of s, i.e., $s =$

$s_{\text{re}} + js_{\text{im}}$. Correspondingly, the PDF is transformed into

$$f_{\rho,\theta}(s_{\text{re}} + \rho\cos\theta, s_{\text{im}} + \rho\sin\theta|s) = \frac{\rho}{2\pi\sigma^2}\exp\Big(-\frac{\rho^2}{2\sigma^2}\Big).$$

In order to prove Theorem 2.5, we need to consider sum constellation based on the Eisenstein integers and the Gaussian integers separately.

1. The decision regions of constellation based on the Eisenstein integers can be divided into seven types, namely, types A $\sim$ G in Fig. 2.14. For the outer points there are three types (B, C, and D); for the inner points there are two types (A and E) ; and for the edge points there are two types (F and G). The number of each decision region type is shown in Table 2.1.

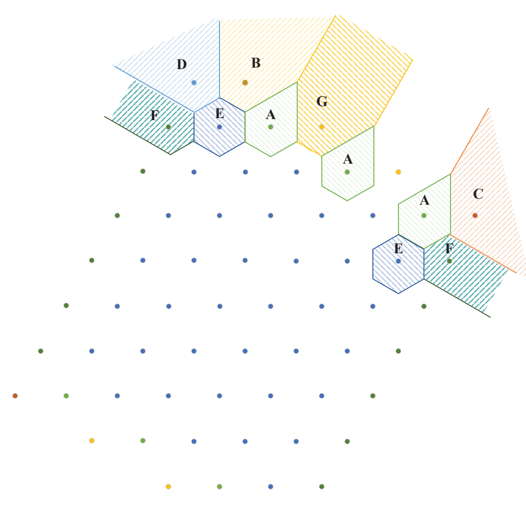

Figure 2.14: Decision region type of Eisenstein integers based sum constellation.

The correct decision probability of each type is calculated as follows, where the

Table 2.1: Type numbers for Eisenstein integers based constellation

Type	K is even	Type	K is odd
A	$2^{K/2}-2$	A	$2^{(K+1)/2}-2$
B	2	B	2
C	2	C	2
D	2	D	2
E	$(2^{K/2}-2)^2$	E	$(2^{(K-1)/2}-2)(2^{(K+1)/2}-2)$
F	$2(2^{K/2}-2)$	F	$2(2^{(K-1)/2}-2)$
G	$2^{K/2}-4$	G	$2^{(K+1)/2}-4$

details are shown in Appendix 2.G.

$$
\begin{aligned}
P_A &= 1-\tfrac{4}{\pi}\int_0^{\frac{\pi}{6}} e^{\left(-\frac{d^2}{8\cos^2\theta\sigma^2}\right)}d\theta-\tfrac{1}{\pi}\int_0^{\frac{\pi}{3}} e^{\left(-\frac{d^2}{8\cos^2\theta\sigma^2}\right)}d\theta.\\
P_B &= 1-\tfrac{2}{\pi}\int_0^{\frac{\pi}{6}} e^{\left(-\frac{d^2}{8\cos^2\theta\sigma^2}\right)}d\theta-\tfrac{1}{2\pi}\int_0^{\frac{\pi}{3}} e^{\left(-\frac{d^2}{8\cos^2\theta\sigma^2}\right)}d\theta-\tfrac{1}{2\pi}\int_0^{\frac{\pi}{2}} e^{\left(-\frac{d^2}{8\cos^2\theta\sigma^2}\right)}d\theta\\
&\quad-\tfrac{1}{2\pi}\int_{\frac{\pi}{6}}^{\frac{\pi}{3}} e^{\left(-\frac{3d^2}{8\cos^2\theta\sigma^2}\right)}d\theta.
\end{aligned}
$$

$$
\begin{aligned}
P_C &= 1-\tfrac{1}{\pi}\int_0^{\frac{\pi}{6}} e^{\left(-\frac{d^2}{8\cos^2\theta\sigma^2}\right)}d\theta-\tfrac{1}{2\pi}\int_0^{\frac{\pi}{3}} e^{\left(-\frac{d^2}{8\cos^2\theta\sigma^2}\right)}d\theta-\tfrac{1}{2\pi}\int_0^{\frac{\pi}{2}} e^{\left(-\frac{d^2}{8\cos^2\theta\sigma^2}\right)}d\theta\\
&\quad-\tfrac{1}{2\pi}\int_{\frac{\pi}{6}}^{\frac{\pi}{2}} e^{\left(-\frac{3d^2}{8\cos^2\theta\sigma^2}\right)}d\theta.\\
P_D &= 1-\tfrac{2}{\pi}\int_0^{\frac{\pi}{6}} e^{\left(-\frac{d^2}{8\cos^2\theta\sigma^2}\right)}d\theta-\tfrac{1}{\pi}\int_0^{\frac{\pi}{2}} e^{\left(-\frac{d^2}{8\cos^2\theta\sigma^2}\right)}d\theta.\\
P_E &= 1-\tfrac{6}{\pi}\int_0^{\frac{\pi}{6}} e^{\left(-\frac{d^2}{8\cos^2\theta\sigma^2}\right)}d\theta.\\
P_F &= 1-\tfrac{3}{\pi}\int_0^{\frac{\pi}{6}} e^{\left(-\frac{d^2}{8\cos^2\theta\sigma^2}\right)}d\theta-\tfrac{1}{\pi}\int_0^{\frac{\pi}{2}} e^{\left(-\frac{d^2}{8\cos^2\theta\sigma^2}\right)}d\theta\\
P_G &= 1-\tfrac{2}{\pi}\int_0^{\frac{\pi}{6}} e^{\left(-\frac{d^2}{8\cos^2\theta\sigma^2}\right)}d\theta-\tfrac{1}{\pi}\int_0^{\frac{\pi}{3}} e^{\left(-\frac{d^2}{8\cos^2\theta\sigma^2}\right)}d\theta-\tfrac{1}{\pi}\int_{\frac{\pi}{6}}^{\frac{\pi}{2}} e^{\left(-\frac{3d^2}{8\cos^2\theta\sigma^2}\right)}d\theta
\end{aligned}
$$

Therefore, the error probability is given as follows.

- When K is even

$$
\begin{aligned}
P_e &= 1 - \Big((2^{K/2}-2)P_A + 2P_B + 2P_C + 2P_D \\
&\quad +(2^{K/2}-2)^2P_E + 2(2^{K/2}-2)P_F + (2^{K/2}-4)P_G\Big)/2^K \\
&= \frac{6(1-2^{-K/2+1}+2^{-K})}{\pi}\int_0^{\frac{\pi}{6}} e^{\left(-\frac{d^2}{8\cos^2\theta\sigma^2}\right)}d\theta + \frac{2^{-K/2+1}-2^{-K+2}}{\pi}\int_0^{\frac{\pi}{3}} e^{\left(-\frac{d^2}{8\cos^2\theta\sigma^2}\right)}d\theta \\
&\quad + \frac{2^{-K/2+1}}{\pi}\int_0^{\frac{\pi}{2}} e^{\left(-\frac{d^2}{8\cos^2\theta\sigma^2}\right)}d\theta + \frac{2^{-K}}{\pi}\int_{\frac{\pi}{6}}^{\frac{\pi}{3}} e^{\left(-\frac{3d^2}{8\cos^2\theta\sigma^2}\right)}d\theta \\
&\quad + \frac{2^{-K/2}-2^{-K}3}{\pi}\int_{\frac{\pi}{6}}^{\frac{\pi}{2}} e^{\left(-\frac{3d^2}{8\cos^2\theta\sigma^2}\right)}d\theta.
\end{aligned}
$$

- When K is odd

$$
\begin{aligned}
P_e &= 1 - \Big((2^{(K+1)/2}-2)P_A + 2P_B + 2P_C + 2P_D + (2^{(K-1)/2}-2)(2^{(K+1)/2}-2)P_E \\
&\quad +2(2^{(K-1)/2}-2)P_F + (2^{(K+1)/2}-4)P_G\Big)/2^K \\
&= \frac{6(1-2^{-(K-1)/2}-2^{-(K+1)/2}+2^{-K})}{\pi}\int_0^{\frac{\pi}{6}} e^{\left(-\frac{d^2}{8\cos^2\theta\sigma^2}\right)}d\theta \\
&\quad + \frac{2^{-(K-3)/2}-2^{-K+2}}{\pi}\int_0^{\frac{\pi}{3}} e^{\left(-\frac{d^2}{8\cos^2\theta\sigma^2}\right)}d\theta + \frac{2^{-(K-1)/2}}{\pi}\int_0^{\frac{\pi}{2}} e^{\left(-\frac{d^2}{8\cos^2\theta\sigma^2}\right)}d\theta \\
&\quad + \frac{2^{-K}}{\pi}\int_{\frac{\pi}{6}}^{\frac{\pi}{3}} e^{\left(-\frac{3d^2}{8\cos^2\theta\sigma^2}\right)}d\theta + \frac{2^{-(K-1)/2}-2^{-K}3}{\pi}\int_{\frac{\pi}{6}}^{\frac{\pi}{2}} e^{\left(-\frac{3d^2}{8\cos^2\theta\sigma^2}\right)}d\theta.
\end{aligned}
$$

2. The decision region of sum constellations based on the Gaussian integers can be divided into four types, namely types A $\sim$ D in Fig.2.15. For the corners there are two types (B and C); for the inner points there is only one type (A); and for the edge points, there is only one type (D). The number of each decision region type is shown in Table 2.2.

   The correct decision probability of each type is calculated as follows, where the

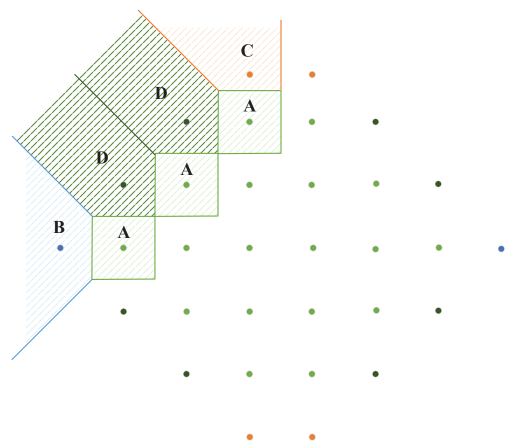

Figure 2.15: Decision region type of Gaussian integers based sum constellation.

Table 2.2: Type numbers for Gaussian integers based constellation

Type	K is odd
A	$2^K - 2^{(K+3)/2} + 2$
B	2
C	4
D	$2^{(K+3)/2} - 8$

details are shown in Appendix 2.H.

$$P_A = 1 - \frac{4}{\pi}\int_0^{\frac{\pi}{4}} e^{\left(-\frac{d^2}{8\cos^2\theta\sigma^2}\right)} d\theta.$$
$$P_B = 1 - \frac{1}{\pi}\int_0^{\frac{\pi}{2}} e^{\left(-\frac{d^2}{4\cos^2\theta\sigma^2}\right)} d\theta - \frac{1}{\pi}\int_0^{\frac{\pi}{4}} e^{\left(-\frac{d^2}{8\cos^2\theta\sigma^2}\right)} d\theta.$$
$$P_C = 1 - \frac{1}{2\pi}\int_0^{\frac{\pi}{2}} e^{\left(-\frac{d^2}{4\cos^2\theta\sigma^2}\right)} d\theta - \frac{3}{2\pi}\int_0^{\frac{\pi}{4}} e^{\left(-\frac{d^2}{8\cos^2\theta\sigma^2}\right)} d\theta - \frac{1}{2\pi}\int_0^{\frac{\pi}{2}} e^{\left(-\frac{d^2}{8\cos^2\theta\sigma^2}\right)} d\theta.$$
$$P_D = 1 - \frac{2}{\pi}\int_0^{\frac{\pi}{4}} e^{\left(-\frac{d^2}{8\cos^2\theta\sigma^2}\right)} d\theta - \frac{1}{\pi}\int_0^{\frac{\pi}{2}} e^{\left(-\frac{d^2}{4\cos^2\theta\sigma^2}\right)} d\theta.$$

Therefore, the error probability is given as follows.

$$
\begin{aligned}
P_e &= 1 - \left((2^K - 2^{(K+3)/2} + 2)P_A + 2P_B + 4P_C + (2^{(K+3)/2} - 8)P_D\right)/2^K \\
&= \frac{4(1-2^{-(K-1)/2})}{\pi}\int_0^{\frac{\pi}{4}} e^{\left(-\frac{d^2}{8\cos^2\theta\sigma^2}\right)} d\theta + \frac{4(2^{-(K+1)/2} - 2^{-K})}{\pi}\int_0^{\frac{\pi}{2}} e^{\left(-\frac{d^2}{4\cos^2\theta\sigma^2}\right)} d\theta \\
&\quad + \frac{2^{-(K-1)}}{\pi}\int_0^{\frac{\pi}{2}} e^{\left(-\frac{d^2}{8\cos^2\theta\sigma^2}\right)} d\theta.
\end{aligned}
$$

Representing the P_e by the combination of the SEP of M-ary PSK constellations ($M = 2, 3, 6$), we have the claim. □

2.G Appendix: Correct decision probability of each type for sum constellation based on Eisenstein integers

For convenience, we let $d = 1$ in the following figures.

1. Type-A

   For this type of region, as shown in Fig. 2.16, by the property of the polar system, the correct decision probability P_A can be calculated in two parts, i.e., $P_{S_{a1}}$ and $P_{S_{a2}}$. The correct decision probability is given as follows.

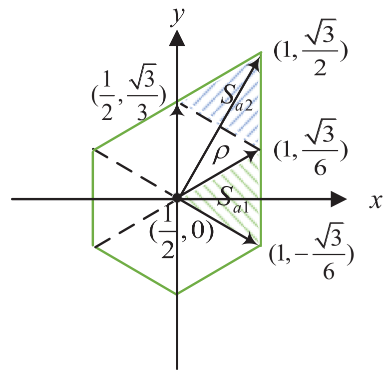

Figure 2.16: Decision region of type-A for Eisenstein integers based sum constellation

$$
\begin{aligned}
P_A &= 6P_{S_{a1}} + P_{S_{a2}} \\
&= 6\int_{-\frac{\pi}{6}}^{\frac{\pi}{6}} \int_{0}^{\frac{d}{2\cos\theta}} \frac{\rho}{2\pi\sigma^2} e^{\left(-\frac{\rho^2}{2\sigma^2}\right)} d\rho d\theta + \left\{ \int_{\frac{\pi}{6}}^{\frac{\pi}{3}} \int_{\frac{d}{2\cos(\theta-\frac{\pi}{3})}}^{\frac{d}{2\cos\theta}} \frac{\rho}{2\pi\sigma^2} e^{\left(-\frac{\rho^2}{2\sigma^2}\right)} d\rho d\theta \right. \\
&\quad \left. + \int_{\frac{\pi}{3}}^{\frac{\pi}{2}} \int_{\frac{d}{2\cos(\theta-\frac{\pi}{3})}}^{\frac{d}{2\cos(\theta-\frac{2\pi}{3})}} \frac{\rho}{2\pi\sigma^2} e^{\left(-\frac{\rho^2}{2\sigma^2}\right)} d\rho d\theta \right\} \\
&= 1 - \frac{4}{\pi} \int_{0}^{\frac{\pi}{6}} e^{\left(-\frac{d^2}{8\cos^2\theta\sigma^2}\right)} d\theta - \frac{1}{\pi} \int_{0}^{\frac{\pi}{3}} e^{\left(-\frac{d^2}{8\cos^2\theta\sigma^2}\right)} d\theta.
\end{aligned}
$$

2. Type-B

   For this region type, as shown in Fig. 2.17, the correct decision probability P_B can be calculated in four parts. The correct decision probability is calculated as follows.

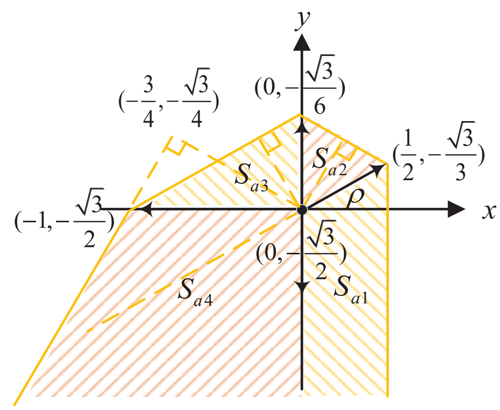

Figure 2.17: Decision region of type-B for Eisenstein integers based sum constellation

$$
\begin{aligned}
P_B &= P_{S_{a1}} + P_{S_{a2}} + P_{S_{a3}} + P_{S_{a4}} \\
&= \int_{-\frac{\pi}{2}}^{\frac{\pi}{6}} \int_0^{\frac{d}{2\cos\theta}} \frac{\rho}{2\pi\sigma^2} e^{\left(-\frac{\rho^2}{2\sigma^2}\right)} d\rho d\theta + \int_{\frac{\pi}{6}}^{\frac{\pi}{2}} \int_0^{\frac{d}{2\cos(\theta-\frac{\pi}{3})}} \frac{\rho}{2\pi\sigma^2} e^{\left(-\frac{\rho^2}{2\sigma^2}\right)} d\rho d\theta \\
&+ \int_{\frac{\pi}{2}}^{\pi} \int_0^{\frac{d}{2\cos(\theta-\frac{2\pi}{3})}} \frac{\rho}{2\pi\sigma^2} e^{\left(-\frac{\rho^2}{2\sigma^2}\right)} d\rho d\theta + \left\{ \int_{\pi}^{\frac{7\pi}{6}} \int_0^{\frac{\sqrt{3}d}{2\cos(\theta-\frac{5\pi}{6})}} \frac{\rho}{2\pi\sigma^2} e^{\left(-\frac{\rho^2}{2\sigma^2}\right)} d\rho d\theta \right. \\
&+ \left. \int_{\frac{7\pi}{6}}^{\frac{3\pi}{2}} \int_0^{\infty} \frac{\rho}{2\pi\sigma^2} e^{\left(-\frac{\rho^2}{2\sigma^2}\right)} d\rho d\theta \right\} \\
&= 1 - \frac{2}{\pi} \int_0^{\frac{\pi}{6}} e^{\left(-\frac{d^2}{8\cos^2\theta\sigma^2}\right)} d\theta - \frac{1}{2\pi} \int_0^{\frac{\pi}{3}} e^{\left(-\frac{d^2}{8\cos^2\theta\sigma^2}\right)} d\theta - \frac{1}{2\pi} \int_0^{\frac{\pi}{2}} e^{\left(-\frac{d^2}{8\cos^2\theta\sigma^2}\right)} d\theta \\
&- \frac{1}{2\pi} \int_{\frac{\pi}{6}}^{\frac{\pi}{3}} e^{\left(-\frac{3d^2}{8\cos^2\theta\sigma^2}\right)} d\theta.
\end{aligned}
$$

3. Type-C

   For this type of region, as shown in Fig. 2.18, we first add the triangle area S_{a2} into the decision region to form a regular shape, denoted by S_{a1}. Then, the correct decision probability P_C can be calculated in these two parts.

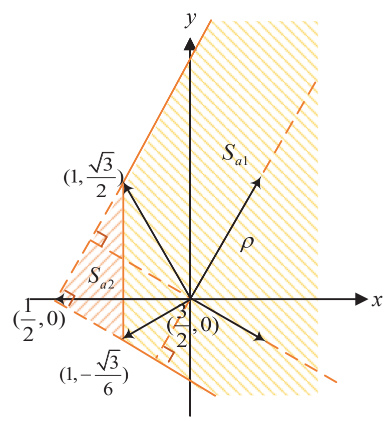

Figure 2.18: Decision region of type-C for Eisenstein integers based sum constellation

For part S_{a1},

$$P_{S_{a1}} = \int_{-\frac{\pi}{6}}^{\frac{\pi}{3}} \int_{0}^{\infty} \frac{\rho}{2\pi\sigma^2} e^{\left(-\frac{\rho^2}{2\sigma^2}\right)} d\rho d\theta + \int_{\frac{\pi}{3}}^{\pi} \int_{0}^{\frac{\sqrt{3}d}{2\cos(\theta-\frac{5\pi}{6})}} \frac{\rho}{2\pi\sigma^2} e^{\left(-\frac{\rho^2}{2\sigma^2}\right)} d\rho d\theta$$
$$+ \int_{\pi}^{\frac{11\pi}{6}} \int_{0}^{\frac{d}{2\cos(\theta-\frac{4\pi}{3})}} \frac{\rho}{2\pi\sigma^2} e^{\left(-\frac{\rho^2}{2\sigma^2}\right)} d\rho d\theta.$$

Then, for part S_{a2},

$$P_{S_{a2}} = \int_{\frac{2\pi}{3}}^{\pi} \int_{\frac{d}{2\cos(\theta-\pi)}}^{\frac{\sqrt{3}d}{2\cos(\theta-\frac{5\pi}{6})}} \frac{\rho}{2\pi\sigma^2} e^{\left(-\frac{\rho^2}{2\sigma^2}\right)} d\rho d\theta + \int_{\pi}^{\frac{7\pi}{6}} \int_{\frac{d}{2\cos(\theta-\pi)}}^{\frac{d}{2\cos(\theta-\frac{4\pi}{3})}} \frac{\rho}{2\pi\sigma^2} e^{\left(-\frac{\rho^2}{2\sigma^2}\right)} d\rho d\theta.$$

Thus, the correct decision probability is shown as follows.

$$\begin{aligned}
P_C &= P_{S_{a1}} - P_{S_{a2}} \\
&= 1 - \frac{1}{\pi} \int_{0}^{\frac{\pi}{6}} e^{\left(-\frac{d^2}{8\cos^2\theta\sigma^2}\right)} d\theta - \frac{1}{2\pi} \int_{0}^{\frac{\pi}{3}} e^{\left(-\frac{d^2}{8\cos^2\theta\sigma^2}\right)} d\theta \\
&\quad - \frac{1}{2\pi} \int_{0}^{\frac{\pi}{2}} e^{\left(-\frac{d^2}{8\cos^2\theta\sigma^2}\right)} d\theta - \frac{1}{2\pi} \int_{\frac{\pi}{6}}^{\frac{\pi}{2}} e^{\left(-\frac{3d^2}{8\cos^2\theta\sigma^2}\right)} d\theta.
\end{aligned}$$

4. Type-D

   For this type of region, as shown in Fig. 2.19, we similarly add a triangle area S_{a2} into the decision region to form a regular shape, denoted by S_{a1}. Then, the correct decision probability P_D can be calculated in these two parts. For part

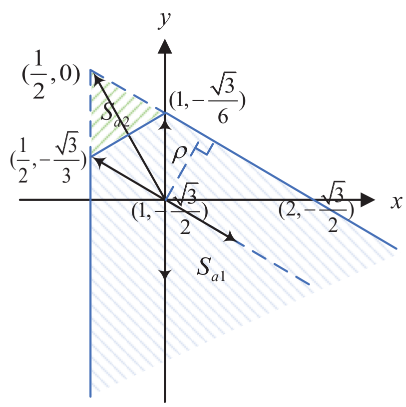

Figure 2.19: Decision region of type-D for Eisenstein integers based sum constellation

S_{a1},

$$P_{S_{a1}} = \int_{\frac{3\pi}{2}}^{\frac{11\pi}{6}} \int_0^{\infty} \frac{\rho}{2\pi\sigma^2} e^{\left(-\frac{\rho^2}{2\sigma^2}\right)} d\rho d\theta + \int_{-\frac{\pi}{6}}^{\frac{2\pi}{3}} \int_0^{\frac{d}{2\cos(\theta-\frac{\pi}{3})}} \frac{\rho}{2\pi\sigma^2} e^{\left(-\frac{\rho^2}{2\sigma^2}\right)} d\rho d\theta$$
$$+ \int_{\frac{2\pi}{3}}^{\frac{3\pi}{2}} \int_0^{\frac{d}{2\cos(\theta-\pi)}} \frac{\rho}{2\pi\sigma^2} e^{\left(-\frac{\rho^2}{2\sigma^2}\right)} d\rho d\theta$$

Then, for part S_{a2},

$$P_{S_{a2}} = \int_{\frac{\pi}{2}}^{\frac{2\pi}{3}} \int_{\frac{d}{2\cos(\theta-\frac{2\pi}{3})}}^{\frac{d}{2\cos(\theta-\frac{\pi}{3})}} \frac{\rho}{2\pi\sigma^2} e^{\left(-\frac{\rho^2}{2\sigma^2}\right)} d\rho d\theta + \int_{\frac{2\pi}{3}}^{\frac{5\pi}{6}} \int_{\frac{d}{2\cos(\theta-\frac{2\pi}{3})}}^{\frac{d}{2\cos(\theta-\pi)}} \frac{\rho}{2\pi\sigma^2} e^{\left(-\frac{\rho^2}{2\sigma^2}\right)} d\rho d\theta$$

Thus, the correct decision probability is given as follows.

$$P_D = P_{S_{a1}} - P_{S_{a2}} = 1 - \frac{2}{\pi}\int_0^{\frac{\pi}{6}} e^{\left(-\frac{d^2}{8\cos^2\theta\sigma^2}\right)} d\theta - \frac{1}{\pi}\int_0^{\frac{\pi}{2}} e^{\left(-\frac{d^2}{8\cos^2\theta\sigma^2}\right)} d\theta.$$

5. Type-E

The correct decision probability for a type-E region, as shown in Fig. 2.20, is given as follows.

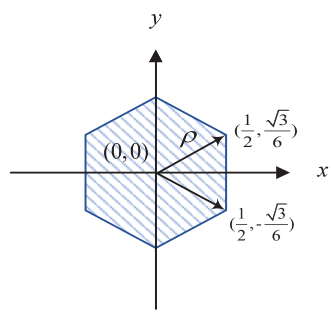

Figure 2.20: Decision region of type-E for Eisenstein integers based sum constellation

$$P_E = 6\int_{-\frac{\pi}{6}}^{\frac{\pi}{6}}\int_0^{\frac{d}{2\cos\theta}} \frac{\rho}{2\pi\sigma^2} e^{\left(-\frac{\rho^2}{2\sigma^2}\right)} d\rho d\theta = 1 - \frac{6}{\pi}\int_0^{\frac{\pi}{6}} e^{\left(-\frac{d^2}{8\cos^2\theta\sigma^2}\right)} d\theta.$$

6. Type-F

The correct decision probability for a type-F region, as shown in Fig. 2.21, is given as follows.

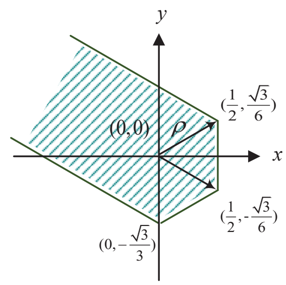

Figure 2.21: Decision region of type-F for Eisenstein integers based sum constellation

$$\begin{aligned}
P_F &= 2\int_{-\frac{\pi}{6}}^{\frac{\pi}{6}}\int_0^{\frac{d}{2\cos\theta}} \frac{\rho}{2\pi\sigma^2} e^{\left(-\frac{\rho^2}{2\sigma^2}\right)} d\rho d\theta + 2\int_{\frac{\pi}{6}}^{\frac{5\pi}{6}}\int_0^{\frac{d}{2\cos(\theta-\frac{\pi}{3})}} \frac{\rho}{2\pi\sigma^2} e^{\left(-\frac{\rho^2}{2\sigma^2}\right)} d\rho d\theta \\
&= \frac{1}{\pi}\int_{-\frac{\pi}{6}}^{\frac{\pi}{6}} \left(1-e^{\left(-\frac{d^2}{8\cos^2\theta\sigma^2}\right)}\right) d\theta + \frac{1}{\pi}\int_{\frac{\pi}{6}}^{\frac{5\pi}{6}} \left(1-e^{\left(-\frac{d^2}{8\cos^2(\theta-\frac{\pi}{3})\sigma^2}\right)}\right) d\theta \\
&= 1 - \frac{3}{\pi}\int_0^{\frac{\pi}{6}} e^{\left(-\frac{d^2}{8\cos^2\theta\sigma^2}\right)} d\theta - \frac{1}{\pi}\int_0^{\frac{\pi}{2}} e^{\left(-\frac{d^2}{8\cos^2\theta\sigma^2}\right)} d\theta
\end{aligned}$$

7. Type-G

   The correct decision probability for type-G, as shown in Fig. 2.22, is given as follows.

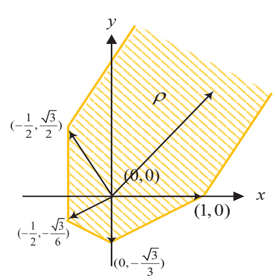

Figure 2.22: Decision region of type-G for Eisenstein integers based sum constellation

$$
\begin{aligned}
P_G =& \int_{-\frac{\pi}{6}}^{\frac{\pi}{6}} \int_{0}^{\frac{d}{2\cos\theta}} \frac{\rho}{2\pi\sigma^2} e^{\left(-\frac{\rho^2}{2\sigma^2}\right)} d\rho d\theta + 2\int_{-\frac{\pi}{2}}^{0} \int_{0}^{\frac{d}{2\cos(\theta+\frac{\pi}{3})}} \frac{\rho}{2\pi\sigma^2} e^{\left(-\frac{\rho^2}{2\sigma^2}\right)} d\rho d\theta \\
&+ 2\int_{0}^{\frac{\pi}{3}} \int_{0}^{\frac{\sqrt{3}d}{2\cos(\theta+\frac{\pi}{6})}} \frac{\rho}{2\pi\sigma^2} e^{\left(-\frac{\rho^2}{2\sigma^2}\right)} d\rho d\theta \\
=& \frac{1}{2\pi}\int_{-\frac{\pi}{6}}^{\frac{\pi}{6}} \left(1 - e^{\left(-\frac{d^2}{8\cos^2\theta\sigma^2}\right)}\right) d\theta + \frac{1}{\pi}\int_{-\frac{\pi}{2}}^{0} \left(1 - e^{\left(-\frac{d^2}{8\cos^2(\theta+\frac{\pi}{3})\sigma^2}\right)}\right) d\theta \\
&+ \frac{1}{\pi}\int_{0}^{\frac{\pi}{3}} \left(1 - e^{\left(-\frac{3d^2}{8\cos^2(\theta+\frac{\pi}{6})\sigma^2}\right)}\right) d\theta \\
=& 1 - \frac{2}{\pi}\int_{0}^{\frac{\pi}{6}} e^{\left(-\frac{d^2}{8\cos^2\theta\sigma^2}\right)} d\theta - \frac{1}{\pi}\int_{0}^{\frac{\pi}{3}} e^{\left(-\frac{d^2}{8\cos^2\theta\sigma^2}\right)} d\theta - \frac{1}{\pi}\int_{\frac{\pi}{6}}^{\frac{\pi}{2}} e^{\left(-\frac{3d^2}{8\cos^2\theta\sigma^2}\right)} d\theta
\end{aligned}
$$

2.H Appendix: Correct decision probability of each type for sum constellation based on Gaussian integers

For convenience, we let $d = 1$ in the following figures.

1. Type-A

   The decision region for a type-A region is shown in Fig. 2.23, and the correct decision probability is given as follows.

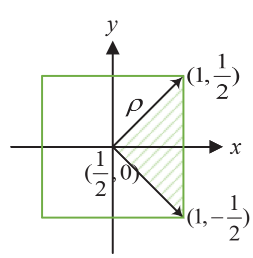

Figure 2.23: Decision region of type-A for Gaussian integers based sum constellation

$$P_A = 4\int_{-\frac{\pi}{4}}^{\frac{\pi}{4}}\int_{0}^{\frac{d}{2\cos\theta}} \frac{\rho}{2\pi\sigma^2} e^{\left(-\frac{\rho^2}{2\sigma^2}\right)} d\rho d\theta = 1 - \frac{4}{\pi}\int_{0}^{\frac{\pi}{4}} e^{\left(-\frac{d^2}{8\cos^2\theta\sigma^2}\right)} d\theta.$$

2. Type-B

For this region type, shown in Fig. 2.24, we add a triangle area S_{a2} into the decision region to form a regular shape, denoted by S_{a1}. Then, the correct decision probability P_B can be calculated in these two parts. For part S_{a1},

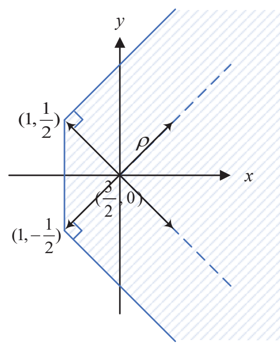

Figure 2.24: Decision region of type-B for Gaussian integers based sum constellation

$$P_{S_{a1}} = \int_{-\frac{\pi}{4}}^{\frac{\pi}{4}}\int_{0}^{\infty} \frac{\rho}{2\pi\sigma^2} e^{\left(-\frac{\rho^2}{2\sigma^2}\right)} d\rho d\theta + \int_{\frac{\pi}{4}}^{\pi}\int_{0}^{\frac{\sqrt{2}d}{2\cos(\theta-\frac{3\pi}{4})}} \frac{\rho}{2\pi\sigma^2} e^{\left(-\frac{\rho^2}{2\sigma^2}\right)} d\rho d\theta$$
$$+ \int_{\pi}^{\frac{7\pi}{4}}\int_{0}^{\frac{\sqrt{2}d}{2\cos(\theta-\frac{5\pi}{4})}} \frac{\rho}{2\pi\sigma^2} e^{\left(-\frac{\rho^2}{2\sigma^2}\right)} d\rho d\theta$$

Then, for part S_{a2},

$$P_{S_{a2}} = \int_{\frac{3\pi}{4}}^{\pi}\int_{\frac{d}{2\cos(\theta-\pi)}}^{\frac{\sqrt{2}d}{2\cos(\theta-\frac{3\pi}{4})}} \frac{\rho}{2\pi\sigma^2} e^{\left(-\frac{\rho^2}{2\sigma^2}\right)} d\rho d\theta + \int_{\pi}^{\frac{5\pi}{4}}\int_{\frac{d}{2\cos(\theta-\pi)}}^{\frac{\sqrt{2}d}{2\cos(\theta-\frac{5\pi}{4})}} \frac{\rho}{2\pi\sigma^2} e^{\left(-\frac{\rho^2}{2\sigma^2}\right)} d\rho d\theta$$

Thus, the correct decision probability is given as follows.

$$P_B = P_{S_{a1}} - P_{S_{a2}} = 1 - \frac{1}{\pi}\int_0^{\frac{\pi}{2}} e^{\left(-\frac{d^2}{4\cos^2\theta\sigma^2}\right)} d\theta - \frac{1}{\pi}\int_0^{\frac{\pi}{4}} e^{\left(-\frac{d^2}{8\cos^2\theta\sigma^2}\right)} d\theta.$$

3. Type-C

   The correct decision probability for a type-C region, as shown in Fig. 2.25, is given as follows.

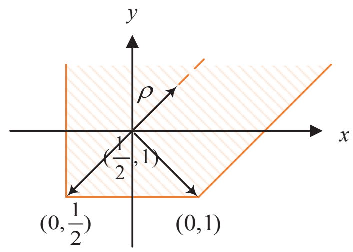

Figure 2.25: Decision region of type-C for Gaussian integers based sum constellation

$$\begin{aligned}
P_C &= P_{S_{a1}} + P_{S_{a2}} + P_{S_{a3}} + P_{S_{a4}} \\
&= \int_{-\frac{\pi}{4}}^{\frac{\pi}{4}} \int_0^{\frac{\sqrt{2}d}{2\cos(\theta+\frac{\pi}{4})}} \frac{\rho}{2\pi\sigma^2} e^{\left(-\frac{\rho^2}{2\sigma^2}\right)} d\rho d\theta + \int_{\frac{\pi}{4}}^{\frac{\pi}{2}} \int_0^{\infty} \frac{\rho}{2\pi\sigma^2} e^{\left(-\frac{\rho^2}{2\sigma^2}\right)} d\rho d\theta \\
&+ \int_{\frac{\pi}{2}}^{\frac{5\pi}{4}} \int_0^{\frac{d}{2\cos(\theta-\pi)}} \frac{\rho}{2\pi\sigma^2} e^{\left(-\frac{\rho^2}{2\sigma^2}\right)} d\rho d\theta + \int_{\frac{5\pi}{4}}^{\frac{7\pi}{4}} \int_0^{\frac{d}{2\cos(\theta-\frac{3\pi}{2})}} \frac{\rho}{2\pi\sigma^2} e^{\left(-\frac{\rho^2}{2\sigma^2}\right)} d\rho d\theta \\
&= 1 - \frac{1}{2\pi}\int_0^{\frac{\pi}{2}} e^{\left(-\frac{d^2}{4\cos^2\theta\sigma^2}\right)} d\theta - \frac{3}{2\pi}\int_0^{\frac{\pi}{4}} e^{\left(-\frac{d^2}{8\cos^2\theta\sigma^2}\right)} d\theta - \frac{1}{2\pi}\int_0^{\frac{\pi}{2}} e^{\left(-\frac{d^2}{8\cos^2\theta\sigma^2}\right)} d\theta.
\end{aligned}$$

4. Type-D

   The correct decision probability for a type-D region, as shown in Fig. 2.26, is given as follows.

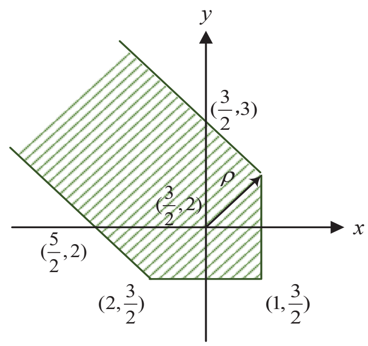

Figure 2.26: Decision region of type-D for Gaussian integers based sum constellation

$$
\begin{aligned}
P_D &= 2\int_{-\frac{\pi}{4}}^{\frac{\pi}{4}}\int_0^{\frac{d}{2\cos\theta}} \frac{\rho}{2\pi\sigma^2}e^{\left(-\frac{\rho^2}{2\sigma^2}\right)}d\rho d\theta + 2\int_{\frac{\pi}{4}}^{\frac{3\pi}{4}}\int_0^{\frac{\sqrt{2}d}{2\cos(\theta-\frac{\pi}{4})}} \frac{\rho}{2\pi\sigma^2}e^{\left(-\frac{\rho^2}{2\sigma^2}\right)}d\rho d\theta \\
&= \frac{1}{\pi}\int_{-\frac{\pi}{4}}^{\frac{\pi}{4}}\left(1-e^{\left(-\frac{d^2}{8\cos^2\theta\sigma^2}\right)}\right)d\theta + \frac{1}{\pi}\int_{\frac{\pi}{4}}^{\frac{3\pi}{4}}\left(1-e^{\left(-\frac{d^2}{4\cos^2(\theta-\frac{\pi}{4})\sigma^2}\right)}\right)d\theta \\
&= 1-\frac{2}{\pi}\int_0^{\frac{\pi}{4}} e^{\left(-\frac{d^2}{8\cos^2\theta\sigma^2}\right)}d\theta - \frac{1}{\pi}\int_0^{\frac{\pi}{2}} e^{\left(-\frac{d^2}{4\cos^2\theta\sigma^2}\right)}d\theta.
\end{aligned}
$$

Chapter 3

Non-coherent Multiuser Constellation Design for Multi-hop Relay Channels

Abstract

Inspired by a potential application in communication along high-speed trains, in this chapter we design constellations that enable non-coherent communication over a multi-hop amplify-and-forward relay channel in which both the source and the relays have data to send to the destination. The constellations are designed in such a way that the product constellation that arrives at the destination is uniquely facterizable into its constituent components. This enables us to reduce the complexity of the receiver to a simple phase-quantization receiver analogous to the coherent detector for single-user M-ary PSK signalling. Closed-form expressions for the symbol error probability are obtained.

3.1 Introduction

Over recent years there has been a significant increase in the demand for high-speed train(HST) communications, for applications such as handling safety-related messaging, or passenger-facing services. Many of these applications require fast, high capacity, low-latency connections [80]. To more towards these goals, mobile operators will need to use a wider range of spectrum. Therefore, 5G millimeter wave (mmWave) bands, ranging from 24 GHz to 40 GHz, are receiving increasing attention. However, different from conventional sub-6GHz train radio systems, mmWave systems will incur severe signal attenuation due to propagation loss, blockage, mobility sensitivity and other effects, such as rain attenuation. This may result in significant performance loss. A promising approach to efficiently mitigate these effects and increase coverage and capacity in mmWave networks, is to employ multi-hop relay-assisted communication. The link quality is improved by dividing the data transmission between a source and its destination over a large distance into several segments, where the signal strength in each segment is enhanced by intermediate relay nodes.

The two most widely adopted enhancement strategies for the relays are decode-and-forward (DF), and amplify-and-forward (AF). In this chapter we will adopt the AF strategy, as it is much simpler to implement. However, the relays will not be limited to simply relaying the signal from the source. They will have their own data to send to the destination, too. One way in which the transmission of the data from the relays could be incorporated would be by allocating orthogonal subchannels to each relay, such as time slots or frequency bands. However, this strategy allocates the resources inefficiently (due to the orthogonality requirement), and is not suitable for a system with strictly low-latency requirements. Hence, in this paper, our design objective is to design a signalling scheme that will allow the source and the relays to transmit information simultaneously at the symbol level. The primary idea that underlies our approach is to properly extend the concept of a uniquely-factorable constellation set (UFCS) proposed in [25, 26, 52, 99, 103], to a set of uniquely-factorable constellations.

The main contributions of this chapter are summarized as follows:

- A set of uniquely factorable constellations is designed based on the multi-hop relay-assisted system to allow the source and the relays to transmit their information simultaneously at the symbol level. The uniquely-factorable constellation set is based on phase-shift keying constellations.
- With such construction, We derive a maximum likelihood (ML) receiver that enables the system to operate non-coherently with respect to the channel from the source to the first relay. Furthermore, we show that this ML receiver can be reduced to a symbol-by-symbol detector that only requires phase quantization. That receiver is analogous to a coherent single-user detector for PSK signalling.
- A closed form expression for the symbol error probability (SEP) of the ML detector is derived, showing that the diversity gain is proportional to SNR^{-1}.

3.2 System Model

A motivating application for the communication scheme developed in this chapter arises in communication along a high speed train, as illustrated in Fig. 3.1. A mobile user (the source) in a carriage wishes to communicate with a destination node several carriages away. To do so, the source communicates to the relay node in its carriage.

The message is then passed over several hops to the destination. At each hop, the relay may incorporate its own data for the destination.

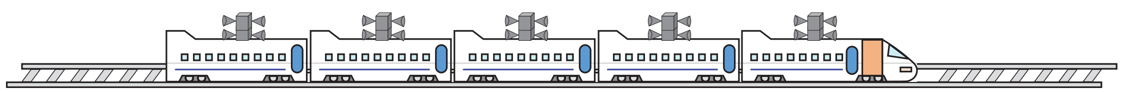

Figure 3.1: Multi-hop communication model on a high-speed train.

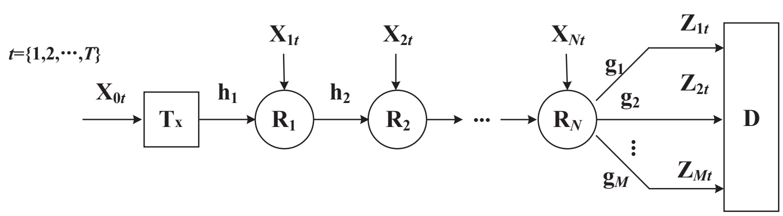

Figure 3.2: System model.

The development of the communication system that we will propose is based on the abstract system model in Fig. 3.2. This model consists of a single antenna transmitter, denoted by Tx that has data symbols $s_{0,t}$, $t = 1, 2, \cdots, T$, to send to the M-antenna destination, denoted by D. The transmission is assisted by N single antenna relays, each of which has its own data symbols, $s_{i,t}$, $i = 1, 2, \cdots, N$, $t = 1, 2, \cdots, T$, to send to the destination. Each relay operates by amplifying and forwarding the signal that it receives, and it encodes its own data in the phase of the amplification. That is, if we let y_i denote the signal received by the i-th relay at the t-th instant, then the signal transmitted by that relay is $\sqrt{\beta_i} s_{i,t} y_{i,t}$, where $\sqrt{\beta_i}$ is the amplifier gain of the relay, and $s_{i,t}$, with $|s_{i,t}| = 1$, is the data symbol for the i-th relay. Analogously, the signal transmitted by the source is $\sqrt{\beta_0} s_{0,t}$. We will model the channel to the i-th relay as being narrow band with a baseband equivalent (complex-valued) gain of h_i, with zero-mean circular additive white Gaussian noise of variance σ^2. Let

$$x_{i-1,t} = \sqrt{\beta_{i-1}} s_{i-1,t}, \text{ for } i = 1, \ldots, N. \tag{3.2.1}$$

Hence, we can write

$$y_{i,t} = h_i x_{i-1,t} y_{i-1,t} + \eta_{i,t} \tag{3.2.2}$$

where $\eta_{i,t} \sim \mathcal{CN}(0, \sigma^2)$ and since we envision operating at mmWave frequencies, where the attenuation due to path loss is high, we assume that any interference from the previous relay falls significantly below the noise floor. We define $y_{0,t} = 1$ for all t because the input of the channel to relay 1 depends only on the symbol from the source. We will assume that all channel coefficients are subject to Rayleigh distribution; i.e., $h_i \sim \mathcal{CN}(0, 1)$.

In the last hop, the N-th relay transmits to the destination, which has M antennas. The signal received by the m-th antenna at the destination can be written as

$$z_{m,t} = g_m x_{N,t} y_{N,t} + \xi_{m,t}, \tag{3.2.3}$$

where g_m is the (complex-valued) channel gain from the N-th relay to the m-th antenna at the destination and $\xi_{m,t} \sim \mathcal{CN}(0, \sigma^2)$.

The destination seeks to detect the signals transmitted by the source and the relays from its measurements $\{z_{m,t}\}_{m=1,t=1}^{M,T}$. We will consider a scenario in which the relays and the destination are in fixed relative positions and hence we can assume that the destination knows the (complex) channel gains $h_2, h_3, \cdots, h_N$ and $g_1, g_2, \cdots, g_M$. However, the source may be in motion relative to the first relay, and hence the detector will operate in a non-coherent manner (e.g., [62, 110]) with respect to h_1. That is, the receiver will operate without knowledge of h_1, but it does know that h_1 is Rayleigh distributed.

The key result of this chapter is that we will show how the constellations employed by the source and the relays at each time instant $\{\mathcal{S}_{i,t}\}_{i=0,t=1}^{N,T}$ can be designed so that using a block size of only $T = 2$, we can detect the source's symbols $\{s_{0,t} \in \mathcal{S}_{0,t}\}_{t=1}^{2}$, and all the relay symbols $\{s_{i,t} \in \mathcal{S}_{i,t}\}_{i=1,t=1}^{N,2}$. Furthermore, this detection problem can be reduced to a scalar maximum phase alignment problem over the product constellation formed by $\{s_{i,t}\}_{i=0,t=1}^{N,2}$.

3.3 Uniquely-Factorable Constellation Design

The development of our signalling scheme will be based on the notion of a uniquely factorable constellation set.

Definition 3.1 *A set of constellations $\mathcal{S}_1, \mathcal{S}_2, \ldots, \mathcal{S}_r$ ($r \geq 2$) is said to be a uniquely-factorable constellation set (UFCS) if the existence of $s_1, \tilde{s}_1 \in \mathcal{S}_1$, $s_2, \tilde{s}_2 \in \mathcal{S}_2$, $\ldots$, $s_r, \tilde{s}_r \in \mathcal{S}_r$ which satisfy $s_1 s_2 \cdots s_r = \tilde{s}_1 \tilde{s}_2 \cdots \tilde{s}_r$, implies that $s_1 = \tilde{s}_1$, $s_2 = \tilde{s}_2$, $\ldots$, $s_r = \tilde{s}_r$.*

In the following theorem we show how a set of carefully rotated M-ary phase shift keying (M-PSK) constellations forms a UFCS.

Theorem 3.1 *Consider a set of r constellations $\{\mathcal{S}_i,\ 1 \leq i \leq r\}$ in which the cardinality of the i-th constellation is $|\mathcal{S}_i| = 2^{q_i}$ and in which the constellations are constructed as*

$$\mathcal{S}_1 = \left\{ \exp\left(\frac{j2\pi n_1}{2^{q_1}} \right) \right\}_{n_1=0}^{2^{q_1}-1}, \tag{3.3.1}$$

and for any $2 \leq i \leq r$

$$\mathcal{S}_i = \left\{ \exp\left(\frac{j2\pi n_i \prod_{k=1}^{i-1}(2^{q_k}-1)}{2^{\sum_{k=1}^{i} q_k}} \right) \right\}_{n_i=0}^{2^{q_i}-1}. \tag{3.3.2}$$

Such a set of constellations constitutes a UFCS.

Proof The proof is provided in Appendix 3.A. □

In the following theorem, we will show how to decompose a standard uniform PSK constellation with 2^q points, where $q = \sum_{k=1}^{r} q_k$ into a UFCS containing r constellations, the k-th of which is of size 2^{q_k}.

Theorem 3.2 *Let $\mathcal{S}$ denote the standard uniform 2^q-ary PSK constellation, i.e.,*

$$\mathcal{S} = \left\{ \exp\left(\frac{j2\pi n}{2^q} \right) \right\}_{n=0}^{2^q-1}. \tag{3.3.3}$$

Given r and $\{q_k\}_{k=1}^{r}$ such that $q = \sum_{k=1}^{r} q_k$, construct the constellations

$$\mathcal{S}_1 = \left\{ \exp\left(\frac{j2\pi n_1}{2^{q_1}} \right) \right\}_{n_1=0}^{2^{q_1}-1}, \tag{3.3.4}$$

and for $2 \leq i \leq r$,

$$\mathcal{S}_i = \left\{ \exp\left(\frac{j2\pi n_i \prod_{k=1}^{i-1}(2^{q_k}-1)}{2^{\sum_{k=1}^{i} q_k}} \right) \right\}_{n_i=0}^{2^{q_i}-1}. \tag{3.3.5}$$

Then, for any $s \in \mathcal{S}$, there exists a set of $s_i \in \mathcal{S}_i, 1 \leq i \leq r$, such that $s_1 s_2 \cdots s_r = s$. Thus $\{\mathcal{S}_i\}_{i=1}^{r}$ constitutes a UFCS. In particular, given $s = \exp(\frac{j2\pi n}{2^q}) \in \mathcal{S}$, where $n \in \{0, 1, \ldots, 2^{q-1}\}$, s_1 and s_i ($2 \leq i \leq r$) are uniquely and explicitly determined by

$s_1 = \exp(\frac{j2\pi n_1}{2^{q_1}})$ *and* $s_i = \exp(\frac{j2\pi n_i \prod_{k=1}^{i-1}(2^{q_k}-1)}{2^{\sum_{k=1}^{i} q_k}})$, *where*

$$n_i \equiv \frac{(n - \sum_{t=i+1}^{r} n_t 2^{\sum_{k=t+1}^{r} q_k} \prod_{k=1}^{t-1}(2^{q_k}-1)) \prod_{k=1}^{i-1}(2^{q_k}-1)^{2^{q_i-1}-1}}{2^{\sum_{k=i+1}^{r} q_k}} \bmod 2^{q_i}$$

and $n_1 \equiv \frac{n - \sum_{t=2}^{r} n_t 2^{\sum_{k=t+1}^{r} q_k} \prod_{k=1}^{t-1}(2^{q_k}-1)}{2^{\sum_{k=2}^{r} q_k}} \bmod 2^{q_1}$, *for* $0 \le n_1 \le 2^{q_1}-1$ *and* $0 \le n_i \le 2^{q_i}-1$.

Proof The proof is provided in Appendix 3.B. □

3.4 Signalling scheme and power allocation

The distinguishing feature of a uniquely factorable constellation set is that we can uniquely determine the constituent symbols from their product. Since the relays in our system introduce their data in a multiplicative manner, cf., (3.3.1) and (3.3.2), such a set appears to be well suited to the problem at hand. We will consider a system in which non-coherent detection will be performed on blocks of $T = 2$ transmissions from each user. For reasons that will become soon apparent, the constellations used by the source, $\{\mathcal{S}_{0,t}\}_{t=1}^{2}$, and those used by relays, $\{\mathcal{S}_{i,t}\}_{i=0,t=1}^{N,2}$ will be selected so that they form a UFCS. That is, $\{\mathcal{S}_{i,t}\}_{i=0,t=1}^{N,2}$ forms a UFCS.

Given our model for the amplified symbols $x_{i,t}$ transmitted by source and the relays (cf. (3.2.1)) and the signals transmitted by the relays (cf. (3.2.2)), we will allocate power to the relay nodes according to the long-term average (i.e., over an asymptotically large number of channel realizations.) Since the constellations are normalized so that $|\mathcal{S}_{i,t}| = 1$ means that the transmitted power of the source is β_0. This must be less that the source's average power constraint P_0. We will let P_i denote the average power constraint for i-th relay ($1 \leq i \leq N$). Since our system performs amplify and forward relaying, the transmitted average power for the i-th relay is

$$\begin{aligned}
\mathbb{E}[|y_{i,t}x_{i,t}|^2] &= \beta_i \mathbb{E}[|y_{i,t}|^2] \\
&= \beta_i \mathbb{E}[|h_i y_{i-1,t} x_{i-1,t} + \eta_{i,t}|^2] \\
&= \beta_i (\mathbb{E}[|h_i|^2]\mathbb{E}[|y_{i-1,t}|^2]\mathbb{E}[|x_{i-1,t}|^2] + \mathbb{E}[|\eta_{i,t}|^2]) \\
&= \beta_{i-1}\beta_i \mathbb{E}[|y_{i-1,t}|^2] + \beta_i \mathbb{E}[|\eta_{i,t}|^2] \\
&= \beta_0 \prod_{k=1}^{i} \beta_k \mathbb{E}[|y_{0,t}|^2] + \sum_{j=1}^{i} \prod_{k=j}^{i} \beta_k \sigma^2 \\
&= \beta_0 \prod_{k=1}^{i} \beta_k + \sum_{j=1}^{i} \prod_{k=j}^{i} \beta_k \sigma^2,
\end{aligned} \tag{3.4.1}$$

where we have used the normalization of the constellations, and the assumptions of independent Rayleigh fading channels, and additive Gaussian noise. In order to satisfy the power constraints, the amplifier gains must satisfy

$$\beta_0 \prod_{k=1}^{i} \beta_k + \sum_{j=1}^{i} \prod_{k=j}^{i} \beta_k \sigma^2 \leq P_i. \tag{3.4.2}$$

In general, the link quality is proportional to the transmitted power. If the relays have access to a continuous (inexpensive) power source, such as the power supplied to an electric train, it is reasonable to operate each relay so that it transmits using its maximum average power P_i. In that case, (3.4.2) holds with equality, and the relay power gains β_i can be recursively calculated as

$$\beta_i = \frac{P_i}{\beta_0 \prod_{k=1}^{i-1} \beta_k + \sum_{j=1}^{i-1} \prod_{k=j}^{i-1} \beta_k \sigma^2 + \sigma^2}. \tag{3.4.3}$$

We observe that (3.4.3) enables us to set the relay amplification gains without the relays needing to know the channel realizations.

3.5 Maximum Likelihood Detector

In the scenarios that we envision, such as the relaying of messages between the carriages of a high speed train, the (relative) position of the relays and the destination are essentially constant and it is reasonable to model the communication channels as being quasi-static. Therefore, in detecting the symbols sent by the source and the relays, it is reasonable to assume that the destination can obtain, through training, an accurate model of the channels to each antenna in the last hop, $\{g_m\}_{m=1}^{M}$, and of the product channels $H_k = \prod_{i=k}^{N} h_i$ for $k = 2, 3, \cdots, N$. However, in the scenarios that we envision, it is likely that the source will be in an environment that changes on a time scale at which the amount of training required to accurately identify $H_1 = h_1 H_2$ is significant. Therefore, the detector at the destination will operate in a non-coherent manner with respect to h_1; e.g., [62, 110]. That is, it will operate with knowledge of the distribution of h_1, but without the knowledge of the particular realization of h_1. As with many approaches to non-coherent communication (e.g., [62, 110]), we will consider a block of symbols of length T and will seek to jointly detect all the symbols transmitted by the source and all the relays in that interval, $\{s_{i,t}\}_{i=0,t=1}^{N,T}$, from the signals received at the destination $\{\mathbf{z}_t\}_{t=1}^{T}$ given knowledge of the channels $\{g_m\}_{m=1}^{M}$ and the product channels $\{H_k\}_{k=2}^{N}$, but without knowledge of $H_1 = h_1 H_2$, where $\mathbf{z}_t = [z_{1,t}, z_{2,t}, \ldots, z_{M,t}]^T$.

To simplify our notation, let us define the (amplified) product symbols $X_{k,t} = \prod_{i=k}^{N} x_{i,t}$ for $k = 0, \ldots, N$, where $x_{i,t}$ was given in (3.2.1). According to (3.2.2) and

(3.2.3), we can write $y_{N,t}$ as

$$\begin{aligned} y_{N,t} &= h_N x_{N-1,t} y_{N-1,t} + \eta_{N,t} \\ &= h_N x_{N-1,t}(h_{N-1} x_{N-2,t} y_{N-2,t}) + h_N x_{N-1,t}\eta_{N-1,t} + \eta_{N,t} \\ &= H_1 \prod_{i=0}^{N-1} x_{i,t} + \sum_{j=2}^{N} \{H_j \eta_{j-1,t} \prod_{i=j-1}^{N-1} x_{i,t}\} + \eta_{N,t}. \end{aligned} \tag{3.5.1}$$

Thus, we have $x_{N,t}y_{N,t} = H_1 X_{0,t} + \sum_{j=2}^{N}\{H_j X_{j-1,t}\eta_{j-1,t}\} + x_{N,t}\eta_{N,t}$. For simplicity, we will explicitly formulate the maximum likelihood detector for the case of $T = 2$, but the extension to the general case is straightforward.

Now let us define $\mathbf{z} = [\mathbf{z}_1^T, \mathbf{z}_2^T]^T$, $\boldsymbol{\xi}_t = [\xi_{1,t}, \xi_{2,t}, \dots, \xi_{M,t}]^T$ $\boldsymbol{\xi} = [\boldsymbol{\xi}_1^T, \boldsymbol{\xi}_2^T]^T$, and $\mathbf{g} = [g_1, g_2, \dots, g_M]^T$. Then, if we let $\otimes$ denote the Kronecker product, we can write

$$\begin{aligned} \mathbf{z} &= \begin{pmatrix} x_{N,1}y_{N,1} \\ x_{N,2}y_{N,2} \end{pmatrix} \otimes \mathbf{g} + \boldsymbol{\xi} \\ &= H_1 \begin{pmatrix} X_{0,1} \\ X_{0,2} \end{pmatrix} \otimes \mathbf{g} + H_2 \begin{pmatrix} \eta_{1,1}X_{1,1} \\ \eta_{1,2}X_{1,2} \end{pmatrix} \otimes \mathbf{g} + \cdots \\ &\quad + H_N \begin{pmatrix} \eta_{N-1,1}X_{N-1,1} \\ \eta_{N-1,2}X_{N-1,2} \end{pmatrix} \otimes \mathbf{g} + \begin{pmatrix} \eta_{N,1}x_{N,1} \\ \eta_{N,2}x_{N,2} \end{pmatrix} \otimes \mathbf{g} + \boldsymbol{\xi}. \end{aligned} \tag{3.5.2}$$

Let $\mathbf{X}_0 = \begin{pmatrix} X_{0,1} \\ X_{0,2} \end{pmatrix} \otimes \mathbf{I}_M$, where $\mathbf{I}_M$ is the identity matrix of size M, and let

$\mathbf{D}_k = \begin{pmatrix} \eta_{k,1}X_{k,1} \\ \eta_{k,2}X_{k,2} \end{pmatrix} \otimes \mathbf{I}_M$ for $1 \leq k \leq N-1$. Then, we can write

$$\mathbf{z} = H_1\mathbf{X}_0\mathbf{g} + \sum_{k=1}^{N-1} H_{k+1}\mathbf{D}_k\mathbf{g} + \mathbf{D}_N\mathbf{g} + \boldsymbol{\xi}. \tag{3.5.3}$$

Let $\mathbf{x} = [x_{1,t}, x_{2,t}, \ldots, x_{N,t}]^T$, $\mathbf{x} = [x_1^T, x_2^T]$ and $\mathbf{G} = \mathbf{g}\mathbf{g}^H$. Since $\{x_{i,t}\}$ are simply amplified versions of the symbols $\{s_{i,t}\}$, we can formulate the maximum likelihood detector in terms of the conditional distribution of $\mathbf{z}$ given $\{x_{i,t}\}$, the channels to the destination $\mathbf{g}$, and the product channels H_i, $2 \leq i \leq N$. Conditioned on those terms, each component of $\mathbf{z}$ in (3.5.3) is an independent zero mean Gaussian random variable, and hence the conditional distribution of $\mathbf{z}$ is a zero-mean Gaussian distribution. The covariance of that distribution is

$$\begin{aligned}\boldsymbol{\Sigma} &= \mathbb{E}[\mathbf{z}\mathbf{z}^H|\mathbf{x}, H_2, \ldots, H_N, \mathbf{g}] \\ &= |H_2|^2\mathbf{X}_0\mathbf{G}\mathbf{X}_0^H + \sum_{k=1}^{N-1} |H_{k+1}|^2\mathbb{E}[\mathbf{D}_k\mathbf{G}\mathbf{D}_k^H] + \mathbb{E}[\mathbf{D}_N\mathbf{G}\mathbf{D}_N^H] + \boldsymbol{\Xi},\end{aligned} \tag{3.5.4}$$

where $\boldsymbol{\Xi} = \mathbb{E}\left[\boldsymbol{\xi}\boldsymbol{\xi}^H\right] = \begin{pmatrix} \sigma_{N+1}^2 \\ \sigma_{N+1}^2 \end{pmatrix} \otimes \mathbf{I}_M$, and $\mathbf{x}$ represents the all transmitted symbols. For notational simplicity, let $\boldsymbol{\Omega} = \{H_2, \ldots, H_N, \mathbf{g}\}$. Thus, the received signal has the conditional probability density

$$f(\mathbf{z}|\mathbf{x}, \boldsymbol{\Omega}) = \frac{1}{\pi^{2M}|\boldsymbol{\Sigma}|} e^{-\mathbf{z}^H\boldsymbol{\Sigma}^{-1}\mathbf{z}}. \tag{3.5.5}$$

Therefore, the maximum likelihood detector becomes

$$
\begin{aligned}
\hat{\mathbf{x}} &= \arg\max_{\mathbf{x}} f(\mathbf{z}|\mathbf{x}, \boldsymbol{\Omega}) \\
&= \arg\max_{\mathbf{x}} \frac{1}{\pi^{2M}|\boldsymbol{\Sigma}|} e^{-\mathbf{z}^H \boldsymbol{\Sigma}^{-1} \mathbf{z}} \\
&= \arg\max_{\mathbf{x}} -\mathbf{z}^H \boldsymbol{\Sigma}^{-1} \mathbf{z},
\end{aligned} \tag{3.5.6}
$$

where the last equality results from the fact that $|\boldsymbol{\Sigma}|$ is a constant with respect to $\mathbf{x}$ (see (3.C.9) in Appendix 3.C).

Although the ML detector in (3.5.6) has a simple form, if the source transmits q_0 bits per channel use and the i-th relay transmits q_i, then in the classic implementation, we must construct and invert the matrix $\boldsymbol{\Sigma}$ a total of $2^{\sum_{i=0}^{N} q_i}$ times, resulting in a high computational load.

3.6 Fast Detector

In this section, we will show how the structure of our signalling set and our transmission scheme enable us to reduce the ML detection problem to a simple "phase quantization" detector. As in Sect. 3.4, we let $\mathcal{S}_{i,t}$ denote the constellation used by node i at time slot t. This constellation has q_i elements. The set $\{s_{i,t}\}_{i=0,t=1}^{N,2}$ forms a uniquely factorable constellation set and $\mathcal{S}$ denotes the corresponding "product constellation" with $2^{\sum_{i=0}^{N} q_i}$ elements; see Theorem 3.2. Let $\tilde{\mathcal{S}}$ denote the scaled version of that constellation in which each element is scaled by $\prod_{i=0}^{N} \beta_i$.

Theorem 3.3 *The ML detector can be reduced to a symbol-by-symbol detector, that seeks the maximum value of* $\Re(B\mathbf{z}_1^H \mathbf{G}\mathbf{z}_2)$ *with respect to the argument* B*, where* $B = X_{0,1}X_{0,2}^* \in \tilde{\mathcal{S}}$*.*

Proof The proof is provided in Appendix 3.C. □

By making the mild approximation outlined below, the detector can be simplified to

$$\max_{B\in\tilde{\mathcal{S}}} \Re(B\mathbf{z}_1^H\mathbf{z}_2). \tag{3.6.1}$$

In particular, for $t = 1, 2$, let $\tilde{y}_t = x_{N,t}y_{N,t}$, according to (3.2.3), we have $\mathbf{z}_t = \mathbf{g}\tilde{y}_t + \boldsymbol{\xi}_t$. Then, we note that

$$\begin{aligned}\mathbf{z}_1^H\mathbf{G}\mathbf{z}_2 &= \Big((\mathbf{g}^H\tilde{y}_1^* + \boldsymbol{\xi}_1^H)\mathbf{g}\Big)\Big(\mathbf{g}^H(\mathbf{g}\tilde{y}_2 + \boldsymbol{\xi}_2)\Big)\\ &= \|\mathbf{g}\|^2\Big(\|\mathbf{g}\|^2\tilde{y}_1^*\tilde{y}_2 + \tilde{y}_2\boldsymbol{\xi}_1^H\mathbf{g} + \tilde{y}_1^*\mathbf{g}^H\boldsymbol{\xi}_2 + \boldsymbol{\xi}_1^H\mathbf{u}_1\mathbf{u}_1^H\boldsymbol{\xi}_2\Big)\end{aligned} \tag{3.6.2}$$

where $\mathbf{u}_1 = \mathbf{g}/\|\mathbf{g}\|$, and

$$\begin{aligned}\mathbf{z}_1^H\mathbf{z}_2 &= (\mathbf{g}^H\tilde{y}_1^* + \boldsymbol{\xi}_1^H)(\mathbf{g}\tilde{y}_2 + \boldsymbol{\xi}_2)\\ &= \|\mathbf{g}\|^2\tilde{y}_1^*\tilde{y}_2 + \tilde{y}_2\boldsymbol{\xi}_1^H\mathbf{g} + \tilde{y}_1^*\mathbf{g}^H\boldsymbol{\xi}_2 + \boldsymbol{\xi}_1^H\boldsymbol{\xi}_2.\end{aligned} \tag{3.6.3}$$

These expressions only differ by a real-valued scaling and the last term, which is a product of the noise components and is typically much smaller than the other components. An alternative derivation of this simplified detector is provided in Appendices 3.D and 3.E.

An advantage of the simplified detector in (3.6.1) is that it only needs the received signals (and $\prod_{i=0}^{N}\beta_i$) and does not require explicit knowledge of any of the channels.

3.7 Symbol Error Probability

In this section, we derive a closed-form expression for the symbol error probability of the simplified detector in (3.6.1).

According to the system model and (3.5.5), we know that $\mathbf{z}|\mathbf{x}, \boldsymbol{\Omega} \sim \mathcal{CN}(\mathbf{0}, \boldsymbol{\Sigma})$. Let $\boldsymbol{\Sigma}_{ij} = \mathbb{E}[\mathbf{z}_i \mathbf{z}_j^H | \mathbf{x}, \boldsymbol{\Omega}]$ with $1 \leq i, j \leq 2$. Then, the covariance matrix of $\mathbf{z}$ can be rewritten as

$$\boldsymbol{\Sigma} = \mathbb{E}[\mathbf{z}\mathbf{z}^H | \mathbf{x}, \boldsymbol{\Omega}] = \begin{bmatrix} \boldsymbol{\Sigma}_{11} & \boldsymbol{\Sigma}_{12} \\ \boldsymbol{\Sigma}_{21} & \boldsymbol{\Sigma}_{22} \end{bmatrix}. \tag{3.7.1}$$

Since

$$\begin{bmatrix} \mathbf{I} & \mathbf{0} \\ -\boldsymbol{\Sigma}_{21}\boldsymbol{\Sigma}_{11}^{-1} & \mathbf{I} \end{bmatrix} \begin{bmatrix} \boldsymbol{\Sigma}_{11} & \boldsymbol{\Sigma}_{12} \\ \boldsymbol{\Sigma}_{21} & \boldsymbol{\Sigma}_{22} \end{bmatrix} \begin{bmatrix} \mathbf{I} & -\boldsymbol{\Sigma}_{11}^{-1}\boldsymbol{\Sigma}_{12} \\ \mathbf{0} & \mathbf{I} \end{bmatrix} = \begin{bmatrix} \boldsymbol{\Sigma}_{11} & \mathbf{0} \\ \mathbf{0} & -\boldsymbol{\Sigma}_{21}\boldsymbol{\Sigma}_{11}^{-1}\boldsymbol{\Sigma}_{12} + \boldsymbol{\Sigma}_{22} \end{bmatrix}, \tag{3.7.2}$$

we have

$$\begin{aligned} \boldsymbol{\Sigma}^{-1} = \begin{bmatrix} \boldsymbol{\Sigma}_{11} & \boldsymbol{\Sigma}_{12} \\ \boldsymbol{\Sigma}_{21} & \boldsymbol{\Sigma}_{22} \end{bmatrix}^{-1} &= \begin{bmatrix} \mathbf{I} & -\boldsymbol{\Sigma}_{11}^{-1}\boldsymbol{\Sigma}_{12} \\ \mathbf{0} & \mathbf{I} \end{bmatrix} \begin{bmatrix} \boldsymbol{\Sigma}_{11} & \mathbf{0} \\ \mathbf{0} & -\boldsymbol{\Sigma}_{21}\boldsymbol{\Sigma}_{11}^{-1}\boldsymbol{\Sigma}_{12} + \boldsymbol{\Sigma}_{22} \end{bmatrix}^{-1} \begin{bmatrix} \mathbf{I} & \mathbf{0} \\ -\boldsymbol{\Sigma}_{21}\boldsymbol{\Sigma}_{11}^{-1} & \mathbf{I} \end{bmatrix} \\ &= \begin{bmatrix} \boldsymbol{\Sigma}_{11}^{-1} + \boldsymbol{\Sigma}_{11}^{-1}\boldsymbol{\Sigma}_{12}(-\boldsymbol{\Sigma}_{21}\boldsymbol{\Sigma}_{11}^{-1}\boldsymbol{\Sigma}_{12} + \boldsymbol{\Sigma}_{22})^{-1}\boldsymbol{\Sigma}_{21}\boldsymbol{\Sigma}_{11}^{-1} & -\boldsymbol{\Sigma}_{11}^{-1}\boldsymbol{\Sigma}_{12}(-\boldsymbol{\Sigma}_{21}\boldsymbol{\Sigma}_{11}^{-1}\boldsymbol{\Sigma}_{12} + \boldsymbol{\Sigma}_{22})^{-1} \\ -(-\boldsymbol{\Sigma}_{21}\boldsymbol{\Sigma}_{11}^{-1}\boldsymbol{\Sigma}_{12} + \boldsymbol{\Sigma}_{22})^{-1}\boldsymbol{\Sigma}_{21}\boldsymbol{\Sigma}_{11}^{-1} & (-\boldsymbol{\Sigma}_{21}\boldsymbol{\Sigma}_{11}^{-1}\boldsymbol{\Sigma}_{12} + \boldsymbol{\Sigma}_{22})^{-1} \end{bmatrix}. \end{aligned} \tag{3.7.3}$$

Note that we also have $\mathbf{z}_1|\mathbf{x}, \boldsymbol{\Omega} \sim \mathcal{CN}(\mathbf{0}, \boldsymbol{\Sigma}_{11})$, thus, the conditional probability density functions (PDFs) of $\mathbf{z}$ and $\mathbf{z}_1$ are given by

$$f(\mathbf{z}|\mathbf{x}, \boldsymbol{\Omega}) = \frac{1}{\pi^{2M}|\boldsymbol{\Sigma}|} e^{-\mathbf{z}^H \boldsymbol{\Sigma}^{-1} \mathbf{z}}, \tag{3.7.4}$$

and

$$f(\mathbf{z}_1|\mathbf{x},\mathbf{\Omega}) = \frac{1}{\pi^M|\mathbf{\Sigma}_{11}|}e^{-\mathbf{z}_1^H\mathbf{\Sigma}_{11}^{-1}\mathbf{z}_1}. \tag{3.7.5}$$

Since $f(\mathbf{z}|\mathbf{x},\mathbf{\Omega}) = f((\mathbf{z}_1^T,\mathbf{z}_2^T)^T|\mathbf{x},\mathbf{\Omega}) = f(\mathbf{z}_1|\mathbf{x})f(\mathbf{z}_2|\mathbf{z}_1,\mathbf{x},\mathbf{\Omega})$, we have

$$f(\mathbf{z}_2|\mathbf{z}_1,\mathbf{x}) = \frac{f(\mathbf{z})}{f(\mathbf{z}_1)} = \frac{1}{\pi^M\frac{|\mathbf{\Sigma}|}{|\mathbf{\Sigma}_{11}|}}e^{-(\mathbf{z}^H\mathbf{\Sigma}^{-1}\mathbf{z}-\mathbf{z}_1^H\mathbf{\Sigma}_{11}^{-1}\mathbf{z}_1)}. \tag{3.7.6}$$

Furthermore, we have

$$\mathbf{z}^H\mathbf{\Sigma}^{-1}\mathbf{z} - \mathbf{z}_1^H\mathbf{\Sigma}_{11}^{-1}\mathbf{z}_1 = (\mathbf{z}_2^H - \mathbf{z}_1^H\mathbf{\Sigma}_{11}^{-1}\mathbf{\Sigma}_{12})(-\mathbf{\Sigma}_{21}\mathbf{\Sigma}_{11}^{-1}\mathbf{\Sigma}_{12} + \mathbf{\Sigma}_{22})^{-1}(\mathbf{z}_2 - \mathbf{\Sigma}_{21}\mathbf{\Sigma}_{11}^{-1}\mathbf{z}_1). \tag{3.7.7}$$

Due to the fact that $\mathbf{\Sigma}_{12} = \mathbf{\Sigma}_{21}^H$ and $\mathbf{\Sigma}_{11} = \mathbf{\Sigma}_{11}^H$, we have $(\mathbf{\Sigma}_{21}\mathbf{\Sigma}_{11}^{-1}\mathbf{z}_1)^H = \mathbf{z}_1^H\mathbf{\Sigma}_{11}^{-1}\mathbf{\Sigma}_{12}$. Therefore, (3.7.7) can be rewritten as

$$\mathbf{z}^H\mathbf{\Sigma}^{-1}\mathbf{z} - \mathbf{z}_1^H\mathbf{\Sigma}_{11}^{-1}\mathbf{z}_1 = (\mathbf{z}_2^H - (\mathbf{\Sigma}_{21}\mathbf{\Sigma}_{11}^{-1}\mathbf{z}_1)^H)(-\mathbf{\Sigma}_{21}\mathbf{\Sigma}_{11}^{-1}\mathbf{\Sigma}_{12} + \mathbf{\Sigma}_{22})^{-1}(\mathbf{z}_2 - \mathbf{\Sigma}_{21}\mathbf{\Sigma}_{11}^{-1}\mathbf{z}_1). \tag{3.7.8}$$

Moreover, according to (3.7.2), we know that the determinant

$$\left|\begin{matrix}\mathbf{I} & \mathbf{0}\\ -\mathbf{\Sigma}_{21}\mathbf{\Sigma}_{11}^{-1} & \mathbf{I}\end{matrix}\right|\left|\begin{matrix}\mathbf{\Sigma}_{11} & \mathbf{\Sigma}_{12}\\ \mathbf{\Sigma}_{21} & \mathbf{\Sigma}_{22}\end{matrix}\right|\left|\begin{matrix}\mathbf{I} & -\mathbf{\Sigma}_{11}^{-1}\mathbf{\Sigma}_{12}\\ \mathbf{0} & \mathbf{I}\end{matrix}\right| = \left|\begin{matrix}\mathbf{\Sigma}_{11} & \mathbf{0}\\ \mathbf{0} & \mathbf{\Sigma}_{22} - \mathbf{\Sigma}_{21}\mathbf{\Sigma}_{11}^{-1}\mathbf{\Sigma}_{12}\end{matrix}\right|, \tag{3.7.9}$$

i.e., $|\mathbf{\Sigma}| = |\mathbf{\Sigma}_{11}| \times |\mathbf{\Sigma}_{22} - \mathbf{\Sigma}_{21}\mathbf{\Sigma}_{11}^{-1}\mathbf{\Sigma}_{12}|$. Therefore

$$\frac{|\mathbf{\Sigma}|}{|\mathbf{\Sigma}_{11}|} = |\mathbf{\Sigma}_{22} - \mathbf{\Sigma}_{21}\mathbf{\Sigma}_{11}^{-1}\mathbf{\Sigma}_{12}|. \tag{3.7.10}$$

By combining (3.7.8) and (3.7.10), we have

$$f(\mathbf{z}_2|\mathbf{z}_1,\mathbf{x},\boldsymbol{\Omega}) = \frac{1}{\pi^M|\boldsymbol{\Sigma}_{22}-\boldsymbol{\Sigma}_{21}\boldsymbol{\Sigma}_{11}^{-1}\boldsymbol{\Sigma}_{12}|}e^{-(\mathbf{z}_2^H-(\boldsymbol{\Sigma}_{21}\boldsymbol{\Sigma}_{11}^{-1}\mathbf{z}_1)^H)(\boldsymbol{\Sigma}_{22}-\boldsymbol{\Sigma}_{21}\boldsymbol{\Sigma}_{11}^{-1}\boldsymbol{\Sigma}_{12})^{-1}(\mathbf{z}_2-\boldsymbol{\Sigma}_{21}\boldsymbol{\Sigma}_{11}^{-1}\mathbf{z}_1)}, \tag{3.7.11}$$

i.e.,

$$\mathbf{z}_2|\mathbf{z}_1,\mathbf{x},\boldsymbol{\Omega} \sim \mathcal{CN}(\boldsymbol{\Sigma}_{21}\boldsymbol{\Sigma}_{11}^{-1}\mathbf{z}_1, -\boldsymbol{\Sigma}_{21}\boldsymbol{\Sigma}_{11}^{-1}\boldsymbol{\Sigma}_{12}+\boldsymbol{\Sigma}_{22}). \tag{3.7.12}$$

Now, let us consider the simplified detector in (3.6.1) and let $U = \mathbf{z}_1^H\mathbf{z}_2$. The conditional distribution of U conditioned on $\mathbf{z}_1$ and $\mathbf{x}$ is

$$U|\mathbf{z}_1,\mathbf{x},\boldsymbol{\Omega} = \mathbf{z}_1^H\mathbf{z}_2|\mathbf{z}_1,\mathbf{x} \sim \mathcal{CN}\Big(\mathbf{z}_1^H\boldsymbol{\Sigma}_{21}\boldsymbol{\Sigma}_{11}^{-1}\mathbf{z}_1, \mathbf{z}_1^H(-\boldsymbol{\Sigma}_{21}\boldsymbol{\Sigma}_{11}^{-1}\boldsymbol{\Sigma}_{12}+\boldsymbol{\Sigma}_{22})\mathbf{z}_1\Big), \tag{3.7.13}$$

Since

$$\begin{aligned} f(U|\mathbf{x},\boldsymbol{\Omega}) &= f(\mathbf{z}_1^H\mathbf{z}_2|\mathbf{x},\boldsymbol{\Omega}) \\ &= f(\mathbf{z}_1^H\mathbf{z}_2|\mathbf{z}_1,\mathbf{x},\boldsymbol{\Omega})f(\mathbf{z}_1|\mathbf{x},\boldsymbol{\Omega}), \end{aligned} \tag{3.7.14}$$

we have

$$\begin{aligned} f(U|\mathbf{x}) &= \int_{\boldsymbol{\Omega}}\int_{\mathbf{z}_1} \frac{1}{\pi^M\mathbf{z}_1^H(-\boldsymbol{\Sigma}_{21}\boldsymbol{\Sigma}_{11}^{-1}\boldsymbol{\Sigma}_{12}+\boldsymbol{\Sigma}_{22})\mathbf{z}_1} e^{-\frac{|u-\mathbf{z}_1^H\boldsymbol{\Sigma}_{21}\boldsymbol{\Sigma}_{11}^{-1}\mathbf{z}_1|^2}{\mathbf{z}_1^H(-\boldsymbol{\Sigma}_{21}\boldsymbol{\Sigma}_{11}^{-1}\boldsymbol{\Sigma}_{12}+\boldsymbol{\Sigma}_{22})\mathbf{z}_1}} \frac{1}{\pi^M|\boldsymbol{\Sigma}_{11}|} \\ &\quad \times e^{-\mathbf{z}_1^H\boldsymbol{\Sigma}_{11}^{-1}\mathbf{z}_1} f(\boldsymbol{\Omega})d\mathbf{z}_1 d\boldsymbol{\Omega} \\ &= \frac{1}{\pi^{2M}|\boldsymbol{\Sigma}_{11}|}\int_{\mathbf{g},H_2,\ldots,H_N} f(\mathbf{g})f(H_2,\ldots,H_N)\int_{\mathbf{z}_1}\frac{1}{\mathbf{z}_1^H(-\boldsymbol{\Sigma}_{21}\boldsymbol{\Sigma}_{11}^{-1}\boldsymbol{\Sigma}_{12}+\boldsymbol{\Sigma}_{22})\mathbf{z}_1} \\ &\quad \times e^{-\frac{|u-\mathbf{z}_1^H\boldsymbol{\Sigma}_{21}\boldsymbol{\Sigma}_{11}^{-1}\mathbf{z}_1|^2}{\mathbf{z}_1^H(-\boldsymbol{\Sigma}_{21}\boldsymbol{\Sigma}_{11}^{-1}\boldsymbol{\Sigma}_{12}+\boldsymbol{\Sigma}_{22})\mathbf{z}_1}} e^{-\mathbf{z}_1^H\boldsymbol{\Sigma}_{11}^{-1}\mathbf{z}_1} d\mathbf{z}_1 d\mathbf{g} d(H_2,\ldots,H_N) \end{aligned} \tag{3.7.15}$$

According to (3.C.6) in Appendix 3.C, we know that

$$\boldsymbol{\Sigma}_{11} = \mathbb{E}[\mathbf{z}_1\mathbf{z}_1^H|\mathbf{x},\boldsymbol{\Omega}] = \sigma^2\Big(\mathbf{I}_M + \frac{A}{\sigma^2}\mathbf{g}\mathbf{g}^H\Big) \tag{3.7.16}$$

and

$$\begin{aligned}\mathbf{\Sigma}_{11}^{-1} &= \sigma^{-2}\Big(\mathbf{I}_M - \frac{\frac{|X_{0,1}|^2}{\sigma^2} + \sum_{k=1}^{N-1}|H_{k+1}|^2|X_{k,1}|^2 + |X_{N,1}|^2}{1 + (\frac{|X_{0,1}|^2}{\sigma^2} + \sum_{k=1}^{N-1}|H_{k+1}|^2|X_{k,1}|^2 + |X_{N,1}|^2)\|\mathbf{g}\|^2}\mathbf{g}\mathbf{g}^H\Big) \\ &= \sigma^{-2}\Big(\mathbf{I}_M - \frac{\mathbf{g}\mathbf{g}^H}{(\frac{A}{\sigma^2})^{-1} + \|\mathbf{g}\|^2}\Big),\end{aligned} \tag{3.7.17}$$

with $A = |H_2|^2 E \prod_{i=1}^{N}\beta_i + (\sum_{k=1}^{N-1}|H_{k+1}|^2\prod_{i=k}^{N}\beta_i + \beta_N)\sigma^2$. Moreover, according to $B = X_{0,1}X_{0,2}^*$, we have

$$\begin{aligned}\mathbf{\Sigma}_{12} &= \mathbb{E}[\mathbf{z}_1\mathbf{z}_2^H|\mathbf{x},\mathbf{\Omega}] = B|H_2|^2\mathbf{g}\mathbf{g}^H, \\ \mathbf{\Sigma}_{21} &= \mathbb{E}[\mathbf{z}_2\mathbf{z}_1^H|\mathbf{x},\mathbf{\Omega}] = B^*|H_2|^2\mathbf{g}\mathbf{g}^H,\end{aligned} \tag{3.7.18}$$

and

$$\mathbf{\Sigma}_{22} = \mathbb{E}[\mathbf{z}_2\mathbf{z}_2^H|\mathbf{x},\mathbf{\Omega}] = \sigma^2\Big(\mathbf{I}_M + \frac{A}{\sigma^2}\mathbf{g}\mathbf{g}^H\Big). \tag{3.7.19}$$

Since the matrix $\mathbf{z}_1\mathbf{z}_1^H$ can be diagonalized by a matrix $\mathbf{W}$, the columns of which are the eigenvectors of $\mathbf{z}_1\mathbf{z}_1^H$, i.e., $\mathbf{z}_1\mathbf{z}_1^H = \mathbf{W}\begin{bmatrix}\|\mathbf{z}_1\|^2 & \dots & 0\\ \vdots & \ddots & \vdots \\ 0 & \dots & 0\end{bmatrix}\mathbf{W}^H$, we have

$$\begin{aligned}\mathbf{z}_1^H\mathbf{g}\mathbf{g}^H\mathbf{z}_1 &= \mathrm{tr}(\mathbf{z}_1^H\mathbf{g}\mathbf{g}^H\mathbf{z}_1) = \mathrm{tr}(\mathbf{g}^H\mathbf{z}_1\mathbf{z}_1^H\mathbf{g}) \\ &= \|\mathbf{z}_1\|^2|\tilde{g}_1|^2,\end{aligned} \tag{3.7.20}$$

where $\tilde{\mathbf{g}} = (\tilde{g}_1,\dots,\tilde{g}_M)^T = \mathbf{W}^H\mathbf{g}$. Since $\mathbf{W}^H\mathbf{W} = \mathbf{W}\mathbf{W}^H = \mathbf{I}$ and $\mathbf{g} \sim \mathcal{CN}(0,\mathbf{I}_M)$, we know that $\tilde{\mathbf{g}} \sim \mathcal{CN}(0,\mathbf{I}_M)$. Let $C = \frac{A}{\sigma^2}$. Then, we have the following equations,

$$|\mathbf{\Sigma}_{11}| = |\sigma^2(\mathbf{I}_M + C\mathbf{g}\mathbf{g}^H)| = \sigma^{2M}(C\|\mathbf{g}\|^2 + 1), \tag{3.7.21}$$

$$\begin{aligned}
\mathbf{z}_1^H \boldsymbol{\Sigma}_{21}\boldsymbol{\Sigma}_{11}^{-1}\mathbf{z}_1 &= \sigma^{-2}B^*(\mathbf{z}_1^H\mathbf{g}\mathbf{g}^H\mathbf{z}_1 - \frac{\|\mathbf{g}\|^2\mathbf{z}_1^H\mathbf{g}\mathbf{g}^H\mathbf{z}_1}{C^{-1}+\|\mathbf{g}\|^2}) \\
&= \sigma^{-2}B^*(1-\frac{\|\mathbf{g}\|^2}{C^{-1}+\|\mathbf{g}\|^2})\mathbf{z}_1^H\mathbf{g}\mathbf{g}^H\mathbf{z}_1 \\
&= \frac{\sigma^{-2}B^*}{1+C\|\tilde{\mathbf{g}}\|^2}\|\mathbf{z}_1\|^2|\tilde{g}_1|^2,
\end{aligned} \tag{3.7.22}$$

$$\begin{aligned}
&\mathbf{z}_1^H(-\boldsymbol{\Sigma}_{21}\boldsymbol{\Sigma}_{11}^{-1}\boldsymbol{\Sigma}_{12}+\boldsymbol{\Sigma}_{22})\mathbf{z}_1 \\
&= -\mathbf{z}_1^H\sigma^{-2}|B|^2(\|\mathbf{g}\|^2\mathbf{g}\mathbf{g}^H - \frac{\|\mathbf{g}\|^4\mathbf{g}\mathbf{g}^H}{C^{-1}+\|\mathbf{g}\|^2})\mathbf{z}_1 + \sigma^2\mathbf{z}_1^H\mathbf{z}_1 + \sigma^2C\mathbf{z}_1^H\mathbf{g}\mathbf{g}^H\mathbf{z}_1 \\
&= -\frac{\sigma^{-2}|B|^2}{1+C\|\mathbf{g}\|^2}\|\mathbf{g}\|^2\|\mathbf{z}_1\|^2|\mathbf{g}^H\mathbf{w}_1|^2 + \sigma^2\|\mathbf{z}_1\|^2 + \sigma^2C\|\mathbf{z}_1\|^2|\mathbf{g}^H\mathbf{w}_1|^2 \\
&= (\sigma^2C - \frac{\sigma^{-2}E^2\prod_{i=1}^N\beta_i^2\|\tilde{\mathbf{g}}\|^2}{1+C\|\tilde{\mathbf{g}}\|^2})\|\mathbf{z}_1\|^2|\tilde{g}_1|^2 + \sigma^2\|\mathbf{z}_1\|^2,
\end{aligned} \tag{3.7.23}$$

and

$$\begin{aligned}
\mathbf{z}_1^H\boldsymbol{\Sigma}_{11}^{-1}\mathbf{z}_1 &= \mathbf{z}_1^H\sigma^{-2}(\mathbf{I}_M - \frac{\mathbf{g}\mathbf{g}^H}{C^{-1}+\|\mathbf{g}\|^2})\mathbf{z}_1 \\
&= \frac{-\sigma^{-2}C}{1+C\|\tilde{\mathbf{g}}\|^2}\|\mathbf{z}_1\|^2|\tilde{g}_1|^2 + \sigma^{-2}\|\mathbf{z}_1\|^2.
\end{aligned} \tag{3.7.24}$$

Therefore, the conditional PDF can be written as

$$\begin{aligned}
f(U|\mathbf{x}) &= \int_{H_2,\ldots,H_N,\mathbf{g}} \frac{1}{\pi^{2M}|\boldsymbol{\Sigma}_{11}|} f(\mathbf{g})f(H_2,\ldots,H_N)\int_{\mathbf{z}_1}\frac{1}{\mathbf{z}_1^H(-\boldsymbol{\Sigma}_{21}\boldsymbol{\Sigma}_{11}^{-1}\boldsymbol{\Sigma}_{12}+\boldsymbol{\Sigma}_{22})\mathbf{z}_1} \\
&\quad\times e^{-\frac{|u-\mathbf{z}_1^H\boldsymbol{\Sigma}_{21}\boldsymbol{\Sigma}_{11}^{-1}\mathbf{z}_1|^2}{\mathbf{z}_1^H(-\boldsymbol{\Sigma}_{21}\boldsymbol{\Sigma}_{11}^{-1}\boldsymbol{\Sigma}_{12}+\boldsymbol{\Sigma}_{22})\mathbf{z}_1}} e^{-\mathbf{z}_1^H\boldsymbol{\Sigma}_{11}^{-1}\mathbf{z}_1} d\mathbf{z}_1 d\mathbf{g} d(H_2,\ldots,H_N) \\
&= \int_{(H_2,\ldots,H_N,\mathbf{g})}\frac{f(\mathbf{g})f(H_2,\ldots,H_N)}{\pi^{2M}\sigma^{2M}(C\|\mathbf{g}\|^2+1)}\int_{\mathbf{z}_1}\frac{1}{((\sigma^2C-\frac{\sigma^{-2}E^2\prod_{i=1}^N\beta_i^2\|\tilde{\mathbf{g}}\|^2}{1+C\|\tilde{\mathbf{g}}\|^2})\|\mathbf{z}_1\|^2|\tilde{g}_1|^2+\sigma^2\|\mathbf{z}_1\|^2)} \\
&\quad\times e^{-\frac{|u-\frac{\sigma^{-2}B^*}{1+C\|\tilde{\mathbf{g}}\|^2}\|\mathbf{z}_1\|^2|\tilde{g}_1|^2|^2}{(\sigma^2C-\frac{\sigma^{-2}|B|^2\|\tilde{\mathbf{g}}\|^2}{1+C\|\tilde{\mathbf{g}}\|^2})\|\mathbf{z}_1\|^2|\tilde{g}_1|^2+\sigma^2\|\mathbf{z}_1\|^2}} e^{-(\frac{-\sigma^{-2}C}{1+C\|\tilde{\mathbf{g}}\|^2}\|\mathbf{z}_1\|^2|\tilde{g}_1|^2+\sigma^{-2}\|\mathbf{z}_1\|^2)} d\mathbf{z}_1 d\mathbf{g} d(H_2,\ldots,H_N)
\end{aligned} \tag{3.7.25}$$

For a point $s_k = \sqrt{E}e^{\frac{j2\pi k}{Q}}$ of Q-PSK, we know that its corresponding symbol error probability is $P_e = \frac{1}{\pi}\int_0^{\frac{\pi(Q-1)}{Q}} e^{-\frac{E\sin^2\frac{\pi}{Q}}{2\tau^2\sin^2\theta}}d\theta$ with the PDF $f(y|s_k) = \frac{1}{2\pi\tau^2}e^{-\frac{|y-s_k|^2}{2\tau^2}}$. Thus, with letting $\sqrt{E_m} = \frac{\sigma^{-2}\prod_{i=0}^{N}\beta_i}{1+C\|\tilde{\mathbf{g}}\|^2}\|\mathbf{z}_1\|^2|\tilde{g}_1|^2$, we have

$$\begin{aligned}
&P_e(U|H_2,\ldots,H_N,\mathbf{g})\\
&=\int_{\mathbf{z}_1}\int_0^{\frac{\pi(Q-1)}{Q}} e^{-\frac{E_m\sin^2\frac{\pi}{Q}}{\mathbf{z}_1^H(-\boldsymbol{\Sigma}_{21}\boldsymbol{\Sigma}_{11}^{-1}\boldsymbol{\Sigma}_{12}+\boldsymbol{\Sigma}_{22})\mathbf{z}_1\sin^2\theta}}d\theta\frac{1}{\pi^{2M}|\boldsymbol{\Sigma}_{11}|}e^{-\mathbf{z}_1^H\boldsymbol{\Sigma}_{11}^{-1}\mathbf{z}_1}d\mathbf{z}_1\\
&=\int_{\mathbf{z}_1}\frac{1}{\pi^{2M}}\int_0^{\frac{\pi(Q-1)}{Q}} e^{-\frac{\frac{\sigma^{-4}\prod_{i=0}^{N}\beta_i^2}{(1+C\|\tilde{\mathbf{g}}\|^2)^2}\|\mathbf{z}_1\|^4|\tilde{g}_1|^4\sin^2\frac{\pi}{Q}}{((\sigma^2C-\frac{\sigma^{-2}\prod_{i=0}^{N}\beta_i^2\|\tilde{\mathbf{g}}\|^2}{1+C\|\tilde{\mathbf{g}}\|^2})\|\mathbf{z}_1\|^2|\tilde{g}_1|^2+\sigma^2\|\mathbf{z}_1\|^2)\sin^2\theta}}\frac{1}{\sigma^{2M}(C\|\mathbf{g}\|^2+1)}\\
&\quad\times e^{-(\frac{-\sigma^{-2}C}{1+C\|\tilde{\mathbf{g}}\|^2}\|\mathbf{z}_1\|^2|\tilde{g}_1|^2+\sigma^{-2}\|\mathbf{z}_1\|^2)}d\theta d\mathbf{z}_1
\end{aligned}\tag{3.7.26}$$

Consider the polar system, and let $r^2 = \|\mathbf{z}_1\|^2$, then (3.7.26) can be rewritten as

$$\begin{aligned}
&P_e(U|H_2,\ldots,H_N,\mathbf{g})\\
&=\int_0^{\frac{\pi(Q-1)}{Q}}\frac{1}{\pi^{2M}\sigma^{2M}(C\|\mathbf{g}\|^2+1)}\int_0^{\infty} e^{-\frac{\frac{\sigma^{-4}\prod_{i=0}^{N}\beta_i^2}{(1+C\|\tilde{\mathbf{g}}\|^2)^2}r^4|\tilde{g}_1|^4\sin^2\frac{\pi}{Q}}{((\sigma^2C-\frac{\sigma^{-2}\prod_{i=0}^{N}\beta_i^2\|\tilde{\mathbf{g}}\|^2}{1+C\|\tilde{\mathbf{g}}\|^2})r^2|\tilde{g}_1|^2+\sigma^2r^2)\sin^2\theta}}\\
&\quad\times e^{-(\frac{-\sigma^{-2}C}{1+C\|\tilde{\mathbf{g}}\|^2}r^2|\tilde{g}_1|^2+\sigma^{-2}r^2)}\frac{2\pi^M}{\Gamma(M)}r^{2M-1}drd\theta\\
&=\int_0^{\frac{\pi(Q-1)}{Q}}\frac{2(C\|\mathbf{g}\|^2+1)^{-1}}{\pi^M\sigma^{2M}\Gamma(M)}\int_0^{\infty} e^{-\frac{\sigma^{-6}|B|^2|\tilde{g}_1|^4\sin^2\frac{\pi}{Q}r^2}{(1+C\|\tilde{\mathbf{g}}\|^2)((C|\tilde{g}_1|^2+1)(1+C\|\tilde{\mathbf{g}}\|^2)-\sigma^{-4}|B|^2\|\tilde{\mathbf{g}}\|^2|\tilde{g}_1|^2)\sin^2\theta}}\\
&\quad\times e^{-(\frac{-\sigma^{-2}C}{1+C\|\tilde{\mathbf{g}}\|^2}r^2|\tilde{g}_1|^2+\sigma^{-2}r^2)}r^{2M-1}drd\theta\\
&=\int_0^{\frac{\pi(Q-1)}{Q}}\frac{1}{\pi^M\sigma^{2M}\Gamma(M)(C\|\mathbf{g}\|^2+1)}\int_0^{\infty}t^{M-1}\\
&\quad\times e^{-\frac{t}{\sigma^2}\frac{\sigma^{-4}|B|^2|\tilde{g}_1|^4\sin^2\frac{\pi}{Q}+(1+C\|\tilde{\mathbf{g}}\|^2-C|\tilde{g}_1|^2)((C|\tilde{g}_1|^2+1)(1+C\|\tilde{\mathbf{g}}\|^2)-\sigma^{-4}|B|^2\|\tilde{\mathbf{g}}\|^2|\tilde{g}_1|^2)\sin^2\theta}{(1+C\|\tilde{\mathbf{g}}\|^2)((C|\tilde{g}_1|^2+1)(1+C\|\tilde{\mathbf{g}}\|^2)-\sigma^{-4}|B|^2\|\tilde{\mathbf{g}}\|^2|\tilde{g}_1|^2)\sin^2\theta}}dtd\theta
\end{aligned}\tag{3.7.27}$$

Since $\int_0^\infty x^n e^{-\mu x} dx = n!\mu^{-n-1}$, then we have

$$P_e(U|H_2,\ldots,H_N,\mathbf{g}) = \int_0^{\frac{\pi(Q-1)}{Q}} \frac{(C\|\mathbf{g}\|^2+1)^{-1}}{\pi^M}$$
$$\left(\frac{(1+C\|\tilde{\mathbf{g}}\|^2)((C|\tilde{g}_1|^2+1)(1+C\|\tilde{\mathbf{g}}\|^2)-\sigma^{-4}|B|^2\|\tilde{\mathbf{g}}\|^2|\tilde{g}_1|^2)\sin^2\theta}{\sigma^{-4}|B|^2|\tilde{g}_1|^4\sin^2\frac{\pi}{Q}+(1+C\|\tilde{\mathbf{g}}\|^2-C|\tilde{g}_1|^2)((C|\tilde{g}_1|^2+1)(1+C\|\tilde{\mathbf{g}}\|^2)-\sigma^{-4}|B|^2\|\tilde{\mathbf{g}}\|^2|\tilde{g}_1|^2)\sin^2\theta}\right)^M d\theta$$
$$= \int_0^{\frac{\pi(Q-1)}{Q}} \frac{1}{\pi^M}\times$$
$$\frac{(1+C\|\tilde{\mathbf{g}}\|^2)^{M-1}\left(((C|\tilde{g}_1|^2+1)(1+C\|\tilde{\mathbf{g}}\|^2)-\sigma^{-4}|B|^2\|\tilde{\mathbf{g}}\|^2|\tilde{g}_1|^2)\sin^2\theta\right)^M}{\left(\sigma^{-4}|B|^2|\tilde{g}_1|^4\sin^2\frac{\pi}{Q}+(1+C\|\tilde{\mathbf{g}}\|^2-C|\tilde{g}_1|^2)((C|\tilde{g}_1|^2+1)(1+C\|\tilde{\mathbf{g}}\|^2)-\sigma^{-4}|B|^2\|\tilde{\mathbf{g}}\|^2|\tilde{g}_1|^2)\sin^2\theta\right)^M} d\theta, \tag{3.7.28}$$

with the fact that $\Gamma(M) = (M-1)!$. Let SNR $= \frac{\beta_0}{\sigma^2}$. Since $C = \frac{|H_2|^2\prod_{i=0}^N \beta_i}{\sigma^2} + \sum_{k=1}^{N-1}|H_{k+1}|^2\prod_{i=k}^N \beta_i + \beta_N$, we know that the highest order of $P_e(U|H_2,\ldots,H_N,\mathbf{g})$ is SNR^{-1}.

Theorem 3.4 *If the channel coefficients are given, then the conditional symbol error probability is given by*

$$P_e(U|H_2,\ldots,H_N)$$
$$= \int_0^{\frac{\pi(Q-1)}{Q}} \int_0^\infty \frac{e^{-v}R_3^{M-1}}{\pi^{M+1}\Gamma(M-1)} \left(\sum_{k=0}^{M-2}\sum_{t=k}^{M-2}\sum_{i=1}^{M-t-1} \frac{(-1)^t k! \binom{M}{k}\binom{M-2}{t-k} R_1^k R_2^{M-k-i-1} R_3^{-i}}{(M-t-i-1)!} \right.$$
$$+ \sum_{k=1}^{M}\sum_{t=\max\{M-1,k\}}^{M-2+k} \binom{M}{k}\binom{M-2}{t-k}(-1)^t R_1^k R_2^{t-k}\sum_{i=1}^{t-M+1}\frac{(-R_3)^{t-M-i+1}(i-1)!}{R_2^i(t-M+1)!}$$
$$\left. - \sum_{k=1}^{M}\sum_{t=\max\{M-1,k\}}^{M-2+k} \binom{M}{k}\binom{M-2}{t-k}(-1)^t R_1^k R_2^{t-k}\frac{(-R_3)^{t-M+1}}{(t-M+1)!}e^{R_2R_3}Ei(-R_2R_3)\right) dv d\theta, \tag{3.7.29}$$

where $C = \frac{|H_2|^2 \prod_{i=0}^{N} \beta_i}{\sigma^2} + \sum_{k=1}^{N-1} |H_{k+1}|^2 \prod_{i=k}^{N} \beta_i + \beta_N$, $D_s = C^2 - \sigma^{-4}|B|^2$, $R_1 = \frac{\sigma^{-4}|B|^2 v^2 \sin^2 \frac{\pi}{Q}}{(CD_s v^2 + D_s v)\sin^2 \theta}$, $R_2 = \frac{(D_s v^2 + 2Cv + 1)\sin^2 \theta + \sigma^{-4}|B|^2 v^2 \sin^2 \frac{\pi}{Q}}{(CD_s v^2 + D_s v)\sin^2 \theta}$, *and* $R_3 = Cv + 1$.

Proof The proof is provided in Appendix 3.F. $\square$

3.8 Numerical Results

Computer simulations are carried out in this section. The system SNR is defined by $\eta \triangleq 1/2\sigma^2$. For simplicity, we denote a vector consisting of power coefficients by $\Delta = (P_0, \ldots, P_N)$.

Fig. 3.3 and Fig. 3.4 show the frame error performance (FER) comparison with different constellation sizes and different relay numbers, respectively. (Here, by FER we mean one minus probability that all symbols from all users in the block of $T = 2$ channel uses are received correctly.) Both the ML detector and simplified detector are considered. In Fig. 3.3, $\Delta = (5, 10, 15)$, $N = 2$, $M = 2$, $|\mathcal{S}_{i,t}| = 2$ for $i = 0, 1$ and $t = 1, 2$. The different curves arise from different choices for the size of the constellation for the second relay. We make two choices, $|\mathcal{S}_{2,t}| = 4, 2$ for $t = 1, 2$, which imply in these scenarios that 256-PSK and 64-PSK constellations are received at the destination, respectively. In Fig. 3.4, we make three choices for the number of relays, $N = 3, 2, 1$, along with $M = 2$, $|\mathcal{S}_{i,t}| = 2$ for $0 \le i \le N$, $t = 1, 2$ and $\Delta = (5, 10, 15, 20)$, $\Delta = (5, 10, 15)$ and $\Delta = (5, 10)$, respectively, which implies that 256-PSK, 64-PSK, and 16-PSK constellations are also received at the destination in this experiment. From these two figures, it can be seen that, simplified detector exhibits a similar performance with ML detector. Moreover, the frame error decreases with SNR in a way that was predicted by the diversity gain result after (3.7.26). The differing rates of the transmission account for the offsets between the curves at high SNRs.

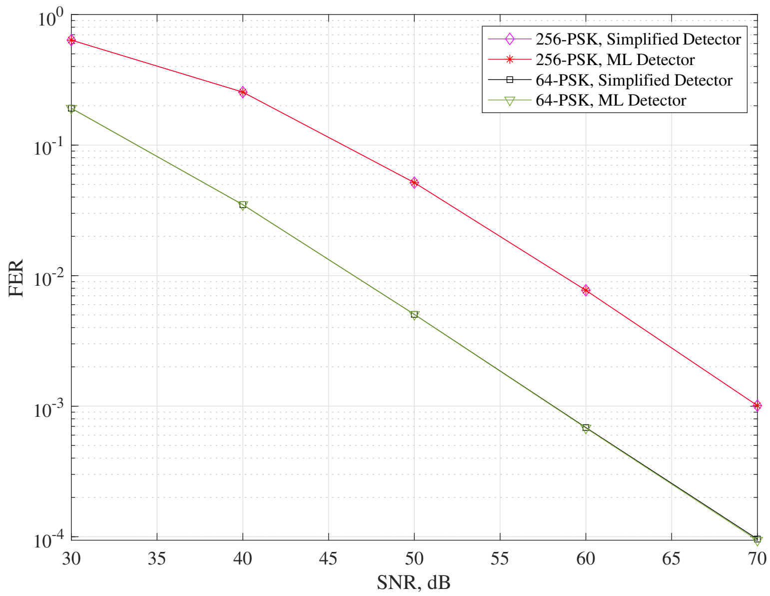

Figure 3.3: Comparison among two-relay based system with different constellation sizes.

Fig. 3.5 shows the performance comparison when the number of antennas M increases, where $\Delta = (5, 10, 15)$, $N = 2$, $|\mathcal{S}_{i,t}| = 2$ for $0 \leq i \leq N$ and $t = 1, 2$. It can be seen that the performance cannot be significantly improved by increasing M.

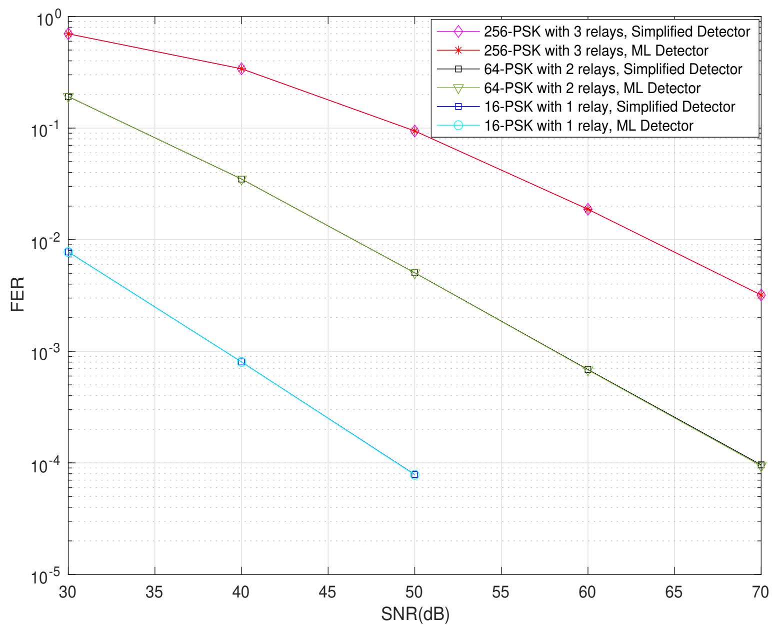

Figure 3.4: Comparison among the proposed scheme for different relay numbers.

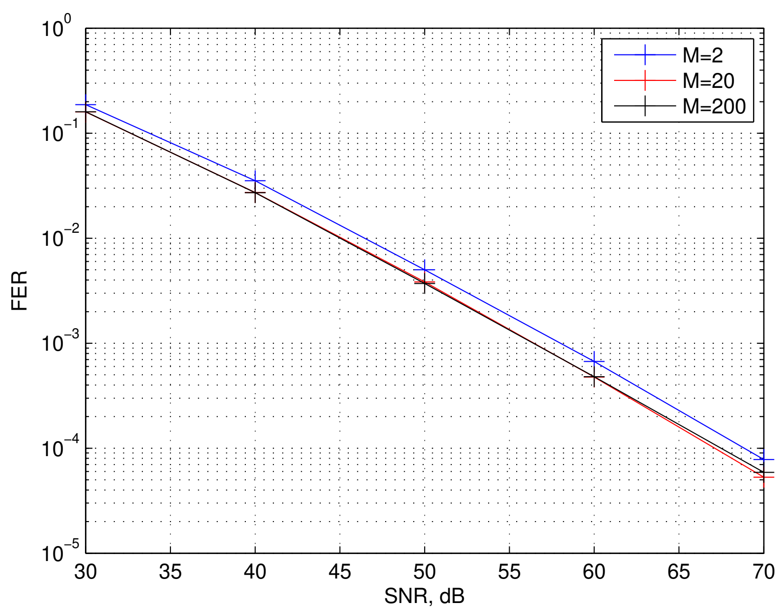

Figure 3.5: Comparison among the proposed scheme for different antenna numbers.

3.9 Conclusions

In this chapter, we developed a novel approach to communicating non-coherently over a multi-hop relay-assisted system that allows the source and the relay to transmit their own information. By employing uniquely factorable constellations, we were able to reduce the ML detector to a simple symbol-by-symbol detector that employs phase quantization. In addition, the symbol error probability formula was given, showing that the system achieves a diversity gain of 1.

3.A Appendix: Proof of Theorem 3.1

Let $q = \sum_{k=1}^{r} q_k$, $s_1 = \exp(\frac{j2\pi n_1}{2^{q_1}})$ and $\tilde{s}_1 = \exp(\frac{j2\pi \tilde{n}_1}{2^{q_1}})$, $s_i = \exp(\frac{j2\pi n_i \prod_{k=1}^{i-1}(2^{q_k}-1)}{2^{\sum_{k=1}^{i} q_k}})$ and $\tilde{s}_i = \exp(\frac{j2\pi \tilde{n}_i \prod_{k=1}^{i-1}(2^{q_k}-1)}{2^{\sum_{k=1}^{i} q_k}})$, where $0 \leq n_i, \tilde{n}_i \leq 2^{q_i} - 1$ and $2 \leq i \leq r$.

According to the property of the PSK constellation, the equation $s_1 s_2 \cdots s_r = \tilde{s}_1 \tilde{s}_2 \cdots \tilde{s}_r$ is equivalent to

$$n_1 2^{\sum_{k=2}^{r} q_k} + \sum_{i=2}^{r} n_i 2^{\sum_{k=i+1}^{r} q_k} \prod_{k=1}^{i-1}(2^{q_k}-1) = \tilde{n}_1 2^{\sum_{k=2}^{r} q_k} + \sum_{i=2}^{r} \tilde{n}_i 2^{\sum_{k=i+1}^{r} q_k} \prod_{k=1}^{i-1}(2^{q_k}-1) \bmod 2^q, \tag{3.A.1}$$

i.e.,

$$(n_1 - \tilde{n}_1) 2^{\sum_{k=2}^{r} q_k} + \sum_{i=2}^{r} (n_i - \tilde{n}_i) 2^{\sum_{k=i+1}^{r} q_k} \prod_{k=1}^{i-1}(2^{q_k} - 1) \equiv 0 \bmod 2^q, \tag{3.A.2}$$

where the notation $a \equiv b \bmod m$ means $m|(a-b)$.

Since $2^{q_r}|2^q$, we have $(n_r - \tilde{n}_r)\prod_{k=1}^{r-1}(2^{q_k}-1) \equiv 0 \bmod 2^{q_r}$. Moreover, due to the fact that $(\prod_{k=1}^{r-1}(2^{q_k}-1), 2^{q_r}) = 1$, then we have $2^{q_r}|(n_r - \tilde{n}_r)$. Since $0 \leq n_r, \tilde{n}_r \leq 2^{q_r} - 1$, we can obtain $n_r = \tilde{n}_r$, and as a result, (3.A.2) can be reduced to

$$(n_1 - \tilde{n}_1)2^{\sum_{k=2}^{r} q_k} + \sum_{i=2}^{r-1}(n_i - \tilde{n}_i)2^{\sum_{k=i+1}^{r} q_k}\prod_{k=1}^{i-1}(2^{q_k} - 1) \equiv 0 \bmod 2^q. \tag{3.A.3}$$

Dividing both sides by 2^{q_r} yields

$$(n_1-\tilde{n}_1)2^{\sum_{k=2}^{r-1} q_k}+\sum_{i=2}^{r-1}(n_i-\tilde{n}_i)2^{\sum_{k=i+1}^{r-1} q_k}\prod_{k=1}^{i-1}(2^{q_k}-1) \equiv 0 \bmod 2^{q-q_r} = 2^{\sum_{k=1}^{r-1} q_k}. \tag{3.A.4}$$

Similarly, since $2^{q_{r-1}}|2^{\sum_{k=1}^{r-1} q_k}$, we have $(n_{r-1} - \tilde{n}_{r-1})\prod_{k=1}^{r-2}(2^{q_k} - 1) \equiv 0 \bmod 2^{q_r}$, and $2^{q_{r-1}}|(n_{r-1} - \tilde{n}_{r-1})$ based on the fact that $(\prod_{k=1}^{r-2}(2^{q_k} - 1), 2^{q_{r-1}}) = 1$. Since $0 \le n_r, \tilde{n}_r \le 2^{q_r} - 1$, we have $n_{r-1} = \tilde{n}_{r-1}$.

Repeatedly, we can obtain that $n_i = \tilde{n}_i$ for any $i \ge 2$ and (3.A.2) can be reduced to

$$(n_1 - \tilde{n}_1) \equiv 0 \bmod 2^{q_1}, \tag{3.A.5}$$

which suggests that $2^{q_1}|(n_1 - \tilde{n}_1)$. Since $0 \le n_1, \tilde{n}_1 \le 2^{q_1} - 1$, we have $n_1 = \tilde{n}_1$. Therefore, $s_i = \tilde{s}_i$ for any $1 \le i \le r$ and such a set of $\{\mathcal{S}_i\}$ constitutes a UFCS. The proof is completed.

3.B Appendix: Proof of Theorem 3.2

Let $s = \exp(\frac{j2\pi n}{2^q})$, $s_1 = \exp(\frac{j2\pi n_1}{2^{q_1}})$, and $s_i = \exp(\frac{j2\pi n_i \prod_{k=1}^{i-1}(2^{q_k}-1)}{2^{\sum_{k=1}^{i} q_k}})$ for $2 \le i \le r$. Then, equation $s_1 s_2 \cdots s_r = s$ is equivalent to

$$n_1 2^{\sum_{k=2}^{r} q_k} + \sum_{i=2}^{r} n_i 2^{\sum_{k=i+1}^{r} q_k}\prod_{k=1}^{i-1}(2^{q_k} - 1) \equiv n \bmod 2^q. \tag{3.B.1}$$

Since $2^{q_r}|2^q$, we have

$$n_r \prod_{k=1}^{r-1}(2^{q_k}-1) \equiv n \bmod 2^{q_r}. \tag{3.B.2}$$

Due to the fact that 2^{q_r} and any $2^{q_k}-1$ $(1 \le k \le j-1)$ are co-prime, with the help of Euler theorem, we have

$$\prod_{k=1}^{r-1}(2^{q_k}-1)^{2^{q_r-1}} \equiv 1 \bmod 2^{q_r}. \tag{3.B.3}$$

By combining (3.B.2) and (3.B.3), we can obtain

$$n_r \equiv n \prod_{k=1}^{r-1}(2^{q_k}-1)^{2^{q_r-1}-1} \bmod 2^{q_r}. \tag{3.B.4}$$

There is only one solution to (3.B.4), such that $0 \le n_r \le 2^{q_r}-1$. In other words, the solution to n_r is unique. On the other hand, according to (3.B.2), we have $2^{q_r}|(n - n_r \prod_{k=1}^{r-1}(2^{q_k}-1))$. Therefore, (3.B.1) can be reduced to

$$n_1 2^{\sum_{k=2}^{r-1} q_k} + \sum_{i=2}^{r-1} n_i 2^{\sum_{k=i+1}^{r-1} q_k} \prod_{k=1}^{i-1}(2^{q_k}-1) \equiv \frac{(n - n_r \prod_{k=1}^{r-1}(2^{q_k}-1))}{2^{q_r}} \bmod 2^{q-q_r} = 2^{\sum_{k=1}^{r-1} q_k}. \tag{3.B.5}$$

Similarly, since $2^{q_{r-1}}|2^{\sum_{k=1}^{r-1} q_k}$, we have

$$n_{r-1} \prod_{k=1}^{r-2}(2^{q_k}-1) \equiv \frac{(n - n_r \prod_{k=1}^{r-1}(2^{q_k}-1))}{2^{q_r}} \bmod 2^{q_{r-1}}. \tag{3.B.6}$$

Moreover, since $2^{q_{r-1}}$ and any $2^{q_k}-1$ $(1 \le k \le r-2)$ are co-prime, with the help of Euler theorem, we have,

$$\prod_{k=1}^{r-2}(2^{q_k}-1)^{2^{q_{r-1}-1}} \equiv 1 \bmod 2^{q_{r-1}}. \tag{3.B.7}$$

Then, by combining (3.B.6) and (3.B.7), we can arrive at

$$n_{r-1} \equiv \frac{(n - n_r \prod_{k=1}^{r-1}(2^{q_k}-1)) \prod_{k=1}^{r-2}(2^{q_k}-1)^{2^{q_{r-1}-1}-1}}{2^{q_r}} \bmod 2^{q_{r-1}}, \tag{3.B.8}$$

which can also be uniquely determined for $0 \le n_{r-1} \le 2^{q_{r-1}}-1$.

Repeatedly, we can obtain that for any $i \ge 2$,

$$n_i \equiv \frac{(n - \sum_{t=i+1}^{r} n_t 2^{\sum_{k=t+1}^{r} q_k} \prod_{k=1}^{t-1}(2^{q_k}-1)) \prod_{k=1}^{i-1}(2^{q_k}-1)^{2^{q_i-1}-1}}{2^{\sum_{k=i+1}^{r} q_k}} \bmod 2^{q_i}, \tag{3.B.9}$$

which is also uniquely determined for $0 \le n_i \le 2^{q_i}-1$. Then, according to (3.B.1), we have

$$n_1 \equiv \frac{n - \sum_{t=2}^{r} n_t 2^{\sum_{k=t+1}^{r} q_k} \prod_{k=1}^{t-1}(2^{q_k}-1)}{2^{\sum_{k=2}^{r} q_k}} \bmod 2^{q_1}, \tag{3.B.10}$$

where n_1 can also be uniquely determined for $0 \le n_1 \le 2^{q_1}-1$. This complete the proof of Theorem 3.2.

3.C Appendix: Proof for Theorem 3.3

Proof For ML detection, we have

$$\hat{\mathbf{x}} = \arg\max_{\mathbf{x}} -\mathbf{z}^H \mathbf{\Sigma}^{-1}\mathbf{z}, \tag{3.C.1}$$

where according to (3.5.4), we have that

$$\mathbf{\Sigma} = |H_2|^2\mathbf{X}_0\mathbf{G}\mathbf{X}_0^H + \sum_{k=1}^{N-1} |H_{k+1}|^2\mathbb{E}[\mathbf{D}_k\mathbf{G}\mathbf{D}_k^H] + \mathbb{E}[\mathbf{D}_N\mathbf{G}\mathbf{D}_N^H] + \mathbf{\Xi} \tag{3.C.2}$$

Since the matrix $\mathbf{G} = \mathbf{g}\mathbf{g}^H$ is rank-1, it can be written as $\mathbf{G} = \|\mathbf{g}\|^2\mathbf{u}_1\mathbf{u}_1^H$, where $\mathbf{u}_1 = \mathbf{g}/\|\mathbf{g}\|$. Hence

$$\mathbf{D}_k\mathbf{G}\mathbf{D}_k^H = \|\mathbf{g}\|^2 \begin{bmatrix} |\eta_{k,1}|^2|X_{k+1,1}|^2\mathbf{u}_1\mathbf{u}_1^H & \eta_{k,1}\eta_{k,2}^*X_{k+1,1}X_{k+1,2}^*\mathbf{u}_1\mathbf{u}_1^H \\ \eta_{k,2}\eta_{k,1}^*X_{k+1,2}X_{k+1,1}^*\mathbf{u}_1\mathbf{u}_1^H & |\eta_{k,2}|^2|X_{k+1,2}|^2\mathbf{u}_1\mathbf{u}_1^H \end{bmatrix}. \tag{3.C.3}$$

Therefore, we have

$$\begin{aligned}\mathbb{E}[\mathbf{D}_k\mathbf{G}\mathbf{D}_k^H] &= \|\mathbf{g}\|^2\mathbb{E} \begin{bmatrix} |\eta_{k,1}|^2|X_{k+1,1}|^2\mathbf{u}_1\mathbf{u}_1^H & \eta_{k,1}\eta_{k,2}^*X_{k+1,1}X_{k+1,2}^*\mathbf{u}_1\mathbf{u}_1^H \\ \eta_{k,2}\eta_{k,1}^*X_{k+1,2}X_{k+1,1}^*\mathbf{u}_1\mathbf{u}_1^H & |\eta_{k,2}|^2|X_{k+1,2}|^2\mathbf{u}_1\mathbf{u}_1^H \end{bmatrix} \\ &= \|\mathbf{g}\|^2 \begin{bmatrix} \sigma^2|X_{k+1,1}|^2\mathbf{u}_1\mathbf{u}_1^H & \mathbf{0} \\ \mathbf{0} & \sigma^2|X_{k+1,2}|^2\mathbf{u}_1\mathbf{u}_1^H. \end{bmatrix}. \end{aligned} \tag{3.C.4}$$

Similarly, we have

$$\mathbf{X}_0\mathbf{G}\mathbf{X}_0^H = \|\mathbf{g}\|^2 \begin{bmatrix} |X_{0,1}|^2\mathbf{u}_1\mathbf{u}_1^H & X_{0,1}X_{0,2}^*\mathbf{u}_1\mathbf{u}_1^H \\ X_{0,2}X_{0,1}^*\mathbf{u}_1\mathbf{u}_1^H & |X_{0,2}|^2\mathbf{u}_1\mathbf{u}_1^H \end{bmatrix}. \tag{3.C.5}$$

Now we can rewrite (3.C.2) as follows

$$\begin{aligned}\mathbf{\Sigma} =&|H_2|^2\|\mathbf{g}\|^2\begin{bmatrix}|X_{0,1}|^2\mathbf{u}_1\mathbf{u}_1^H & X_{0,1}X_{0,2}^*\mathbf{u}_1\mathbf{u}_1^H\\ X_{0,2}X_{0,1}^*\mathbf{u}_1\mathbf{u}_1^H & |X_{0,2}|^2\mathbf{u}_1\mathbf{u}_1^H\end{bmatrix}+\sum_{k=1}^{N-1}|H_{k+1}|^2\|\mathbf{g}\|^2\begin{bmatrix}\sigma^2|X_{k,1}|^2\mathbf{u}_1\mathbf{u}_1^H & \mathbf{0}\\ \mathbf{0} & \sigma^2|X_{k,2}|^2\mathbf{u}_1\mathbf{u}_1^H\end{bmatrix}\\ &+\|\mathbf{g}\|^2\begin{bmatrix}\sigma^2|X_{N,1}|^2\mathbf{u}_1\mathbf{u}_1^H & \mathbf{0}\\ \mathbf{0} & \sigma^2|X_{N,2}|^2\mathbf{u}_1\mathbf{u}_1^H\end{bmatrix}+\mathbf{\Xi}\\ &=\sigma^2\begin{bmatrix}\mathbf{V} & \mathbf{0}\\ \mathbf{0} & \mathbf{V}\end{bmatrix}\begin{bmatrix}\frac{\|\mathbf{g}\|^2}{\sigma^2}A+1 & \dots & 0 & \frac{\|\mathbf{g}\|^2}{\sigma^2}B & \dots & 0\\ \vdots & \ddots & \vdots & \vdots & \ddots & \vdots\\ 0 & \dots & 1 & 0 & \dots & 0\\ \frac{\|\mathbf{g}\|^2}{\sigma^2}B^* & \dots & 0 & \frac{\|\mathbf{g}\|^2}{\sigma^2}A+1 & \dots & 0\\ \vdots & \ddots & \vdots & \vdots & \ddots & \vdots\\ 0 & \dots & 0 & 0 & \dots & 1\end{bmatrix}\begin{bmatrix}\mathbf{V}^H & \mathbf{0}\\ \mathbf{0} & \mathbf{V}^H\end{bmatrix}\end{aligned} \tag{3.C.6}$$

where $\mathbf{V}=[\mathbf{u}_1,\mathbf{W}]$ and the columns of $\mathbf{W}\in\mathbb{C}^{M\times(M-1)}$ form an orthogonal basis for the subspace that is the orthogonal complement of $\mathbf{u}_1$ in $\mathbb{C}^M$. Since $|X_{i,1}|=|X_{i,2}|$ for all $i=0,1,\dots,N$, we can define

$$\begin{aligned}A&=|H_2|^2|X_{0,j}|^2+\sigma^2\sum_{k=1}^{N-1}|H_{k+1}|^2|X_{k,j}|^2+\sigma^2|X_{N,j}|^2\\ &=|H_2|^2\prod_{i=0}^{N}\beta_i+(\sum_{k=1}^{N-1}|H_{k+1}|^2\prod_{i=k}^{N}\beta_i+\beta_N)\sigma^2.\end{aligned} \tag{3.C.7}$$

Furthermore, as defined before, $B\in\tilde{\mathcal{S}}$. Let

$$\Phi=\begin{vmatrix}\frac{\|\mathbf{g}\|^2}{\sigma^2}A+1 & \frac{\|\mathbf{g}\|^2}{\sigma^2}B\\ \frac{\|\mathbf{g}\|^2}{\sigma^2}B^* & \frac{\|\mathbf{g}\|^2}{\sigma^2}A+1\end{vmatrix}. \tag{3.C.8}$$

Then, we know that

$$|\mathbf{\Sigma}|=\sigma^{4M}\Phi. \tag{3.C.9}$$

By taking the block matrix inverse (see [71, section 9.1.3]), we have

$$\begin{bmatrix} \frac{\|\mathbf{g}\|^2}{\sigma^2}A+1 & \dots & 0 & \frac{\|\mathbf{g}\|^2}{\sigma^2}B & \dots & 0 \\ \vdots & \ddots & \vdots & \vdots & \ddots & \vdots \\ 0 & \dots & 1 & 0 & \dots & 0 \\ \frac{\|\mathbf{g}\|^2}{\sigma^2}B^* & \dots & 0 & \frac{\|\mathbf{g}\|^2}{\sigma^2}A+1 & \dots & 0 \\ \vdots & \ddots & \vdots & \vdots & \ddots & \vdots \\ 0 & \dots & 0 & 0 & \dots & 1 \end{bmatrix}^{-1} = \begin{bmatrix} (\frac{\|\mathbf{g}\|^2}{\sigma^2}A+1)/\Phi & \dots & 0 & -\frac{\|\mathbf{g}\|^2}{\sigma^2}B/\Phi & \dots & 0 \\ \vdots & \ddots & \vdots & \vdots & \ddots & \vdots \\ 0 & \dots & 1 & 0 & \dots & 0 \\ -\frac{\|\mathbf{g}\|^2}{\sigma^2}B^*/\Phi & \dots & 0 & (\frac{\|\mathbf{g}\|^2}{\sigma^2}A+1)/\Phi & \dots & 0 \\ \vdots & \ddots & \vdots & \vdots & \ddots & \vdots \\ 0 & \dots & 0 & 0 & \dots & 1 \end{bmatrix}. \tag{3.C.10}$$

Then, we have

$$\begin{aligned} \mathbf{\Sigma}^{-1} &= \sigma^{-2}\begin{bmatrix} \mathbf{V} & \mathbf{0} \\ \mathbf{0} & \mathbf{V} \end{bmatrix} \begin{bmatrix} (\frac{\|\mathbf{g}\|^2}{\sigma^2}A+1)/\Phi & \dots & 0 & -\frac{\|\mathbf{g}\|^2}{\sigma^2}B/\Phi & \dots & 0 \\ \vdots & \ddots & \vdots & \vdots & \ddots & \vdots \\ 0 & \dots & 1 & 0 & \dots & 0 \\ -\frac{\|\mathbf{g}\|^2}{\sigma^2}B^*/\Phi & \dots & 0 & (\frac{\|\mathbf{g}\|^2}{\sigma^2}A+1)/\Phi & \dots & 0 \\ \vdots & \ddots & \vdots & \vdots & \ddots & \vdots \\ 0 & \dots & 0 & 0 & \dots & 1 \end{bmatrix} \begin{bmatrix} \mathbf{V}^H & \mathbf{0} \\ \mathbf{0} & \mathbf{V}^H \end{bmatrix} \\ &= \begin{bmatrix} (\frac{A}{\sigma^4\Phi} + \frac{1-\Phi}{\sigma^2\|\mathbf{g}\|^2 T})\mathbf{g}\mathbf{g}^H & -\frac{B}{\sigma^4\Phi}\mathbf{g}\mathbf{g}^H \\ -\frac{B^*}{\sigma^4\Phi}\mathbf{g}\mathbf{g}^H & (\frac{A}{\sigma^4\Phi} + \frac{1-\Phi}{\sigma^2\|\mathbf{g}\|^2\Phi})\mathbf{g}\mathbf{g}^H \end{bmatrix} + \frac{1}{\sigma^2}\begin{bmatrix} \mathbf{I}_M & \mathbf{0} \\ \mathbf{0} & \mathbf{I}_M \end{bmatrix} \\ &= \frac{1}{\sigma^4 T}\begin{bmatrix} \frac{A\|\mathbf{g}\|^2+\sigma^2(1-\Phi)}{\|\mathbf{g}\|^2}\mathbf{I}_M & -B\mathbf{I}_M \\ -B^*\mathbf{I}_M & \frac{A\|\mathbf{g}\|^2+\sigma^2(1-\Phi)}{\|\mathbf{g}\|^2}\mathbf{I}_M \end{bmatrix} \begin{bmatrix} \mathbf{G} & \mathbf{0} \\ \mathbf{0} & \mathbf{G} \end{bmatrix} + \frac{1}{\sigma^2}\begin{bmatrix} \mathbf{I}_M & \mathbf{0} \\ \mathbf{0} & \mathbf{I}_M \end{bmatrix}. \end{aligned} \tag{3.C.11}$$

Therefore,

$$\begin{aligned} \mathbf{z}^H\mathbf{\Sigma}^{-1}\mathbf{z} =& \frac{1}{\sigma^4\Phi}\begin{pmatrix} \mathbf{z}_1 \\ \mathbf{z}_2 \end{pmatrix}^H \left(\begin{bmatrix} \frac{A\|\mathbf{g}\|^2+\sigma^2(1-\Phi)}{\|\mathbf{g}\|^2}\mathbf{I}_M & -B\mathbf{I}_M \\ -B^*\mathbf{I}_M & \frac{A\|\mathbf{g}\|^2+\sigma^2(1-\Phi)}{\|\mathbf{g}\|^2}\mathbf{I}_M \end{bmatrix} \begin{bmatrix} \mathbf{G} & \mathbf{0} \\ \mathbf{0} & \mathbf{G} \end{bmatrix} \right) \begin{pmatrix} \mathbf{z}_1 \\ \mathbf{z}_2 \end{pmatrix} \\ &+ \frac{1}{\sigma^2}\begin{pmatrix} \mathbf{z}_1 \\ \mathbf{z}_2 \end{pmatrix}^H \begin{pmatrix} \mathbf{z}_1 \\ \mathbf{z}_2 \end{pmatrix}. \end{aligned} \tag{3.C.12}$$

Since the second term does not depend on the symbols, we can restrict attention to the first term. For that term we have

$$\frac{1}{\sigma^4\Phi}\begin{pmatrix}\mathbf{z}_1\\\mathbf{z}_2\end{pmatrix}^H\left(\begin{bmatrix}\frac{A\|\mathbf{g}\|^2+\sigma^2(1-\Phi)}{\|\mathbf{g}\|^2}\mathbf{I}_M & -B\mathbf{I}_M\\ -B^*\mathbf{I}_M & \frac{A\|\mathbf{g}\|^2+\sigma^2(1-\Phi)}{\|\mathbf{g}\|^2}\mathbf{I}_M\end{bmatrix}\begin{bmatrix}\mathbf{G} & \mathbf{0}\\ \mathbf{0} & \mathbf{G}\end{bmatrix}\right)\begin{pmatrix}\mathbf{z}_1\\\mathbf{z}_2\end{pmatrix}$$
$$= \frac{1}{\sigma^4\Phi}\frac{A\|\mathbf{g}\|^2+\sigma^2(1-\Phi)}{\|\mathbf{g}\|^2}(\mathbf{z}_1^H\mathbf{G}\mathbf{z}_1+\mathbf{z}_2^H\mathbf{G}\mathbf{z}_2) - \frac{1}{\sigma^4\Phi}(B^*\mathbf{z}_2^H\mathbf{G}\mathbf{z}_1+B\mathbf{z}_1^H\mathbf{G}\mathbf{z}_2) \tag{3.C.13}$$

Moreover, we also have $B^*\mathbf{z}_2^H\mathbf{G}\mathbf{z}_1+B\mathbf{z}_1^H\mathbf{G}\mathbf{z}_2 = \Re(B\mathbf{z}_1^H\mathbf{G}\mathbf{z}_2)$. Since $\mathbf{z}_1^H\mathbf{G}\mathbf{z}_1+\mathbf{z}_2^H\mathbf{G}\mathbf{z}_2$ is determined solely by $\mathbf{z}$ and $\mathbf{G}$, and A and Φ are independent of the data symbols, we have the claim. □

3.D Appendix: Lemma for ML detector with eigenvalues

Lemma 3.1 *Let* $\mathbf{S} = \begin{bmatrix}\mathbf{z}_1 & \mathbf{z}_2\end{bmatrix}\begin{bmatrix}0 & B^*\\ B & 0\end{bmatrix}\begin{bmatrix}\mathbf{z}_1^H\\ \mathbf{z}_2^H\end{bmatrix}$ *and* $\mathbf{S} = \mathbf{U}\mathbf{\Lambda}\mathbf{U}^H$ *be its eigenvalue decomposition and let* $\bar{g}_i$ *denote the elements of* $\bar{\mathbf{g}}$. *Then, the ML detection problem can be reformulated as* $\hat{x} = \arg\max \lambda_1|\bar{g}_1|^2+\lambda_2|\bar{g}_2|^2$. *Note that* $\bar{g}_i = u_i^H\mathbf{g}$, *where* u_i *is the* i*-th column of* $\mathbf{U}$.

Proof The term $\Re(B\mathbf{z}_1^H\mathbf{G}\mathbf{z}_2) = B^*\mathbf{z}_2^H\mathbf{G}\mathbf{z}_1 + B\mathbf{z}_1^H\mathbf{G}\mathbf{z}_2$ can be rewritten as follows,

$$\begin{aligned}
& B^*\mathbf{z}_2^H\mathbf{G}\mathbf{z}_1 + B\mathbf{z}_1^H\mathbf{G}\mathbf{z}_2 \\
&= \mathrm{tr}(B^*\mathbf{z}_2^H\mathbf{G}\mathbf{z}_1) + \mathrm{tr}(B\mathbf{z}_1^H\mathbf{G}\mathbf{z}_2) \\
&= \mathrm{tr}(B^*\mathbf{g}^H\mathbf{z}_1\mathbf{z}_2^H\mathbf{g}) + \mathrm{tr}(B\mathbf{g}^H\mathbf{z}_2\mathbf{z}_1^H\mathbf{g}) \\
&= \mathbf{g}^H \begin{bmatrix} \mathbf{z}_1 & \mathbf{z}_2 \end{bmatrix} \begin{bmatrix} 0 & B^* \\ B & 0 \end{bmatrix} \begin{bmatrix} \mathbf{z}_1^H \\ \mathbf{z}_2^H \end{bmatrix} \mathbf{g}.
\end{aligned} \tag{3.D.1}$$

Let $\mathbf{S} = \begin{bmatrix} \mathbf{z}_1 & \mathbf{z}_2 \end{bmatrix} \begin{bmatrix} 0 & B^* \\ B & 0 \end{bmatrix} \begin{bmatrix} \mathbf{z}_1^H \\ \mathbf{z}_2^H \end{bmatrix}$, where $\mathrm{rank}(\mathbf{S}) \leq 2$. Then, we consider the eigenvalue decomposition (EVD) of $\mathbf{S}$, i.e., $\mathbf{S} = \mathbf{U}\boldsymbol{\Lambda}\mathbf{U}^H$. Here, we assume that λ_1 is the largest in absolute value with the remaining nonzero eigenvalues are arranged in descending order, the eigenvectors are reordered to correspond with the ordering of the eigenvalues, resulting in $\mathbf{U}$. Furthermore, let $\bar{\mathbf{g}} = \mathbf{U}^H\mathbf{g}$. Then, we have

$$B^*\mathbf{z}_2^H\mathbf{G}\mathbf{z}_1 + B\mathbf{z}_1^H\mathbf{G}\mathbf{z}_2 = \bar{\mathbf{g}}^H\boldsymbol{\Lambda}\bar{\mathbf{g}} \tag{3.D.2}$$

Since $\mathrm{rank}(\mathbf{S}) \leq 2$, there are at most two nonzero eigenvalues λ_1 and λ_2. Thus, (3.D.2) can be further written as

$$B^*\mathbf{z}_2^H\mathbf{G}\mathbf{z}_1 + B\mathbf{z}_1^H\mathbf{G}\mathbf{z}_2 = \lambda_1|\bar{g}_1|^2 + \lambda_2|\bar{g}_2|^2. \tag{3.D.3}$$

Thus, we have the claim. □

3.E Appendix: Proof of further simplified detector

We observed that, for different $B \in \tilde{\mathcal{S}}$, the first two eigenvectors corresponding to the non-zero eigenvalues of $\mathbf{S}$ are in a similar shape, resulting in $|\bar{g}_1|$ and $|\bar{g}_2|$ being almost constant. Based on this result, we have the following lemma.

Lemma 3.2 *Let $g(\lambda_1, \lambda_2) = \lambda_1|\bar{g}_1|^2 + \lambda_2|\bar{g}_2|^2$. Assume that $\lambda_1^* = \max \lambda_1$ and $\lambda_2^* = \max \lambda_2$. The maximum value of $g(\lambda_1, \lambda_2)$ is given by $g(\lambda_1^*, \lambda_2^*)$, i.e., $g(\lambda_1, \lambda_2) \leq g(\lambda_1^*, \lambda_2^*)$ for any pair of λ_1 and λ_2 given in (3.E.3) and (3.E.4), respectively.*

Proof Let $\Delta = |B|^2(\|\mathbf{z}_1\|^2\|\mathbf{z}_2\|^2 - |\mathbf{z}_1^H\mathbf{z}_2|^2)$, and $w = \Re(B\mathbf{z}_1^H\mathbf{z}_2)$. Then we have $\lambda_1 = w + \sqrt{w^2 + \Delta}$ and $\lambda_2 = w - \sqrt{w^2 + \Delta}$. According to Cauchy-Schwarz inequality, we know that $\|\mathbf{z}_1\|^2\|\mathbf{z}_2\|^2 \geq |\mathbf{z}_1^H\mathbf{z}_2|^2$, i.e., $\Delta \geq 0$. Therefore, $\sqrt{w^2 + \Delta} \geq |w|$, resulting in $-1 \leq \frac{w}{\sqrt{w^2+\Delta}} \leq 1$. Thus, $\frac{d\lambda_1}{dw} = 1 + \frac{w}{\sqrt{w^2+\Delta}} \geq 0$, which suggests that λ_1 increases with the increase of w. Furthermore, we have $\lambda_2 = w - \sqrt{w^2 + \Delta} = \frac{-\Delta}{w+\sqrt{w^2+\Delta}} = -\frac{\Delta}{\lambda_1}$, which suggests that maximum λ_2 can be obtained by maximizing λ_1, i,e, $\lambda_2^* = -\frac{\Delta}{\lambda_1^*}$. Since $g(\lambda_1, \lambda_2)$ increases with the increase of λ_1 and λ_2, we have $g(\lambda_1, \lambda_2) \leq g(\lambda_1^*, \lambda_2^*)$. The proof is completed. □

Based on the property that the matrix $\mathbf{AB}$ and $\mathbf{BA}$ have the same nonzero eigenvalues, then finding the nonzero eigenvalues of $\mathbf{S}$ can be transfered to find that of

$$\tilde{\mathbf{S}} = \begin{bmatrix} 0 & B^* \\ B & 0 \end{bmatrix} \begin{bmatrix} \mathbf{z}_1^H \\ \mathbf{z}_2^H \end{bmatrix} \begin{bmatrix} \mathbf{z}_1 & \mathbf{z}_2 \end{bmatrix} = \begin{bmatrix} B^*\mathbf{z}_2^H\mathbf{z}_1 & B^*\|\mathbf{z}_2\|^2 \\ B\|\mathbf{z}_1\|^2 & B\mathbf{z}_1^H\mathbf{z}_2 \end{bmatrix}. \tag{3.E.1}$$

Consider the eigenvalues of (3.E.1), we have

$$\begin{aligned}\det(\lambda\mathbf{I}-\tilde{\mathbf{S}}) &= (\lambda - B^*\mathbf{z}_2^H\mathbf{z}_1)(\lambda - B\mathbf{z}_1^H\mathbf{z}_2) - |B|^2\|\mathbf{z}_1\|^2\|\mathbf{z}_2\|^2 \\ &= \lambda^2 - 2\Re(B\mathbf{z}_1^H\mathbf{z}_2)\lambda + |B|^2|\mathbf{z}_1^H\mathbf{z}_2|^2 - |B|^2\|\mathbf{z}_1\|^2\|\mathbf{z}_2\|^2.\end{aligned} \tag{3.E.2}$$

Then, the eigenvalues are the roots of (3.E.2), i.e.,

$$\begin{aligned}\lambda_1 &= \frac{2\Re(B\mathbf{z}_1^H\mathbf{z}_2) + \sqrt{4\Re^2(B\mathbf{z}_1^H\mathbf{z}_2) - 4|B|^2(|\mathbf{z}_1^H\mathbf{z}_2|^2 - \|\mathbf{z}_1\|^2\|\mathbf{z}_2\|^2)}}{2} \\ &= \Re(B\mathbf{z}_1^H\mathbf{z}_2) + \sqrt{\Re^2(B\mathbf{z}_1^H\mathbf{z}_2) + |B|^2(\|\mathbf{z}_1\|^2\|\mathbf{z}_2\|^2 - |\mathbf{z}_1^H\mathbf{z}_2|^2)}\end{aligned} \tag{3.E.3}$$

(the largest one), and

$$\lambda_2 = \Re(B\mathbf{z}_1^H\mathbf{z}_2) - \sqrt{\Re^2(B\mathbf{z}_1^H\mathbf{z}_2) + |B|^2(\|\mathbf{z}_1\|^2\|\mathbf{z}_2\|^2 - |\mathbf{z}_1^H\mathbf{z}_2|^2)} \tag{3.E.4}$$

According to proof of Lemma 3.2, we know that λ_2^* can be obtained by λ_1^* and λ_1 increases with the increase of $\Re(B\mathbf{z}_1^H\mathbf{z}_2)$. Then, we have the further simplified detector $\max\limits_{B\in\tilde{\mathcal{S}}} \Re(B\mathbf{z}_1^H\mathbf{z}_2)$.

3.F Appendix: Symbol Error Probability

Let $D = \sum_{k=1}^{N-1} |H_{k+1}|^2 \prod_{i=k}^{N} \beta_i + \beta_N$. Then, we have $C = \frac{A}{\sigma^2} = \frac{|H_2|^2 \prod_{i=0}^{N} \beta_i}{\sigma^2} + \sum_{k=1}^{N-1} |H_{k+1}|^2 \prod_{i=k}^{N} \beta_i + \beta_N = \frac{|H_2|^2|B|}{\sigma^2} + D$. For simplicity, we denote, $D_s = C^2 -$

$\sigma^{-4}|B|^2 = (|H_2|^2-1)\frac{|B|}{\sigma^2} + \frac{2|H_2|^2|B|D}{\sigma^2} + D^2$. Then, we have

$$
\begin{aligned}
&(C|\tilde{g}_1|^2+1)(1+C\|\tilde{\mathbf{g}}\|^2) - \sigma^{-4}|B|^2\|\tilde{\mathbf{g}}\|^2|\tilde{g}_1|^2 \\
&= (1+C|\tilde{g}_1|^2)(1+C|\tilde{g}_1|^2 + C\sum_{k=2}^{M}|\tilde{g}_k|^2) - \sigma^{-4}|B|^2||\tilde{g}_1|^2 + \sum_{k=2}^{M}|\tilde{g}_k|^2)|\tilde{g}_1|^2 \\
&= D_s|\tilde{g}_1|^4 + (2C + D_s\sum_{k=2}^{M}|\tilde{g}_k|^2)|\tilde{g}_1|^2 + (1+C\sum_{k=2}^{M}|\tilde{g}_k|^2)
\end{aligned}
\tag{3.F.1}
$$

and

$$
\begin{aligned}
&\sigma^{-4}|B|^2|\tilde{g}_1|^4\sin^2\frac{\pi}{Q} + (1+C\|\tilde{\mathbf{g}}\|^2 - C|\tilde{g}_1|^2)((C|\tilde{g}_1|^2+1)(1+C\|\tilde{\mathbf{g}}\|^2) - \sigma^{-4}|B|^2\|\tilde{\mathbf{g}}\|^2|\tilde{g}_1|^2)\sin^2\theta \\
&= \left(\sin^2\theta(1+C\sum_{k=2}^{M}|\tilde{g}_k|^2)D_s + \sigma^{-4}\sin^2\frac{\pi}{Q}|B|^2\right)|\tilde{g}_1|^4 + \sin^2\theta(1+C\sum_{k=2}^{M}|\tilde{g}_k|^2)^2 \\
&+ \sin^2\theta(1+C\sum_{k=2}^{M}|\tilde{g}_k|^2)(2C + D_s\sum_{k=2}^{M}|\tilde{g}_k|^2)|\tilde{g}_1|^2.
\end{aligned}
\tag{3.F.2}
$$

Let $\tilde{g}_1 = \tilde{r}e^{j\phi}$, $T_1 = 1 + C\sum_{k=2}^{M}|\tilde{g}_k|^2$, and $T_2 = 2C + D_s\sum_{k=2}^{M}|\tilde{g}_k|^2$. Since $f(\tilde{g}_1) = \frac{1}{\pi}e^{-|\tilde{g}_1|^2} = \frac{1}{\pi}e^{-\tilde{r}^2}$, we have

$$
\begin{aligned}
&P_e(U|s_k, H_2, \ldots, H_N, \tilde{g}_2, \ldots, \tilde{g}_M) \\
&= \frac{2\pi}{\pi^M}\int_0^{\frac{\pi(Q-1)}{Q}}\int_0^{\infty}\frac{\tilde{r}}{\pi}e^{-\tilde{r}^2}\frac{(C\tilde{r}^2+T_1)^{M-1}\left((D_s\tilde{r}^4 + T_2\tilde{r}^2 + T_1)\sin^2\theta\right)^M}{\left((\sigma^{-4}\sin^2\frac{\pi}{Q}|B|^2 + T_1D_s\sin^2\theta)\tilde{r}^4 + T_1T_2\sin^2\theta\tilde{r}^2 + T_1^2\sin^2\theta\right)^M}d\tilde{r}d\theta \\
&= \frac{1}{\pi^M}\int_0^{\frac{\pi(Q-1)}{Q}}\int_0^{\infty}e^{-\omega}\frac{(Cx+T_1)^{M-1}\left((D_s\omega^2 + T_2\omega + T_1)\sin^2\theta\right)^M}{\left((\sigma^{-4}\sin^2\frac{\pi}{Q}|B|^2 + T_1D_s\sin^2\theta)\omega^2 + T_1T_2\sin^2\theta\omega + T_1^2\sin^2\theta\right)^M}d\omega d\theta
\end{aligned}
\tag{3.F.3}
$$

Moreover, if we let $\omega = T_1 v$, then we have

$$
\begin{aligned}
&P_e(U|s_k, H_2, \ldots, H_N, \tilde{g}_2, \ldots, \tilde{g}_M) \\
&= \frac{1}{\pi^M} \int_0^{\frac{\pi(Q-1)}{Q}} \int_0^{\infty} e^{-T_1 v} \frac{(CT_1 v + T_1)^{M-1} \left((D_s T_1^2 v^2 + T_2 T_1 v + T_1)\sin^2\theta\right)^M T_1}{\left((\sigma^{-4}\sin^2\frac{\pi}{Q}|B|^2 + T_1 \sin^2\theta D_s)T_1^2 v^2 + T_1^2 T_2 \sin^2\theta v + T_1^2 \sin^2\theta\right)^M} dv d\theta \\
&= \frac{1}{\pi^M} \int_0^{\frac{\pi(Q-1)}{Q}} \int_0^{\infty} e^{-T_1 v} \frac{(Cv + 1)^{M-1} \left((D_s T_1 v^2 + T_2 v + 1)\sin^2\theta\right)^M}{\left((\sigma^{-4}\sin^2\frac{\pi}{Q}|B|^2 + T_1 D_s \sin^2\theta)v^2 + T_2 \sin^2\theta v + \sin^2\theta\right)^M} dv d\theta
\end{aligned} \tag{3.F.4}
$$

Consider the polar system and further let $\tilde{\mathbf{g}}_s = (\tilde{g}_2, \ldots, \tilde{g}_M)$ and $\tilde{r}_s^2 = \|\tilde{\mathbf{g}}_s\|^2 = \sum_{k=2}^M |\tilde{g}_k|^2$, then we have

$$
\begin{aligned}
&P_e(U|H_2, \ldots, H_N) \\
&= \frac{1}{\pi^M} \int_0^{\frac{\pi(Q-1)}{Q}} \int_0^{\infty} \int_0^{\infty} \frac{1}{\pi^M} e^{-\tilde{r}_s^2} e^{-T_1 v} \frac{(Cv + 1)^{M-1} \left((D_s T_1 v^2 + T_2 v + 1)\sin^2\theta\right)^M}{\left((\sigma^{-4}\sin^2\frac{\pi}{Q}|B|^2 + T_1 D_s \sin^2\theta)v^2 + T_2 \sin^2\theta v + \sin^2\theta\right)^M} \\
&\quad \times \frac{2\pi^{M-1}}{\Gamma(M-1)} \tilde{r}_s^{2(M-1)-1} dv d\tilde{r}_s d\theta
\end{aligned} \tag{3.F.5}
$$

Let $y = \tilde{r}_s^2$. Since $T_1 = 1 + C\sum_{k=2}^M |\tilde{g}_k|^2 = 1 + Cy$, and $T_2 = 2C + D_s \sum_{k=2}^M |\tilde{g}_k|^2 = 2C + D_s y$, the integrand of (3.F.15) can be rewritten as

$$
\begin{aligned}
&\frac{e^{-y} e^{-(1+Cy)v}}{\pi^{M+1}\Gamma(M-1)} \frac{(Cv + 1)^{M-1} \left((D_s(1 + Cy)v^2 + (2C + D_s y)v + 1)\sin^2\theta\right)^M y^{M-2}}{\left((\sigma^{-4}\sin^2\frac{\pi}{Q}|B|^2 + (1 + Cy)D_s \sin^2\theta)v^2 + (2C + D_s y)\sin^2\theta v + \sin^2\theta\right)^M} \\
&= \frac{e^{-v} e^{-(Cv+1)y}}{\pi^{M+1}\Gamma(M-1)} \frac{(Cv + 1)^{M-1} \left((CD_s v^2 + D_s v)\sin^2\theta y + (D_s v^2 + 2Cv + 1)\sin^2\theta\right)^M y^{M-2}}{\left((CD_s v^2 + D_s v)\sin^2\theta y + (D_s v^2 + 2Cv + 1)\sin^2\theta + \sigma^{-4}|B|^2 v^2 \sin^2\frac{\pi}{Q}\right)^M}
\end{aligned} \tag{3.F.6}
$$

Moreover, since $(1-x)^M = \sum_{k=0}^{M} \begin{pmatrix} M \\ k \end{pmatrix} (-1)^k x^k$, where $\begin{pmatrix} M \\ k \end{pmatrix} = \frac{M!}{k!(M-k)!}$, we have

$$\frac{(Cv+1)^{M-1}\left((CD_s v^2 + D_s v)\sin^2\theta y + (D_s v^2 + 2Cv + 1)\sin^2\theta\right)^M}{\left((CD_s v^2 + D_s v)\sin^2\theta y + (D_s v^2 + 2Cv + 1)\sin^2\theta + \sigma^{-4}|B|^2 v^2 \sin^2\frac{\pi}{Q}\right)^M}$$
$$= (Cv+1)^{M-1}\left(1 - \frac{\sigma^{-4}|B|^2 v^2 \sin^2\frac{\pi}{Q}}{(CD_s v^2 + D_s v)\sin^2\theta y + (D_s v^2 + 2Cv + 1)\sin^2\theta + \sigma^{-4}|B|^2 v^2 \sin^2\frac{\pi}{Q}}\right)^M$$
$$= (Cv+1)^{M-1}\sum_{k=0}^{M}\frac{\begin{pmatrix} M \\ k \end{pmatrix}(-1)^k(\sigma^{-4}|B|^2 v^2 \sin^2\frac{\pi}{Q})^k}{\left((CD_s v^2 + D_s v)\sin^2\theta y + (D_s v^2 + 2Cv + 1)\sin^2\theta + \sigma^{-4}|B|^2 v^2 \sin^2\frac{\pi}{Q}\right)^k}. \tag{3.F.7}$$

Let $R_1 = \frac{\sigma^{-4}|B|^2 v^2 \sin^2\frac{\pi}{Q}}{(CD_s v^2 + D_s v)\sin^2\theta}$, $R_2 = \frac{(D_s v^2 + 2Cv + 1)\sin^2\theta + \sigma^{-4}|B|^2 v^2 \sin^2\frac{\pi}{Q}}{(CD_s v^2 + D_s v)\sin^2\theta}$, and $R_3 = Cv + 1$. Then, the integral in (3.F.15) can be rewritten as

$$\frac{1}{\pi^{M+1}}\int_0^{\frac{\pi(Q-1)}{Q}}\int_0^{\infty}\frac{e^{-v}}{\Gamma(M-1)}R_3^{M-1}\int_0^{\infty}e^{-R_3 y}y^{M-2}\sum_{k=0}^{M}\begin{pmatrix} M \\ k \end{pmatrix}(-1)^k\left(\frac{R_1}{y+R_2}\right)^k dy dv d\theta. \tag{3.F.8}$$

Consider the integral of y first, we have

$$\begin{aligned}
&\int_0^\infty e^{-R_3 y} y^{M-2} \sum_{k=0}^{M} \begin{pmatrix} M \\ k \end{pmatrix} (-1)^k \left(\frac{R_1}{y+R_2}\right)^k dy \\
&= \int_0^\infty e^{-R_3 y} \sum_{k=0}^{M} \begin{pmatrix} M \\ k \end{pmatrix} (-1)^k \left(\frac{R_1}{y+R_2}\right)^k (y+R_2-R_2)^{M-2} dy \\
&= \int_0^\infty e^{-R_3 y} \sum_{k=0}^{M} \begin{pmatrix} M \\ k \end{pmatrix} (-1)^k \left(\frac{R_1}{y+R_2}\right)^k \sum_{j=0}^{M-2} \begin{pmatrix} M-2 \\ j \end{pmatrix} (-1)^j (y+R_2)^{M-2-j} R_2^j dy \\
&= \sum_{k=0}^{M} \sum_{j=0}^{M-2} \begin{pmatrix} M \\ k \end{pmatrix} \begin{pmatrix} M-2 \\ j \end{pmatrix} (-1)^{k+j} R_1^k R_2^j \int_0^\infty e^{-R_3 y} (y+R_2)^{M-2-j-k} dy.
\end{aligned} \tag{3.F.9}$$

We use the following lemma to solve the integral in (3.F.9).

Lemma 3.3 *For $k \geq 0$*

$$\int_0^\infty (y+a)^k e^{-by} dy = \sum_{i=1}^{k+1} \frac{k!}{(k+1-i)!} a^{k+1-i} b^{-i}. \tag{3.F.10}$$

Proof

$$\begin{aligned}
\int_0^\infty (y+a)^k e^{-by} dy &= \int_0^\infty -\frac{1}{b}(y+a)^k de^{-by} \\
&= -\frac{1}{b}(y+a)^k e^{-by}\Big|_0^\infty + \int_0^\infty \frac{k}{b}(y+a)^{k-1} e^{-by} dy \\
&= \frac{a^k}{b} + \int_0^\infty \frac{k}{b}(y+a)^{k-1} e^{-by} dy.
\end{aligned}$$

Similarly, we have

$$\begin{aligned}\int_0^\infty \frac{k}{b}(y+a)^{k-1}e^{-by}dy &= \int_0^\infty -\frac{k}{b^2}(y+a)^{k-1}de^{-by}\\ &= -\frac{k}{b^2}(y+a)^{k-1}e^{-by}\Big|_0^\infty + \int_0^\infty \frac{k(k-1)}{b^2}(y+a)^{k-2}e^{-by}dy\\ &= \frac{ka^{k-1}}{b^2} + \int_0^\infty \frac{k(k-1)}{b^2}(y+a)^{k-2}e^{-by}dy.\end{aligned}$$

Recursively, we know that

$$\begin{aligned}\int_0^\infty (y+a)^k e^{-by}dy &= \frac{a^k}{b} + \frac{ka^{k-1}}{b^2} + \cdots + \frac{k!a}{b^k} + \int_0^\infty \frac{k!}{b^k}e^{-by}dy\\ &= \frac{a^k}{b} + \frac{k!a^{k-1}}{(k-1)!b^2} + \cdots + \frac{k!a}{b^k} - \frac{k!}{b^{k+1}}e^{-by}\Big|_0^\infty\\ &= \sum_{i=1}^{k+1} \frac{k!}{(k+1-i)!}a^{k-i+1}b^{-i}.\end{aligned}$$

The proof is completed. □

Let $E_i(x)$ represent the exponential integral function, i.e., $E_i(x) = \int_{-\infty}^x \frac{e^u}{u}du$. Then, we have the following lemma.

Lemma 3.4

$$\int_0^\infty \frac{e^{-by}}{y+a}dy = -e^{ab}Ei(-ab)$$

Proof Since $E_i(x) = \int_{-\infty}^x \frac{e^u}{u}du$, by substituting $u=-t$, we have

$$E_i(-x) = \int_{-x}^\infty -\frac{e^{-t}}{t}dt, \tag{3.F.11}$$

Then, let $t = b(y+a)$, according to (3.F.11), we have

$$\begin{aligned}
E_i(-\frac{x}{b} - a) &= \int_{-\frac{x}{b}-a}^{\infty} -\frac{e^{-b(y+a)}}{b(y+a)} d(b(y+a)) \\
&= -e^{-ab} \int_{-\frac{x}{b}-a}^{\infty} \frac{e^{-by}}{y+a} dy,
\end{aligned}$$

which suggests that $\int_{-\frac{x}{b}-a}^{\infty} \frac{e^{-by}}{y+a} dy = -e^{ab} E_i(-\frac{x}{b} - a)$.

By substituting $x = -ab$, we have $\int_0^{\infty} \frac{e^{-by}}{y+a} dy = -e^{ab} E_i(-ab)$. The proof is completed. □

Lemma 3.5 *For $k \geq 1$*

$$\int_0^{\infty} \frac{e^{-by}}{(y+a)^k} dy = \sum_{i=1}^{k-1} \frac{(-b)^{k-i-1}(i-1)!}{a^i (k-1)!} - \frac{(-b)^{k-1}}{(k-1)!} e^{ab} Ei(-ab). \tag{3.F.12}$$

Proof

$$\begin{aligned}
\int_0^{\infty} \frac{e^{-by}}{(y+a)^k} dy &= \int_0^{\infty} -\frac{e^{-by}}{k-1} d(y+a)^{-(k-1)} \\
&= -\frac{e^{-by}}{k-1}(y+a)^{-(k-1)}\Big|_0^{\infty} - b\int_0^{\infty} (y+a)^{-(k-1)} \frac{e^{-by}}{k-1} dy \\
&= \frac{a^{-k+1}}{k-1} - \frac{b}{k-1} \int_0^{\infty} \frac{e^{-by}}{(y+a)^{k-1}} dy.
\end{aligned}$$

Similarly, we have

$$
\begin{aligned}
\frac{b}{k-1}\int_0^{\infty}\frac{e^{-by}}{(y+a)^{k-1}}dy &= \frac{b}{k-1}\int_0^{\infty}-\frac{e^{-by}}{k-2}d(y+a)^{-(k-2)} \\
&= -\frac{be^{-by}}{(k-1)(k-2)}(y+a)^{-(k-2)}\big|_0^{\infty} - \frac{b^2}{k-1}\int_0^{\infty}(y+a)^{-(k-2)}\frac{e^{-by}}{k-2}dy \\
&= \frac{ba^{-k+2}}{(k-1)(k-2)} - \frac{b^2}{(k-1)(k-2)}\int_0^{\infty}\frac{e^{-by}}{(y+a)^{k-2}}dy.
\end{aligned}
$$

Recursively, we know that

$$
\begin{aligned}
\int_0^{\infty}\frac{e^{-by}}{(y+a)^{k}}dy &= \frac{a^{-k+1}}{k-1} - \frac{ba^{-k+2}}{(k-1)(k-2)} + \ldots + (-1)^{k-1}\frac{b^{k-1}}{(k-1)!}\int_0^{\infty}\frac{e^{-by}}{y+a}dy \\
&= \frac{(k-2)!}{a^{k-1}(k-1)!} - \frac{b(k-3)!}{a^{k-2}(k-1)!} + \ldots + (-1)^{k-1}\frac{b^{k-1}}{(k-1)!}\int_0^{\infty}\frac{e^{-by}}{y+a}dy \\
&= \sum_{i=1}^{k-1}(-1)^{k-i-1}\frac{b^{k-i-1}(i-1)!}{a^{i}(k-1)!} + (-1)^{k-1}\frac{b^{k-1}}{(k-1)!}\int_0^{\infty}\frac{e^{-by}}{y+a}dy.
\end{aligned}
$$

According to Lemma 3.4, we have

$$
\begin{aligned}
\int_0^{\infty}\frac{e^{-by}}{(y+a)^{k}}dy &= \sum_{i=1}^{k-1}(-1)^{k-i-1}\frac{b^{k-i-1}(i-1)!}{a^{i}(k-1)!} + (-1)^{k-1}\frac{b^{k-1}}{(k-1)!}(-e^{ab}Ei(-ab)) \\
&= \sum_{i=1}^{k-1}\frac{(-b)^{k-i-1}(i-1)!}{a^{i}(k-1)!} - \frac{(-b)^{k-1}}{(k-1)!}e^{ab}Ei(-ab).
\end{aligned}
$$

Therefore, the proof is completed. $\square$

According to the positive and negative properties of $M-2-(k+j)$, the (3.F.9) can be divided into two parts, where one part is $k+j \leq M-2$ and another part is $k+j \geq M-1$. Let $t = k+j$.

For the first part with $t \leq M-2$, according to Lemma 3.3, we have

$$\sum_{k=0}^{M-2}\sum_{t=k}^{M-2}\binom{M}{k}\binom{M-2}{t-k}(-1)^t R_1^k R_2^{t-k}\int_0^\infty e^{-R_3 y}(y+R_2)^{M-2-t}dy$$
$$=\sum_{k=0}^{M-2}\sum_{t=k}^{M-2}\binom{M}{k}\binom{M-2}{t-k}(-1)^t R_1^k R_2^{t-k}\sum_{i=1}^{M-t-1}\frac{k!}{(M-t-i-1)!}R_2^{M-t-i-1}R_3^{-i}$$
$$=\sum_{k=0}^{M-2}\sum_{t=k}^{M-2}\sum_{i=1}^{M-t-1}\binom{M}{k}\binom{M-2}{t-k}\frac{(-1)^t k!}{(M-t-i-1)!}R_1^k R_2^{M-k-i-1}R_3^{-i} \tag{3.F.13}$$

For the second part with $t \geq M-1$, according to Lemma 3.5 we have

$$\sum_{k=1}^{M}\sum_{t=\max\{M-1,k\}}^{M-2+k}\binom{M}{k}\binom{M-2}{t-k}(-1)^t R_1^k R_2^{t-k}\int_0^\infty e^{-R_3 y}(y+R_2)^{-(t-M+2)}dy$$
$$=\sum_{k=1}^{M}\sum_{t=\max\{M-1,k\}}^{M-2+k}\binom{M}{k}\binom{M-2}{t-k}(-1)^t R_1^k R_2^{t-k}\sum_{i=1}^{t-M+1}\frac{(-R_3)^{t-M-i+1}(i-1)!}{R_2^i(t-M+1)!}$$
$$-\sum_{k=1}^{M}\sum_{t=\max\{M-1,k\}}^{M-2+k}\binom{M}{k}\binom{M-2}{t-k}(-1)^t R_1^k R_2^{t-k}\frac{(-R_3)^{t-M+1}}{(t-M+1)!}e^{R_2R_3}Ei(-R_2R_3) \tag{3.F.14}$$

Then, we know that

$$
\begin{aligned}
&P_e(U|H_2,\ldots,H_N)\\
&= \int_0^{\frac{\pi(Q-1)}{Q}} \int_0^{\infty} \frac{e^{-v}R_3^{M-1}}{\pi^{M+1}\Gamma(M-1)} \left(\sum_{k=0}^{M-2}\sum_{t=k}^{M-2}\sum_{i=1}^{M-t-1} \frac{(-1)^t k! \binom{M}{k}\binom{M-2}{t-k} R_1^k R_2^{M-k-i-1} R_3^{-i}}{(M-t-i-1)!} \right.\\
&+\sum_{k=1}^{M}\sum_{t=\max\{M-1,k\}}^{M-2+k} \binom{M}{k}\binom{M-2}{t-k} (-1)^t R_1^k R_2^{t-k} \sum_{i=1}^{t-M+1} \frac{(-R_3)^{t-M-i+1}(i-1)!}{R_2^i (t-M+1)!}\\
&\left. -\sum_{k=1}^{M}\sum_{t=\max\{M-1,k\}}^{M-2+k} \binom{M}{k}\binom{M-2}{t-k} (-1)^t R_1^k R_2^{t-k} \frac{(-R_3)^{t-M+1}}{(t-M+1)!} e^{R_2R_3} Ei(-R_2R_3) \right) dv d\theta
\end{aligned}
\tag{3.F.15}
$$

Chapter 4

Gaussian Semantic Source Coding

Abstract

Semantic source coding differs from conventional source coding in the sense that the decoder is required to reconstruct, possibly in a lossy fashion, not only the observable source realization but also an intrinsic source state that carries certain semantic information. Centralized Gaussian semantic source coding and its distributed counterpart are studied in this work. We explicitly characterize their respective rate-distortion functions for the symmetric setting and the 2-component setting via the analysis of the associated convex optimization problems. These characterizations generalize several classical results in quadratic vector Gaussian source coding and Gaussian multiterminal source coding.

4.1 Introduction

Direct source coding [18] aims to find an efficient bit-sequence representation of an observed source realization, from which that realization can be reconstructed exactly or approximately. In contrast, indirect source coding [5, 24, 96, 97] deals with the situation where the object of interest is not observed directly, but is some hidden state. These two coding problems are closely related. In fact, if the observation is a sufficient statistic for the hidden state, then indirect source coding can be reduced to direct source coding under a suitably constructed surrogate distortion measure [5].

Semantic source coding [39, 58] couples the aforementioned two coding problems by requiring the decoder to reconstruct, possibly in a lossy fashion, both the observable source realization and the hidden source state. This unification is motivated by task-oriented compression (e.g., MPEG Compact Descriptors for Video Analysis [29] and Video Coding for Machines [28, 61, 104]), where the coded representation has the dual responsibility of preserving the extrinsic aspects of the given data (which corresponds to the observable source realization) and capturing its intrinsic semantic features (which are assumed to be carried by the hidden source state). Note that the two objectives of the decoder in semantic source coding are not necessarily aligned. Indeed, with the coding rate fixed, there often exists a tension between faithfully reproducing the extrinsic observation and accurately estimating the intrinsic state. Characterizing this tension in the form of a quantitative tradeoff is a fundamental problem from the information-theoretic perspective.

So far, research on semantic source coding has been exclusively focused on centralized systems with a single encoder having access to all source components, e.g., [38, 57, 58]. However, in practice, there are many situations where the source components are not co-located and have to be processed in a distributed manner. Even when the source components are co-located, distributed processing might still be favored due to implementation constraints (e.g., small receptive fields of neural networks) or complexity considerations. This provides a strong incentive to study distributed semantic source coding and investigate how it differs from its centralized counterpart in terms of the performance limits.

In this work, we consider the quadratic Gaussian versions of both centralized semantic source coding and distributed semantic source coding. The Gaussian version is known to be analytically more tractable. In particular, we obtain several explicit characterizations of the fundamental rate-distortion limits, while explicit characterization of the fundamental rate-distortion tradeoff remains elusive for general source distributions, the external properties of the Gaussian distribution suggest that our results can be used widely as baselines for non-Gaussian distributions.

The rest of this chapter is organized as follows. We introduce the problem definitions in Section 4.2. The rate-distortion function of centralized Gaussian semantic source coding is explicitly characterized for the symmetric setting and the 2-component setting in Section 4.3. The corresponding results for distributed Gaussian semantic source coding are presented in Section 4.4. Section 4.5 contains some numerical simulations and comparisons. We conclude the chapter in Section 4.6.

4.2 Problem Definitions

Let $\mathbf{X} := (X_1, \ldots, X_L)^T$ be an observable vector source, and let S be a state variable carrying certain semantic information. We assume $X_i = S + N_i$, $i = 1, \ldots, L$, where

$S, N_1, \ldots, N_L$ are mutually independent zero-mean Gaussian random variables with variances $\sigma_S^2, \sigma_{N_1}^2, \ldots, \sigma_{N_L}^2$, respectively. The covariance matrix of $\mathbf{X}$, denoted by $\mathbf{K_X}$, can be written as

$$\mathbf{K_X} = \begin{bmatrix} \sigma_S^2 + \sigma_{N_1}^2 & \sigma_S^2 & \ldots & \sigma_S^2 \\ \sigma_S^2 & \sigma_S^2 + \sigma_{N_2}^2 & \ldots & \sigma_S^2 \\ \vdots & \vdots & \ddots & \vdots \\ \sigma_S^2 & \sigma_S^2 & \ldots & \sigma_S^2 + \sigma_{N_L}^2 \end{bmatrix}.$$

According to linear minimum mean square error (MMSE) estimation, it is easy to verify that

$$S = \mathbb{E}[S|\mathbf{X}] + Z = \mathbf{g}^T\mathbf{X} + Z,$$

where Z is a zero-mean Gaussian random variable, independent of $\mathbf{X}$, with variance $\sigma_Z^2 = (\frac{1}{\sigma_S^2} + \frac{1}{\sigma_{N_1}^2} + \ldots + \frac{1}{\sigma_{N_L}^2})^{-1}$, and $\mathbf{g} = (\frac{\sigma_Z^2}{\sigma_{N_1}^2}, \ldots, \frac{\sigma_Z^2}{\sigma_{N_L}^2})^T$. Let $\{(X_1(t), \ldots, X_L(t), S(t), Z(t))\}_{t=1}^{\infty}$ be a joint i.i.d. process induced by $(X_1, \ldots, X_L, S, Z)$.

To set the scene for the contribution of the paper, we define the achievability of an encoding rate R in the cases of centralized and distributed coding in the following ways.

Definition 4.1 *Rate R is said to be achievable with respect to reproduction distortion constraints $D_1, \ldots, D_L$ and semantic distortion constraint D_S via centralized coding if given any $\epsilon > 0$, there exist encoding functions $f^{(n)} : \mathbb{R}^{L\times n} \rightarrow \mathcal{C}^{(n)}$ and decoding* *functions* $g^{(n)}: \mathcal{C}^{(n)} \to \mathbb{R}^{L\times n}$ *and* $g_S^{(n)}: \mathcal{C}^{(n)} \to \mathbb{R}^n$ *for all sufficiently large* n *such that*

$$\frac{1}{n}\log|\mathcal{C}^{(n)}| \leq R+\epsilon,$$
$$\frac{1}{n}\sum_{t=1}^{n}\mathbb{E}[(X_i(t)-\hat{X}_i(t))^2] \leq D_i+\epsilon, \quad i=1,\ldots,L,$$
$$\frac{1}{n}\sum_{t=1}^{n}\mathbb{E}[(S(t)-\hat{S}(t))^2] \leq D_S+\epsilon,$$

where $\hat{\mathbf{X}}^n := g^{(n)}(f^{(n)}(\mathbf{X}^n))$ *(with* $\mathbf{X}(t)$ *and* $\hat{\mathbf{X}}(t)$ *standing for* $(X_1(t),\ldots,X_L(t))^T$ *and* $(\hat{X}_1(t),\ldots,\hat{X}_L(t))^T$*, respectively,* $t=1,\ldots,n$*) and* $\hat{S}^n := g_S^{(n)}(f^{(n)}(\mathbf{X}^n))$*. The infimum of such achievable* R *is denoted by* $R_c(D_1,\ldots,D_L,D_S)$*.*

Definition 4.2 *Rate* R *is said to be achievable with respect to reproduction distortion constraints* $D_1,\ldots,D_L$ *and semantic distortion constraint* D_S *via distributed coding if given any* $\epsilon>0$*, there exist encoding functions* $f_i^{(n)}: \mathbb{R}^n \to \mathcal{C}_i^{(n)}$*,* $i=1,\ldots,L$*, and decoding functions* $g^{(n)}: \mathcal{C}_1^{(n)}\times\ldots\times\mathcal{C}_L^{(n)} \to \mathbb{R}^{L\times n}$ *and* $g_S^{(n)}: \mathcal{C}_1^{(n)}\times\ldots\times\mathcal{C}_L^{(n)} \to \mathbb{R}^n$ *for all sufficiently large* n *such that*

$$\frac{1}{n}\sum_{i=1}^{L}\log|\mathcal{C}_i^{(n)}| \leq R+\epsilon,$$
$$\frac{1}{n}\sum_{t=1}^{n}\mathbb{E}[(X_i(t)-\hat{X}_i(t))^2] \leq D_i+\epsilon, \quad i=1,\ldots,L,$$
$$\frac{1}{n}\sum_{t=1}^{n}\mathbb{E}[(S(t)-\hat{S}(t))^2] \leq D_S+\epsilon,$$

where $\hat{\mathbf{X}}^n := g^{(n)}(f_1^{(n)}(X_1^n),\ldots,f_L^{(n)}(X_L^n))$ *(with* $\hat{\mathbf{X}}(t)$ *standing for* $(\hat{X}_1(t),\ldots,\hat{X}_L(t))^T$*,* $t=1,\ldots,n$*) and* $\hat{S}^n := g_S^{(n)}(f_1^{(n)}(X_1^n),\ldots,f_L^{(n)}(X_L^n))$*. The infimum of such achievable* R *is denoted by* $R_d(D_1,\ldots,D_L,D_S)$*.*

For a given set of distortion metrics, $D_1, \dots, D_L, D_S$, the rate distortion problem is to find the minimum achievable rate. In this work, we will consider distortions $D_i \in (0, \sigma_S^2 + \sigma_{N_i}^2]$, $i = 1, \dots, L$, and $D_S \in (\sigma_Z^2, \sigma_S^2]$, as distortions that are larger result in inactive constraints, and distortions that are smaller are inherently infeasible.

The centralized Gaussian semantic source coding problem considered in the present work differs from that in [58] in two aspects. Firstly, we impose a reproduction distortion constraint on each source component while [58] adopts a trace distortion constraint. Secondly, we consider a special correlation structure where the observable source components are conditionally independent given the hidden state; in contrast, [58] has no such a restriction. It is worth mentioning that the conditional independence assumption is introduced mainly to ensure that the results derived for the centralized Gaussian semantic source coding problem are comparable to those for the distributed counterpart, as the latter problem is likely intractable without this assumption.

To the best of our knowledge, the distributed Gaussian semantic source coding problem formulated above is new. Nevertheless, it has rich connections with various network source coding problems [11, 68, 72, 86, 89] in the literature. In particular, it can be viewed as a coupling of the Gaussian multiterminal source coding problem [6, 12, 66, 82, 86, 89, 102, 105] and the Gaussian CEO problem [7, 11, 67, 69, 72, 85]. In the multiterminal source coding system, many sources are separately encoded and sent to a single destination, and the decoder wishes to reconstruct the original sources. In [6, 82], the inner bound of this problem was given, and Wagner *et al.* [86] gave a complete solution to this problem in the two terminal case of quadratic Gaussian sources and quadratic distortion by proving such inner bound is optimal. Although the vector case [87, 88] and symmetric case [13] are considered, this problem remains open in the general case. As a practical situation of the distributed source coding system, the encoders can not directly access the source outputs but can access their noisy observations, such remote source coding problem is often referred to as CEO problem [7, 67, 68, 69, 90, 91] , where [69] showed the connection of these two source coding problems and [91] gave a comparison with centralized coding in symmetric case.

4.3 Centralized Gaussian Semantic Source Coding

In this section, we take the centralized version of the semantic source coding problem. The coding model of L-symmetric-component setting and 2-component setting are shown in Fig. 4.1 and Fig. 4.2, respectively. The following result is a simple variant of [58, Theorem 2].

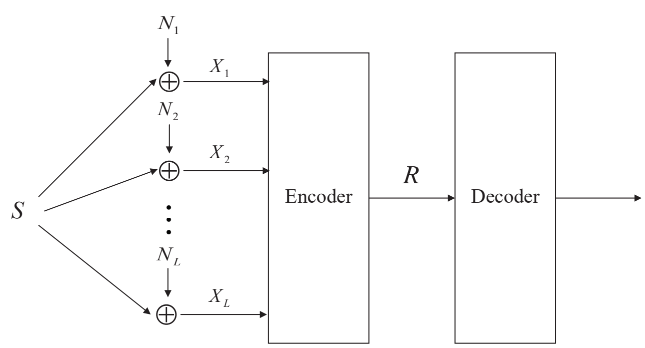

Figure 4.1: Centralized semantic source coding: L-symmetric-component setting.

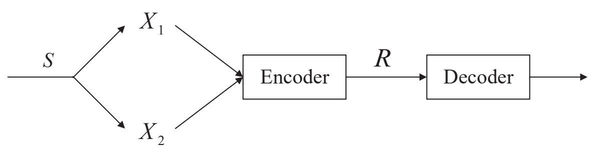

Figure 4.2: Centralized semantic source coding: 2-component setting.

Theorem 4.1 *We have*

$$R_c(D_1,\ldots,D_L,D_S) = \min_{\boldsymbol{\Delta}} \frac{1}{2}\log\frac{\det(\mathbf{K_X})}{\det(\boldsymbol{\Delta})} \tag{4.3.1}$$

$$s.t. \quad \mathbf{0} \prec \boldsymbol{\Delta} \preceq \mathbf{K_X}, \tag{4.3.2}$$

$$\mathrm{diag}(\boldsymbol{\Delta}) \preceq \mathbf{D}, \tag{4.3.3}$$

$$\mathbf{g}^T\boldsymbol{\Delta}\mathbf{g} + \sigma_Z^2 \leq D_S, \tag{4.3.4}$$

where $\mathbf{D}$ *is a diagonal matrix with the i-th diagonal entry being* D_i, $i = 1,\ldots,L$.

Lemma 4.1 $\boldsymbol{\Delta}^*$ *is an optimal solution of the optimization problem in (4.3.1) if it satisfies the constraints (4.3.2)–(4.3.4) and there exist positive semidefinite matrix* $\mathbf{U}$*, a positive semidefinite diagonal matrix* $\boldsymbol{\Lambda}$*, and a nonnegative number* ρ *such that*

$$-(\boldsymbol{\Delta}^*)^{-1} + \mathbf{U} + \boldsymbol{\Lambda} + \rho\mathbf{g}\mathbf{g}^T = \mathbf{0}, \tag{4.3.5}$$

$$\mathbf{U}(\boldsymbol{\Delta}^* - \mathbf{K_X}) = \mathbf{0}, \tag{4.3.6}$$

$$\boldsymbol{\Lambda}(\mathrm{diag}(\boldsymbol{\Delta}^*) - \mathbf{D}) = \mathbf{0}, \tag{4.3.7}$$

$$\rho\left(\mathbf{g}^T\boldsymbol{\Delta}^*\mathbf{g} + \sigma_Z^2 - D_S\right) = 0. \tag{4.3.8}$$

Proof Since (4.3.1) is a convex optimization problem and it has interior points, $\boldsymbol{\Delta}^*$ is an optimal solution if it satisfies the constraints (4.3.2)–(4.3.4) as well as the following KKT conditions [8]:

$$\begin{aligned}
&\nabla_{\mathbf{\Delta}} L(\mathbf{\Delta}; \mathbf{U}, \mathbf{\Lambda}, \rho)|_{\mathbf{\Delta}=\mathbf{\Delta}^*} = \mathbf{0}, \\
&\mathbf{U}(\mathbf{\Delta}^* - \mathbf{K}_{\mathbf{X}}) = \mathbf{0}, \\
&\mathbf{\Lambda}(\mathrm{diag}(\mathbf{\Delta}^*) - \mathbf{D}) = \mathbf{0}, \\
&\rho \left(\mathbf{g}^T \mathbf{\Delta}^* \mathbf{g} + \sigma_Z^2 - D_S\right) = 0,
\end{aligned}$$

where $L(\mathbf{\Delta}; \mathbf{U}, \mathbf{\Lambda}, \rho)$ is the Lagrangian defined as

$$L(\mathbf{\Delta}; \mathbf{U}, \mathbf{\Lambda}, \rho) := -\log\det(\mathbf{\Delta}) + \mathrm{tr}\left(\mathbf{U}(\mathbf{\Delta} - \mathbf{K}_{\mathbf{X}})\right) + \mathrm{tr}\left(\mathbf{\Lambda}(\mathrm{diag}(\mathbf{\Delta}) - \mathbf{D})\right) + \rho(\mathbf{g}^T \mathbf{\Delta}\mathbf{g} + \sigma_Z^2 - D_S)$$

with $\mathbf{U}$, $\mathbf{\Lambda}$, and ρ being a positive semidefinite matrix, a positive semidefinite diagonal matrix, and a nonnegative number, respectively. The proof is complete in view of the fact that $\nabla_{\mathbf{\Delta}} L(\mathbf{\Delta}; \mathbf{U}, \mathbf{\Lambda}, \rho) = -\mathbf{\Delta}^{-1} + \mathbf{U} + \mathbf{\Lambda} + \rho\mathbf{g}\mathbf{g}^T$. □

Next we consider the symmetric setting with $\sigma_{N_1}^2 = \ldots = \sigma_{N_L}^2 = \sigma_N^2$ and $D_1 = \ldots = D_L = D$. An explicit characterization of $R_c(D_1, \ldots, D_L, D_S)$, abbreviated as $R_c(D, D_S)$, is provided by the following result.

Theorem 4.2 *An explicit expression for $R_c(D, D_S)$ is given as follows:*

1. *If $D < \sigma_N^2$ and $D < \frac{(D_S - \sigma_Z^2)\sigma_N^4}{L\sigma_Z^4}$, then*

$$R_c(D, D_S) = \frac{1}{2} \log \frac{L\sigma_S^2 \sigma_N^{2(L-1)} + \sigma_N^{2L}}{D^L}.$$

2. If $D < \frac{L-1}{L}\sigma_N^2 + \frac{(D_S-\sigma_Z^2)\sigma_N^4}{L^2\sigma_Z^4}$ *and* $D \geq \frac{(D_S-\sigma_Z^2)\sigma_N^4}{L\sigma_Z^4}$*, then*

$$R_c(D, D_S) = \frac{1}{2}\log\frac{L\sigma_Z^4(L\sigma_S^2\sigma_N^{2(L-1)} + \sigma_N^{2L})}{(D_S-\sigma_Z^2)\sigma_N^4(\frac{L}{L-1}D - \frac{(D_S-\sigma_Z^2)\sigma_N^4}{L(L-1)\sigma_Z^4})^{L-1}}.$$

3. If $D \geq \sigma_N^2$ *and* $D < \frac{L-1}{L}\sigma_N^2 + \frac{(D_S-\sigma_Z^2)\sigma_N^4}{L^2\sigma_Z^4}$*, then*

$$R_c(D, D_S) = \frac{1}{2}\log\frac{L\sigma_S^2 + \sigma_N^2}{LD - (L-1)\sigma_N^2}.$$

4. If $D \geq \frac{L-1}{L}\sigma_N^2 + \frac{(D_S-\sigma_Z^2)\sigma_N^4}{L^2\sigma_Z^4}$*, then*

$$R_c(D, D_S) = \frac{1}{2}\log\frac{\sigma_S^2 - \sigma_Z^2}{D_S - \sigma_Z^2}.$$

The regions of the (D, D_S) space in which each closed-form expression applies can be visualized using the example in Fig. 4.3.

Proof For each of the four cases, we invoke Lemma 4.1 to verify the optimality of a specific $\mathbf{\Delta}^*$ by explicitly constructing $\mathbf{U}$, $\mathbf{\Lambda}$, and ρ that satisfy the KKT conditions.

1. Consider the following construction:

$$\mathbf{\Delta}^* := \mathbf{D}, \quad \mathbf{U} := \mathbf{0}, \quad \mathbf{\Lambda} := \mathbf{D}^{-1}, \quad \rho := 0.$$

It is clear that (4.3.3) and (4.3.5)–(4.3.8) are satisfied. Moreover, (4.3.4) is also

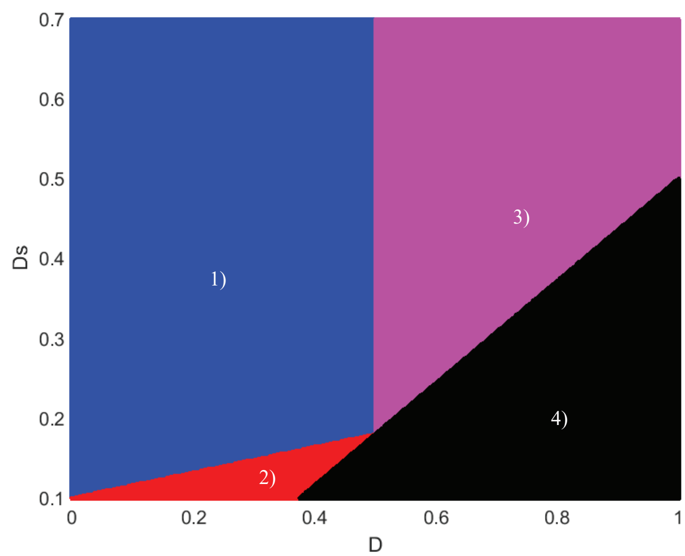

Figure 4.3: Regions of each case of Theorem 4.2, when $\sigma_S^2 = 0.5$, $\sigma_N^2 = 0.5$, and $L = 7$.

satisifed since

$$\mathbf{g}^T \mathbf{\Delta}^* \mathbf{g} + \sigma_Z^2 < D_S \Longleftrightarrow D < \frac{(D_S - \sigma_Z^2)\sigma_N^4}{L\sigma_Z^4}.$$

Note that $\mathbf{\Delta}^* \succ \mathbf{0}$. Also, the eigenvalues of $\mathbf{K_X} - \mathbf{\Delta}^*$ take two possible values $L\sigma_S^2 + \sigma_N^2 - D$ and $\sigma_N^2 - D$; the former is nonnegative when $D \leq \sigma_S^2 + \sigma_N^2$ while the latter is positive when $D < \sigma_N^2$. So (4.3.2) is satisfied as well. Therefore, $\mathbf{\Delta}^*$ is indeed an optimal solution and consequently

$$R_c(D, D_S) = \frac{1}{2} \log \frac{\det(\mathbf{K_X})}{\det(\mathbf{\Delta}^*)} = \frac{1}{2} \log \frac{L\sigma_S^2 \sigma_N^{2(L-1)} + \sigma_N^{2L}}{D^L}.$$

2. Consider the following construction:

$$\mathbf{\Delta}^* := \begin{bmatrix} D & \eta & \dots & \eta \\ \eta & D & \dots & \eta \\ \vdots & \vdots & \ddots & \vdots \\ \eta & \eta & \dots & D \end{bmatrix}, \quad \mathbf{U} := \mathbf{0}, \quad \mathbf{\Lambda} := \begin{bmatrix} \frac{1}{D-\eta} & 0 & \dots & 0 \\ 0 & \frac{1}{D-\eta} & \dots & 0 \\ \vdots & \vdots & \ddots & \vdots \\ 0 & 0 & \dots & \frac{1}{D-\eta} \end{bmatrix},$$
$$\rho := -\frac{\eta\sigma_N^4}{((L-1)\eta + D)(D-\eta)\sigma_Z^4}.$$

where $\eta := \frac{(D_S-\sigma_Z^2)\sigma_N^4}{L(L-1)\sigma_Z^4} - \frac{D}{L-1}$. Note that the eigenvalues of $\mathbf{\Delta}^*$ take two possible values $D + (L-1)\eta$ and $D - \eta$; the former is positive when $D_S > \sigma_Z^2$ while the latter is positive when $D \geq \frac{(D_S-\sigma_Z^2)\sigma_N^4}{L\sigma_Z^4}$. Also, the eigenvalues of $\mathbf{K_X} - \mathbf{\Delta}^*$ take two possible values $L\sigma_S^2 + \sigma_N^2 - D - (L-1)\eta$ and $\sigma_N^2 - D + \eta$; the former is nonnegative when $D_S \leq \sigma_S^2$ while the latter is positive when $D < \frac{L-1}{L}\sigma_N^2 + \frac{(D_S-\sigma_Z^2)\sigma_N^4}{L^2\sigma_Z^4}$. So (4.3.2) is satisfied. It is easy to verify that (4.3.3)–(4.3.8) are also satisfied. Moreover, $D \geq \frac{(D_S-\sigma_Z^2)\sigma_N^4}{L\sigma_Z^4}$ is equivalent to $\eta \leq 0$, which implies $\rho \geq 0$ and $\mathbf{\Lambda} \succ \mathbf{0}$. Therefore, $\mathbf{\Delta}^*$ is indeed an optimal solution and consequently

$$R_c(D, D_S) = \frac{1}{2}\log\frac{\det(\mathbf{K_X})}{\det(\mathbf{\Delta}^*)} = \frac{1}{2}\log\frac{L\sigma_Z^4(L\sigma_S^2\sigma_N^{2(L-1)} + \sigma_N^{2L})}{(D_S-\sigma_Z^2)\sigma_N^4(\frac{L}{L-1}D - \frac{(D_S-\sigma_Z^2)\sigma_N^4}{L(L-1)\sigma_Z^4})^{L-1}}.$$

3. Consider the following construction:

$$\mathbf{\Delta}^* := \begin{bmatrix} D & D-\sigma_N^2 & \dots & D-\sigma_N^2 \\ D-\sigma_N^2 & D & \dots & D-\sigma_N^2 \\ \vdots & \vdots & \ddots & \vdots \\ D-\sigma_N^2 & D-\sigma_N^2 & \dots & D \end{bmatrix},$$

$$\mathbf{U} := \begin{bmatrix} \frac{(L-1)(D-\sigma_N^2)}{(LD-(L-1)\sigma_N^2)\sigma_N^2} & -\frac{D-\sigma_N^2}{(LD-(L-1)\sigma_N^2)\sigma_N^2} & \dots & -\frac{D-\sigma_N^2}{(LD-(L-1)\sigma_N^2)\sigma_N^2} \\ -\frac{D-\sigma_N^2}{(LD-(L-1)\sigma_N^2)\sigma_N^2} & \frac{(L-1)(D-\sigma_N^2)}{(LD-(L-1)\sigma_N^2)\sigma_N^2} & \dots & -\frac{D-\sigma_N^2}{(LD-(L-1)\sigma_N^2)\sigma_N^2} \\ \vdots & \vdots & \ddots & \vdots \\ -\frac{D-\sigma_N^2}{(LD-(L-1)\sigma_N^2)\sigma_N^2} & -\frac{D-\sigma_N^2}{(LD-(L-1)\sigma_N^2)\sigma_N^2} & \dots & \frac{(L-1)(D-\sigma_N^2)}{(LD-(L-1)\sigma_N^2)\sigma_N^2} \end{bmatrix},$$

$$\mathbf{\Lambda} := \begin{bmatrix} \frac{1}{LD-(L-1)\sigma_N^2} & 0 & \dots & 0 \\ 0 & \frac{1}{LD-(L-1)\sigma_N^2} & \dots & 0 \\ \vdots & \vdots & \ddots & \vdots \\ 0 & 0 & \dots & \frac{1}{LD-(L-1)\sigma_N^2} \end{bmatrix}, \quad \rho := 0.$$

The eigenvalues of $\mathbf{\Delta}^*$ take two possible values $LD-(L-1)\sigma_N^2$ and σ_N^2 while the eigenvalues of $\mathbf{K}_{\mathbf{X}}-\mathbf{\Delta}^*$ take two possible values $L(\sigma_S^2+\sigma_N^2-D)$ and 0. So (4.3.2) is satisfied since $LD-(L-1)\sigma_N^2 > 0$ when $D \geq \sigma_N^2$ and $L(\sigma_S^2+\sigma_N^2-D) \geq 0$ when $D_S \leq \sigma_S^2$. It can be verified that (4.3.3)–(4.3.8) are also satisfied. In particular, (4.3.4) holds because

$$\mathbf{g}^T\mathbf{\Delta}^*\mathbf{g} + \sigma_Z^2 < D_S \Longleftrightarrow D < \frac{L-1}{L}\sigma_N^2 + \frac{(D_S-\sigma_Z^2)\sigma_N^4}{L^2\sigma_Z^4}.$$

Moreover, we have $\mathbf{U} \succeq \mathbf{0}$ since its eigenvalues take two possible values 0 and

$\frac{L(D-\sigma_N^2)}{(LD-(L-1)\sigma_N^2)\sigma_N^2}$, the latter of which is nonnegative when $D \geq \sigma_N^2$. It is also clear that $\mathbf{\Lambda} \succ \mathbf{0}$ when $D \geq \sigma_N^2$. Therefore, $\mathbf{\Delta}^*$ is indeed an optimal solution and consequently

$$R_c(D, D_S) = \frac{1}{2}\log\frac{\det(\mathbf{K_X})}{\det(\mathbf{\Delta}^*)} = \frac{1}{2}\log\frac{L\sigma_S^2 + \sigma_N^2}{LD - (L-1)\sigma_N^2}.$$

4. Consider the following construction:

$$\mathbf{\Delta}^* := \begin{bmatrix} \frac{L-1}{L}\sigma_N^2 + \frac{\sigma_N^4(D_S-\sigma_Z^2)}{L^2\sigma_Z^4} & \frac{\sigma_N^4(D_S-\sigma_Z^2)}{L^2\sigma_Z^4} - \frac{\sigma_N^2}{L} & \cdots & \frac{\sigma_N^4(D_S-\sigma_Z^2)}{L^2\sigma_Z^4} - \frac{\sigma_N^2}{L} \\ \frac{\sigma_N^4(D_S-\sigma_Z^2)}{L^2\sigma_Z^4} - \frac{\sigma_N^2}{L} & \frac{L-1}{L}\sigma_N^2 + \frac{\sigma_N^4(D_S-\sigma_Z^2)}{L^2\sigma_Z^4} & \cdots & \frac{\sigma_N^4(D_S-\sigma_Z^2)}{L^2\sigma_Z^4} - \frac{\sigma_N^2}{L} \\ \vdots & \vdots & \ddots & \vdots \\ \frac{\sigma_N^4(D_S-\sigma_Z^2)}{L^2\sigma_Z^4} - \frac{\sigma_N^2}{L} & \frac{\sigma_N^4(D_S-\sigma_Z^2)}{L^2\sigma_Z^4} - \frac{\sigma_N^2}{L} & \cdots & \frac{L-1}{L}\sigma_N^2 + \frac{\sigma_N^4(D_S-\sigma_Z^2)}{L^2\sigma_Z^4} \end{bmatrix},$$

$$\mathbf{U} := \begin{bmatrix} \frac{L-1}{L\sigma_N^2} & -\frac{1}{L\sigma_N^2} & \cdots & -\frac{1}{L\sigma_N^2} \\ -\frac{1}{L\sigma_N^2} & \frac{L-1}{L\sigma_N^2} & \cdots & -\frac{1}{L\sigma_N^2} \\ \vdots & \vdots & \ddots & \vdots \\ -\frac{1}{L\sigma_N^2} & -\frac{1}{L\sigma_N^2} & \cdots & \frac{L-1}{L\sigma_N^2} \end{bmatrix}, \quad \mathbf{\Lambda} := \mathbf{0}, \quad \rho := \frac{1}{D_S - \sigma_Z^2}.$$

The eigenvalues of $\mathbf{\Delta}^*$ take two possible values $\frac{\sigma_N^4(D_S-\sigma_Z^2)}{L\sigma_Z^4}$ and σ_N^2 while the eigenvalues of $\mathbf{K_X} - \mathbf{\Delta}^*$ take two possible values $L\sigma_S^2 + \sigma_N^2 - \frac{\sigma_N^4(D_S-\sigma_Z^2)}{L\sigma_Z^4}$ and 0. So (4.3.2) is satisfied since $\frac{\sigma_N^4(D_S-\sigma_Z^2)}{L\sigma_Z^4} > 0$ when $D_S > \sigma_Z^2$ and $L\sigma_S^2 + \sigma_N^2 - \frac{\sigma_N^4(D_S-\sigma_Z^2)}{L\sigma_Z^4} \geq 0$ when $D_S \leq \sigma_S^2$. It can be verified that (4.3.3)–(4.3.8) are also satisfied. In particular, (4.3.3) holds because it is equivalent to $D \geq \frac{L-1}{L}\sigma_N^2 + \frac{(D_S-\sigma_Z^2)\sigma_N^4}{L^2\sigma_Z^4}$. Moreover, we have $\mathbf{U} \succeq \mathbf{0}$ since its eigenvalues take two possible values 0 and $\frac{1}{\sigma_N^2}$. It is also clear that $\rho > 0$ when $D_S > \sigma_Z^2$. Therefore, $\mathbf{\Delta}^*$ is indeed an optimal solution and consequently

$$R_c(D, D_S) = \frac{1}{2}\log\frac{\det(\mathbf{K}_{\mathbf{X}})}{\det(\mathbf{\Delta}^*)} = \frac{1}{2}\log\frac{\sigma_S^2 - \sigma_Z^2}{D_S - \sigma_Z^2}.$$

This completes the proof of Theorem 4.2. $\square$

The following result deals with the 2-component setting (shown in Fig. 4.2) and provides an explicit characterization of $R_c(D_1, D_2, D_S)$.

Theorem 4.3 *The closed-form expression for $R_c(D_1, D_2, D_S)$ is given as follows:*

1. *If $D_2 \geq \sigma_S^2 + \sigma_{N_2}^2 - \frac{\sigma_S^4(\sigma_S^2+\sigma_{N_1}^2-D_1)}{(\sigma_S^2+\sigma_{N_1}^2)^2}$ and $D_S \geq \sigma_S^2 - \frac{\sigma_S^4(\sigma_S^2+\sigma_{N_1}^2-D_1)}{(\sigma_S^2+\sigma_{N_1}^2)^2}$, then*

$$R_c(D_1, D_2, D_S) = \frac{1}{2}\log\frac{\sigma_S^2 + \sigma_{N_1}^2}{D_1}.$$

2. *If $D_1 \geq \sigma_S^2 + \sigma_{N_1}^2 - \frac{\sigma_S^4(\sigma_S^2+\sigma_{N_2}^2-D_2)}{(\sigma_S^2+\sigma_{N_2}^2)^2}$ and $D_S \geq \sigma_S^2 - \frac{\sigma_S^4(\sigma_S^2+\sigma_{N_2}^2-D_2)}{(\sigma_S^2+\sigma_{N_2}^2)^2}$, then*

$$R_c(D_1, D_2, D_S) = \frac{1}{2}\log\frac{\sigma_S^2 + \sigma_{N_2}^2}{D_2}.$$

3. *If $D_i \geq \sigma_S^2 + \sigma_{N_i}^2 - \frac{\sigma_S^4(\sigma_S^2-D_S)}{(\sigma_S^2-\sigma_Z^2)^2}$, $i = 1, 2$, then*

$$R_c(D_1, D_2, D_S) = \frac{1}{2}\log\frac{\sigma_S^2 - \sigma_Z^2}{D_S - \sigma_Z^2}.$$

4. *If $(\sigma_S^2 + \sigma_{N_1}^2 - D_1)(\sigma_S^2 + \sigma_{N_2}^2 - D_2) \geq \sigma_S^4$ and $D_S \geq \frac{\sigma_Z^4}{\sigma_{N_1}^2}D_1 + \frac{\sigma_Z^4}{\sigma_{N_2}^2}D_2 + \sigma_Z^2$, then*

$$R_c(D_1, D_2, D_S) = \frac{1}{2}\log\frac{(\sigma_S^2 + \sigma_{N_1}^2)(\sigma_S^2 + \sigma_{N_2}^2) - \sigma_S^4}{D_1 D_2}.$$

5. *If* $(\sigma_S^2+\sigma_{N_1}^2-D_1)(\sigma_S^2-D_S)\geq\sigma_S^4$ *and* $D_2\geq\frac{\sigma_{N_2}^4}{\sigma_{N_1}^4}D_1+\frac{\sigma_{N_2}^4}{\sigma_Z^4}(D_S-\sigma_Z^2)$*, then*

$$R_c(D_1,D_2,D_S)=\frac{1}{2}\log\frac{(\sigma_S^2+\sigma_{N_1}^2)(\sigma_S^2-\sigma_Z^2)-\sigma_S^4}{D_1(D_S-\sigma_Z^2)}.$$

6. *If* $(\sigma_S^2+\sigma_{N_2}^2-D_2)(\sigma_S^2-D_S)\geq\sigma_S^4$ *and* $D_1\geq\frac{\sigma_{N_1}^4}{\sigma_{N_2}^4}D_2+\frac{\sigma_{N_1}^4}{\sigma_Z^4}(D_S-\sigma_Z^2)$*, then*

$$R_c(D_1,D_2,D_S)=\frac{1}{2}\log\frac{(\sigma_S^2+\sigma_{N_2}^2)(\sigma_S^2-\sigma_Z^2)-\sigma_S^4}{D_2(D_S-\sigma_Z^2)}.$$

7. *If* $(\sigma_S^2+\sigma_{N_1}^2-D_1)(\sigma_S^2+\sigma_{N_2}^2-D_2)<\sigma_S^4$*,* $D_1<\sigma_S^2+\sigma_{N_1}^2-\frac{\sigma_S^4(\sigma_S^2+\sigma_{N_2}^2-D_2)}{(\sigma_S^2+\sigma_{N_2}^2)^2}$*,* $D_2<\sigma_S^2+\sigma_{N_2}^2-\frac{\sigma_S^4(\sigma_S^2+\sigma_{N_1}^2-D_1)}{(\sigma_S^2+\sigma_{N_1}^2)^2}$*, and* $D_S\geq\frac{\sigma_Z^4}{\sigma_{N_1}^4}D_1+\frac{2\sigma_Z^4}{\sigma_{N_1}^2\sigma_{N_2}^2}(\sigma_S^2-\sqrt{(\sigma_S^2+\sigma_{N_1}^2-D_1)(\sigma_S^2+\sigma_{N_2}^2-D_2)})+\frac{\sigma_Z^4}{\sigma_{N_2}^4}D_2+\sigma_Z^2$*, then*

$$R_c(D_1,D_2,D_S)=\frac{1}{2}\log\frac{(\sigma_S^2+\sigma_{N_1}^2)(\sigma_S^2+\sigma_{N_2}^2)-\sigma_S^4}{D_1D_2-(\sigma_S^2-\sqrt{(\sigma_S^2+\sigma_{N_1}^2-D_1)(\sigma_S^2+\sigma_{N_2}^2-D_2)})^2}.$$

8. *If* $(\sigma_S^2+\sigma_{N_1}^2-D_1)(\sigma_S^2-D_S)<\sigma_S^4$*,* $D_1<\sigma_S^2+\sigma_{N_1}^2-\frac{\sigma_S^4(\sigma_S^2-D_S)}{(\sigma_S^2-\sigma_Z^2)^2}$*,* $D_S<\sigma_S^2-\frac{\sigma_S^4(\sigma_S^2+\sigma_{N_1}^2-D_1)}{(\sigma_S^2+\sigma_{N_1}^2)^2}$*, and* $D_2\geq\frac{\sigma_{N_2}^4}{\sigma_{N_1}^4}D_1-\frac{2\sigma_{N_2}^4}{\sigma_{N_1}^2\sigma_Z^2}(\sigma_S^2-\sqrt{(\sigma_S^2+\sigma_{N_1}^2-D_1)(\sigma_S^2-D_S)})+\frac{\sigma_{N_2}^4}{\sigma_Z^4}(D_S-\sigma_Z^2)$*, then*

$$R_c(D_1,D_2,D_S)=\frac{1}{2}\log\frac{(\sigma_S^2+\sigma_{N_1}^2)(\sigma_S^2-\sigma_Z^2)-\sigma_S^4}{D_1(D_S-\sigma_Z^2)-(\sigma_S^2-\sqrt{(\sigma_S^2+\sigma_{N_1}^2-D_1)(\sigma_S^2-D_S)})^2}.$$

9. *If* $(\sigma_S^2+\sigma_{N_2}^2-D_2)(\sigma_S^2-D_S)<\sigma_S^4$*,* $D_2<\sigma_S^2+\sigma_{N_2}^2-\frac{\sigma_S^4(\sigma_S^2-D_S)}{(\sigma_S^2-\sigma_Z^2)^2}$*,* $D_S<\sigma_S^2-\frac{\sigma_S^4(\sigma_S^2+\sigma_{N_2}^2-D_2)}{(\sigma_S^2+\sigma_{N_2}^2)^2}$*, and* $D_1\geq\frac{\sigma_{N_1}^4}{\sigma_{N_2}^4}D_2-\frac{2\sigma_{N_1}^4}{\sigma_{N_2}^2\sigma_Z^2}(\sigma_S^2-\sqrt{(\sigma_S^2+\sigma_{N_2}^2-D_2)(\sigma_S^2-D_S)})+$

$\frac{\sigma_{N_1}^4}{\sigma_Z^4}(D_S - \sigma_Z^2)$, *then*

$$R_c(D_1, D_2, D_S) = \frac{1}{2}\log \frac{(\sigma_S^2 + \sigma_{N_2}^2)(\sigma_S^2 - \sigma_Z^2) - \sigma_S^4}{D_2(D_S - \sigma_Z^2) - (\sigma_S^2 - \sqrt{(\sigma_S^2 + \sigma_{N_2}^2 - D_2)(\sigma_S^2 - D_S)})^2}.$$

10. Otherwise,

$$R_c(D_1, D_2, D_S) = \frac{1}{2}\log \frac{(\sigma_S^2 + \sigma_{N_1}^2)(\sigma_S^2 + \sigma_{N_2}^2) - \sigma_S^4}{D_1 D_2 - \frac{\sigma_{N_1}^4 \sigma_{N_2}^4}{4\sigma_Z^8}(D_S - \sigma_Z^2 - \frac{\sigma_Z^4}{\sigma_{N_1}^4} D_1 - \frac{\sigma_Z^4}{\sigma_{N_2}^4} D_2)^2}.$$

Remark 4.1 *One can specialize [100, Theorem 6] and [51, Theorem III.1] from Theorem 4.3 by removing semantic distortion constraint D_S, i.e., by considering only Cases 1), 2), 4), and 7) where semantic distortion constraint D_S is inactive.*

The regions of the (D_1, D_2, D_S) space in which each closed-form expression applies can be visualized using the example in Fig. 4.4. For cases 1), 2), 4) and 7), the distortion D_S is inactive, thus the dominant terms are the combination of D_1 and D_2.

Proof For each of the ten cases, we invoke Lemma 4.1 to verify the optimality of a specific $\mathbf{\Delta}^*$ by explicitly constructing $\mathbf{U}$, $\mathbf{\Lambda}$, and ρ that satisfy the KKT conditions.

1. Consider the following construction:

$$\mathbf{\Delta}^* := \begin{bmatrix} D_1 & \frac{\sigma_S^2}{\sigma_S^2+\sigma_{N_1}^2} D_1 \\ \frac{\sigma_S^2}{\sigma_S^2+\sigma_{N_1}^2} D_1 & \sigma_S^2 + \sigma_{N_2}^2 - \frac{\sigma_S^4(\sigma_S^2+\sigma_{N_1}^2 - D_1)}{(\sigma_S^2+\sigma_{N_1}^2)^2} \end{bmatrix},$$

$$\mathbf{U} := \begin{bmatrix} \frac{\sigma_S^4}{((\sigma_S^2+\sigma_{N_1}^2)(\sigma_S^2+\sigma_{N_2}^2)-\sigma_S^4)(\sigma_S^2+\sigma_{N_1}^2)} & -\frac{\sigma_S^2}{(\sigma_S^2+\sigma_{N_1}^2)(\sigma_S^2+\sigma_{N_2}^2)-\sigma_S^4} \\ -\frac{\sigma_S^2}{(\sigma_S^2+\sigma_{N_1}^2)(\sigma_S^2+\sigma_{N_2}^2)-\sigma_S^4} & \frac{\sigma_S^2+\sigma_{N_1}^2}{(\sigma_S^2+\sigma_{N_1}^2)(\sigma_S^2+\sigma_{N_2}^2)-\sigma_S^4} \end{bmatrix}, \ \mathbf{\Lambda} := \begin{bmatrix} \frac{1}{D_1} & 0 \\ 0 & 0 \end{bmatrix}, \ \rho := 0.$$

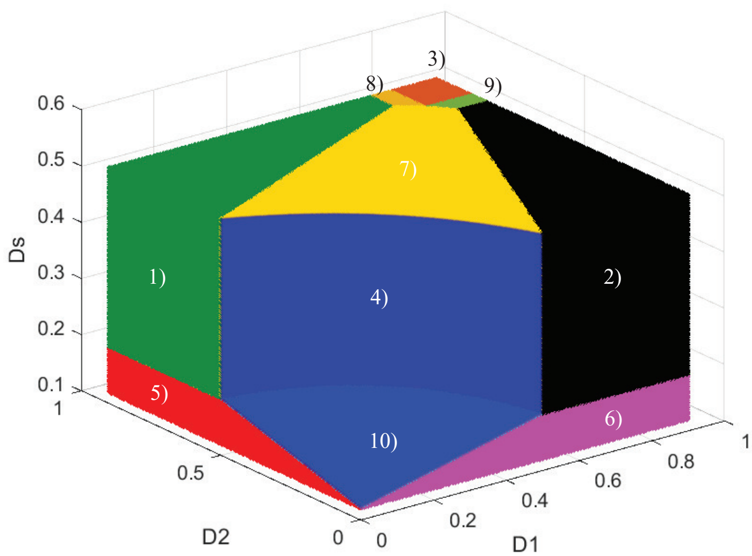

Figure 4.4: Regions of each case of Theorem 4.3, when $\sigma_S^2 = 0.6$, $\sigma_{N_1}^2 = 0.3$, and $\sigma_{N_2}^2 = 0.3$.

Clearly, we have $\mathbf{U} \succeq \mathbf{0}$ and $\mathbf{\Lambda} \succeq \mathbf{0}$. It can be verified that (4.3.5)–(4.3.8) are satisfied. Moreover, (4.3.3) is also satisfied since $D_2 \geq \sigma_S^2 + \sigma_{N_2}^2 - \frac{\sigma_S^4(\sigma_S^2+\sigma_{N_1}^2-D_1)}{(\sigma_S^2+\sigma_{N_1}^2)^2}$. In view of the fact that

$$\mathbf{g}^T \mathbf{\Delta}^* \mathbf{g} \leq D_S - \sigma_Z^2 \Longleftrightarrow D_S \geq \sigma_S^2 - \frac{\sigma_S^4(\sigma_S^2 + \sigma_{N_1}^2 - D_1)}{(\sigma_S^2 + \sigma_{N_1}^2)^2},$$

(4.3.4) is satisfied as well. Finally, (4.3.2) holds because $\mathbf{\Delta}^* \succ \mathbf{0}$ and

$$\mathbf{K_X} - \mathbf{\Delta}^* = \begin{bmatrix} \sigma_S^2 + \sigma_{N_1}^2 - D_1 & \frac{\sigma_S^2(\sigma_S^2+\sigma_{N_1}^2-D_1)}{\sigma_S^2+\sigma_{N_1}^2} \\ \frac{\sigma_S^2(\sigma_S^2+\sigma_{N_1}^2-D_1)}{\sigma_S^2+\sigma_{N_1}^2} & \frac{\sigma_S^4(\sigma_S^2+\sigma_{N_1}^2-D_1)}{(\sigma_S^2+\sigma_{N_1}^2)^2} \end{bmatrix} \succeq \mathbf{0}.$$

Therefore, $\mathbf{\Delta}^*$ is indeed an optimal solution and consequently

$$R_c(D_1, D_2, D_S) = \frac{1}{2} \log \frac{\det(\mathbf{K_X})}{\det(\mathbf{\Delta}^*)} = \frac{1}{2} \log \frac{\sigma_S^2 + \sigma_{N_1}^2}{D_1}.$$

2. This follows from Case 1) by symmetry.

3. Consider the following construction:

$$\mathbf{\Delta}^* := \begin{bmatrix} \sigma_S^2 + \sigma_{N_1}^2 - \frac{\sigma_S^4(\sigma_S^2 - D_S)}{(\sigma_S^2-\sigma_Z^2)^2} & \sigma_S^2 - \frac{\sigma_S^4(\sigma_S^2 - D_S)}{(\sigma_S^2-\sigma_Z^2)^2} \\ \sigma_S^2 - \frac{\sigma_S^4(\sigma_S^2 - D_S)}{(\sigma_S^2-\sigma_Z^2)^2} & \sigma_S^2 + \sigma_{N_2}^2 - \frac{\sigma_S^4(\sigma_S^2 - D_S)}{(\sigma_S^2-\sigma_Z^2)^2} \end{bmatrix},$$

$$\mathbf{U} := \begin{bmatrix} \frac{1}{\sigma_{N_1}^2+\sigma_{N_2}^2} & -\frac{1}{\sigma_{N_1}^2+\sigma_{N_2}^2} \\ -\frac{1}{\sigma_{N_1}^2+\sigma_{N_2}^2} & \frac{1}{\sigma_{N_1}^2+\sigma_{N_2}^2} \end{bmatrix}, \ \mathbf{\Lambda} := \mathbf{0}, \ \rho := \frac{\left((\sigma_S^2+\sigma_{N_1}^2)(\sigma_S^2+\sigma_{N_2}^2) - \sigma_S^4\right)(\sigma_S^2 - \sigma_Z^2)}{\sigma_S^4\left(D_S - \sigma_Z^2\right)\left(\sigma_{N_1}^2 + \sigma_{N_2}^2\right)}.$$

Clearly, we have $\mathbf{U} \succeq \mathbf{0}$ and $\rho \geq 0$. It can be verified that (4.3.4)–(4.3.8) are satisfied. Moreover, (4.3.3) is also satisfied since $D_i \geq \sigma_S^2 + \sigma_{N_i}^2 - \frac{\sigma_S^4(\sigma_S^2-D_S)}{(\sigma_S^2-\sigma_Z^2)^2}$, $i = 1, 2$. Finally, (4.3.2) holds because $\mathbf{\Delta}^* \succ \mathbf{0}$ and

$$\mathbf{K_X} - \mathbf{\Delta}^* = \begin{bmatrix} \frac{\sigma_S^4(\sigma_S^2 - D_S)}{(\sigma_S^2-\sigma_Z^2)^2} & \frac{\sigma_S^4(\sigma_S^2 - D_S)}{(\sigma_S^2-\sigma_Z^2)^2} \\ \frac{\sigma_S^4(\sigma_S^2 - D_S)}{(\sigma_S^2-\sigma_Z^2)^2} & \frac{\sigma_S^4(\sigma_S^2 - D_S)}{(\sigma_S^2-\sigma_Z^2)^2} \end{bmatrix} \succeq \mathbf{0}.$$

Therefore, $\mathbf{\Delta}^*$ is indeed an optimal solution and consequently

$$R_c(D_1, D_2, D_S) = \frac{1}{2}\log\frac{\det(\mathbf{K_X})}{\det(\mathbf{\Delta}^*)} = \frac{1}{2}\log\frac{\sigma_S^2 - \sigma_Z^2}{D_S - \sigma_Z^2}.$$

4. Consider the following construction:

$$\mathbf{\Delta}^* := \mathbf{D}, \quad \mathbf{U} := \mathbf{0}, \quad \mathbf{\Lambda} := \mathbf{D}^{-1}, \quad \rho := 0.$$

It is clear that (4.3.3) and (4.3.5)–(4.3.8) are satisfied. In view of the fact that

$$\mathbf{g}^T\mathbf{\Delta}^*\mathbf{g} \leq D_S - \sigma_Z^2 \Longleftrightarrow D_S \geq \frac{\sigma_Z^4}{\sigma_{N_1}^4}D_1 + \frac{\sigma_Z^4}{\sigma_{N_2}^4}D_2 + \sigma_Z^2,$$

(4.3.4) is satisfied as well. Finally, (4.3.2) holds because $\mathbf{\Delta}^* \succ \mathbf{0}$ and

$$\mathbf{K_X} - \mathbf{\Delta}^* = \begin{bmatrix} \sigma_S^2 + \sigma_{N_1}^2 - D_1 & \sigma_S^2 \\ \sigma_S^2 & \sigma_S^2 + \sigma_{N_2}^2 - D_2 \end{bmatrix} \succeq \mathbf{0},$$

where the last step uses the condition $(\sigma_S^2 + \sigma_{N_1}^2 - D_1)(\sigma_S^2 + \sigma_{N_2}^2 - D_2) \geq \sigma_S^4$. Therefore, $\mathbf{\Delta}^*$ is indeed an optimal solution and consequently

$$R_c(D_1, D_2, D_S) = \frac{1}{2}\log\frac{\det(\mathbf{K_X})}{\det(\mathbf{\Delta}^*)} = \frac{1}{2}\log\frac{(\sigma_S^2 + \sigma_{N_1}^2)(\sigma_S^2 + \sigma_{N_2}^2) - \sigma_S^4}{D_1 D_2}.$$

5. Consider the following construction:

$$\mathbf{\Delta}^* := \begin{bmatrix} D_1 & -\frac{\sigma_{N_2}^2}{\sigma_{N_1}^2}D_1 \\ -\frac{\sigma_{N_2}^2}{\sigma_{N_1}^2}D_1 & \frac{\sigma_{N_2}^4}{\sigma_{N_1}^4}D_1 + \frac{\sigma_{N_2}^4}{\sigma_Z^4}(D_S - \sigma_Z^2) \end{bmatrix}, \ \mathbf{U} := \mathbf{0}, \ \mathbf{\Lambda} := \begin{bmatrix} \frac{1}{D_1} & 0 \\ 0 & 0 \end{bmatrix}, \ \rho := \frac{1}{D_S - \sigma_Z^2}.$$

Clearly, we have $\mathbf{\Lambda} \succeq \mathbf{0}$ and $\rho \geq 0$. It can be verified that (4.3.4)–(4.3.8) are satisfied. Moreover, (4.3.3) is also satisfied since $D_2 \geq \frac{\sigma_{N_2}^4}{\sigma_{N_1}^4}D_1 + \frac{\sigma_{N_2}^4}{\sigma_Z^4}(D_S - \sigma_Z^2)$. Finally, (4.3.2) holds because $\mathbf{\Delta}^* \succ \mathbf{0}$ and

$$\mathbf{K_X} - \mathbf{\Delta}^* = \begin{bmatrix} \sigma_S^2 + \sigma_{N_1}^2 - D_1 & \sigma_S^2 + \frac{\sigma_{N_2}^2}{\sigma_{N_1}^2}D_1 \\ \sigma_S^2 + \frac{\sigma_{N_2}^2}{\sigma_{N_1}^2}D_1 & \sigma_S^2 + \sigma_{N_2}^2 - (\frac{\sigma_{N_2}^4}{\sigma_{N_1}^4}D_1 + \frac{\sigma_{N_2}^4}{\sigma_Z^4}(D_S - \sigma_Z^2)) \end{bmatrix} \succeq \mathbf{0},$$

where the last step uses the condition $\left(\sigma_S^2+\sigma_{N_1}^2-D_1\right)(\sigma_S^2-D_S)>\sigma_S^4$. Therefore, $\mathbf{\Delta}^*$ is indeed an optimal solution and consequently

$$R_c(D_1,D_2,D_S)=\frac{1}{2}\log\frac{\det(\mathbf{K_X})}{\det(\mathbf{\Delta}^*)}=\frac{1}{2}\log\frac{(\sigma_S^2+\sigma_{N_1}^2)(\sigma_S^2-\sigma_Z^2)-\sigma_S^4}{D_1(D_S-\sigma_Z^2)}.$$

6. This follows from Case 5) by symmetry.

7. Consider the following construction:

$$\mathbf{\Delta}^*:=\begin{bmatrix} D_1 & \sigma_S^2-\mu \\ \sigma_S^2-\mu & D_2 \end{bmatrix},\ \mathbf{U}:=\frac{\sigma_S^2-\mu}{\det(\mathbf{\Delta}^*)}\begin{bmatrix} \sqrt{\frac{\sigma_S^2+\sigma_{N_2}^2-D_2}{\sigma_S^2+\sigma_{N_1}^2-D_1}} & -1 \\ -1 & \sqrt{\frac{\sigma_S^2+\sigma_{N_1}^2-D_1}{\sigma_S^2+\sigma_{N_2}^2-D_2}} \end{bmatrix},$$

$$\mathbf{\Lambda}:=\frac{1}{\det(\mathbf{\Delta}^*)}\begin{bmatrix} \sigma_S^2+\sigma_{N_2}^2-\sigma_S^2\sqrt{\frac{\sigma_S^2+\sigma_{N_2}^2-D_2}{\sigma_S^2+\sigma_{N_1}^2-D_1}} & 0 \\ 0 & \sigma_S^2+\sigma_{N_1}^2-\sigma_S^2\sqrt{\frac{\sigma_S^2+\sigma_{N_1}^2-D_1}{\sigma_S^2+\sigma_{N_2}^2-D_2}} \end{bmatrix},\ \rho:=0,$$

where $\mu:=\sqrt{(\sigma_S^2+\sigma_{N_1}^2-D_1)(\sigma_S^2+\sigma_{N_2}^2-D_2)}$. Since $D_1<\sigma_S^2+\sigma_{N_1}^2-\frac{\sigma_S^4(\sigma_S^2+\sigma_{N_2}^2-D_2)}{(\sigma_S^2+\sigma_{N_2}^2)^2}$ and $D_2<\sigma_S^2+\sigma_{N_2}^2-\frac{\sigma_S^4(\sigma_S^2+\sigma_{N_1}^2-D_1)}{(\sigma_S^2+\sigma_{N_1}^2)^2}$, it follows that

$$\sqrt{\frac{\sigma_S^2+\sigma_{N_1}^2-D_1}{\sigma_S^2+\sigma_{N_2}^2-D_2}}<\frac{\sigma_S^2+\sigma_{N_1}^2}{\sigma_S^2}, \tag{4.3.9}$$

$$\sqrt{\frac{\sigma_S^2+\sigma_{N_2}^2-D_2}{\sigma_S^2+\sigma_{N_1}^2-D_1}}<\frac{\sigma_S^2+\sigma_{N_2}^2}{\sigma_S^2}. \tag{4.3.10}$$

Moreover, we have

$$\mathbf{K_X}-\mathbf{\Delta}^*=\begin{bmatrix} \sigma_S^2+\sigma_{N_1}^2-D_1 & \mu \\ \mu & \sigma_S^2+\sigma_{N_2}^2-D_2 \end{bmatrix}\succeq\mathbf{0}$$

and

$$
\begin{aligned}
\mathbf{\Delta}^* &= \mathbf{K_X} - \begin{bmatrix} \sigma_S^2+\sigma_{N_1}^2-D_1 & \mu \\ \mu & \sigma_S^2+\sigma_{N_2}^2-D_2 \end{bmatrix} \\
&\succeq \mathbf{K_X} - \frac{\sigma_S^2}{\mu} \begin{bmatrix} \sigma_S^2+\sigma_{N_1}^2-D_1 & \mu \\ \mu & \sigma_S^2+\sigma_{N_2}^2-D_2 \end{bmatrix} && (4.3.11) \\
&= \mathbf{K_X} - \begin{bmatrix} \sigma_S^2\sqrt{\frac{\sigma_S^2+\sigma_{N_1}^2-D_1}{\sigma_S^2+\sigma_{N_2}^2-D_2}} & \sigma_S^2 \\ \sigma_S^2 & \sigma_S^2\sqrt{\frac{\sigma_S^2+\sigma_{N_2}^2-D_2}{\sigma_S^2+\sigma_{N_1}^2-D_1}} \end{bmatrix} \\
&\succ \mathbf{0}, && (4.3.12)
\end{aligned}
$$

where (4.3.11) is due to the condition $(\sigma_S^2+\sigma_{N_1}^2-D_1)(\sigma_S^2+\sigma_{N_2}^2-D_2) < \sigma_S^4$ while (4.3.12) is due to (4.3.9) and (4.3.10). So (4.3.2) is satisfied. Note that $\mathbf{\Delta}^* \succ \mathbf{0}$ implies $D_1D_2-(\sigma_S^2-\mu)^2 > 0$, which, together with (4.3.9), (4.3.10), and the condition $(\sigma_S^2+\sigma_{N_1}^2-D_1)(\sigma_S^2+\sigma_{N_2}^2-D_2) \le \sigma_S^4$, further implies $\mathbf{U} \succeq \mathbf{0}$ and $\mathbf{\Lambda} \succeq \mathbf{0}$. It can also be verified that (4.3.3) and (4.3.5)–(4.3.8) are satisfied. Finally, (4.3.4) holds because

$$
\mathbf{g}^T\mathbf{\Delta}^*\mathbf{g} \le D_S - \sigma_Z^2 \Longleftrightarrow D_S \ge \frac{\sigma_Z^4}{\sigma_{N_1}^4}D_1 + 2\frac{\sigma_Z^4}{\sigma_{N_1}^2\sigma_{N_2}^2}(\sigma_S^2-\mu) + \frac{\sigma_Z^4}{\sigma_{N_2}^4}D_2 + \sigma_Z^2.
$$

Therefore, $\mathbf{\Delta}^*$ is indeed an optimal solution and consequently

$$
\begin{aligned}
R_c(D_1,D_2,D_S) &= \frac{1}{2}\log\frac{\det(\mathbf{K_X})}{\det(\mathbf{\Delta}^*)} \\
&= \frac{1}{2}\log\frac{(\sigma_S^2+\sigma_{N_1}^2)(\sigma_S^2+\sigma_{N_2}^2)-\sigma_S^4}{D_1D_2-(\sigma_S^2-\sqrt{(\sigma_S^2+\sigma_{N_1}^2-D_1)(\sigma_S^2+\sigma_{N_2}^2-D_2)})^2}.
\end{aligned}
$$

8. Consider the following construction:

$$
\begin{aligned}
\mathbf{\Delta}^* &:= \begin{bmatrix} D_1 & \sigma_S^2 - \nu\sqrt{\sigma_S^2 + \sigma_{N_1}^2 - D_1} \\ \sigma_S^2 - \nu\sqrt{\sigma_S^2 + \sigma_{N_1}^2 - D_1} & \sigma_S^2 + \sigma_{N_2}^2 - \nu^2 \end{bmatrix}, \\
\mathbf{U} &:= \frac{1}{\det(\mathbf{\Delta}^*)} \begin{bmatrix} \frac{\xi_1\nu^2}{\xi_2\sqrt{\sigma_S^2+\sigma_{N_1}^2-D_1}} & -\frac{\xi_1\nu}{\xi_2} \\ -\frac{\xi_1\nu}{\xi_2} & \frac{\xi_1\sqrt{\sigma_S^2+\sigma_{N_1}^2-D_1}}{\xi_2} \end{bmatrix}, \\
\mathbf{\Lambda} &= \frac{1}{\det(\mathbf{\Delta}^*)} \begin{bmatrix} \frac{\xi_3}{\sqrt{\sigma_S^2+\sigma_{N_1}^2-D_1}} - \frac{\sigma_{N_2}^2\xi_4}{\sigma_{N_1}^2\sqrt{\sigma_S^2+\sigma_{N_1}^2-D_1}} & 0 \\ 0 & 0 \end{bmatrix}, \\
\rho &= \frac{\sigma_{N_1}^2\sigma_{N_2}^4\xi_4}{\sigma_Z^4\xi_2\det(\mathbf{\Delta}^*)},
\end{aligned}
$$

where

$$
\begin{aligned}
\nu &:= \frac{\sigma_S^2(\sigma_{N_1}^2+\sigma_{N_2}^2)\sqrt{\sigma_S^2 - D_S}}{\sigma_{N_1}^2(\sigma_S^2-\sigma_Z^2)} - \frac{\sigma_{N_2}^2\sqrt{\sigma_S^2+\sigma_{N_1}^2-D_1}}{\sigma_{N_1}^2}, \\
\xi_1 &:= \sigma_{N_2}^2 D_1 + \sigma_{N_1}^2(\sigma_S^2 - \nu\sqrt{\sigma_S^2+\sigma_{N_1}^2-D_1}), \\
\xi_2 &:= \sigma_{N_2}^2\sqrt{\sigma_S^2+\sigma_{N_1}^2-D_1} + \sigma_{N_2}^2\nu, \\
\xi_3 &:= (\sigma_S^2+\sigma_{N_2}^2)\sqrt{\sigma_S^2+\sigma_{N_1}^2-D_1} - \sigma_S^2\nu, \\
\xi_4 &:= (\sigma_S^2+\sigma_{N_1}^2)\nu - \sigma_S^2\sqrt{\sigma_S^2+\sigma_{N_1}^2-D_1}.
\end{aligned}
$$

It is shown in Appendix 4.A that

$$0 < \sigma_S^2 + \sigma_{N_2}^2 - \nu^2 \leq D_2, \tag{4.3.13}$$

$$\det(\mathbf{\Delta}^*) > 0, \tag{4.3.14}$$

$$\xi_1 \geq 0, \tag{4.3.15}$$

$$\xi_2 > 0, \tag{4.3.16}$$

$$\xi_3 \geq \sigma_{N_2}^2 \sqrt{\sigma_S^2 + \sigma_{N_1}^2 - D_1}, \tag{4.3.17}$$

$$0 \leq \xi_4 \leq \sigma_{N_1}^2 \sqrt{\sigma_S^2 + \sigma_{N_1}^2 - D_1}. \tag{4.3.18}$$

In view of (4.3.14)–(4.3.18), we have $\mathbf{U} \succeq \mathbf{0}$, $\mathbf{\Lambda} \succeq \mathbf{0}$, and $\rho \geq 0$. It follows by (4.3.13) and (4.3.14) that $\mathbf{\Delta}^* \succ \mathbf{0}$. Moreover,

$$\mathbf{K_X} - \mathbf{\Delta}^* = \begin{bmatrix} \sigma_S^2 + \sigma_{N_1}^2 - D_1 & \nu\sqrt{\sigma_S^2 + \sigma_{N_1}^2 - D_1} \\ \nu\sqrt{\sigma_S^2 + \sigma_{N_1}^2 - D_1} & \nu^2 \end{bmatrix} \succeq \mathbf{0}.$$

So (4.3.2) is satisfied. Note that (4.3.13) implies (4.3.3). It can be verified that (4.3.4)–(4.3.8) are satisfied as well. Therefore, $\mathbf{\Delta}^*$ is indeed an optimal solution and consequently

$$\begin{aligned} R_c(D_1, D_2, D_S) &= \frac{1}{2} \log \frac{\det(\mathbf{K_X})}{\det(\mathbf{\Delta}^*)} \\ &= \frac{1}{2} \log \frac{(\sigma_S^2 + \sigma_{N_1}^2)(\sigma_S^2 - \sigma_Z^2) - \sigma_S^4}{D_1(D_S - \sigma_Z^2) - (\sigma_S^2 - \sqrt{(\sigma_S^2 + \sigma_{N_1}^2 - D_1)(\sigma_S^2 - D_S)})^2}. \end{aligned}$$

9. This follows from Case 8) by symmetry.

10. Consider the following construction:

$$\mathbf{\Delta}^* := \begin{bmatrix} D_1 & -\zeta_1 \\ -\zeta_1 & D_2 \end{bmatrix}, \quad \mathbf{U} := \mathbf{0}, \quad \mathbf{\Lambda} := \frac{1}{\det(\mathbf{\Delta}^*)} \begin{bmatrix} \zeta_2 & 0 \\ 0 & \zeta_3 \end{bmatrix}, \quad \rho := \frac{\sigma_{N_1}^2 \sigma_{N_2}^2 \zeta_1}{\sigma_Z^4 \det(\mathbf{\Delta}^*)},$$

where

$$\begin{aligned} \zeta_1 &:= \frac{\sigma_{N_2}^2}{2\sigma_{N_1}^2} D_1 + \frac{\sigma_{N_1}^2}{2\sigma_{N_2}^2} D_2 - \frac{\sigma_{N_1}^2 \sigma_{N_2}^2}{2\sigma_Z^4}(D_S - \sigma_Z^2), \\ \zeta_2 &:= -\frac{\sigma_{N_2}^4}{2\sigma_{N_1}^4} D_1 + \frac{1}{2} D_2 + \frac{\sigma_{N_2}^4}{2\sigma_Z^4}(D_S - \sigma_Z^2), \\ \zeta_3 &:= \frac{1}{2} D_1 - \frac{\sigma_{N_1}^4}{2\sigma_{N_2}^4} D_2 + \frac{\sigma_{N_1}^4}{2\sigma_Z^4}(D_S - \sigma_Z^2). \end{aligned}$$

It is shown in Appendix 4.B that

$$\det(\mathbf{\Delta}^*) > 0, \tag{4.3.19}$$

$$\det(\mathbf{K_X} - \mathbf{\Delta}^*) \geq 0, \tag{4.3.20}$$

$$\zeta_i \geq 0, \quad i = 1, 2, 3. \tag{4.3.21}$$

In view of (4.3.19) and (4.3.21), we have $\mathbf{\Lambda} \succeq \mathbf{0}$ and $\rho \geq 0$. It can be verified that (4.3.3)–(4.3.8) are satisfied. Finally, (4.3.2) holds in light of (4.3.19) and (4.3.20). Therefore, $\mathbf{\Delta}^*$ is indeed an optimal solution and consequently

$$\begin{aligned} R_c(D_1, D_2, D_S) &= \frac{1}{2} \log \frac{\det(\mathbf{K_X})}{\det(\mathbf{\Delta}^*)} \\ &= \frac{1}{2} \log \frac{(\sigma_S^2 + \sigma_{N_1}^2)(\sigma_S^2 + \sigma_{N_2}^2) - \sigma_S^4}{D_1 D_2 - \frac{\sigma_{N_1}^4 \sigma_{N_2}^4}{4\sigma_Z^8}(D_S - \sigma_Z^2 - \frac{\sigma_Z^4}{\sigma_{N_1}^4} D_1 - \frac{\sigma_Z^4}{\sigma_{N_2}^4} D_2)^2}. \end{aligned}$$

This completes the proof of Theorem 4.3. □

4.4 Distributed Gaussian Semantic Source Coding

In this section, we take the decentralized version of the semantic source coding problem. The coding model of L-symmetric-component setting and 2-component setting are shown in Fig. 4.5 and Fig. 4.6, respectively.

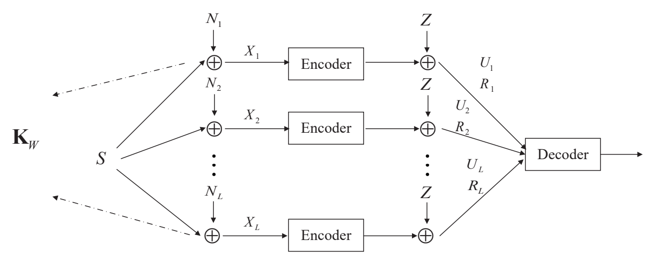

Figure 4.5: Distributed semantic source coding: L-symmetric-component setting.

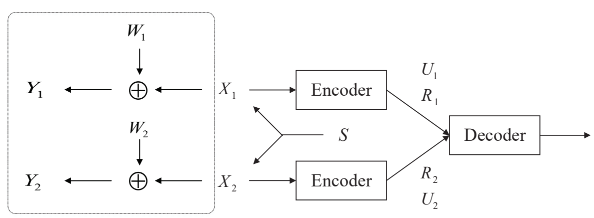

Figure 4.6: Distributed semantic source coding: 2-component setting.

Let $\mathbf{W} := (W_1, \ldots, W_L)^T$ be a Gaussian random vector with mean zero and covariance matrix $\mathbf{K}_{\mathbf{W}}$, which is independent of $\mathbf{X}$. Define that $Y_i = X_i + W_i$, $1 \leq i \leq L$, then we know that $\mathbf{X}$ is jointly Gaussian with $\mathbf{Y} := (Y_1, \ldots, Y_L)^T$. Regarding $\mathbf{Y}$ as a remote source, the distortion covariance matrix of the linear MMSE estimation for $\mathbf{X}$ given $\mathbf{Y}$ is a diagonal matrix $(\mathbf{K}_{\mathbf{X}}^{-1} + \mathbf{K}_{\mathbf{W}}^{-1})^{-1}$. Let $\Omega(\mathbf{K}_{\mathbf{X}})$ denote the set of positive definite matrices $\mathbf{K}_{\mathbf{W}}$ such that $\mathbf{K}_{\mathbf{X}}^{-1} + \mathbf{K}_{\mathbf{W}}^{-1}$ is a diagonal matrix. Furthermore, we let $\mathbf{U} := (U_1, \ldots, U_L)^T$ be L auxiliary random variables jointly distributed with

$\mathbf{X}$ and $\mathbf{Y}$ such that $U_i - X_i - (\mathbf{Y}, X_j, U_j, j \neq i)$ form a Markov chain for $1 \leq i \leq L$. According to [89] and the well-known Berger-Tung upper bound [6],[82], we know that the rate is lower bounded and upper bounded by $H(f_i(X_i^n), 1 \leq i \leq L)$ and $I(\mathbf{X}; \mathbf{U})$, respectively, where $f_i(\cdot)$ denotes the encoding function. Then, we have the following two corresponding optimization problems, where $\mathbf{\Gamma}$ is the distortion covariance matrix of the linear MMSE estimation for $\mathbf{X}$ given $\mathbf{Y}$ and $\mathbf{U}$.

For any $\mathbf{K_W} \in \Omega(\mathbf{K_X})$,

$$\underline{\psi}(D_1, \ldots, D_L, D_S, \mathbf{K_W}) := \min_{\mathbf{\Delta}, \gamma_1, \ldots, \gamma_L} \frac{1}{2} \log \frac{\det(\mathbf{K_X} + \mathbf{K_W}) \det((\mathbf{K_X}^{-1} + \mathbf{K_W}^{-1})^{-1})}{\det(\mathbf{\Delta} + \mathbf{K_W}) \det(\mathbf{\Gamma})} \tag{4.4.1}$$

$$s.t. \quad \mathbf{0} \prec \mathbf{\Delta} \preceq \mathbf{K_X}, \tag{4.4.2}$$

$$0 \prec \mathbf{\Gamma} \preceq \left(\mathbf{\Delta}^{-1} + \mathbf{K_W}^{-1}\right)^{-1}, \tag{4.4.3}$$

$$\mathrm{diag}(\mathbf{\Delta}) \preceq \mathbf{D}, \tag{4.4.4}$$

$$\mathbf{g}^T \mathbf{\Delta} \mathbf{g} + \sigma_Z^2 \leq D_S, \tag{4.4.5}$$

where $\mathbf{\Gamma}$ is a diagonal matrix with the i-th diagonal entry being γ_i, $i = 1, \ldots, L$, and $\mathbf{D}$ is a diagonal matrix with the i-th diagonal entry being D_i, $i = 1, \ldots, L$. We define $\overline{\psi}(D_1, \ldots, D_L, D_S, \mathbf{K_W})$ in a similar way except that the constraint in (4.4.3) is replaced by

$$\mathbf{\Gamma} = (\mathbf{\Delta}^{-1} + \mathbf{K_W}^{-1})^{-1}. \tag{4.4.6}$$

Let

$$\underline{R}_d(D_1,\ldots,D_L,D_s) := \sup_{\mathbf{K_W}\in\Omega(\mathbf{K_X})} \underline{\psi}(D_1,\ldots,D_L,D_S,\mathbf{K_W}),$$
$$\overline{R}_d(D_1,\ldots,D_L,D_s) := \sup_{\mathbf{K_W}\in\Omega(\mathbf{K_X})} \overline{\psi}(D_1,\ldots,D_L,D_S,\mathbf{K_W}).$$

Theorem 4.4 *We have*

$$\underline{R}_d(D_1,\ldots,D_L,D_S) \le R_d(D_1,\ldots,D_L,D_S) \le \overline{R}_d(D_1,\ldots,D_L,D_S).$$

Proof The proof is similar to that of [89, Theorems 1 and 2] and is omitted. □

Lemma 4.2 *Given* $\mathbf{K_W} \in \Omega(\mathbf{K_X})$*,* $(\mathbf{\Delta}^*,\gamma_1^*,\ldots,\gamma_L^*)$ *is an optimal solution of the optimization problem in (4.4.1) if it satisfies the constraints (4.4.2)–(4.4.5) and there exist positive semidefinite matrices* $\mathbf{U}$ *and* $\mathbf{V}$*, a positive semidefinite diagonal matrix* $\mathbf{\Lambda}$*, and a nonnegative number* γ *such that*

$$\begin{aligned}
&-(\mathbf{\Delta}^*+\mathbf{K_W})^{-1}+\mathbf{U}-(\mathbf{\Delta}^*)^{-1}((\mathbf{\Delta}^*)^{-1}+\mathbf{K_W^{-1}})^{-1}\mathbf{\Lambda}((\mathbf{\Delta}^*)^{-1}+\mathbf{K_W^{-1}})^{-1}(\mathbf{\Delta}^*)^{-1}+\mathbf{\Lambda}^*\\
&+\rho\mathbf{g}\mathbf{g}^T=\mathbf{0}, &(4.4.7)\\
&-(\mathbf{\Gamma}^*)^{-1}+\mathrm{diag}(\mathbf{V})=\mathbf{0}, &(4.4.8)\\
&\mathbf{U}(\mathbf{\Delta}^*-\mathbf{K_X})=\mathbf{0}, &(4.4.9)\\
&\mathbf{V}(\mathbf{\Gamma}^*-((\mathbf{\Delta}^*)^{-1}+\mathbf{K_W^{-1}})^{-1})=\mathbf{0}, &(4.4.10)\\
&\mathbf{\Lambda}(\mathrm{diag}(\mathbf{\Delta}^*)-\mathbf{D})=\mathbf{0}, &(4.4.11)\\
&\rho\left(\mathbf{g}^T\mathbf{\Delta}^*\mathbf{g}+\sigma_Z^2-D_S\right)=0, &(4.4.12)
\end{aligned}$$

where $\mathbf{\Gamma}^*$ *is a diagonal matrix with the i-th diagonal entry being* γ_i^**,* $i=1,\ldots,L$*.*

Moreover, if this $(\mathbf{\Delta}^*, \gamma_1^*, \ldots, \gamma_L^*)$ *further satisfies (4.4.6), then*

$$\underline{R}_d(D_1, \ldots, D_L, D_S) = \overline{R}_d(D_1, \ldots, D_L, D_S) = \frac{1}{2}\log\frac{\det(\mathbf{K_X})}{\det(\mathbf{\Delta}^*)}.$$

Proof Since (4.4.1) is a convex optimization problem, $(\mathbf{\Delta}^*, \gamma_1^*, \ldots, \gamma_L^*)$ is an optimal solution if it satisfies the constraints (4.4.2)–(4.4.5) as well as the following KKT conditions [8]:

$$\begin{aligned}
&\nabla_{\mathbf{\Delta}} L(\mathbf{\Delta}, \mathbf{\Gamma}; \mathbf{U}, \mathbf{V}, \mathbf{\Lambda}, \rho)|_{\mathbf{\Delta}=\mathbf{\Delta}^*} = \mathbf{0},\\
&\nabla_{\mathbf{\Gamma}} L(\mathbf{\Delta}, \mathbf{\Gamma}; \mathbf{U}, \mathbf{V}, \mathbf{\Lambda}, \rho)|_{\mathbf{\Gamma}=\mathbf{\Gamma}^*} = \mathbf{0},\\
&\mathbf{U}(\mathbf{\Delta}^* - \mathbf{K_X}) = \mathbf{0},\\
&\mathbf{V}(\mathbf{\Gamma}^* - ((\mathbf{\Delta}^*)^{-1} + \mathbf{K_W^{-1}})^{-1}) = \mathbf{0},\\
&\mathbf{\Lambda}(\mathrm{diag}(\mathbf{\Delta}^*) - \mathbf{D}) = \mathbf{0},\\
&\rho\left(\mathbf{g}^T\mathbf{\Delta}^*\mathbf{g} + \sigma_Z^2 - D_S\right) = 0,
\end{aligned}$$

where $L(\mathbf{\Delta}, \mathbf{\Gamma}; \mathbf{U}, \mathbf{V}, \mathbf{\Lambda}, \rho)$ is the Lagrangian defined as

$$\begin{aligned}
&L(\mathbf{\Delta}, \mathbf{\Gamma}; \mathbf{U}, \mathbf{V}, \mathbf{\Lambda}, \rho)\\
&:= -\log\det(\mathbf{\Delta} + \mathbf{K_W}) - \log(\det(\mathbf{\Gamma})) + \mathrm{tr}(\mathbf{U}(\mathbf{\Delta} - \mathbf{K_X})) + \mathrm{tr}(\mathbf{V}(\mathbf{\Gamma} - (\mathbf{\Delta}^{-1} + \mathbf{K_W^{-1}})^{-1}))\\
&\quad + \mathrm{tr}(\mathbf{\Lambda}(\mathrm{diag}(\mathbf{\Delta}) - \mathbf{D})) + \rho(\mathbf{g}^T\mathbf{\Delta}\mathbf{g} + \sigma_Z^2 - D_S)
\end{aligned}$$

with $\mathbf{U}$ and $\mathbf{V}$ being positive semidefinite matrices, $\mathbf{\Lambda}$ being a positive semidefinite matrix, and ρ being a nonnegative number. This proves (4.4.7)–(4.4.12) in view of the fact that

$$\begin{aligned}\nabla_{\mathbf{\Delta}} L(\mathbf{\Delta}, \mathbf{\Gamma}; \mathbf{U}, \mathbf{V}, \mathbf{\Lambda}, \rho) &= -(\mathbf{\Delta} + \mathbf{K_W})^{-1} + \mathbf{U} - \mathbf{\Delta}^{-1}(\mathbf{\Delta}^{-1} + \mathbf{K_W^{-1}})^{-1}\mathbf{\Lambda}(\mathbf{\Delta}^{-1} + \mathbf{K_W^{-1}})^{-1}\mathbf{\Delta}^{-1} \\ &\quad + \mathbf{\Lambda} + \rho \mathbf{g}\mathbf{g}^T, \\ \nabla_{\mathbf{\Gamma}} L(\mathbf{\Delta}, \mathbf{\Gamma}; \mathbf{U}, \mathbf{V}, \mathbf{\Lambda}, \rho) &= -\mathbf{\Gamma}^{-1} + \mathrm{diag}(\mathbf{V}).\end{aligned}$$

It is clear that if this $(\mathbf{\Delta}^*, \gamma_1^*, \ldots, \gamma_L^*)$ further satisfies (4.4.6), then we must have

$$\underline{R}_d(D_1, \ldots, D_L, D_S) = \overline{R}_d(D_1, \ldots, D_L, D_S) = \frac{1}{2} \log \frac{\det(\mathbf{K_X} + \mathbf{K_W}) \det((\mathbf{K_X^{-1}} + \mathbf{K_W^{-1}})^{-1})}{\det(\mathbf{\Delta}^* + \mathbf{K_W}) \det(((\mathbf{\Delta}^*)^{-1} + \mathbf{K_W^{-1}})^{-1})}.$$

One can readily verify

$$\frac{1}{2} \log \frac{\det(\mathbf{K_X} + \mathbf{K_W}) \det((\mathbf{K_X^{-1}} + \mathbf{K_W^{-1}})^{-1})}{\det(\mathbf{\Delta}^* + \mathbf{K_W}) \det(((\mathbf{\Delta}^*)^{-1} + \mathbf{K_W^{-1}})^{-1})} = \frac{1}{2} \log \frac{\det(\mathbf{K_X})}{\det(\mathbf{\Delta}^*)}.$$

This completes the proof of Lemma 4.2. $\square$

Next we consider the symmetric setting with $\sigma_{N_1}^2 = \ldots = \sigma_{N_L}^2 = \sigma_N^2$ and $D_1 = \ldots = D_L = D$. Let

$$\theta := \frac{\sigma_S^2}{(1 + \beta\sigma_N^2)(1 + \beta(L\sigma_S^2 + \sigma_N^2))},$$

where β is the unique nonnegative solution to

$$\frac{\sigma_N^2}{1 + \beta\sigma_N^2} + \frac{\sigma_S^2}{(1 + \beta\sigma_N^2)(1 + \beta(L\sigma_S^2 + \sigma_N^2))} = D.$$

An explicit characterization of $R_d(D_1, \ldots, D_L, D_S)$, abbreviated as $R_d(D, D_S)$, is provided by the following result.

Theorem 4.5 *An explicit expression for $R_d(D, D_S)$ is given as follows:*

1. *If $D_S \geq \frac{L\sigma_Z^4}{\sigma_N^4}(D + (L-1)\theta) + \sigma_Z^2$, then*

$$R_d(D, D_S) = \frac{1}{2}\log\frac{L\sigma_S^2\sigma_N^{2(L-1)} + \sigma_N^{2L}}{L\theta(D-\theta)^{L-1} + (D-\theta)^L}.$$

2. *If $D_S < \frac{L\sigma_Z^4}{\sigma_N^4}(D + (L-1)\theta) + \sigma_Z^2$, then*

$$R_d(D, D_S) = \frac{1}{2}\log\frac{L^L\sigma_S^2\sigma_Z^{2L}D_S^{L-1}}{\sigma_N^{2L}(D_S - \sigma_Z^2)^L}.$$

The regions of the (D, D_S) space in which each closed-form expression applies can be visualized using the example in Fig. 4.7.

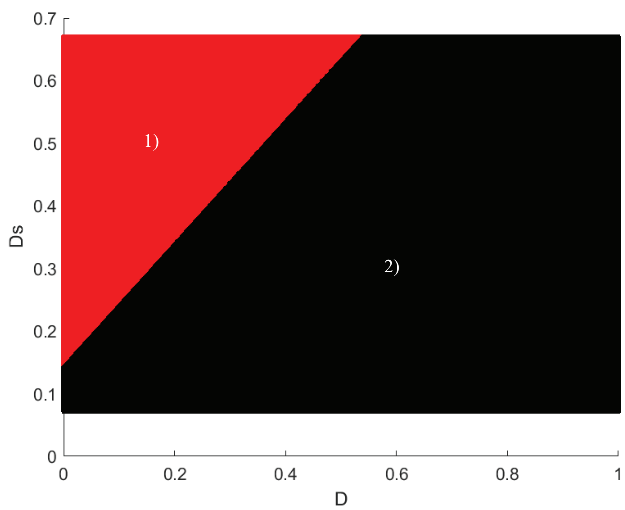

Figure 4.7: Regions of each case of Theorem 4.5, when $\sigma_S^2 = 0.5$, $\sigma_N^2 = 0.5$, and $L = 6$.

Proof For Case 1), semantic distortion constraint D_S is inactive and consequently $R_d(D, D_S)$ can be deduced from the rate-distortion function of symmetric

Gaussian multiterminal source coding [86, Theorem 3][89, Corollary 2]. For Case 2), reproduction distortion constraint D is inactive and consequently $R_d(D, D_S)$ can be deduced from the rate-distortion function of the Gaussian CEO problem [11, 68, 72]. $\square$

The following result deals with the 2-component setting (shown in Fig. 4.6) and provides an explicit characterization of $R_d(D_1, D_2, D_S)$.

Theorem 4.6 *The closed-form expression for $R_d(D_1, D_2, D_S)$ is given as follows:*

1. *If $D_2 \geq \sigma_S^2 + \sigma_{N_2}^2 - \frac{\sigma_S^4(\sigma_S^2+\sigma_{N_1}^2-D_1)}{(\sigma_S^2+\sigma_{N_1}^2)^2}$ and $D_S \geq \sigma_S^2 - \frac{\sigma_S^4(\sigma_S^2+\sigma_{N_1}^2-D_1)}{(\sigma_S^2+\sigma_{N_1}^2)^2}$, then*

$$R_d(D_1, D_2, D_S) = \frac{1}{2}\log\frac{\sigma_S^2 + \sigma_{N_1}^2}{D_1}.$$

2. *If $D_1 \geq \sigma_S^2 + \sigma_{N_1}^2 - \frac{\sigma_S^4(\sigma_S^2+\sigma_{N_2}^2-D_2)}{(\sigma_S^2+\sigma_{N_2}^2)^2}$ and $D_S \geq \sigma_S^2 - \frac{\sigma_S^4(\sigma_S^2+\sigma_{N_2}^2-D_2)}{(\sigma_S^2+\sigma_{N_2}^2)^2}$, then*

$$R_d(D_1, D_2, D_S) = \frac{1}{2}\log\frac{\sigma_S^2 + \sigma_{N_2}^2}{D_2}.$$

3. *If $D_S \geq (\frac{1}{\sigma_S^2}+\frac{1}{\sigma_{N_1}^2}-\frac{1}{\sigma_{N_2}^2})^{-1}$, $D_1 \geq \frac{(\sigma_S^2+\sigma_{N_1}^2)((\sigma_S^2+\sigma_{N_1}^2)D_S-\sigma_S^2\sigma_{N_1}^2)}{\sigma_S^4}$, and $D_2 \geq D_S+\sigma_{N_2}^2$, then*

$$R_d(D_1, D_2, D_S) = \frac{1}{2}\log\frac{\sigma_S^4}{D_S\sigma_S^2 - \sigma_S^2\sigma_{N_1}^2 + D_S\sigma_{N_1}^2}.$$

4. *If $D_S < (\frac{1}{\sigma_S^2}+\frac{1}{\sigma_{N_1}^2}-\frac{1}{\sigma_{N_2}^2})^{-1}$, $D_1 \geq \frac{(D_S^2-\sigma_Z^4)\sigma_{N_1}^4}{4D_S\sigma_Z^4}$, and $D_2 \geq \frac{(D_S^2-\sigma_Z^4)\sigma_{N_2}^4}{4D_S\sigma_Z^4}$, then*

$$R_d(D_1, D_2, D_S) = \frac{1}{2}\log\frac{4\sigma_S^2\sigma_Z^4 D_S}{\sigma_{N_1}^2\sigma_{N_2}^2(D_S - \sigma_Z^2)^2}.$$

5. *If* $D_1 < \sigma_S^2 + \sigma_{N_1}^2 - \frac{\sigma_S^4(\sigma_S^2+\sigma_{N_2}^2-D_2)}{(\sigma_S^2+\sigma_{N_2}^2)^2}$, $D_2 < \sigma_S^2 + \sigma_{N_2}^2 - \frac{\sigma_S^4(\sigma_S^2+\sigma_{N_1}^2-D_1)}{(\sigma_S^2+\sigma_{N_1}^2)^2}$, *and* $D_S \geq \frac{\sigma_Z^4}{\sigma_{N_1}^4}D_1 + \sigma_Z^2\sqrt{1+\frac{4\sigma_Z^4 D_1 D_2}{\sigma_{N_1}^4\sigma_{N_2}^4}} + \frac{\sigma_Z^4}{\sigma_{N_2}^4}D_2$, *then*

$$R_d(D_1, D_2, D_S) = \frac{1}{2}\log\frac{2\sigma_S^2\sigma_Z^2}{\sqrt{\sigma_{N_1}^4\sigma_{N_2}^4 + 4\sigma_Z^4 D_1 D_2} - \sigma_{N_1}^2\sigma_{N_2}^2}.$$

6. *If* $D_1 < \frac{(D_S^2-\sigma_Z^4)\sigma_{N_1}^4}{4D_S\sigma_Z^4}$, $D_S < \min\{(\frac{1}{\sigma_S^2} + \frac{1}{\sigma_{N_1}^2} - \frac{1}{\sigma_{N_2}^2})^{-1}, \sigma_S^2 - \frac{\sigma_S^4(\sigma_S^2+\sigma_{N_1}^2-D_1)}{(\sigma_S^2+\sigma_{N_1}^2)^2}\}$, *and* $D_2 \geq \frac{\sigma_{N_2}^4}{\sigma_{N_1}^4}D_1 - \frac{\sigma_{N_2}^4}{\sigma_Z^2}\sqrt{1+\frac{4D_1D_S}{\sigma_{N_1}^4}} + \frac{\sigma_{N_2}^4}{\sigma_Z^4}D_S$, *then*

$$R_d(D_1, D_2, D_S) = \frac{1}{2}\log\frac{2\sigma_S^2\sigma_Z^2\sigma_{N_1}^2}{\sigma_{N_1}^2\sigma_{N_2}^2\sqrt{\sigma_{N_1}^4 + 4D_1D_S} - 2\sigma_Z^2\sigma_{N_2}^2 D_1 - \sigma_{N_1}^4\sigma_{N_2}^2}.$$

7. *If i)* $D_2 < D_S + \sigma_{N_2}^2$, $(\frac{1}{\sigma_S^2} + \frac{1}{\sigma_{N_1}^2} - \frac{1}{\sigma_{N_2}^2})^{-1} \leq D_S < \sigma_S^2 - \frac{\sigma_S^4(\sigma_S^2+\sigma_{N_2}^2-D_2)}{(\sigma_S^2+\sigma_{N_2}^2)^2}$, *and* $D_1 \geq \frac{\sigma_{N_1}^4}{\sigma_{N_2}^4}D_2 - \frac{\sigma_{N_1}^4}{\sigma_Z^2}\sqrt{1+\frac{4D_2D_S}{\sigma_{N_2}^4}} + \frac{\sigma_{N_1}^4}{\sigma_Z^4}D_S$, *or ii)* $D_2 < \frac{(D_S^2-\sigma_Z^4)\sigma_{N_2}^4}{4D_S\sigma_Z^4}$, $D_S < \min\{(\frac{1}{\sigma_S^2} + \frac{1}{\sigma_{N_1}^2} - \frac{1}{\sigma_{N_2}^2})^{-1}, \sigma_S^2 - \frac{\sigma_S^4(\sigma_S^2+\sigma_{N_2}^2-D_2)}{(\sigma_S^2+\sigma_{N_2}^2)^2}\}$, *and* $D_1 \geq \frac{\sigma_{N_1}^4}{\sigma_{N_2}^4}D_2 - \frac{\sigma_{N_1}^4}{\sigma_Z^2}\sqrt{1+\frac{4D_2D_S}{\sigma_{N_2}^4}} + \frac{\sigma_{N_1}^4}{\sigma_Z^4}D_S$,

$$R_d(D_1, D_2, D_S) = \frac{1}{2}\log\frac{2\sigma_S^2\sigma_Z^2\sigma_{N_2}^2}{\sigma_{N_1}^2\sigma_{N_2}^2\sqrt{\sigma_{N_2}^4 + 4D_2D_S} - 2\sigma_Z^2\sigma_{N_1}^2 D_2 - \sigma_{N_1}^2\sigma_{N_2}^4}.$$

The regions of the (D_1, D_2, D_S) space in which each closed-form expression applies can be visualized using the example in Fig. 4.8, where Fig. 4.8(b) is a rotation of Fig. 4.8(a) along with $D_1 - D_2$ plane.

Proof For Cases 1), 2), and 5), semantic distortion constraint D_S is inactive and consequently $R_d(D_1, D_2, D_S)$ can be deduced from the rate-distortion function of Gaussian two-terminal source coding [86, Theorem 1][89, Theorem 6]. For Cases 3) and 4), reproduction distortion constraints D_1 and D_2 are inactive and consequently

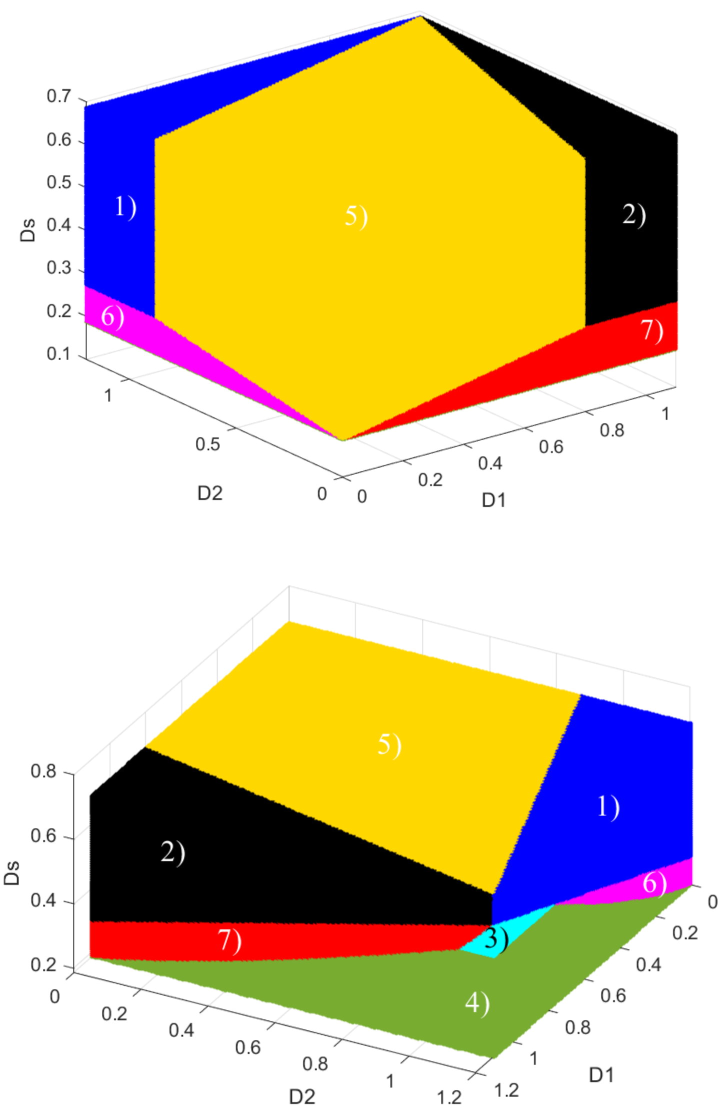

Figure 4.8: Regions of each case of Theorem 4.6, when $\sigma_S^2 = 0.6$, $\sigma_{N_1}^2 = 0.5$, and $\sigma_{N_2}^2 = 0.6$.

$R_d(D_1, D_2, D_S)$ can be deduced from the rate-distortion function of the Gaussian CEO problem [11, 68, 72]. So it remains to analyze Cases 6) and 7).

For Case 6), consider the following construction:

$$\mathbf{\Delta}^* := \begin{bmatrix} D_1 & \frac{\sigma_{N_1}^2\sigma_{N_2}^2}{2\sigma_Z^2}(\tau - \frac{2\sigma_Z^2}{\sigma_{N_1}^4}D_1 - 1) \\ \frac{\sigma_{N_1}^2\sigma_{N_2}^2}{2\sigma_Z^2}(\tau - \frac{2\sigma_Z^2}{\sigma_{N_1}^4}D_1 - 1) & \frac{\sigma_{N_2}^4}{\sigma_{N_1}^4}D_1 - \frac{\sigma_{N_2}^4}{\sigma_Z^2}\tau + \frac{\sigma_{N_2}^4}{\sigma_Z^4}D_S \end{bmatrix},$$

$$\mathbf{\Gamma}^* := \begin{bmatrix} \frac{\sigma_{N_1}^2\sigma_{N_2}^2\sqrt{D_1}(\tau-1)}{2\sigma_Z^2\tau\sqrt{\frac{\sigma_{N_2}^4}{\sigma_{N_1}^4}D_1 - \frac{\sigma_{N_2}^4}{\sigma_Z^2}\tau + \frac{\sigma_{N_2}^4}{\sigma_Z^4}D_S}} & 0 \\ 0 & \frac{\sigma_{N_1}^2\sigma_{N_2}^2\sqrt{\frac{\sigma_{N_2}^4}{\sigma_{N_1}^4}D_1 - \frac{\sigma_{N_2}^4}{\sigma_Z^2}\tau + \frac{\sigma_{N_2}^4}{\sigma_Z^4}D_S}(\tau-1)}{2\sigma_Z^2\tau\sqrt{D_1}} \end{bmatrix},$$

$$\mathbf{U} := \mathbf{0}, \quad \mathbf{V} := \begin{bmatrix} \frac{2\sigma_Z^2\tau\sqrt{\frac{\sigma_{N_2}^4}{\sigma_{N_1}^4}D_1 - \frac{\sigma_{N_2}^4}{\sigma_Z^2}\tau + \frac{\sigma_{N_2}^4}{\sigma_Z^4}D_S}}{\sigma_{N_1}^2\sigma_{N_2}^2\sqrt{D_1}(\tau-1)} & \frac{2\sigma_Z^2\tau}{\sigma_{N_1}^2\sigma_{N_2}^2(\tau-1)} \\ \frac{2\sigma_Z^2\tau}{\sigma_{N_1}^2\sigma_{N_2}^2(\tau-1)} & \frac{2\sigma_Z^2\tau\sqrt{D_1}}{\sigma_{N_1}^2\sigma_{N_2}^2\sqrt{\frac{\sigma_{N_2}^4}{\sigma_{N_1}^4}D_1 - \frac{\sigma_{N_2}^4}{\sigma_Z^2}\tau + \frac{\sigma_{N_2}^4}{\sigma_Z^4}D_S}(\tau-1)} \end{bmatrix},$$

$$\mathbf{\Lambda} := \begin{bmatrix} \frac{2(D_S - \sigma_Z^2\tau)}{\sigma_{N_1}^4\tau(\tau - \frac{2\sigma_Z^2}{\sigma_{N_1}^4}D_1 - 1)} & 0 \\ 0 & 0 \end{bmatrix}, \quad \rho := \frac{2D_1}{\sigma_{N_1}^4\tau(\tau - \frac{2\sigma_Z^2}{\sigma_{N_1}^4}D_1 - 1)}, \quad \mathbf{K_W} := \begin{bmatrix} \omega_1 & \frac{\sigma_Z^2}{\sigma_{N_1}^2\sigma_{N_2}^2} \\ \frac{\sigma_Z^2}{\sigma_{N_1}^2\sigma_{N_2}^2} & \omega_2 \end{bmatrix}^{-1},$$

where

$$\tau := \sqrt{1 + \frac{4D_1D_S}{\sigma_{N_1}^4}},$$

$$\omega_1 := \frac{\tau\sqrt{(\tau - \frac{2\sigma_Z^2}{\sigma_{N_1}^4}D_1)^2 - 1}}{(\tau-1)D_1} - \frac{(\tau - \frac{2\sigma_Z^2}{\sigma_{N_1}^4}D_1)^2 - 1}{2(\tau - \frac{2\sigma_Z^2}{\sigma_{N_1}^4}D_1 - 1)D_1},$$

$$\omega_2 := \frac{\tau\sqrt{(\tau - \frac{2\sigma_Z^2}{\sigma_{N_1}^4}D_1)^2 - 1}}{(\tau-1)(\frac{\sigma_{N_2}^4}{\sigma_{N_1}^4}D_1 - \frac{\sigma_{N_2}^4}{\sigma_Z^2}\tau + \frac{\sigma_{N_2}^4}{\sigma_Z^4}D_S)} - \frac{(\tau - \frac{2\sigma_Z^2}{\sigma_{N_1}^4}D_1)^2 - 1}{2(\tau - \frac{2\sigma_Z^2}{\sigma_{N_1}^4}D_1 - 1)(\frac{\sigma_{N_2}^4}{\sigma_{N_1}^4}D_1 - \frac{\sigma_{N_2}^4}{\sigma_Z^2}\tau + \frac{\sigma_{N_2}^4}{\sigma_Z^4}D_S)}.$$

Since $D_1 < \frac{(D_S^2-\sigma_Z^4)\sigma_{N_1}^4}{4D_S\sigma_Z^4}$, it follows that

$$D_S - \sigma_Z^2\tau > 0. \tag{4.4.13}$$

As a consequence,

$$\frac{\sigma_{N_2}^4}{\sigma_{N_1}^4}D_1 - \frac{\sigma_{N_2}^4}{\sigma_Z^2}\tau + \frac{\sigma_{N_2}^4}{\sigma_Z^4}D_S > \frac{\sigma_{N_2}^4}{\sigma_{N_1}^4}D_1 > 0. \tag{4.4.14}$$

Moreover,

$$\tau - \frac{2\sigma_Z^2}{\sigma_{N_1}^4}D_1 - 1 > 0, \tag{4.4.15}$$

because

$$\begin{aligned}
\tau^2 - \left(\frac{2\sigma_Z^2}{\sigma_{N_1}^4}D_1 - 1\right)^2 &= \frac{4D_1}{\sigma_{N_1}^4}\left(D_S - \sigma_Z^2 - \frac{\sigma_Z^4}{\sigma_{N_1}^4}D_1\right) \\
&> \frac{4D_1}{\sigma_{N_1}^4}\left(\frac{D_S^2 - \sigma_Z^4}{2D_S} - \frac{\sigma_Z^4}{\sigma_{N_1}^4}D_1\right) && (4.4.16) \\
&> 0, && (4.4.17)
\end{aligned}$$

where (4.4.16) is due to $D_S > \sigma_Z^2$, and (4.4.17) is due to $D_1 < \frac{(D_S^2-\sigma_Z^4)\sigma_{N_1}^4}{4D_S\sigma_Z^4}$. In view of (4.4.13)–(4.4.15) and the fact that $\det(\mathbf{V}) = 0$, we have $\mathbf{V} \succeq \mathbf{0}$, $\mathbf{\Lambda} \succeq \mathbf{0}$, and $\rho > 0$. One can readily verify that (4.4.4)–(4.4.12) are satisfied. In addition, it is shown in Appendix 4.C.1 that $\mathbf{K_W} \in \Omega(\mathbf{K_X})$ and $\mathbf{0} \prec \mathbf{\Delta}^* \preceq \mathbf{K_X}$ (i.e., (4.4.2)), which, together with (4.4.6), further implies (4.4.3). Therefore, in light of Lemma 4.2,

$$R_d(D_1, D_2, D_S) = \frac{1}{2}\log\frac{\det(\mathbf{K_X})}{\det(\mathbf{\Delta}^*)} = \frac{1}{2}\log\frac{2\sigma_S^2\sigma_Z^2\sigma_{N_1}^2}{\sigma_{N_1}^2\sigma_{N_2}^2\sqrt{\sigma_{N_1}^4 + 4D_1D_S} - 2\sigma_Z^2\sigma_{N_2}^2D_1 - \sigma_{N_1}^4\sigma_{N_2}^2}.$$

For Case 7), similar construction can be applied, and one can readily verify that (4.4.4)–(4.4.12) and $\mathbf{K_W} \in \Omega(\mathbf{K_X})$ are satisfied. It is shown in Appendix 4.C.2 that $\mathbf{0} \prec \mathbf{\Delta}^* \preceq \mathbf{K_X}$ is satisfied, implying (4.4.3) with (4.4.6). □

Remark 4.2 *It should be pointed out that the chosen of* $\mathbf{K_W}$ *is not unique. In different cases (regions), we actually know which constraints are active and which are inactive. The Lagrange multipliers can be calculated by using that information, for example, we let the corresponding multiplier be zero if the constraint is inactive.*

4.5 Numerical Results

In this section, we carry out computer simulations to compare the performance between centralized encoding and distributed encoding methods, where both two terminals case and symmetric model based L terminals case are considered.

4.5.1 Encoding for symmetric L Terminals

Fig. 4.9 shows the comparison between centralized/distributed source coding with $L = 2, 7, 20$ terminals. It can be seen that with the increasing of L, the rate gap between centralized and distributed model is increased. The asymptotic performance is considered in Fig. 4.10 with $L = 100$ and $L = 1000$. The reflection point divides the rate curve into two parts, and each of them is only dominated by D_S and D, respectively.

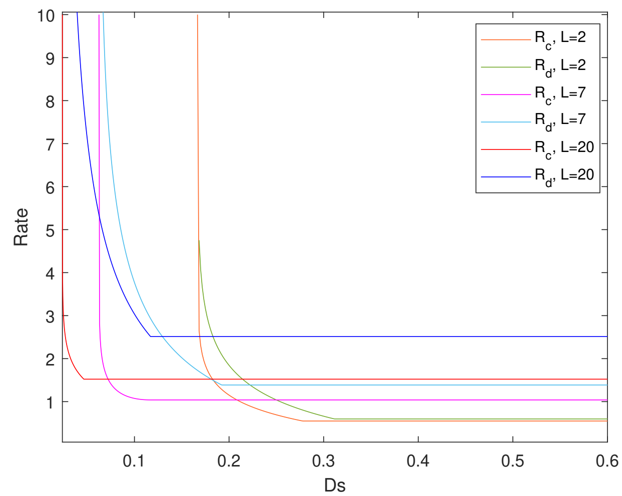

Figure 4.9: Comparison between centralized/distributed source coding with $\sigma_S^2 = 0.5$, $\sigma_N^2 = 0.5$ and $D = 0.5$.

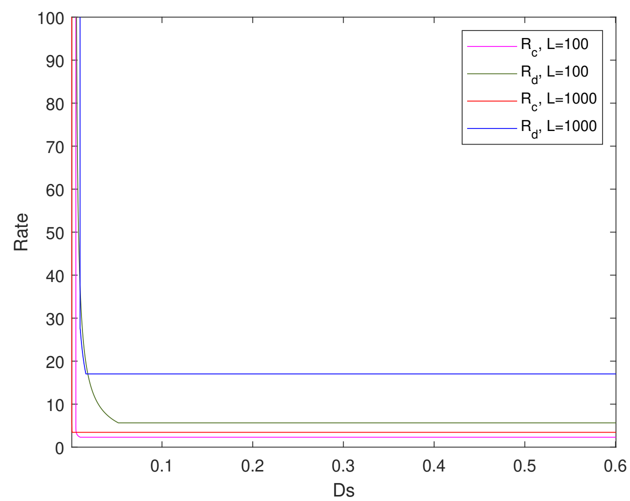

Figure 4.10: Comparison between centralized/distributed source coding with $\sigma_S^2 = 0.5$, $\sigma_N^2 = 0.5$ and $D = 0.5$.

4.5.2 Encoding for Two Terminals

Let $\rho = \frac{\sigma_S^2}{\sqrt{(\sigma_S^2+\sigma_{N_1}^2)(\sigma_S^2+\sigma_{N_2}^2)}}$ and $r_i = \frac{D_i}{\sigma_S^2+\sigma_{N_i}^2}$ $(i = 1, 2)$. Fig. 4.11 and Fig. 4.12 show the rate comparison between the centralized source coding and distributed source coding with two terminals, where $\sigma_{N_1}^2 = 0.4$, $\sigma_{N_2}^2 = 0.6$, and $\rho = 0.5$. From all these figures, we can see that when D_S is large, the rate of distributed system is matched with that of centralized system, this is because at this time the condition of D_S is inactive.

In Fig. 4.11 and Fig. 4.12, r_1 and r_2 are fixed, respectively. It can be seen that when D_S is relatively high, the asymptotic rate decreases with the increasing of r_2 or r_1.

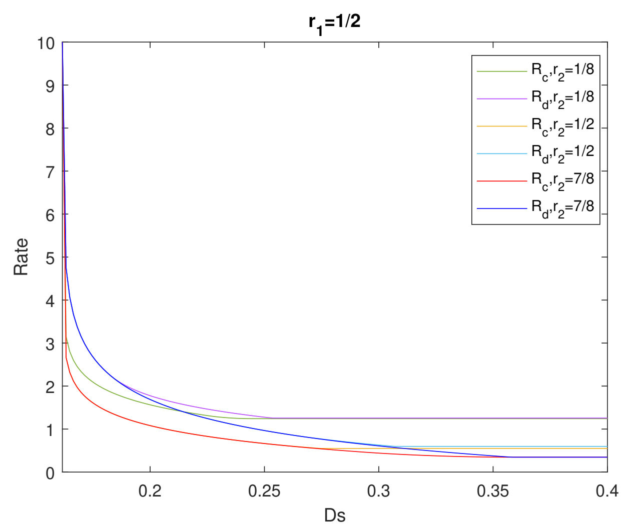

Figure 4.11: Comparison between centralized/distributed source coding with $r_1 = 1/2$.

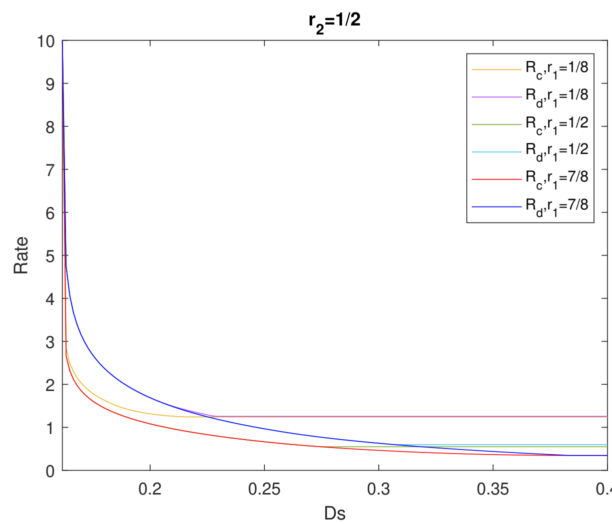

Figure 4.12: Comparison between centralized/distributed source coding with $r_2 = 1/2$.

4.6 Conclusion

We have studied centralized Gaussian semantic source coding and its distributed counterpart in terms of their rate-distortion functions. There are several directions worthy of pursuing for future work. For example, it is of great interest to investigate more general correlation structures between the observable variables and the state variable. The i.i.d. assumption adopted in our work also appears to be overly restrictive. This can be remedied by considering the one-shot formulation, which is better justified from a practical perspective. One may further go beyond the quadratic Gaussian setting to deal with more realistic source models and loss functions. Here the notorious technical difficulties inherent in distributed source coding will likely become a roadblock. Nevertheless, it remains promising to make good progress within the log-loss framework [17] that is most relevant to machine learning applications.

4.A Appendix: Proof of (4.3.13)–(4.3.18)

- Proof of (4.3.13): It can be verified that

$$\begin{aligned}
&\sigma_S^2 + \sigma_{N_2}^2 - \nu^2 \\
&= \frac{\sigma_{N_2}^4}{\sigma_{N_1}^4} D_1 - \frac{2\sigma_{N_2}^4}{\sigma_{N_1}^2 \sigma_Z^2}\kappa + \frac{\sigma_{N_2}^4}{\sigma_Z^4}(D_S - \sigma_Z^2) \\
&= \begin{bmatrix} -\frac{\sigma_{N_2}^2}{\sigma_{N_1}^2} & \frac{\sigma_{N_2}^2}{\sigma_Z^2} \end{bmatrix} \begin{bmatrix} D_1 & \kappa \\ \kappa & D_S - \sigma_Z^2 \end{bmatrix} \begin{bmatrix} -\frac{\sigma_{N_2}^2}{\sigma_{N_1}^2} \\ \frac{\sigma_{N_2}^2}{\sigma_Z^2} \end{bmatrix},
\end{aligned}$$

where $\kappa := \sigma_S^2 - \sqrt{(\sigma_S^2 + \sigma_{N_1}^2 - D_1)(\sigma_S^2 - D_S)}$. As a consequence,

$$D_2 \geq \sigma_S^2 + \sigma_{N_2}^2 - \nu^2 \iff D_2 \geq \frac{\sigma_{N_2}^4}{\sigma_{N_1}^4} D_1 - \frac{2\sigma_{N_2}^4}{\sigma_{N_1}^2 \sigma_Z^2}\kappa + \frac{\sigma_{N_2}^4}{\sigma_Z^4}(D_S - \sigma_Z^2).$$

Since $D_1 < \sigma_S^2 + \sigma_{N_1}^2 - \frac{\sigma_S^4(\sigma_S^2 - D_S)}{(\sigma_S^2 - \sigma_Z^2)^2}$ and $D_S < \sigma_S^2 - \frac{\sigma_S^4(\sigma_S^2 + \sigma_{N_1}^2 - D_1)}{(\sigma_S^2 + \sigma_{N_1}^2)^2}$, we have

$$\sqrt{\frac{\sigma_S^2 + \sigma_{N_1}^2 - D_1}{\sigma_S^2 - D_S}} < \frac{\sigma_S^2 + \sigma_{N_1}^2}{\sigma_S^2}, \tag{4.A.1}$$

$$\sqrt{\frac{\sigma_S^2 - D_S}{\sigma_S^2 + \sigma_{N_1}^2 - D_1}} < \frac{\sigma_S^2 - \sigma_Z^2}{\sigma_S^2}. \tag{4.A.2}$$

Note that

$$
\begin{aligned}
&\begin{bmatrix} D_1 & \kappa \\ \kappa & D_S - \sigma_Z^2 \end{bmatrix} \\
&= \begin{bmatrix} \sigma_S^2 + \sigma_{N_1}^2 & \sigma_S^2 \\ \sigma_S^2 & \sigma_S^2 - \sigma_Z^2 \end{bmatrix} - \begin{bmatrix} \sigma_S^2 + \sigma_{N_1}^2 - D_1 & \sigma_S^2 - \kappa \\ \sigma_S^2 - \kappa & \sigma_S^2 - D_S \end{bmatrix} \\
&\succeq \begin{bmatrix} \sigma_S^2 + \sigma_{N_1}^2 & \sigma_S^2 \\ \sigma_S^2 & \sigma_S^2 - \sigma_Z^2 \end{bmatrix} - \frac{\sigma_S^2}{\sigma_S^2 - \kappa} \begin{bmatrix} \sigma_S^2 + \sigma_{N_1}^2 - D_1 & \sigma_S^2 - \kappa \\ \sigma_S^2 - \kappa & \sigma_S^2 - D_S \end{bmatrix} && (4.A.3) \\
&= \begin{bmatrix} \sigma_S^2 + \sigma_{N_1}^2 & \sigma_S^2 \\ \sigma_S^2 & \sigma_S^2 - \sigma_Z^2 \end{bmatrix} - \begin{bmatrix} \sigma_S^2 \sqrt{\frac{\sigma_S^2 + \sigma_{N_1}^2 - D_1}{\sigma_S^2 - D_S}} & \sigma_S^2 \\ \sigma_S^2 & \sigma_S^2 \sqrt{\frac{\sigma_S^2 - D_S}{\sigma_S^2 + \sigma_{N_1}^2 - D_1}} \end{bmatrix} \\
&\succ \mathbf{0}, && (4.A.4)
\end{aligned}
$$

where (4.A.3) is due to the condition $(\sigma_S^2 + \sigma_{N_1}^2 - D_1)(\sigma_S^2 - D_S) < \sigma_S^4$ while (4.A.4) is due to (4.A.1) and (4.A.2). Therefore,

$$
\sigma_S^2 + \sigma_{N_2}^2 - \nu^2 = \begin{bmatrix} -\frac{\sigma_{N_2}^2}{\sigma_{N_1}^2} & \frac{\sigma_{N_2}^2}{\sigma_Z^2} \end{bmatrix} \begin{bmatrix} D_1 & \kappa \\ \kappa & D_S - \sigma_Z^2 \end{bmatrix} \begin{bmatrix} -\frac{\sigma_{N_2}^2}{\sigma_{N_1}^2} \\ \frac{\sigma_{N_2}^2}{\sigma_Z^2} \end{bmatrix} > 0.
$$

- Proof of (4.3.14): It can be verified that

$$
\begin{aligned}
\det(\boldsymbol{\Delta}^*) &= \frac{((\sigma_S^2 + \sigma_{N_1}^2)(\sigma_S^2 + \sigma_{N_2}^2) - \sigma_S^4)^2}{\sigma_S^4 \sigma_{N_1}^4} (D_1(D_S - \sigma_Z^2) - \kappa^2) \\
&> 0, && (4.A.5)
\end{aligned}
$$

where (4.A.5) is due to (4.A.4).

- Proof of (4.3.15): It can be verified that

$$\xi_1 = \frac{\sigma_S^2(\sigma_{N_1}^2 + \sigma_{N_2}^2)(\sigma_S^2 - \sqrt{(\sigma_S^2 + \sigma_{N_1}^2 - D_1)(\sigma_S^2 - D_S)})}{\sigma_S^2 - \sigma_Z^2} \geq 0,$$

where the inequality follows from the condition $(\sigma_S^2 + \sigma_{N_1}^2 - D_1)(\sigma_S^2 - D_S) < \sigma_S^4$.

- Proof of (4.3.16): It can be verified that

$$\xi_2 = \frac{\sigma_S^2(\sigma_{N_1}^2 + \sigma_{N_2}^2)\sqrt{\sigma_S^2 - D_S}}{\sigma_S^2 - \sigma_Z^2} > 0,$$

where the inequality is due to $D_S < \sigma_S^2 - \frac{\sigma_S^4(\sigma_S^2+\sigma_{N_1}^2-D_1)}{(\sigma_S^2+\sigma_{N_1}^2)^2} \leq \sigma_S^2$.

- Proof of (4.3.17): Since $D_1 < \sigma_S^2 + \sigma_{N_1}^2 - \frac{\sigma_S^4(\sigma_S^2-D_S)}{(\sigma_S^2-\sigma_Z^2)^2}$, it follows that $\sqrt{\sigma_S^2 - D_S} \leq \frac{\sigma_S^2-\sigma_Z^2}{\sigma_S^2}\sqrt{\sigma_S^2 + \sigma_{N_1}^2 - D_1}$ and consequently

$$\begin{aligned} \nu &\leq \frac{(\sigma_{N_1}^2 + \sigma_{N_2}^2)\sqrt{\sigma_S^2 + \sigma_{N_1}^2 - D_1}}{\sigma_{N_1}^2} - \frac{\sigma_{N_2}^2\sqrt{\sigma_S^2 + \sigma_{N_1}^2 - D_1}}{\sigma_{N_1}^2} \\ &= \sqrt{\sigma_S^2 + \sigma_{N_1}^2 - D_1}. \end{aligned} \tag{4.A.6}$$

Therefore, we have

$$\begin{aligned} \xi_3 &\geq (\sigma_S^2 + \sigma_{N_2}^2)\sqrt{\sigma_S^2 + \sigma_{N_1}^2 - D_1} - \sigma_S^2\sqrt{\sigma_S^2 + \sigma_{N_1}^2 - D_1} \\ &= \sigma_{N_2}^2\sqrt{\sigma_S^2 + \sigma_{N_1}^2 - D_1}. \end{aligned}$$

- Proof of (4.3.18): Note that

$$\xi_4 \le (\sigma_S^2+\sigma_{N_1}^2)\sqrt{\sigma_S^2+\sigma_{N_1}^2-D_1} - \sigma_S^2\sqrt{\sigma_S^2+\sigma_{N_1}^2-D_1} \tag{4.A.7}$$
$$= \sigma_{N_1}^2\sqrt{\sigma_S^2+\sigma_{N_1}^2-D_1},$$

where (4.A.7) is due to (4.A.6). Since $D_S < \sigma_S^2 - \frac{\sigma_S^4(\sigma_S^2+\sigma_{N_1}^2-D_1)}{(\sigma_S^2+\sigma_{N_1}^2)^2}$, it follows that $\sqrt{\sigma_S^2-D_S} \ge \frac{\sigma_S^2}{\sigma_S^2+\sigma_{N_1}^2}\sqrt{\sigma_S^2+\sigma_{N_1}^2-D_1}$ and consequently

$$\nu \ge \left(\frac{\sigma_S^4(\sigma_{N_1}^2+\sigma_{N_2}^2)}{(\sigma_S^2-\sigma_Z^2)(\sigma_S^2+\sigma_{N_1}^2)} - \sigma_{N_2}^2\right)\frac{\sqrt{\sigma_S^2+\sigma_{N_1}^2-D_1}}{\sigma_{N_1}^2}$$
$$= \frac{\sigma_S^2}{\sigma_S^2+\sigma_{N_1}^2}\sqrt{\sigma_S^2+\sigma_{N_1}^2-D_1}.$$

Therefore, we have

$$\xi_4 \ge (\sigma_S^2+\sigma_{N_1}^2)\frac{\sigma_S^2}{\sigma_S^2+\sigma_{N_1}^2}\sqrt{\sigma_S^2+\sigma_{N_1}^2-D_1} - \sigma_S^2\sqrt{\sigma_S^2+\sigma_{N_1}^2-D_1} \tag{4.A.8}$$
$$= 0.$$

4.B Appendix: Proof of (4.3.19)–(4.3.21)

We start with some technical lemmas.

Lemma 4.3 *(4.3.21) implies (4.3.19).*

Proof Since $D_S \le \frac{\sigma_Z^4}{\sigma_{N_1}^4}D_1 + \frac{\sigma_Z^4}{\sigma_{N_2}^4}D_2 + \sigma_Z^2$, it follows that $D_S - \sigma_Z^2 \le (\frac{\sigma_Z^2}{\sigma_{N_1}^2}\sqrt{D_1} + \frac{\sigma_Z^2}{\sigma_{N_2}^2}\sqrt{D_2})^2$, which implies $\sqrt{D_S-\sigma_Z^2} \le \frac{\sigma_Z^2}{\sigma_{N_1}^2}\sqrt{D_1} + \frac{\sigma_Z^2}{\sigma_{N_2}^2}\sqrt{D_2}$. Consider the following two cases separately.

- $0 \leq \sqrt{D_S - \sigma_Z^2} - \frac{\sigma_Z^2}{\sigma_{N_2}^2}\sqrt{D_2} \leq \frac{\sigma_Z^2}{\sigma_{N_1}^2}\sqrt{D_1}$ or $0 \leq \sqrt{D_S - \sigma_Z^2} - \frac{\sigma_Z^2}{\sigma_{N_1}^2}\sqrt{D_1} \leq \frac{\sigma_Z^2}{\sigma_{N_2}^2}\sqrt{D_2}$: We have $D_1 \geq (\frac{\sigma_{N_1}^2}{\sigma_Z^2}\sqrt{D_S - \sigma_Z^2} - \frac{\sigma_{N_1}^2}{\sigma_{N_2}^2}\sqrt{D_2})^2$ or $D_2 \geq (\frac{\sigma_{N_2}^2}{\sigma_Z^2}\sqrt{D_S - \sigma_Z^2} - \frac{\sigma_{N_2}^2}{\sigma_{N_1}^2}\sqrt{D_1})^2$.

- $\sqrt{D_S - \sigma_Z^2} - \frac{\sigma_Z^2}{\sigma_{N_2}^2}\sqrt{D_2} \leq 0 \leq \frac{\sigma_Z^2}{\sigma_{N_1}^2}\sqrt{D_1}$ and $\sqrt{D_S - \sigma_Z^2} - \frac{\sigma_Z^2}{\sigma_{N_1}^2}\sqrt{D_1} \leq 0 \leq \frac{\sigma_Z^2}{\sigma_{N_2}^2}\sqrt{D_2}$: Without loss of generality, we assume that $\frac{\sqrt{D_1}}{\sigma_{N_1}^2} \geq \frac{\sqrt{D_2}}{\sigma_{N_2}^2}$. It can be verified that $(\sqrt{D_S - \sigma_Z^2} - \frac{\sigma_Z^2}{\sigma_{N_2}^2}\sqrt{D_2})^2 \leq (\frac{\sigma_Z^2}{\sigma_{N_2}^2}\sqrt{D_2})^2 \leq (\frac{\sigma_Z^2}{\sigma_{N_1}^2}\sqrt{D_1})^2$, which implies $D_1 \geq (\frac{\sigma_{N_1}^2}{\sigma_Z^2}\sqrt{D_S - \sigma_Z^2} - \frac{\sigma_{N_1}^2}{\sigma_{N_2}^2}\sqrt{D_2})^2$.

Thus, we always have $D_1 \geq (\frac{\sigma_{N_1}^2}{\sigma_Z^2}\sqrt{D_S - \sigma_Z^2} - \frac{\sigma_{N_1}^2}{\sigma_{N_2}^2}\sqrt{D_2})^2$ or $D_2 \geq (\frac{\sigma_{N_2}^2}{\sigma_Z^2}\sqrt{D_S - \sigma_Z^2} - \frac{\sigma_{N_2}^2}{\sigma_{N_1}^2}\sqrt{D_1})^2$, which, together with (4.3.21), yields

$$\frac{\sigma_{N_1}^4}{\sigma_{N_2}^4}D_2 + \frac{(D_S - \sigma_Z^2)\sigma_{N_1}^4}{\sigma_Z^4} \geq D_1 \geq \left(\frac{\sigma_{N_1}^2}{\sigma_Z^2}\sqrt{D_S - \sigma_Z^2} - \frac{\sigma_{N_1}^2}{\sigma_{N_2}^2}\sqrt{D_2}\right)^2 \tag{4.B.1}$$

or

$$\frac{\sigma_{N_2}^4}{\sigma_{N_1}^4}D_1 + \frac{(D_S - \sigma_Z^2)\sigma_{N_2}^4}{\sigma_Z^4} \geq D_2 \geq \left(\frac{\sigma_{N_2}^2}{\sigma_Z^2}\sqrt{D_S - \sigma_Z^2} - \frac{\sigma_{N_2}^2}{\sigma_{N_1}^2}\sqrt{D_1}\right)^2. \tag{4.B.2}$$

Since

$$\begin{aligned}\det(\mathbf{\Delta}^*) = &-\frac{\sigma_{N_2}^4}{4\sigma_{N_1}^4}D_1^2 - \frac{\sigma_{N_1}^4}{4\sigma_{N_2}^4}D_2^2 + \frac{1}{2}D_1D_2 + \frac{(D_S - \sigma_Z^2)\sigma_{N_2}^4}{2\sigma_Z^4}D_1 + \frac{(D_S - \sigma_Z^2)\sigma_{N_1}^4}{2\sigma_Z^4}D_2 \\ &- \left(\frac{(D_S - \sigma_Z^2)\sigma_{N_1}^2\sigma_{N_2}^2}{2\sigma_Z^4}\right)^2,\end{aligned}$$

it follows that (4.3.19) holds when

$$\left|D_1 - \frac{\sigma_{N_1}^4}{\sigma_{N_2}^4}D_2 - \frac{(D_S - \sigma_Z^2)\sigma_{N_1}^4}{\sigma_Z^4}\right| \leq \frac{2\sigma_{N_1}^4}{\sigma_Z^2\sigma_{N_2}^2}\sqrt{(D_S - \sigma_Z^2)D_2} \tag{4.B.3}$$

or

$$\left|D_2 - \frac{\sigma_{N_2}^4}{\sigma_{N_1}^4}D_1 - \frac{(D_S - \sigma_Z^2)\sigma_{N_2}^4}{\sigma_Z^4}\right| \leq \frac{2\sigma_{N_2}^4}{\sigma_Z^2\sigma_{N_1}^2}\sqrt{(D_S - \sigma_Z^2)D_1}. \tag{4.B.4}$$

The proof is complete in view of the fact that (4.B.3) and (4.B.4) are implied by (4.B.1) and (4.B.2), respectively. □

Lemma 4.4 *$\zeta_2 < 0$ and $\zeta_3 < 0$ cannot hold simultaneously. Moreover, $\zeta_1 < 0$ implies $\zeta_2 \geq 0$ and $\zeta_3 \geq 0$.*

Proof Note that $\zeta_2 < 0$ and $\zeta_3 < 0$ are respectively equivalent to

$$\begin{aligned} D_1 &> \frac{\sigma_{N_1}^4}{\sigma_{N_2}^4}D_2 + \frac{(D_S - \sigma_Z^2)\sigma_{N_1}^4}{\sigma_Z^4}, \\ D_1 &< \frac{\sigma_{N_1}^4}{\sigma_{N_2}^4}D_2 - \frac{(D_S - \sigma_Z^2)\sigma_{N_1}^4}{\sigma_Z^4}, \end{aligned}$$

which clearly cannot hold simultaneously.

Moreover, note that $\zeta_1 < 0$ is equivalent to

$$D_S > \frac{\sigma_Z^4}{\sigma_{N_1}^4}D_1 + \frac{\sigma_Z^4}{\sigma_{N_2}^4}D_2 + \sigma_Z^2 \tag{4.B.5}$$

while $\zeta_2 \geq 0$ and $\zeta_3 \geq 0$ are respectively equivalent to

$$D_S \geq \frac{\sigma_Z^4}{\sigma_{N_1}^4}D_1 - \frac{\sigma_Z^4}{\sigma_{N_2}^4}D_2 + \sigma_Z^2, \tag{4.B.6}$$

$$D_S \geq -\frac{\sigma_Z^4}{\sigma_{N_1}^4}D_1 + \frac{\sigma_Z^4}{\sigma_{N_2}^4}D_2 + \sigma_Z^2. \tag{4.B.7}$$

Clearly, (4.B.5) implies (4.B.6) and (4.B.7). □

Lemma 4.5 *If* $D_S < \frac{\sigma_Z^4}{\sigma_{N_1}^4}D_1 + \frac{2\sigma_Z^4}{\sigma_{N_1}^2\sigma_{N_2}^2}(\sigma_S^2 - \sqrt{(\sigma_S^2+\sigma_{N_1}^2-D_1)(\sigma_S^2+\sigma_{N_2}^2-D_2)}) + \frac{\sigma_Z^4}{\sigma_{N_2}^4}D_2 + \sigma_Z^2$, *then* $D_1 < \sigma_S^2 + \sigma_{N_1}^2 - \frac{\sigma_S^4(\sigma_S^2-D_S)}{(\sigma_S^2-\sigma_Z^2)^2}$ *and* $D_2 < \sigma_S^2 + \sigma_{N_2}^2 - \frac{\sigma_S^4(\sigma_S^2-D_S)}{(\sigma_S^2-\sigma_Z^2)^2}$ *cannot hold simultaneously.*

Proof Assume $D_1 < \sigma_S^2 + \sigma_{N_1}^2 - \frac{\sigma_S^4(\sigma_S^2-D_S)}{(\sigma_S^2-\sigma_Z^2)^2}$ and $D_2 < \sigma_S^2 + \sigma_{N_2}^2 - \frac{\sigma_S^4(\sigma_S^2-D_S)}{(\sigma_S^2-\sigma_Z^2)^2}$. We have

$$\begin{aligned}
D_S &< \frac{\sigma_Z^4}{\sigma_{N_1}^4}D_1 + \frac{2\sigma_Z^4}{\sigma_{N_1}^2\sigma_{N_2}^2}(\sigma_S^2 - \sqrt{(\sigma_S^2+\sigma_{N_1}^2-D_1)(\sigma_S^2+\sigma_{N_2}^2-D_2)}) + \frac{\sigma_Z^4}{\sigma_{N_2}^4}D_2 + \sigma_Z^2 \\
&= -\left(\frac{\sigma_Z^2}{\sigma_{N_1}^2}\sqrt{\sigma_S^2+\sigma_{N_1}^2-D_1} + \frac{\sigma_Z^2}{\sigma_{N_2}^2}\sqrt{\sigma_S^2+\sigma_{N_2}^2-D_2}\right)^2 + \sigma_S^2\left(\frac{\sigma_Z^2}{\sigma_{N_1}^2}+\frac{\sigma_Z^2}{\sigma_{N_2}^2}\right)^2 \\
&\quad + \frac{\sigma_Z^4}{\sigma_{N_1}^2} + \frac{\sigma_Z^4}{\sigma_{N_2}^2} + \sigma_Z^2 \\
&< -\left(\frac{\sigma_Z^2}{\sigma_{N_1}^2}+\frac{\sigma_Z^2}{\sigma_{N_2}^2}\right)^2\frac{\sigma_S^4(\sigma_S^2-D_S)}{(\sigma_S^2-\sigma_Z^2)^2} + \sigma_S^2\left(\frac{\sigma_Z^2}{\sigma_{N_1}^2}+\frac{\sigma_Z^2}{\sigma_{N_2}^2}\right)^2 + \frac{\sigma_Z^4}{\sigma_{N_1}^2} + \frac{\sigma_Z^4}{\sigma_{N_2}^2} + \sigma_Z^2 \\
&= D_S,
\end{aligned}$$

which leads to a contradiction. This proves Lemma 4.5. □

Lemma 4.6 *The following conditions are equivalent:*

$$\begin{aligned}
&(\sigma_S^2+\sigma_{N_1}^2-D_1)(\sigma_S^2+\sigma_{N_2}^2-D_2) < \left(\sigma_S^2 + \frac{\sigma_{N_2}^2}{2\sigma_{N_1}^2}D_1 + \frac{\sigma_{N_1}^2}{2\sigma_{N_2}^2}D_2 - \frac{(D_S-\sigma_Z^2)\sigma_{N_1}^2\sigma_{N_2}^2}{2\sigma_Z^4}\right)^2 \\
&\iff (\sigma_S^2+\sigma_{N_1}^2-D_1)(\sigma_S^2-D_S) < \left(\sigma_S^2 + \frac{\sigma_Z^2\sigma_{N_1}^2}{2\sigma_{N_2}^4}D_2 - \frac{\sigma_Z^2}{2\sigma_{N_1}^2}D_1 - \frac{(D_S-\sigma_Z^2)\sigma_{N_1}^2}{2\sigma_Z^2}\right)^2 \\
&\iff (\sigma_S^2+\sigma_{N_2}^2-D_2)(\sigma_S^2-D_S) < \left(\sigma_S^2 + \frac{\sigma_Z^2\sigma_{N_2}^2}{2\sigma_{N_1}^4}D_1 - \frac{\sigma_Z^2}{2\sigma_{N_2}^2}D_2 - \frac{(D_S-\sigma_Z^2)\sigma_{N_2}^2}{2\sigma_Z^2}\right)^2.
\end{aligned}$$

Proof It can be verified that

$$\begin{aligned}
&\left(\sigma_S^2+\frac{\sigma_{N_2}^2}{2\sigma_{N_1}^2}D_1+\frac{\sigma_{N_1}^2}{2\sigma_{N_2}^2}D_2-\frac{(D_S-\sigma_Z^2)\sigma_{N_1}^2\sigma_{N_2}^2}{2\sigma_Z^4}\right)^2-(\sigma_S^2+\sigma_{N_1}^2-D_1)(\sigma_S^2+\sigma_{N_2}^2-D_2)\\
&=\frac{\sigma_{N_2}^4}{\sigma_Z^4}\left(\left(\sigma_S^2+\frac{\sigma_Z^2\sigma_{N_1}^2}{2\sigma_{N_2}^4}D_2-\frac{\sigma_Z^2}{2\sigma_{N_1}^2}D_1-\frac{(D_S-\sigma_Z^2)\sigma_{N_1}^2}{2\sigma_Z^2}\right)^2-(\sigma_S^2+\sigma_{N_1}^2-D_1)(\sigma_S^2-D_S)\right)\\
&=\frac{\sigma_{N_1}^4}{\sigma_Z^4}\left(\left(\sigma_S^2+\frac{\sigma_Z^2\sigma_{N_2}^2}{2\sigma_{N_1}^4}D_1-\frac{\sigma_Z^2}{2\sigma_{N_2}^2}D_2-\frac{(D_S-\sigma_Z^2)\sigma_{N_2}^2}{2\sigma_Z^2}\right)^2-(\sigma_S^2+\sigma_{N_2}^2-D_2)(\sigma_S^2-D_S)\right),
\end{aligned}$$

from which the desired result follows immediately. $\square$

Lemma 4.7 *If* $D_1 \geq \sigma_S^2+\sigma_{N_1}^2-\frac{\sigma_S^4(\sigma_S^2+\sigma_{N_2}^2-D_2)}{(\sigma_S^2+\sigma_{N_2}^2)^2}$ *and* $(\sigma_S^2+\sigma_{N_1}^2-D_1)(\sigma_S^2+\sigma_{N_2}^2-D_2)\geq \left(\sigma_S^2+\frac{\sigma_{N_2}^2}{2\sigma_{N_1}^2}D_1+\frac{\sigma_{N_1}^2}{2\sigma_{N_2}^2}D_2-\frac{(D_S-\sigma_Z^2)\sigma_{N_1}^2\sigma_{N_2}^2}{2\sigma_Z^4}\right)^2$, *then* $D_S\geq\sigma_S^2-\frac{\sigma_S^4(\sigma_S^2+\sigma_{N_2}^2-D_2)}{(\sigma_S^2+\sigma_{N_2}^2)^2}$.

Proof Since $D_1 \geq \sigma_S^2+\sigma_{N_1}^2-\frac{\sigma_S^4(\sigma_S^2+\sigma_{N_2}^2-D_2)}{(\sigma_S^2+\sigma_{N_2}^2)^2}$, i.e., $\sigma_S^2+\sigma_{N_1}^2-D_1\leq\frac{\sigma_S^4(\sigma_S^2+\sigma_{N_2}^2-D_2)}{(\sigma_S^2+\sigma_{N_2}^2)^2}$, we have $(\sigma_S^2+\sigma_{N_1}^2-D_1)(\sigma_S^2+\sigma_{N_2}^2-D_2)\leq\frac{\sigma_S^4(\sigma_S^2+\sigma_{N_2}^2-D_2)^2}{(\sigma_S^2+\sigma_{N_2}^2)^2}$, which, together with the fact that $(\sigma_S^2+\sigma_{N_1}^2-D_1)(\sigma_S^2+\sigma_{N_2}^2-D_2)\geq\left(\sigma_S^2+\frac{\sigma_{N_2}^2}{2\sigma_{N_1}^2}D_1+\frac{\sigma_{N_1}^2}{2\sigma_{N_2}^2}D_2-\frac{(D_S-\sigma_Z^2)\sigma_{N_1}^2\sigma_{N_2}^2}{2\sigma_Z^4}\right)^2$, implies

$$\left(\sigma_S^2+\frac{\sigma_{N_2}^2}{2\sigma_{N_1}^2}D_1+\frac{\sigma_{N_1}^2}{2\sigma_{N_2}^2}D_2-\frac{(D_S-\sigma_Z^2)\sigma_{N_1}^2\sigma_{N_2}^2}{2\sigma_Z^4}\right)^2\leq\frac{\sigma_S^4(\sigma_S^2+\sigma_{N_2}^2-D_2)^2}{(\sigma_S^2+\sigma_{N_2}^2)^2}. \quad (4.B.8)$$

If $\sigma_S^2+\frac{\sigma_{N_2}^2}{2\sigma_{N_1}^2}D_1+\frac{\sigma_{N_1}^2}{2\sigma_{N_2}^2}D_2-\frac{(D_S-\sigma_Z^2)\sigma_{N_1}^2\sigma_{N_2}^2}{2\sigma_Z^4}\geq 0$, taking the square root on both sides of the inequality in (4.B.8) gives $\sigma_S^2+\frac{\sigma_{N_2}^2}{2\sigma_{N_1}^2}D_1+\frac{\sigma_{N_1}^2}{2\sigma_{N_2}^2}D_2-\frac{(D_S-\sigma_Z^2)\sigma_{N_1}^2\sigma_{N_2}^2}{2\sigma_Z^4}\leq\frac{\sigma_S^2(\sigma_S^2+\sigma_{N_2}^2-D_2)}{\sigma_S^2+\sigma_{N_2}^2}$, i.e.,

$$D_S\geq\frac{\sigma_Z^4}{\sigma_{N_1}^4}D_1+\left(\frac{\sigma_Z^4}{\sigma_{N_2}^4}+\frac{2\sigma_Z^4\sigma_S^2}{\sigma_{N_1}^2\sigma_{N_2}^2(\sigma_S^2+\sigma_{N_2}^2)}\right)D_2+\sigma_Z^2. \quad (4.B.9)$$

On the other hand, if $\sigma_S^2+\frac{\sigma_{N_2}^2}{2\sigma_{N_1}^2}D_1+\frac{\sigma_{N_1}^2}{2\sigma_{N_2}^2}D_2-\frac{(D_S-\sigma_Z^2)\sigma_{N_1}^2\sigma_{N_2}^2}{2\sigma_Z^4}<0$, i.e. $D_S>\frac{\sigma_Z^4}{\sigma_{N_1}^4}D_1+$

$\frac{\sigma_Z^4}{\sigma_{N_2}^4}D_2 + \sigma_Z^2 + \frac{2\sigma_Z^4\sigma_S^2}{\sigma_{N_1}^2\sigma_{N_2}^2}$, we still have (4.B.9) since $\sigma_S^2 \geq \frac{\sigma_S^2}{\sigma_S^2+\sigma_{N_2}^2}D_2$. Combining (4.B.9) with the fact that $D_1 \geq \sigma_S^2 + \sigma_{N_1}^2 - \frac{\sigma_S^4(\sigma_S^2+\sigma_{N_2}^2-D_2)}{(\sigma_S^2+\sigma_{N_2}^2)^2}$ yields the desired inequality. $\square$

In view of Lemma 4.3, it suffices to focus on (4.3.20) and (4.3.21). We shall show that the complement of (4.3.20) and (4.3.21) is already covered by Cases 1)–9).

4.B.1 $\det(\mathbf{K_X} - \boldsymbol{\Delta}^*) < 0$ and $\zeta_1 \geq 0$

According to Lemma 4.4, there is no need to consider the scenario $\zeta_2 < 0$ and $\zeta_3 < 0$. So it remains to handle the following scenarios: 1) $\zeta_2 < 0$ and $\zeta_3 \geq 0$, 2) $\zeta_2 \geq 0$ and $\zeta_3 < 0$, 3) $\zeta_2 \geq 0$ and $\zeta_3 \geq 0$.

$\zeta_2 < 0$ **and** $\zeta_3 \geq 0$

We only need to consider the situation $(\sigma_S^2+\sigma_{N_2}^2-D_2)(\sigma_S^2-D_S) < \sigma_S^4$ since otherwise the condition of Case 6) is met.

- $D_1 < \sigma_S^2 + \sigma_{N_1}^2 - \frac{\sigma_S^4\left(\sigma_S^2-D_S\right)}{\left(\sigma_S^2-\sigma_Z^2\right)^2}$ and $D_2 < \sigma_S^2 + \sigma_{N_2}^2 - \frac{\sigma_S^4\left(\sigma_S^2-D_S\right)}{\left(\sigma_S^2-\sigma_Z^2\right)^2}$: This is excluded by Lemma 4.5 since $\det(\mathbf{K_X} - \boldsymbol{\Delta}^*) < 0$ and $\zeta_1 \geq 0$ imply $D_S < \frac{\sigma_Z^4}{\sigma_{N_1}^4}D_1 + \frac{2\sigma_Z^4}{\sigma_{N_1}^2\sigma_{N_2}^2}(\sigma_S^2 - \sqrt{(\sigma_S^2+\sigma_{N_1}^2-D_1)(\sigma_S^2+\sigma_{N_2}^2-D_2)}) + \frac{\sigma_Z^4}{\sigma_{N_2}^4}D_2 + \sigma_Z^2$.
- $D_1 \geq \sigma_S^2 + \sigma_{N_1}^2 - \frac{\sigma_S^4\left(\sigma_S^2-D_S\right)}{\left(\sigma_S^2-\sigma_Z^2\right)^2}$ and $D_2 < \sigma_S^2 + \sigma_{N_2}^2 - \frac{\sigma_S^4\left(\sigma_S^2-D_S\right)}{\left(\sigma_S^2-\sigma_Z^2\right)^2}$:
  - $D_S < \sigma_S^2 - \frac{\sigma_S^4(\sigma_S^2+\sigma_{N_2}^2-D_2)}{(\sigma_S^2+\sigma_{N_2}^2)^2}$: The condition of Case 9) is met.

– $D_S \geq \sigma_S^2 - \frac{\sigma_S^4(\sigma_S^2+\sigma_{N_2}^2-D_2)}{(\sigma_S^2+\sigma_{N_2}^2)^2}$: Note that

$$\begin{aligned}
D_1 &> \frac{\sigma_{N_1}^4}{\sigma_{N_2}^4}D_2 + \frac{(D_S-\sigma_Z^2)\sigma_{N_1}^4}{\sigma_Z^4} && \text{(4.B.10)}\\
&\geq \frac{\sigma_{N_1}^4}{\sigma_{N_2}^4}D_2 + \frac{\sigma_{N_1}^4}{\sigma_Z^4}\left(\sigma_S^2 - \frac{\sigma_S^4(\sigma_S^2+\sigma_{N_2}^2-D_2)}{(\sigma_S^2+\sigma_{N_2}^2)^2}\right) - \frac{\sigma_{N_1}^4}{\sigma_Z^4}\sigma_Z^2 && \text{(4.B.11)}\\
&= \frac{(\sigma_S^2+\sigma_{N_2}^2)\sigma_{N_1}^2+\sigma_S^2\sigma_{N_2}^2}{\sigma_S^2+\sigma_{N_2}^2} + \frac{\sigma_{N_1}^4\left(\sigma_S^2+\sigma_{N_2}^2\right)^2 + \left((\sigma_S^2+\sigma_{N_2}^2)\sigma_{N_1}^2+\sigma_S^2\sigma_{N_2}^2\right)^2}{(\sigma_S^2+\sigma_{N_2}^2)^2\sigma_{N_2}^4}D_2,
\end{aligned}$$

where (4.B.10) and (4.B.11) are due to $\zeta_2 < 0$ and $D_S \geq \sigma_S^2 - \frac{\sigma_S^4(\sigma_S^2+\sigma_{N_2}^2-D_2)}{(\sigma_S^2+\sigma_{N_2}^2)^2}$, respectively. Therefore,

$$\begin{aligned}
\sigma_S^2+\sigma_{N_1}^2-D_1 &< \sigma_S^2+\sigma_{N_1}^2 - \frac{(\sigma_S^2+\sigma_{N_2}^2)\sigma_{N_1}^2+\sigma_S^2\sigma_{N_2}^2}{\sigma_S^2+\sigma_{N_2}^2}\\
&\qquad - \frac{\sigma_{N_1}^4\left(\sigma_S^2+\sigma_{N_2}^2\right)^2 + \left((\sigma_S^2+\sigma_{N_2}^2)\sigma_{N_1}^2+\sigma_S^2\sigma_{N_2}^2\right)^2}{(\sigma_S^2+\sigma_{N_2}^2)^2\sigma_{N_2}^4}D_2\\
&= \frac{\sigma_S^4}{\sigma_S^2+\sigma_{N_2}^2} - \frac{\sigma_{N_1}^4\left(\sigma_S^2+\sigma_{N_2}^2\right)^2 + \left((\sigma_S^2+\sigma_{N_2}^2)\sigma_{N_1}^2+\sigma_S^2\sigma_{N_2}^2\right)^2}{(\sigma_S^2+\sigma_{N_2}^2)^2\sigma_{N_2}^4}D_2\\
&< \frac{\sigma_S^4}{\sigma_S^2+\sigma_{N_2}^2} - \frac{\sigma_S^4}{(\sigma_S^2+\sigma_{N_2}^2)^2}D_2 && \text{(4.B.12)}\\
&= \frac{\sigma_S^4}{(\sigma_S^2+\sigma_{N_2}^2)^2}\left(\sigma_S^2+\sigma_{N_2}^2-D_2\right),
\end{aligned}$$

where (4.B.12) is due to $\frac{\sigma_{N_1}^4\left(\sigma_S^2+\sigma_{N_2}^2\right)^2 + \left((\sigma_S^2+\sigma_{N_2}^2)\sigma_{N_1}^2+\sigma_S^2\sigma_{N_2}^2\right)^2}{(\sigma_S^2+\sigma_{N_2}^2)^2\sigma_{N_2}^4} \geq \frac{\sigma_S^4}{(\sigma_S^2+\sigma_{N_2}^2)^2}$. Thus, we have $D_1 > \sigma_S^2+\sigma_{N_1}^2 - \frac{\sigma_S^4(\sigma_S^2+\sigma_{N_2}^2-D_2)}{(\sigma_S^2+\sigma_{N_2}^2)^2}$. Now one can readily see that the condition of Case 2) is met.

- $D_2 \geq \sigma_S^2 + \sigma_{N_2}^2 - \frac{\sigma_S^4(\sigma_S^2 - D_S)}{(\sigma_S^2-\sigma_Z^2)^2}$: Note that

$$
\begin{aligned}
D_1 &> \frac{\sigma_{N_1}^4}{\sigma_{N_2}^4} D_2 + \frac{(D_S - \sigma_Z^2)\sigma_{N_1}^4}{\sigma_Z^4} && (4.B.13)\\
&\geq \frac{\sigma_{N_1}^4}{\sigma_{N_2}^4}\left(\sigma_S^2 + \sigma_{N_2}^2 - \frac{\sigma_S^4\left(\sigma_S^2 - D_S\right)}{\left(\sigma_S^2 - \sigma_Z^2\right)^2}\right) + \frac{(D_S - \sigma_Z^2)\sigma_{N_1}^4}{\sigma_Z^4} && (4.B.14)\\
&= \frac{\sigma_{N_1}^4}{\sigma_{N_1}^2 + \sigma_{N_2}^2} + \left(\frac{\sigma_{N_1}^4\sigma_S^4}{\sigma_{N_2}^4\left(\sigma_S^2 - \sigma_Z^2\right)^2} + \frac{\sigma_{N_1}^4}{\sigma_Z^4}\right)(D_S - \sigma_Z^2),
\end{aligned}
$$

where (4.B.13) and (4.B.14) are due to $\zeta_2 < 0$ and $D_2 \geq \sigma_S^2 + \sigma_{N_2}^2 - \frac{\sigma_S^4(\sigma_S^2 - D_S)}{(\sigma_S^2-\sigma_Z^2)^2}$, respectively. Therefore,

$$
\begin{aligned}
&D_1 - \left(\sigma_S^2 + \sigma_{N_1}^2 - \frac{\sigma_S^4\left(\sigma_S^2 - D_S\right)}{\left(\sigma_S^2 - \sigma_Z^2\right)^2}\right)\\
&> \frac{\sigma_{N_1}^4}{\sigma_{N_1}^2 + \sigma_{N_2}^2} + \left(\frac{\sigma_{N_1}^4\sigma_S^4}{\sigma_{N_2}^4\left(\sigma_S^2 - \sigma_Z^2\right)^2} + \frac{\sigma_{N_1}^4}{\sigma_Z^4}\right)(D_S - \sigma_Z^2) - \left(\sigma_S^2 + \sigma_{N_1}^2 - \frac{\sigma_S^4\left(\sigma_S^2 - D_S\right)}{\left(\sigma_S^2 - \sigma_Z^2\right)^2}\right)\\
&= \left(\frac{\sigma_{N_1}^4\sigma_S^4}{\sigma_{N_2}^4\left(\sigma_S^2 - \sigma_Z^2\right)^2} + \frac{\sigma_S^4\sigma_{N_1}^4\left(\frac{\sigma_{N_1}^2}{\sigma_Z^2} + \frac{\sigma_S^2}{\sigma_S^2 - \sigma_Z^2}\right)}{\sigma_Z^2(\sigma_S^2 - \sigma_Z^2)(\sigma_S^2 + \sigma_{N_2}^2)\sigma_{N_1}^2 + \sigma_S^2\sigma_{N_2}^2)}\right)(D_S - \sigma_Z^2)\\
&\geq 0.
\end{aligned}
$$

Thus, we have $D_1 > \sigma_S^2 + \sigma_{N_1}^2 - \frac{\sigma_S^4\left(\sigma_S^2 - D_S\right)}{\left(\sigma_S^2-\sigma_Z^2\right)^2}$. Now one can readily see that the condition of Case 3) is met.

$\zeta_2 \geq 0$ **and** $\zeta_3 < 0$

This is symmetric to the scenario $\zeta_2 < 0$ and $\zeta_3 \geq 0$, thus is covered by Cases 1), 3), 5), and 8).

$\zeta_2 \geq 0$ **and** $\zeta_3 \geq 0$

We have

$$
\begin{aligned}
&(\sigma_S^2+\sigma_{N_1}^2-D_1)\left(\sigma_S^2+\sigma_{N_2}^2-\left(\frac{\sigma_{N_2}^4}{\sigma_{N_1}^4}D_1+\frac{(D_S-\sigma_Z^2)\sigma_{N_2}^4}{\sigma_Z^4}\right)\right)\\
&\leq (\sigma_S^2+\sigma_{N_1}^2-D_1)(\sigma_S^2+\sigma_{N_2}^2-D_2) && \text{(4.B.15)}\\
&< \left(\sigma_S^2+\frac{\sigma_{N_2}^2}{2\sigma_{N_1}^2}D_1+\frac{\sigma_{N_1}^2}{2\sigma_{N_2}^2}D_2-\frac{(D_S-\sigma_Z^2)\sigma_{N_1}^2\sigma_{N_2}^2}{2\sigma_Z^4}\right)^2 && \text{(4.B.16)}\\
&\leq \left(\sigma_S^2+\frac{\sigma_{N_2}^2}{\sigma_{N_1}^2}D_1\right)^2, && \text{(4.B.17)}
\end{aligned}
$$

where (4.B.15) is due to $\zeta_3 \geq 0$, (4.B.16) is due to $\det(\mathbf{K_X}-\mathbf{\Delta}^*)<0$, and (4.B.17) is due to $\zeta_1 \geq 0$ and $\zeta_3 \geq 0$. It can be verified that

$$
\begin{aligned}
&(\sigma_S^2+\sigma_{N_1}^2-D_1)\left(\sigma_S^2+\sigma_{N_2}^2-\left(\frac{\sigma_{N_2}^4}{\sigma_{N_1}^4}D_1+\frac{(D_S-\sigma_Z^2)\sigma_{N_2}^4}{\sigma_Z^4}\right)\right)-\left(\sigma_S^2+\frac{\sigma_{N_2}^2}{\sigma_{N_1}^2}D_1\right)^2\\
&=\frac{\left((\sigma_S^2+\sigma_{N_1}^2)(\sigma_S^2+\sigma_{N_2}^2)-\sigma_S^4\right)^2}{\sigma_S^4\sigma_{N_1}^4}\left((\sigma_S^2+\sigma_{N_1}^2-D_1)(\sigma_S^2-D_S)-\sigma_S^4\right). && \text{(4.B.18)}
\end{aligned}
$$

Therefore, (4.B.17) implies $(\sigma_S^2+\sigma_{N_1}^2-D_1)(\sigma_S^2-D_S)<\sigma_S^4$. Similarly, it can be shown that $(\sigma_S^2+\sigma_{N_2}^2-D_2)(\sigma_S^2-D_S)<\sigma_S^4$.

- $D_1<\sigma_S^2+\sigma_{N_1}^2-\frac{\sigma_S^4(\sigma_S^2-D_S)}{(\sigma_S^2-\sigma_Z^2)^2}$ and $D_2<\sigma_S^2+\sigma_{N_2}^2-\frac{\sigma_S^4(\sigma_S^2-D_S)}{(\sigma_S^2-\sigma_Z^2)^2}$: This is excluded by Lemma 4.5 since $\det(\mathbf{K_X}-\mathbf{\Delta}^*)<0$ and $\zeta_1 \geq 0$ imply $D_S<\frac{\sigma_Z^4}{\sigma_{N_1}^4}D_1+\frac{2\sigma_Z^4}{\sigma_{N_1}^2\sigma_{N_2}^2}(\sigma_S^2-\sqrt{(\sigma_S^2+\sigma_{N_1}^2-D_1)(\sigma_S^2+\sigma_{N_2}^2-D_2)})+\frac{\sigma_Z^4}{\sigma_{N_2}^4}D_2+\sigma_Z^2$.
- $D_1\geq\sigma_S^2+\sigma_{N_1}^2-\frac{\sigma_S^4(\sigma_S^2-D_S)}{(\sigma_S^2-\sigma_Z^2)^2}$ and $D_2<\sigma_S^2+\sigma_{N_2}^2-\frac{\sigma_S^4(\sigma_S^2-D_S)}{(\sigma_S^2-\sigma_Z^2)^2}$:
  - $D_S<\sigma_S^2-\frac{\sigma_S^4(\sigma_S^2+\sigma_{N_2}^2-D_2)}{(\sigma_S^2+\sigma_{N_2}^2)^2}$: According to Lemma 4.6, $\det(\mathbf{K_X}-\mathbf{\Delta}^*)<0$ is

equivalent to

$$(\sigma_S^2+\sigma_{N_2}^2-D_2)(\sigma_S^2-D_S) < \left(\sigma_S^2+\frac{\sigma_Z^2\sigma_{N_2}^2}{2\sigma_{N_1}^4}D_1-\frac{\sigma_Z^2}{2\sigma_{N_2}^2}D_2-\frac{(D_S-\sigma_Z^2)\sigma_{N_2}^2}{2\sigma_Z^2}\right)^2. \tag{4.B.19}$$

Moreover, we have

$$\begin{aligned}
&\sigma_S^2+\frac{\sigma_Z^2\sigma_{N_2}^2}{2\sigma_{N_1}^4}D_1-\frac{\sigma_Z^2}{2\sigma_{N_2}^2}D_2-\frac{(D_S-\sigma_Z^2)\sigma_{N_2}^2}{2\sigma_Z^2}\\
&\geq \sigma_S^2-\frac{\sigma_Z^2}{\sigma_{N_2}^2}D_2 \qquad (4.B.20)\\
&=\frac{\sigma_S^2\sigma_{N_1}^2(\sigma_S^2+\sigma_{N_2}^2-D_2)+\sigma_S^2\sigma_{N_2}^2}{\sigma_{N_1}^2(\sigma_S^2+\sigma_{N_2}^2)+\sigma_S^2\sigma_{N_2}^2}\\
&\geq 0,
\end{aligned}$$

where (4.B.20) is due to $\zeta_1 \geq 0$. Therefore, (4.B.19) implies

$$\sqrt{(\sigma_S^2+\sigma_{N_2}^2-D_2)(\sigma_S^2-D_S)} < \sigma_S^2+\frac{\sigma_Z^2\sigma_{N_2}^2}{2\sigma_{N_1}^4}D_1-\frac{\sigma_Z^2}{2\sigma_{N_2}^2}D_2-\frac{(D_S-\sigma_Z^2)\sigma_{N_2}^2}{2\sigma_Z^2},$$

i.e., $D_1 > \frac{\sigma_{N_1}^4}{\sigma_{N_2}^4}D_2-\frac{2\sigma_{N_1}^4}{\sigma_S^2\sigma_{N_2}^2}(\sigma_S^2-\sqrt{(\sigma_S^2+\sigma_{N_2}^2-D_2)(\sigma_S^2-D_S)})+\frac{\sigma_{N_1}^4}{\sigma_Z^4}(D_S-\sigma_Z^2)$. Now one can readily see that the condition of Case 9) is met.

– $D_S \geq \sigma_S^2 - \frac{\sigma_S^4(\sigma_S^2+\sigma_{N_2}^2-D_2)}{(\sigma_S^2+\sigma_{N_2}^2)^2}$: Note that

$$\begin{aligned}
D_1 &\geq \frac{\sigma_{N_1}^4}{\sigma_Z^4}(D_S - \sigma_Z^2) - \frac{\sigma_{N_1}^4}{\sigma_{N_2}^4} D_2 && (4.B.21)\\
&\geq \frac{\sigma_{N_1}^4}{\sigma_Z^4}\left(\sigma_S^2 - \frac{\sigma_S^4(\sigma_S^2+\sigma_{N_2}^2-D_2)}{(\sigma_S^2+\sigma_{N_2}^2)^2} - \sigma_Z^2\right) - \frac{\sigma_{N_1}^4}{\sigma_{N_2}^4} D_2 && (4.B.22)\\
&= \frac{(\sigma_S^2+\sigma_{N_2}^2)\sigma_{N_1}^2 + \sigma_S^2\sigma_{N_2}^2}{\sigma_S^2+\sigma_{N_2}^2} + \left(\frac{((\sigma_S^2+\sigma_{N_2}^2)\sigma_{N_1}^2 + \sigma_S^2\sigma_{N_2}^2)^2 - \sigma_{N_1}^4(\sigma_S^2+\sigma_{N_2}^2)^2}{\sigma_{N_2}^4(\sigma_S^2+\sigma_{N_2}^2)^2}\right) D_2 \\
&\geq \frac{(\sigma_S^2+\sigma_{N_2}^2)\sigma_{N_1}^2 + \sigma_S^2\sigma_{N_2}^2}{\sigma_S^2+\sigma_{N_2}^2} + \frac{\sigma_S^4}{(\sigma_S^2+\sigma_{N_2}^2)^2} D_2, && (4.B.23)
\end{aligned}$$

where (4.B.21) is due to $\zeta_1 \geq 0$, (4.B.22) is due to $D_S \geq \sigma_S^2 - \frac{\sigma_S^4(\sigma_S^2+\sigma_{N_2}^2-D_2)}{(\sigma_S^2+\sigma_{N_2}^2)^2}$, and (4.B.23) is due to $\frac{((\sigma_S^2+\sigma_{N_2}^2)\sigma_{N_1}^2+\sigma_S^2\sigma_{N_2}^2)^2-\sigma_{N_1}^4(\sigma_S^2+\sigma_{N_2}^2)^2}{\sigma_{N_2}^4(\sigma_S^2+\sigma_{N_2}^2)^2} \geq \frac{\sigma_S^4}{(\sigma_S^2+\sigma_{N_2}^2)^2}$. Therefore,

$$\begin{aligned}
&\sigma_S^2 + \sigma_{N_1}^2 - D_1 && (4.B.24)\\
&\leq \sigma_S^2 + \sigma_{N_1}^2 - \frac{(\sigma_S^2+\sigma_{N_2}^2)\sigma_{N_1}^2 + \sigma_S^2\sigma_{N_2}^2}{\sigma_S^2+\sigma_{N_2}^2} - \frac{\sigma_S^4}{(\sigma_S^2+\sigma_{N_2}^2)^2} D_2 && (4.B.25)\\
&= \frac{\sigma_S^4}{(\sigma_S^2+\sigma_{N_2}^2)^2}(\sigma_S^2+\sigma_{N_2}^2 - D_2), && (4.B.26)
\end{aligned}$$

which implies $D_1 \geq \sigma_S^2 + \sigma_{N_1}^2 - \frac{\sigma_S^4(\sigma_S^2+\sigma_{N_2}^2-D_2)}{(\sigma_S^2+\sigma_{N_2}^2)^2}$. So the condition of Case 2) is met.

- $D_1 < \sigma_S^2 + \sigma_{N_1}^2 - \frac{\sigma_S^4(\sigma_S^2-D_S)}{(\sigma_S^2-\sigma_Z^2)^2}$ and $D_2 \geq \sigma_S^2 + \sigma_{N_2}^2 - \frac{\sigma_S^4(\sigma_S^2-D_S)}{(\sigma_S^2-\sigma_Z^2)^2}$: This is symmetric to $D_1 \geq \sigma_S^2 + \sigma_{N_1}^2 - \frac{\sigma_S^4(\sigma_S^2-D_S)}{(\sigma_S^2-\sigma_Z^2)^2}$ and $D_2 < \sigma_S^2 + \sigma_{N_2}^2 - \frac{\sigma_S^4(\sigma_S^2-D_S)}{(\sigma_S^2-\sigma_Z^2)^2}$, thus is covered by Cases 1) and 8).

- $D_1 \geq \sigma_S^2 + \sigma_{N_1}^2 - \frac{\sigma_S^4(\sigma_S^2-D_S)}{(\sigma_S^2-\sigma_Z^2)^2}$ and $D_2 \geq \sigma_S^2 + \sigma_{N_2}^2 - \frac{\sigma_S^4(\sigma_S^2-D_S)}{(\sigma_S^2-\sigma_Z^2)^2}$: The condition of Case 3) is met.

4.B.2 $\det(\mathbf{K}_{\mathbf{X}} - \mathbf{\Delta}^*) < 0$ and $\zeta_1 < 0$

According to Lemma 4.4, $\zeta_1 < 0$ implies $\zeta_2 \geq 0$ and $\zeta_3 \geq 0$. Moreover, we only need to consider the situation $(\sigma_S^2 + \sigma_{N_1}^2 - D_1)(\sigma_S^2 + \sigma_{N_2}^2 - D_2) < \sigma_S^4$ since otherwise the condition of Case 4) is met. Note that

$$
\begin{aligned}
&(\sigma_S^2 + \sigma_{N_1}^2 - D_1)\left(\sigma_S^2 + \sigma_{N_2}^2 - \left(\frac{\sigma_{N_2}^4}{\sigma_{N_1}^4} D_1 + \frac{(D_S - \sigma_Z^2)\sigma_{N_2}^4}{\sigma_Z^4}\right)\right) \\
&\leq (\sigma_S^2 + \sigma_{N_1}^2 - D_1)(\sigma_S^2 + \sigma_{N_2}^2 - D_2) \qquad (4.B.27) \\
&< \sigma_S^4 \\
&< \left(\sigma_S^2 + \frac{\sigma_{N_2}^2}{\sigma_{N_1}^2} D_1\right)^2,
\end{aligned}
$$

where (4.B.27) is due to $\zeta_3 \geq 0$. Therefore, in view of (4.B.18), we must have $(\sigma_S^2 + \sigma_{N_1}^2 - D_1)(\sigma_S^2 - D_S) < \sigma_S^4$. Similarly, it can be shown that $(\sigma_S^2 + \sigma_{N_2}^2 - D_2)(\sigma_S^2 - D_S) < \sigma_S^4$.

- $D_1 \geq \sigma_S^2 + \sigma_{N_1}^2 - \frac{\sigma_S^4(\sigma_S^2 + \sigma_{N_2}^2 - D_2)}{(\sigma_S^2 + \sigma_{N_2}^2)^2}$:
  - $D_S \geq \sigma_S^2 - \frac{\sigma_S^4(\sigma_S^2 + \sigma_{N_2}^2 - D_2)}{(\sigma_S^2 + \sigma_{N_2}^2)^2}$: The condition of Case 2) is met.
  - $D_S < \sigma_S^2 - \frac{\sigma_S^4(\sigma_S^2 + \sigma_{N_2}^2 - D_2)}{(\sigma_S^2 + \sigma_{N_2}^2)^2}$:

    i) $D_2 < \sigma_S^2 + \sigma_{N_2}^2 - \frac{\sigma_S^4(\sigma_S^2 - D_S)}{(\sigma_S^2 - \sigma_Z^2)^2}$: According to Lemma 4.6, $\det(\mathbf{K}_{\mathbf{X}} - \mathbf{\Delta}^*) < 0$ is equivalent to

$$
(\sigma_S^2 + \sigma_{N_2}^2 - D_2)(\sigma_S^2 - D_S) < \left(\sigma_S^2 + \frac{\sigma_Z^2 \sigma_{N_2}^2}{2\sigma_{N_1}^4} D_1 - \frac{\sigma_Z^2}{2\sigma_{N_2}^2} D_2 - \frac{(D_S - \sigma_Z^2)\sigma_{N_2}^2}{2\sigma_Z^2}\right)^2. \qquad (4.B.28)
$$

It can be verified that

$$\begin{aligned}
&\sigma_S^2 + \frac{\sigma_Z^2\sigma_{N_2}^2}{2\sigma_{N_1}^4}D_1 - \frac{\sigma_Z^2}{2\sigma_{N_2}^2}D_2 - \frac{(D_S-\sigma_Z^2)\sigma_{N_2}^2}{2\sigma_Z^2}\\
&> \sigma_S^2 + \frac{\sigma_Z^2\sigma_{N_2}^2}{2\sigma_{N_1}^4}\left(\sigma_S^2+\sigma_{N_1}^2-\frac{\sigma_S^4(\sigma_S^2+\sigma_{N_2}^2-D_2)}{(\sigma_S^2+\sigma_{N_2}^2)^2}\right) - \frac{\sigma_Z^2}{2\sigma_{N_2}^2}D_2 + \frac{\sigma_{N_2}^2}{2}\\
&\quad - \frac{\sigma_{N_2}^2}{2\sigma_Z^2}\left(\sigma_S^2 - \frac{\sigma_S^4(\sigma_S^2+\sigma_{N_2}^2-D_2)}{(\sigma_S^2+\sigma_{N_2}^2)^2}\right)\\
&= \sigma_S^2\left(1-\frac{D_2}{\sigma_S^2+\sigma_{N_2}^2}\right)\\
&\geq 0.
\end{aligned}$$

So taking the square root on both sides of the inequality in (4.B.28) gives $\sqrt{(\sigma_S^2+\sigma_{N_2}^2-D_2)(\sigma_S^2-D_S)} < \sigma_S^2 + \frac{\sigma_Z^2\sigma_{N_2}^2}{2\sigma_{N_1}^4}D_1 - \frac{\sigma_Z^2}{2\sigma_{N_2}^2}D_2 - \frac{(D_S-\sigma_Z^2)\sigma_{N_2}^2}{2\sigma_Z^2}$, i.e., $D_1 > \frac{\sigma_{N_1}^4}{\sigma_{N_2}^4}D_2 - \frac{2\sigma_{N_1}^4}{\sigma_S^2\sigma_{N_2}^2}(\sigma_S^2 - \sqrt{(\sigma_S^2+\sigma_{N_2}^2-D_2)(\sigma_S^2-D_S)}) + \frac{\sigma_{N_1}^4}{\sigma_Z^4}(D_S-\sigma_Z^2)$. Now one can readily see that the condition of Case 9) is met.

ii) $D_2 \geq \sigma_S^2+\sigma_{N_2}^2 - \frac{\sigma_S^4(\sigma_S^2-D_S)}{(\sigma_S^2-\sigma_Z^2)^2}$: It can be verified that

$$\begin{aligned}
D_1 &\geq \sigma_S^2+\sigma_{N_1}^2 - \frac{\sigma_S^4(\sigma_S^2+\sigma_{N_2}^2-D_2)}{(\sigma_S^2+\sigma_{N_2}^2)^2}\\
&\geq \sigma_S^2+\sigma_{N_1}^2 - \frac{\sigma_S^8(\sigma_S^2-D_S)}{(\sigma_S^2+\sigma_{N_2}^2)^2(\sigma_S^2-\sigma_Z^2)^2}\\
&\geq \sigma_S^2+\sigma_{N_1}^2 - \frac{\sigma_S^4(\sigma_S^2-D_S)}{(\sigma_S^2-\sigma_Z^2)^2}.
\end{aligned}$$

So the condition of Case 3) is met.

- $D_2 \geq \sigma_S^2+\sigma_{N_2}^2 - \frac{\sigma_S^4(\sigma_S^2+\sigma_{N_1}^2-D_1)}{(\sigma_S^2+\sigma_{N_1}^2)^2}$: This is symmetric to $D_1 \geq \sigma_S^2+\sigma_{N_1}^2 - \frac{\sigma_S^4(\sigma_S^2+\sigma_{N_2}^2-D_2)}{(\sigma_S^2+\sigma_{N_2}^2)^2}$, thus is covered by Cases 1), 3), and 8).
- $D_1 < \sigma_S^2+\sigma_{N_1}^2 - \frac{\sigma_S^4(\sigma_S^2+\sigma_{N_2}^2-D_2)}{(\sigma_S^2+\sigma_{N_2}^2)^2}$ and $D_2 < \sigma_S^2+\sigma_{N_2}^2 - \frac{\sigma_S^4(\sigma_S^2+\sigma_{N_1}^2-D_1)}{(\sigma_S^2+\sigma_{N_1}^2)^2}$:

– $D_S \geq \frac{\sigma_Z^4}{\sigma_{N_1}^4} D_1 + \frac{2\sigma_Z^4}{\sigma_{N_1}^2 \sigma_{N_2}^2}(\sigma_S^2 - \sqrt{(\sigma_S^2 + \sigma_{N_1}^2 - D_1)(\sigma_S^2 + \sigma_{N_2}^2 - D_2)}) + \frac{\sigma_Z^4}{\sigma_{N_2}^4} D_2 + \sigma_Z^2$: The condition of Case 7) is met.

– $D_S < \frac{\sigma_Z^4}{\sigma_{N_1}^4} D_1 + \frac{2\sigma_Z^4}{\sigma_{N_1}^2 \sigma_{N_2}^2}(\sigma_S^2 - \sqrt{(\sigma_S^2 + \sigma_{N_1}^2 - D_1)(\sigma_S^2 + \sigma_{N_2}^2 - D_2)}) + \frac{\sigma_Z^4}{\sigma_{N_2}^4} D_2 + \sigma_Z^2$: Since $D_1 < \sigma_S^2 + \sigma_{N_1}^2 - \frac{\sigma_S^4(\sigma_S^2 + \sigma_{N_2}^2 - D_2)}{(\sigma_S^2 + \sigma_{N_2}^2)^2}$, i.e., $\sigma_S^2 + \sigma_{N_1}^2 - D_1 > \frac{\sigma_S^4(\sigma_S^2 + \sigma_{N_2}^2 - D_2)}{(\sigma_S^2 + \sigma_{N_2}^2)^2}$, we have

$$\sqrt{(\sigma_S^2 + \sigma_{N_1}^2 - D_1)(\sigma_S^2 + \sigma_{N_2}^2 - D_2)} \geq \sigma_S^2 - \frac{\sigma_S^2}{\sigma_S^2 + \sigma_{N_2}^2} D_2. \qquad (4.B.29)$$

It can be verified that

$$\begin{aligned}
D_S &< \frac{\sigma_Z^4}{\sigma_{N_1}^4} D_1 + \frac{2\sigma_Z^4}{\sigma_{N_1}^2 \sigma_{N_2}^2}(\sigma_S^2 - \sqrt{(\sigma_S^2 + \sigma_{N_1}^2 - D_1)(\sigma_S^2 + \sigma_{N_2}^2 - D_2)}) + \frac{\sigma_Z^4}{\sigma_{N_2}^4} D_2 + \sigma_Z^2 \\
&< \frac{\sigma_Z^4}{\sigma_{N_1}^4}\left(\sigma_S^2 + \sigma_{N_1}^2 - \frac{\sigma_S^4(\sigma_S^2 + \sigma_{N_2}^2 - D_2)}{(\sigma_S^2 + \sigma_{N_2}^2)^2}\right) + \frac{2\sigma_Z^4 \sigma_S^2}{\sigma_{N_1}^2 \sigma_{N_2}^2 (\sigma_S^2 + \sigma_{N_2}^2)} D_2 \\
&\quad + \frac{\sigma_Z^4}{\sigma_{N_2}^4} D_2 + \sigma_Z^2 \qquad (4.B.30) \\
&= \frac{\sigma_S^2 \sigma_{N_2}^2}{\sigma_S^2 + \sigma_{N_2}^2} + \frac{\sigma_S^4((\sigma_S^2 + \sigma_{N_1}^2)\sigma_{N_2}^2 + \sigma_S^2 \sigma_{N_1}^2)^2 - 2\sigma_S^8 \sigma_{N_2}^4}{(\sigma_S^2 + \sigma_{N_2}^2)^2((\sigma_S^2 + \sigma_{N_1}^2)\sigma_{N_2}^2 + \sigma_S^2 \sigma_{N_1}^2)^2} D_2 \\
&< \frac{\sigma_S^2 \sigma_{N_2}^2}{\sigma_S^2 + \sigma_{N_2}^2} + \frac{\sigma_S^4((\sigma_S^2 + \sigma_{N_1}^2)\sigma_{N_2}^2 + \sigma_S^2 \sigma_{N_1}^2)^2}{(\sigma_S^2 + \sigma_{N_2}^2)^2((\sigma_S^2 + \sigma_{N_1}^2)\sigma_{N_2}^2 + \sigma_S^2 \sigma_{N_1}^2)^2} D_2 \\
&= \sigma_S^2 - \frac{\sigma_S^4(\sigma_S^2 + \sigma_{N_2}^2 - D_2)}{(\sigma_S^2 + \sigma_{N_2}^2)^2},
\end{aligned}$$

where (4.B.30) is due to $D_1 < \sigma_S^2 + \sigma_{N_1}^2 - \frac{\sigma_S^4(\sigma_S^2 + \sigma_{N_2}^2 - D_2)}{(\sigma_S^2 + \sigma_{N_2}^2)^2}$ and (4.B.29).

In light of Lemma 4.5, $D_1 < \sigma_S^2 + \sigma_{N_1}^2 - \frac{\sigma_S^4\left(\sigma_S^2 - D_S\right)}{\left(\sigma_S^2 - \sigma_Z^2\right)^2}$ and $D_2 < \sigma_S^2 + \sigma_{N_2}^2 - \frac{\sigma_S^4\left(\sigma_S^2 - D_S\right)}{\left(\sigma_S^2 - \sigma_Z^2\right)^2}$ cannot hold simultaneously. So it suffices to consider the following possibilities.

i) $D_1 \geq \sigma_S^2 + \sigma_{N_1}^2 - \frac{\sigma_S^4(\sigma_S^2 - D_S)}{(\sigma_S^2 - \sigma_Z^2)^2}$ and $D_2 < \sigma_S^2 + \sigma_{N_2}^2 - \frac{\sigma_S^4(\sigma_S^2 - D_S)}{(\sigma_S^2 - \sigma_Z^2)^2}$: According to Lemma 4.6, $\det(\mathbf{K_X} - \mathbf{\Delta}^*) < 0$ is equivalent to

$$(\sigma_S^2 + \sigma_{N_2}^2 - D_2)(\sigma_S^2 - D_S) < \left(\sigma_S^2 + \frac{\sigma_Z^2\sigma_{N_2}^2}{2\sigma_{N_1}^4}D_1 - \frac{\sigma_Z^2}{2\sigma_{N_2}^2}D_2 - \frac{(D_S - \sigma_Z^2)\sigma_{N_2}^2}{2\sigma_Z^2}\right)^2. \tag{4.B.31}$$

It can be verified that

$$\begin{aligned}
&\sigma_S^2 + \frac{\sigma_Z^2\sigma_{N_2}^2}{2\sigma_{N_1}^4}D_1 - \frac{\sigma_Z^2}{2\sigma_{N_2}^2}D_2 - \frac{(D_S - \sigma_Z^2)\sigma_{N_2}^2}{2\sigma_Z^2} \\
&> \sigma_S^2 + \frac{\sigma_Z^2\sigma_{N_2}^2}{2\sigma_{N_1}^4}D_1 - \frac{\sigma_Z^2}{2\sigma_{N_2}^2}D_2 \\
&\quad - \frac{\sigma_{N_2}^2}{2\sigma_Z^2}\left(\frac{\sigma_Z^4}{\sigma_{N_1}^4}D_1 + \frac{2\sigma_Z^4}{\sigma_{N_1}^2\sigma_{N_2}^2}(\sigma_S^2 - \sqrt{(\sigma_S^2 + \sigma_{N_1}^2 - D_1)(\sigma_S^2 + \sigma_{N_2}^2 - D_2)}) + \frac{\sigma_Z^4}{\sigma_{N_2}^4}D_2\right) \\
&= \sigma_S^2 - \frac{\sigma_Z^2}{\sigma_{N_2}^2}D_2 - \frac{\sigma_Z^2}{\sigma_{N_1}^2}(\sigma_S^2 - \sqrt{(\sigma_S^2 + \sigma_{N_1}^2 - D_1)(\sigma_S^2 + \sigma_{N_2}^2 - D_2)}) \\
&\geq \sigma_S^2 - \frac{\sigma_Z^2}{\sigma_{N_2}^2}D_2 - \frac{\sigma_Z^2}{\sigma_{N_1}^2}\left(\sigma_S^2 - \sigma_S^2 + \frac{\sigma_S^2}{\sigma_S^2 + \sigma_{N_2}^2}D_2\right) \qquad (4.B.32) \\
&= \frac{\sigma_S^2\sigma_{N_1}^2(\sigma_S^2 + \sigma_{N_2}^2)(\sigma_S^2 + \sigma_{N_2}^2 - D_2) + \sigma_S^4\sigma_{N_2}^2(\sigma_S^2 + \sigma_{N_2}^2 - D_2)}{(\sigma_S^2 + \sigma_{N_2}^2)(\sigma_{N_1}^2(\sigma_S^2 + \sigma_{N_2}^2) + \sigma_S^2\sigma_{N_2}^2)} \\
&\geq 0,
\end{aligned}$$

where (4.B.32) is due to (4.B.29). So taking the square root on both sides of the inequality in (4.B.31) gives $\sqrt{(\sigma_S^2 + \sigma_{N_2}^2 - D_2)(\sigma_S^2 - D_S)} < \sigma_S^2 + \frac{\sigma_Z^2\sigma_{N_2}^2}{2\sigma_{N_1}^4}D_1 - \frac{\sigma_Z^2}{2\sigma_{N_2}^2}D_2 - \frac{(D_S - \sigma_Z^2)\sigma_{N_2}^2}{2\sigma_Z^2}$, i.e., $D_1 > \frac{\sigma_{N_1}^4}{\sigma_{N_2}^4}D_2 - \frac{2\sigma_{N_1}^4}{\sigma_S^2\sigma_{N_2}^2}(\sigma_S^2 - \sqrt{(\sigma_S^2 + \sigma_{N_2}^2 - D_2)(\sigma_S^2 - D_S)}) + \frac{\sigma_{N_1}^4}{\sigma_Z^4}(D_S - \sigma_Z^2)$. Now one can readily see that the condition of Case 9) is met.

ii) $D_1 < \sigma_S^2 + \sigma_{N_1}^2 - \frac{\sigma_S^4(\sigma_S^2 - D_S)}{(\sigma_S^2 - \sigma_Z^2)^2}$ and $D_2 \geq \sigma_S^2 + \sigma_{N_2}^2 - \frac{\sigma_S^4(\sigma_S^2 - D_S)}{(\sigma_S^2 - \sigma_Z^2)^2}$: This is symmetric to $D_1 \geq \sigma_S^2 + \sigma_{N_1}^2 - \frac{\sigma_S^4(\sigma_S^2 - D_S)}{(\sigma_S^2 - \sigma_Z^2)^2}$ and $D_2 < \sigma_S^2 + \sigma_{N_2}^2 - \frac{\sigma_S^4(\sigma_S^2 - D_S)}{(\sigma_S^2 - \sigma_Z^2)^2}$, thus is covered by Case 8).

iii) $D_1 \geq \sigma_S^2 + \sigma_{N_1}^2 - \frac{\sigma_S^4(\sigma_S^2 - D_S)}{(\sigma_S^2 - \sigma_Z^2)^2}$ and $D_2 \geq \sigma_S^2 + \sigma_{N_2}^2 - \frac{\sigma_S^4(\sigma_S^2 - D_S)}{(\sigma_S^2 - \sigma_Z^2)^2}$: The condition of Case 3) is met.

4.B.3 $\det(\mathbf{K_X} - \mathbf{\Delta}^*) \geq 0$ and $\zeta_1 < 0$

According to Lemma 4.4, $\zeta_1 < 0$ implies $\zeta_2 \geq 0$ and $\zeta_3 \geq 0$.

- $(\sigma_S^2 + \sigma_{N_1}^2 - D_1)(\sigma_S^2 + \sigma_{N_2}^2 - D_2) \geq \sigma_S^4$: The condition of Case 4) is met.
- $(\sigma_S^2 + \sigma_{N_1}^2 - D_1)(\sigma_S^2 + \sigma_{N_2}^2 - D_2) < \sigma_S^4$:
  - $D_1 \geq \sigma_S^2 + \sigma_{N_1}^2 - \frac{\sigma_S^4(\sigma_S^2 + \sigma_{N_2}^2 - D_2)}{(\sigma_S^2 + \sigma_{N_2}^2)^2}$: It follows by Lemma 4.7 that $D_S \geq \sigma_S^2 - \frac{\sigma_S^4(\sigma_S^2 + \sigma_{N_2}^2 - D_2)}{(\sigma_S^2 + \sigma_{N_2}^2)^2}$. So the condition of Case 2) is met.
  - $D_2 \geq \sigma_S^2 + \sigma_{N_2}^2 - \frac{\sigma_S^4(\sigma_S^2 + \sigma_{N_1}^2 - D_1)}{(\sigma_S^2 + \sigma_{N_1}^2)^2}$: This is symmetric to $D_1 \geq \sigma_S^2 + \sigma_{N_1}^2 - \frac{\sigma_S^4(\sigma_S^2 + \sigma_{N_2}^2 - D_2)}{(\sigma_S^2 + \sigma_{N_2}^2)^2}$, thus is covered by Case 1).
  - $D_1 < \sigma_S^2 + \sigma_{N_1}^2 - \frac{\sigma_S^4(\sigma_S^2 + \sigma_{N_2}^2 - D_2)}{(\sigma_S^2 + \sigma_{N_2}^2)^2}$ and $D_2 < \sigma_S^2 + \sigma_{N_2}^2 - \frac{\sigma_S^4(\sigma_S^2 + \sigma_{N_1}^2 - D_1)}{(\sigma_S^2 + \sigma_{N_1}^2)^2}$: Note that $\det(\mathbf{K_X} - \mathbf{\Delta}^*) \geq 0$ implies $D_S \geq \frac{\sigma_Z^4}{\sigma_{N_1}^4} D_1 + \frac{2\sigma_Z^4}{\sigma_{N_1}^2 \sigma_{N_2}^2}(\sigma_S^2 - \sqrt{(\sigma_S^2 + \sigma_{N_1}^2 - D_1)(\sigma_S^2 + \sigma_{N_2}^2 - D_2)}) + \frac{\sigma_Z^4}{\sigma_{N_2}^4} D_2 + \sigma_Z^2$. So the condition of Case 7) is met.

4.B.4 $\det(\mathbf{K_X} - \mathbf{\Delta}^*) \geq 0$ and $\zeta_1 \geq 0$

According to Lemma 4.4, there is no need to consider the scenario $\zeta_2 < 0$ and $\zeta_3 < 0$. So it remains to handle the following scenarios: 1) $\zeta_2 \geq 0$ and $\zeta_3 < 0$ and 2) $\zeta_2 < 0$ and $\zeta_3 \geq 0$. Note that the remaining scenario $\zeta_2 \geq 0$ and $\zeta_3 \geq 0$ is the desired one.

$\zeta_2 \geq 0$ **and** $\zeta_3 < 0$

We have

$$\begin{aligned}
&(\sigma_S^2 + \sigma_{N_1}^2 - D_1)\left(\sigma_S^2 + \sigma_{N_2}^2 - \left(\frac{\sigma_{N_2}^4}{\sigma_{N_1}^4} D_1 + \frac{(D_S - \sigma_Z^2)\sigma_{N_2}^4}{\sigma_Z^4}\right)\right) \\
&\geq (\sigma_S^2 + \sigma_{N_1}^2 - D_1)(\sigma_S^2 + \sigma_{N_2}^2 - D_2) \qquad (4.B.33) \\
&\geq \left(\sigma_S^2 + \frac{\sigma_{N_2}^2}{2\sigma_{N_1}^2} D_1 + \frac{\sigma_{N_1}^2}{2\sigma_{N_2}^2} D_2 - \frac{(D_S - \sigma_Z^2)\sigma_{N_1}^2\sigma_{N_2}^2}{2\sigma_Z^4}\right)^2 \qquad (4.B.34) \\
&> \left(\sigma_S^2 + \frac{\sigma_{N_2}^2}{\sigma_{N_1}^2} D_1\right)^2, \qquad (4.B.35)
\end{aligned}$$

where (4.B.33) is due to $\zeta_3 < 0$, (4.B.34) is due to $\det(\mathbf{K_X} - \boldsymbol{\Delta}^*) \geq 0$, and (4.B.35) is due to $\zeta_1 \geq 0$ and $\zeta_3 < 0$. In view of (4.B.18),

$$\begin{aligned}
&(\sigma_S^2 + \sigma_{N_1}^2 - D_1)\left(\sigma_S^2 + \sigma_{N_2}^2 - \left(\frac{\sigma_{N_2}^4}{\sigma_{N_1}^4} D_1 + \frac{(D_S - \sigma_Z^2)\sigma_{N_2}^4}{\sigma_Z^4}\right)\right) > \left(\sigma_S^2 + \frac{\sigma_{N_2}^2}{\sigma_{N_1}^2} D_1\right)^2 \\
&\Longleftrightarrow (\sigma_S^2 + \sigma_{N_1}^2 - D_1)(\sigma_S^2 - D_S) > \sigma_S^4.
\end{aligned}$$

So the condition of Case 5) is met.

$\zeta_2 < 0$ **and** $\zeta_3 \geq 0$

This is symmetric to $\zeta_2 \geq 0$ and $\zeta_3 < 0$, thus is covered by Case 6).

4.C Appendix: Proof of (4.4.3)

4.C.1 $\mathbf{K_W} \in \Omega(\mathbf{K_X})$ and $\mathbf{0} \prec \boldsymbol{\Delta}^* \preceq \mathbf{K_X}$ for Case 6)

Note that we have the following equalities:

1. $\left(\frac{\sigma_{N_2}^4}{\sigma_{N_1}^4}D_1 - \frac{\sigma_{N_2}^4}{\sigma_Z^2}\sqrt{1+\frac{4D_SD_1}{\sigma_{N_1}^4}} + \frac{\sigma_{N_2}^4}{\sigma_Z^4}D_S\right)D_1 = \left(\frac{\sigma_{N_1}^2\sigma_{N_2}^2}{2\sigma_Z^2}\sqrt{\left(\sqrt{1+\frac{4D_SD_1}{\sigma_{N_1}^4}} - \frac{2\sigma_Z^2D_1}{\sigma_{N_1}^4}\right)^2 - 1}\right)^2$

2. $\det(\mathbf{K}_\Delta^*) = \frac{\sigma_{N_1}^4\sigma_{N_2}^4}{2\sigma_Z^4}\left(\sqrt{1+\frac{4D_SD_1}{\sigma_{N_1}^4}} - \frac{2\sigma_Z^2D_1}{\sigma_{N_1}^4} - 1\right)$

3. Let $\theta = \frac{\sqrt{1+\frac{4D_SD_1}{\sigma_{N_1}^4} - \frac{2\sigma_Z^2D_1}{\sigma_{N_1}^4} - 1}}{\sqrt{\left(\sqrt{1+\frac{4D_SD_1}{\sigma_{N_1}^4}} - \frac{2\sigma_Z^2D_1}{\sigma_{N_1}^4}\right)^2 - 1}}$, then we have

   (a) $1-\theta^2 \geq 0$:

   (b) $\det(\mathbf{K}_\Delta^*) = (1-\theta^2)\left(\frac{\sigma_{N_2}^4}{\sigma_{N_1}^4}D_1 - \frac{\sigma_{N_2}^4}{\sigma_Z^2}\sqrt{1+\frac{4D_SD_1}{\sigma_{N_1}^4}} + \frac{\sigma_{N_2}^4}{\sigma_Z^4}D_S\right)D_1$.

   (c) $\frac{\theta\sqrt{\left(\frac{\sigma_{N_2}^4}{\sigma_{N_1}^4}D_1 - \frac{\sigma_{N_2}^4}{\sigma_Z^2}\sqrt{1+\frac{4D_SD_1}{\sigma_{N_1}^4}} + \frac{\sigma_{N_2}^4}{\sigma_Z^4}D_S\right)D_1}}{(1-\theta^2)\left(\frac{\sigma_{N_2}^4}{\sigma_{N_1}^4}D_1 - \frac{\sigma_{N_2}^4}{\sigma_Z^2}\sqrt{1+\frac{4D_SD_1}{\sigma_{N_1}^4}} + \frac{\sigma_{N_2}^4}{\sigma_Z^4}D_S\right)D_1} = \frac{\sigma_Z^2}{\sigma_{N_1}^2\sigma_{N_2}^2}$

Now we'd like to show that $\mathbf{K}_W^{-1} \succeq 0$, which implies that $\mathbf{K}_W \succeq 0$. The ω_1 and ω_2 can be rewritten as

$$\omega_1 = \frac{(1-\theta^2)\frac{\sigma_{N_1}^2\sigma_{N_2}^2}{2\sigma_Z^2}\sqrt{\left(\sqrt{1+\frac{4D_SD_1}{\sigma_{N_1}^4}} - \frac{2\sigma_Z^2D_1}{\sigma_{N_1}^4}\right)^2 - 1} - \frac{\sigma_{N_1}^2\sigma_{N_2}^2}{2\sigma_Z^2}\frac{\sqrt{1+\frac{4D_SD_1}{\sigma_{N_1}^4}}-1}{\sqrt{1+\frac{4D_SD_1}{\sigma_{N_1}^4}}}}{(1-\theta^2)\frac{\sigma_{N_1}^2\sigma_{N_2}^2}{2\sigma_Z^2}\frac{\sqrt{1+\frac{4D_SD_1}{\sigma_{N_1}^4}}-1}{\sqrt{1+\frac{4D_SD_1}{\sigma_{N_1}^4}}}D_1} \tag{4.C.1}$$

and

$$\omega_2 = \frac{(1-\theta^2)\frac{\sigma_{N_1}^2\sigma_{N_2}^2}{2\sigma_Z^2}\sqrt{\left(\sqrt{1+\frac{4D_SD_1}{\sigma_{N_1}^4}} - \frac{2\sigma_Z^2D_1}{\sigma_{N_1}^4}\right)^2 - 1} - \frac{\sigma_{N_1}^2\sigma_{N_2}^2}{2\sigma_Z^2}\frac{\sqrt{1+\frac{4D_SD_1}{\sigma_{N_1}^4}}-1}{\sqrt{1+\frac{4D_SD_1}{\sigma_{N_1}^4}}}}{(1-\theta^2)\frac{\sigma_{N_1}^2\sigma_{N_2}^2}{2\sigma_Z^2}\frac{\sqrt{1+\frac{4D_SD_1}{\sigma_{N_1}^4}}-1}{\sqrt{1+\frac{4D_SD_1}{\sigma_{N_1}^4}}}\left(\frac{\sigma_{N_2}^4}{\sigma_{N_1}^4}D_1 - \frac{\sigma_{N_2}^4}{\sigma_Z^2}\sqrt{1+\frac{4D_SD_1}{\sigma_{N_1}^4}} + \frac{\sigma_{N_2}^4}{\sigma_Z^4}D_S\right)}. \tag{4.C.2}$$

According to (4.4.13), we have

$$\left(\sqrt{1+\frac{4D_SD_1}{\sigma_{N_1}^4}}-\frac{2\sigma_Z^2D_1}{\sigma_{N_1}^4}\right)^2-1-\left(\left(\sqrt{1+\frac{4D_SD_1}{\sigma_{N_1}^4}}-\frac{2\sigma_Z^2D_1}{\sigma_{N_1}^4}-1\right)+\left(\frac{\sqrt{1+\frac{4D_SD_1}{\sigma_{N_1}^4}}-1}{\sqrt{1+\frac{4D_SD_1}{\sigma_{N_1}^4}}}\right)\right)^2 \tag{4.C.3}$$

$$=\left(\sqrt{1+\frac{4D_SD_1}{\sigma_{N_1}^4}}-\frac{2\sigma_Z^2D_1}{\sigma_{N_1}^4}\right)^2-1-\left(\sqrt{1+\frac{4D_SD_1}{\sigma_{N_1}^4}}-\frac{2\sigma_Z^2D_1}{\sigma_{N_1}^4}-\frac{1}{\sqrt{1+\frac{4D_SD_1}{\sigma_{N_1}^4}}}\right)^2 \tag{4.C.4}$$

$$=2\left(\sqrt{1+\frac{4D_SD_1}{\sigma_{N_1}^4}}-\frac{2\sigma_Z^2D_1}{\sigma_{N_1}^4}\right)\frac{1}{\sqrt{1+\frac{4D_SD_1}{\sigma_{N_1}^4}}}-\left(1+\frac{1}{1+\frac{4D_SD_1}{\sigma_{N_1}^4}}\right) \tag{4.C.5}$$

$$=\frac{\frac{4D_SD_1}{\sigma_{N_1}^4}-\frac{4\sigma_Z^2D_1}{\sigma_{N_1}^4}\sqrt{1+\frac{4D_SD_1}{\sigma_{N_1}^4}}}{1+\frac{4D_SD_1}{\sigma_{N_1}^4}}=\frac{\frac{4D_1}{\sigma_{N_1}^4}\left(D_S-\sigma_Z^2\sqrt{1+\frac{4D_SD_1}{\sigma_{N_1}^4}}\right)}{1+\frac{4D_SD_1}{\sigma_{N_1}^4}}>0, \tag{4.C.6}$$

which implies that

$$\sqrt{\left(\sqrt{1+\frac{4D_SD_1}{\sigma_{N_1}^4}}-\frac{2\sigma_Z^2D_1}{\sigma_{N_1}^4}\right)^2-1}>\left(\sqrt{1+\frac{4D_SD_1}{\sigma_{N_1}^4}}-\frac{2\sigma_Z^2D_1}{\sigma_{N_1}^4}-1\right)+\left(\frac{\sqrt{1+\frac{4D_SD_1}{\sigma_{N_1}^4}}-1}{\sqrt{1+\frac{4D_SD_1}{\sigma_{N_1}^4}}}\right). \tag{4.C.7}$$

Since $\sqrt{1+\frac{4D_SD_1}{\sigma_{N_1}^4}}-\frac{2\sigma_Z^2D_1}{\sigma_{N_1}^4}-1=\theta\sqrt{\left(\sqrt{1+\frac{4D_SD_1}{\sigma_{N_1}^4}}-\frac{2\sigma_Z^2D_1}{\sigma_{N_1}^4}\right)^2-1}$, we have

$$(1-\theta)\sqrt{\left(\sqrt{1+\frac{4D_SD_1}{\sigma_{N_1}^4}}-\frac{2\sigma_Z^2D_1}{\sigma_{N_1}^4}\right)^2-1}>\frac{\sqrt{1+\frac{4D_SD_1}{\sigma_{N_1}^4}}-1}{\sqrt{1+\frac{4D_SD_1}{\sigma_{N_1}^4}}}, \tag{4.C.8}$$

resulting in

$$(1-\theta^2)\sqrt{\left(\sqrt{1+\frac{4D_SD_1}{\sigma_{N_1}^4}}-\frac{2\sigma_Z^2D_1}{\sigma_{N_1}^4}\right)^2-1} > (1+\theta)\frac{\sqrt{1+\frac{4D_SD_1}{\sigma_{N_1}^4}}-1}{\sqrt{1+\frac{4D_SD_1}{\sigma_{N_1}^4}}}. \tag{4.C.9}$$

Thus, we know that

$$(1-\theta^2)\sqrt{\left(\sqrt{1+\frac{4D_SD_1}{\sigma_{N_1}^4}}-\frac{2\sigma_Z^2D_1}{\sigma_{N_1}^4}\right)^2-1} - \frac{\sqrt{1+\frac{4D_SD_1}{\sigma_{N_1}^4}}-1}{\sqrt{1+\frac{4D_SD_1}{\sigma_{N_1}^4}}} > 0, \tag{4.C.10}$$

which implies that $\omega_1 > 0$ and $\omega_2 > 0$. Moreover, according to (3c), we know that

$$\det(\mathbf{K}_W^{-1}) = \omega_1\omega_2 - \left(\frac{\sigma_Z^2}{\sigma_{N_1}^2\sigma_{N_2}^2}\right)^2 \tag{4.C.11}$$

$$= \left(\frac{(1-\theta^2)\frac{\sigma_{N_1}^2\sigma_{N_2}^2}{2\sigma_Z^2}\sqrt{\left(\sqrt{1+\frac{4D_SD_1}{\sigma_{N_1}^4}}-\frac{2\sigma_Z^2D_1}{\sigma_{N_1}^4}\right)^2-1} - \frac{\sigma_{N_1}^2\sigma_{N_2}^2}{2\sigma_Z^2}\frac{\sqrt{1+\frac{4D_SD_1}{\sigma_{N_1}^4}}-1}{\sqrt{1+\frac{4D_SD_1}{\sigma_{N_1}^4}}}}{(1-\theta^2)\frac{\sigma_{N_1}^2\sigma_{N_2}^2}{2\sigma_Z^2}\frac{\sqrt{1+\frac{4D_SD_1}{\sigma_{N_1}^4}}-1}{\sqrt{1+\frac{4D_SD_1}{\sigma_{N_1}^4}}}D_1}\right) \tag{4.C.12}$$

$$\times\left(\frac{(1-\theta^2)\frac{\sigma_{N_1}^2\sigma_{N_2}^2}{2\sigma_Z^2}\sqrt{\left(\sqrt{1+\frac{4D_SD_1}{\sigma_{N_1}^4}}-\frac{2\sigma_Z^2D_1}{\sigma_{N_1}^4}\right)^2-1} - \frac{\sigma_{N_1}^2\sigma_{N_2}^2}{2\sigma_Z^2}\frac{\sqrt{1+\frac{4D_SD_1}{\sigma_{N_1}^4}}-1}{\sqrt{1+\frac{4D_SD_1}{\sigma_{N_1}^4}}}}{(1-\theta^2)\frac{\sigma_{N_1}^2\sigma_{N_2}^2}{2\sigma_Z^2}\frac{\sqrt{1+\frac{4D_SD_1}{\sigma_{N_1}^4}}-1}{\sqrt{1+\frac{4D_SD_1}{\sigma_{N_1}^4}}}\left(\frac{\sigma_{N_2}^4}{\sigma_{N_1}^4}D_1-\frac{\sigma_{N_2}^4}{\sigma_Z^2}\sqrt{1+\frac{4D_SD_1}{\sigma_{N_1}^4}}+\frac{\sigma_{N_2}^4}{\sigma_Z^4}D_S\right)}\right) \tag{4.C.13}$$

$$-\left(\frac{\theta\sqrt{\left(\frac{\sigma_{N_2}^4}{\sigma_{N_1}^4}D_1-\frac{\sigma_{N_2}^4}{\sigma_Z^2}\sqrt{1+\frac{4D_SD_1}{\sigma_{N_1}^4}}+\frac{\sigma_{N_2}^4}{\sigma_Z^4}D_S\right)D_1}}{(1-\theta^2)\left(\frac{\sigma_{N_2}^4}{\sigma_{N_1}^4}D_1-\frac{\sigma_{N_2}^4}{\sigma_Z^2}\sqrt{1+\frac{4D_SD_1}{\sigma_{N_1}^4}}+\frac{\sigma_{N_2}^4}{\sigma_Z^4}D_S\right)D_1}\right)^2 \tag{4.C.14}$$

$$=\frac{\left((1-\theta^2)\sqrt{\left(\sqrt{1+\frac{4D_SD_1}{\sigma_{N_1}^4}}-\frac{2\sigma_Z^2D_1}{\sigma_{N_1}^4}\right)^2-1}-\frac{\sqrt{1+\frac{4D_SD_1}{\sigma_{N_1}^4}}-1}{\sqrt{1+\frac{4D_SD_1}{\sigma_{N_1}^4}}}\right)^2-\left(\theta\frac{\sqrt{1+\frac{4D_SD_1}{\sigma_{N_1}^4}}-1}{\sqrt{1+\frac{4D_SD_1}{\sigma_{N_1}^4}}}\right)^2}{\left((1-\theta^2)\frac{\sqrt{1+\frac{4D_SD_1}{\sigma_{N_1}^4}}-1}{\sqrt{1+\frac{4D_SD_1}{\sigma_{N_1}^4}}}\right)^2\left(\frac{\sigma_{N_2}^4}{\sigma_{N_1}^4}D_1-\frac{\sigma_{N_2}^4}{\sigma_Z^2}\sqrt{1+\frac{4D_SD_1}{\sigma_{N_1}^4}}+\frac{\sigma_{N_2}^4}{\sigma_Z^4}D_S\right)D_1}>0, \tag{4.C.15}$$

where the inequality holds according to (4.C.9).

It can be verified that (4.4.4)–(4.4.12) are satisfied. Since $D_S<\sigma_S^2-\frac{\sigma_S^4(\sigma_S^2+\sigma_{N_1}^2-D_1)}{(\sigma_S^2+\sigma_{N_1}^2)^2}$, we also have

$$\left(\left(\frac{\sigma_{N_1}^4}{2}+\sigma_S^2\sigma_{N_1}^2\right)\sqrt{1+\frac{4D_SD_1}{\sigma_{N_1}^4}}\right)^2-\left(\sigma_S^2D_1+\frac{\sigma_{N_1}^4}{2}+(\sigma_S^2+\sigma_{N_1}^2)D_S\right)^2 \tag{4.C.16}$$

$$=\sigma_S^2\sigma_{N_1}^4\left(\sigma_S^2+\sigma_{N_1}^2\right)+\left(2\sigma_S^2(\sigma_S^2+\sigma_{N_1}^2)+\sigma_{N_1}^4\right)D_1D_S-\sigma_{N_1}^4\left(\sigma_S^2+\sigma_{N_1}^2\right)D_S \tag{4.C.17}$$

$$-\sigma_S^4D_1^2-(\sigma_S^2+\sigma_{N_1}^2)^2D_S^2-\sigma_S^2\sigma_{N_1}^4D_1 \tag{4.C.18}$$

$$=\sigma_S^2\sigma_{N_1}^4\left(\sigma_S^2+\sigma_{N_1}^2-D_1\right)-\left(\sigma_S^2+\sigma_{N_1}^2-D_1\right)\sigma_{N_1}^4D_S \tag{4.C.19}$$

$$+2\sigma_S^2(\sigma_S^2+\sigma_{N_1}^2)D_1D_S-\sigma_S^4D_1^2-(\sigma_S^2+\sigma_{N_1}^2)^2D_S^2 \tag{4.C.20}$$

$$=\sigma_{N_1}^4\left(\sigma_S^2+\sigma_{N_1}^2-D_1\right)\left(\sigma_S^2-D_S\right)-\left((\sigma_S^2+\sigma_{N_1}^2)D_S-\sigma_S^2D_1\right)^2 \tag{4.C.21}$$

- if $(\sigma_S^2 + \sigma_{N_1}^2)D_S \geq \sigma_S^2 D_1$, we have

$$\sigma_{N_1}^4 \left(\sigma_S^2 + \sigma_{N_1}^2 - D_1\right)\left(\sigma_S^2 - D_S\right) - \left((\sigma_S^2 + \sigma_{N_1}^2)D_S - \sigma_S^2 D_1\right)^2 \tag{4.C.22}$$

$$\geq \left(\frac{\sigma_S^2\sigma_{N_1}^2}{\sigma_S^2 + \sigma_{N_1}^2}\left(\sigma_S^2 + \sigma_{N_1}^2 - D_1\right)\right)^2 - \left((\sigma_S^2 + \sigma_{N_1}^2)D_S - \sigma_S^2 D_1\right)^2 \tag{4.C.23}$$

$$\geq \left(\frac{\sigma_S^2\sigma_{N_1}^2}{\sigma_S^2 + \sigma_{N_1}^2}\left(\sigma_S^2 + \sigma_{N_1}^2 - D_1\right)\right)^2 \tag{4.C.24}$$

$$- \left((\sigma_S^2 + \sigma_{N_1}^2)\left(\sigma_S^2 - \frac{\sigma_S^4(\sigma_S^2 + \sigma_{N_1}^2 - D_1)}{(\sigma_S^2 + \sigma_{N_1}^2)^2}\right) - \sigma_S^2 D_1\right)^2 \tag{4.C.25}$$

$$= \left(\frac{\sigma_S^2\sigma_{N_1}^2}{\sigma_S^2 + \sigma_{N_1}^2}\left(\sigma_S^2 + \sigma_{N_1}^2 - D_1\right)\right)^2 - \left(\frac{\sigma_S^2\sigma_{N_1}^2}{\sigma_S^2 + \sigma_{N_1}^2}\left(\sigma_S^2 + \sigma_{N_1}^2 - D_1\right)\right)^2 \tag{4.C.26}$$

$$= 0. \tag{4.C.27}$$

- if $(\sigma_S^2 + \sigma_{N_1}^2)D_S < \sigma_S^2 D_1$, we also have

$$\sigma_{N_1}^4 \left(\sigma_S^2 + \sigma_{N_1}^2 - D_1\right)\left(\sigma_S^2 - D_S\right) - \left(\sigma_S^2 D_1 - (\sigma_S^2 + \sigma_{N_1}^2)D_S\right)^2 \tag{4.C.28}$$

$$= \left(\sigma_S^2 + \sigma_{N_1}^2\right)^2 \left(\frac{\sigma_{N_1}^2}{\sigma_S^2 + \sigma_{N_1}^2}\left(\sigma_S^2 + \sigma_{N_1}^2 - D_1\right)\frac{\sigma_{N_1}^2}{\sigma_S^2 + \sigma_{N_1}^2}\left(\sigma_S^2 - D_S\right)\right. \tag{4.C.29}$$

$$\left. - \left(\frac{\sigma_S^2}{\sigma_S^2 + \sigma_{N_1}^2}D_1 - D_S\right)^2\right) \tag{4.C.30}$$

Then, we have

$$
\begin{aligned}
& D_S + \sigma_{N_1}^2 - \frac{(D_S^2 - \sigma_Z^4)\sigma_{N_1}^4}{4D_S\sigma_Z^4} && \text{(4.C.31)}\\
&= \frac{4D_S\sigma_Z^4(D_S + \sigma_{N_1}^2) - (D_S^2 - \sigma_Z^4)\sigma_{N_1}^4}{4D_S\sigma_Z^4} && \text{(4.C.32)}\\
&= \frac{4\sigma_Z^4 D_S^2 + 4\sigma_Z^4\sigma_{N_1}^2 D_S + \sigma_Z^4\sigma_{N_1}^4 - D_S^2\sigma_{N_1}^4}{4D_S\sigma_Z^4}\sigma_{N_1}^4 && \text{(4.C.33)}\\
&= \frac{\left(2\sigma_Z^2 D_S + \sigma_Z^2\sigma_{N_1}^2\right)^2 - D_S^2\sigma_{N_1}^4}{4D_S\sigma_Z^4}. && \text{(4.C.34)}
\end{aligned}
$$

Since $\sigma_{N_2}^2 \geq \sigma_{N_1}^2$ and $\sigma_S^2 \geq D_S$, we also have

$$
\begin{aligned}
& 2\sigma_Z^2 D_S + \sigma_Z^2\sigma_{N_1}^2 - D_S\sigma_{N_1}^2 && \text{(4.C.35)}\\
&= \frac{2\sigma_S^2\sigma_{N_1}^2\sigma_{N_2}^2 D_S + \sigma_S^2\sigma_{N_1}^4\sigma_{N_2}^2 - \sigma_{N_1}^2((\sigma_S^2 + \sigma_{N_2}^2)\sigma_{N_1}^2 + \sigma_S^2\sigma_{N_2}^2)D_S}{(\sigma_S^2 + \sigma_{N_1}^2)\sigma_{N_2}^2 + \sigma_S^2\sigma_{N_1}^2} && \text{(4.C.36)}\\
&= \frac{\sigma_{N_1}^2}{(\sigma_S^2 + \sigma_{N_1}^2)\sigma_{N_2}^2 + \sigma_S^2\sigma_{N_1}^2}\left(\sigma_S^2\sigma_{N_2}^2 D_S - (\sigma_S^2 + \sigma_{N_2}^2)\sigma_{N_1}^2 D_S + \sigma_S^2\sigma_{N_1}^2\sigma_{N_2}^2\right) && \text{(4.C.37)}\\
&= \frac{\sigma_{N_1}^2}{(\sigma_S^2 + \sigma_{N_1}^2)\sigma_{N_2}^2 + \sigma_S^2\sigma_{N_1}^2}\left(\sigma_S^2(\sigma_{N_2}^2 - \sigma_{N_1}^2)D_S + (\sigma_S^2 - D_S)\sigma_{N_1}^2\sigma_{N_2}^2\right) \geq 0, && \text{(4.C.38)}
\end{aligned}
$$

resulting in $D_1 < D_S + \sigma_{N_1}^2$.

Then, we know that

$$
\begin{aligned}
& \frac{\sigma_{N_1}^2}{\sigma_S^2 + \sigma_{N_1}^2}\left(\sigma_S^2 + \sigma_{N_1}^2 - D_1\right) - \left(\frac{\sigma_S^2}{\sigma_S^2 + \sigma_{N_1}^2}D_1 - D_S\right) && \text{(4.C.39)}\\
&= \sigma_{N_1}^2 + D_S - D_1 > 0 && \text{(4.C.40)}
\end{aligned}
$$

and

$$\frac{\sigma_{N_1}^2}{\sigma_S^2+\sigma_{N_1}^2}\left(\sigma_S^2-D_S\right)-\left(\frac{\sigma_S^2}{\sigma_S^2+\sigma_{N_1}^2}D_1-D_S\right) \tag{4.C.41}$$

$$=\frac{\sigma_S^2}{\sigma_S^2+\sigma_{N_1}^2}\left(\sigma_{N_1}^2+D_S-D_1\right)>0 \tag{4.C.42}$$

Thus, we always have $\sigma_{N_1}^4\left(\sigma_S^2+\sigma_{N_1}^2-D_1\right)(\sigma_S^2-D_S)-\left((\sigma_S^2+\sigma_{N_1}^2)D_S-\sigma_S^2D_1\right)^2>0$. Then, we know that

$$\det(\mathbf{K_X}-\mathbf{K}_\Delta^*) \tag{4.C.43}$$

$$=\left(\sigma_S^2+\sigma_{N_1}^2-D_1\right)\left(\sigma_S^2+\sigma_{N_2}^2-\left(\frac{\sigma_{N_2}^4}{\sigma_{N_1}^4}D_1-\frac{\sigma_{N_2}^4}{\sigma_Z^2}\sqrt{1+\frac{4D_SD_1}{\sigma_{N_1}^4}}+\frac{\sigma_{N_2}^4}{\sigma_Z^4}D_S\right)\right) \tag{4.C.44}$$

$$-\left(\sigma_S^2-\frac{\sigma_{N_1}^2\sigma_{N_2}^2}{2\sigma_Z^2}\left(\sqrt{1+\frac{4D_SD_1}{\sigma_{N_1}^4}}-\frac{2\sigma_Z^2D_1}{\sigma_{N_1}^4}-1\right)\right)^2 \tag{4.C.45}$$

$$=\left((\sigma_S^2+\sigma_{N_1}^2)\sigma_{N_2}^2+\sigma_S^2\sigma_{N_1}^2\right)+\left(\frac{\sigma_{N_1}^4\sigma_{N_2}^4}{2\sigma_Z^4}+\frac{\sigma_{N_2}^2\left((\sigma_S^2+\sigma_{N_1}^2)\sigma_{N_2}^2+\sigma_S^2\sigma_{N_1}^2\right)}{\sigma_Z^2}\right)\sqrt{1+\frac{4D_SD_1}{\sigma_{N_1}^4}} \tag{4.C.46}$$

$$-\left(\left(\frac{\sigma_{N_1}^4\sigma_{N_2}^4}{2\sigma_Z^2}+\frac{\sigma_S^2\sigma_{N_1}^2\sigma_{N_2}^2}{\sigma_Z^2}\right)\frac{2\sigma_Z^2}{\sigma_{N_1}^4}+\sigma_S^2+\sigma_{N_2}^2+(\sigma_S^2+\sigma_{N_1}^2)\frac{\sigma_{N_2}^4}{\sigma_{N_1}^4}\right)D_1-\left(\frac{\sigma_{N_1}^4\sigma_{N_2}^4}{2\sigma_Z^4}+\frac{\sigma_S^2\sigma_{N_1}^2\sigma_{N_2}^2}{\sigma_Z^2}\right) \tag{4.C.47}$$

$$-(\sigma_S^2+\sigma_{N_1}^2)\frac{\sigma_{N_2}^4}{\sigma_Z^4}D_S \tag{4.C.48}$$

$$=\left(\frac{\left((\sigma_S^2+\sigma_{N_1}^2)\sigma_{N_2}^2+\sigma_S^2\sigma_{N_1}^2\right)^2}{2\sigma_S^4}+\frac{\left((\sigma_S^2+\sigma_{N_1}^2)\sigma_{N_2}^2+\sigma_S^2\sigma_{N_1}^2\right)^2}{\sigma_S^2\sigma_{N_1}^2}\right)\sqrt{1+\frac{4D_SD_1}{\sigma_{N_1}^4}} \tag{4.C.49}$$

$$
-\frac{\left((\sigma_S^2+\sigma_{N_1}^2)\sigma_{N_2}^2+\sigma_S^2\sigma_{N_1}^2\right)^2}{\sigma_S^2\sigma_{N_1}^4}D_1-\frac{\left((\sigma_S^2+\sigma_{N_1}^2)\sigma_{N_2}^2+\sigma_S^2\sigma_{N_1}^2\right)^2}{2\sigma_S^4}-(\sigma_S^2+\sigma_{N_1}^2)\frac{\sigma_{N_2}^4}{\sigma_Z^4}D_S \tag{4.C.50}
$$

$$
=\frac{\left((\sigma_S^2+\sigma_{N_1}^2)\sigma_{N_2}^2+\sigma_S^2\sigma_{N_1}^2\right)^2}{\sigma_S^4\sigma_{N_1}^4}\left(\left(\frac{\sigma_{N_1}^4}{2}+\sigma_S^2\sigma_{N_1}^2\right)\sqrt{1+\frac{4D_SD_1}{\sigma_{N_1}^4}}\right. \tag{4.C.51}
$$

$$
\left.-\left(\sigma_S^2D_1+\frac{\sigma_{N_1}^4}{2}+(\sigma_S^2+\sigma_{N_1}^2)D_S\right)\right)\geq 0. \tag{4.C.52}
$$

Thus, (4.4.3) holds because $\mathbf{K}_\Delta^* \succ \mathbf{0}$, and

$$
\mathbf{K_X}-\mathbf{K}_\Delta^* \tag{4.C.53}
$$

$$
=\begin{bmatrix} \sigma_S^2+\sigma_{N_1}^2-D_1 & \sigma_S^2-\frac{\sigma_{N_1}^2\sigma_{N_2}^2}{2\sigma_Z^2}\left(\sqrt{1+\frac{4D_SD_1}{\sigma_{N_1}^4}}-\frac{2\sigma_Z^2D_1}{\sigma_{N_1}^4}-1\right) \\ \sigma_S^2-\frac{\sigma_{N_1}^2\sigma_{N_2}^2}{2\sigma_Z^2}\left(\sqrt{1+\frac{4D_SD_1}{\sigma_{N_1}^4}}-\frac{2\sigma_Z^2D_1}{\sigma_{N_1}^4}-1\right) & \sigma_S^2+\sigma_{N_2}^2-\left(\frac{\sigma_{N_2}^4}{\sigma_{N_1}^4}D_1-\frac{\sigma_{N_2}^4}{\sigma_Z^2}\sqrt{1+\frac{4D_SD_1}{\sigma_{N_1}^4}}+\frac{\sigma_{N_2}^4}{\sigma_Z^4}D_S\right) \end{bmatrix} \tag{4.C.54}
$$

$$
\succeq \mathbf{0} \tag{4.C.55}
$$

Therefore, $\mathbf{K}_\Delta^*$ is indeed an optimal solution and consequently

$$
R_d(D_1,D_2,D_S)=\frac{1}{2}\log\frac{2\sigma_S^2\sigma_Z^2\sigma_{N_1}^2}{\sigma_{N_1}^2\sigma_{N_2}^2\sqrt{\sigma_{N_1}^4+4D_1D_S}-2\sigma_Z^2\sigma_{N_2}^2D_1-\sigma_{N_1}^4\sigma_{N_2}^2}.
$$

4.C.2 $\mathbf{0} \prec \boldsymbol{\Delta}^* \preceq \mathbf{K_X}$ for Case 7)

For Case 7), we'd like to show that, we always have $D_2 < \frac{(D_S^2-\sigma_Z^4)\sigma_{N_2}^4}{4D_S\sigma_Z^4}$, and $D_2 < D_S+\sigma_{N_2}^2$, thus the similar result from Case 6) can be applied.

For i), since $(\frac{1}{\sigma_S^2} + \frac{1}{\sigma_{N_1}^2} - \frac{1}{\sigma_{N_2}^2})^{-1} \leq D_S$, we know that

$$D_S \geq \frac{\sigma_S^2 \sigma_{N_1}^2 \sigma_{N_2}^2}{\sigma_{N_2}^2(\sigma_S^2 + \sigma_{N_1}^2) - \sigma_S^2 \sigma_{N_1}^2} \tag{4.C.56}$$

$$= \frac{\sigma_S^2 \sigma_{N_1}^2 \sigma_{N_2}^2}{\sigma_{N_2}^2(\sigma_S^2 + \sigma_{N_1}^2) + \sigma_S^2 \sigma_{N_1}^2 - 2\sigma_S^2 \sigma_{N_1}^2} \tag{4.C.57}$$

$$= \frac{\sigma_Z^2 \sigma_{N_2}^2}{\sigma_{N_2}^2 - 2\sigma_Z^2}, \tag{4.C.58}$$

resulting in $\sigma_{N_2}^2 \leq \frac{(\sigma_{N_2}^2 - 2\sigma_Z^2)D_S}{\sigma_Z^2}$. Then, we have

$$D_2 < D_S + \sigma_{N_2}^2 \tag{4.C.59}$$

$$\leq D_S + \frac{(\sigma_{N_2}^2 - 2\sigma_Z^2)D_S}{\sigma_Z^2} \tag{4.C.60}$$

$$= \frac{(\sigma_{N_2}^2 - \sigma_Z^2)D_S}{\sigma_Z^2} \tag{4.C.61}$$

Moreover, we also have

$$D_S \sigma_{N_2}^2 - 2\sigma_Z^2 D_S - \sigma_Z^2 \sigma_{N_2}^2 \tag{4.C.62}$$

$$= D_S\left(\sigma_{N_2}^2 - 2\sigma_Z^2\right) - \sigma_Z^2 \sigma_{N_2}^2 \tag{4.C.63}$$

$$\geq D_S\left(\sigma_{N_2}^2 - 2\sigma_Z^2\right) - \sigma_Z^2 \frac{(\sigma_{N_2}^2 - 2\sigma_Z^2)D_S}{\sigma_Z^2} = 0, \tag{4.C.64}$$

which implies that

$$\frac{(D_S^2-\sigma_Z^4)\sigma_{N_2}^4}{4D_S\sigma_Z^4}-\frac{(\sigma_{N_2}^2-\sigma_Z^2)D_S}{\sigma_Z^2} \tag{4.C.65}$$

$$=\frac{(D_S^2-\sigma_Z^4)\sigma_{N_2}^4-4D_S^2\sigma_Z^2(\sigma_{N_2}^2-\sigma_Z^2)}{4D_S\sigma_Z^4} \tag{4.C.66}$$

$$=\frac{D_S^2(\sigma_{N_2}^4-4\sigma_{N_2}^2\sigma_Z^2+4\sigma_Z^4)-\sigma_Z^4\sigma_{N_2}^4}{4D_S\sigma_Z^4} \tag{4.C.67}$$

$$=\frac{D_S^2(\sigma_{N_2}^2-2\sigma_Z^2)^2-\sigma_Z^4\sigma_{N_2}^4}{4D_S\sigma_Z^4}\geq 0. \tag{4.C.68}$$

Thus, we always have $D_2<\frac{(D_S^2-\sigma_Z^4)\sigma_{N_2}^4}{4D_S\sigma_Z^4}$.

For ii), since $D_S<(\frac{1}{\sigma_S^2}+\frac{1}{\sigma_{N_1}^2}-\frac{1}{\sigma_{N_2}^2})^{-1}$, we have

$$D_S+\sigma_{N_2}^2-\frac{(D_S^2-\sigma_Z^4)\sigma_{N_2}^4}{4D_S\sigma_Z^4} \tag{4.C.69}$$

$$=\frac{(D_S+\sigma_{N_2}^2)4D_S\sigma_Z^4-(D_S^2-\sigma_Z^4)\sigma_{N_2}^4}{4D_S\sigma_Z^4} \tag{4.C.70}$$

$$=\frac{4\sigma_Z^4D_S^2+4\sigma_Z^4\sigma_{N_2}^2D_S+\sigma_Z^4\sigma_{N_2}^4-D_S^2\sigma_{N_2}^4}{4D_S\sigma_Z^4} \tag{4.C.71}$$

$$=\frac{\left(2\sigma_Z^2D_S+\sigma_Z^2\sigma_{N_2}^2\right)^2-D_S^2\sigma_{N_2}^4}{4D_S\sigma_Z^4} \tag{4.C.72}$$

and

$$
\begin{aligned}
&2\sigma_Z^2 D_S + \sigma_Z^2\sigma_{N_2}^2 - D_S\sigma_{N_2}^2 && (4.C.73)\\
&= \frac{2\sigma_S^2\sigma_{N_1}^2\sigma_{N_2}^2 D_S - ((\sigma_S^2+\sigma_{N_1}^2)\sigma_{N_2}^2 + \sigma_S^2\sigma_{N_1}^2)\sigma_{N_2}^2 D_S + \sigma_S^2\sigma_{N_1}^2\sigma_{N_2}^4}{(\sigma_S^2+\sigma_{N_2}^2)\sigma_{N_1}^2 + \sigma_S^2\sigma_{N_2}^2} && (4.C.74)\\
&= \frac{\sigma_S^2\sigma_{N_1}^2\sigma_{N_2}^2 D_S - (\sigma_S^2+\sigma_{N_1}^2)\sigma_{N_2}^4 D_S + \sigma_S^2\sigma_{N_1}^2\sigma_{N_2}^4}{(\sigma_S^2+\sigma_{N_2}^2)\sigma_{N_1}^2 + \sigma_S^2\sigma_{N_2}^2} && (4.C.75)\\
&= \frac{\sigma_{N_2}^2}{(\sigma_S^2+\sigma_{N_2}^2)\sigma_{N_1}^2 + \sigma_S^2\sigma_{N_2}^2}\left(\sigma_S^2\sigma_{N_1}^2\sigma_{N_2}^2 - \left((\sigma_S^2+\sigma_{N_1}^2)\sigma_{N_2}^2 - \sigma_S^2\sigma_{N_1}^2\right)\right) D_S && (4.C.76)\\
&\geq \frac{\sigma_{N_2}^2\left(\sigma_S^2\sigma_{N_1}^2\sigma_{N_2}^2 - \left((\sigma_S^2+\sigma_{N_1}^2)\sigma_{N_2}^2 - \sigma_S^2\sigma_{N_1}^2\right)\left(\frac{1}{\sigma_S^2}+\frac{1}{\sigma_{N_1}^2}-\frac{1}{\sigma_{N_2}^2}\right)^{-1}\right)}{(\sigma_S^2+\sigma_{N_2}^2)\sigma_{N_1}^2 + \sigma_S^2\sigma_{N_2}^2} && (4.C.77)\\
&= \frac{\sigma_S^2\sigma_{N_1}^2\sigma_{N_2}^4\left((\sigma_S^2+\sigma_{N_1}^2)\sigma_{N_2}^2 - \sigma_S^2\sigma_{N_1}^2 - (\sigma_S^2+\sigma_{N_1}^2)\sigma_{N_2}^2 + \sigma_S^2\sigma_{N_1}^2\right)}{\left((\sigma_S^2+\sigma_{N_2}^2)\sigma_{N_1}^2 + \sigma_S^2\sigma_{N_2}^2\right)\left((\sigma_S^2+\sigma_{N_1}^2)\sigma_{N_2}^2 - \sigma_S^2\sigma_{N_1}^2\right)} = 0, && (4.C.78)
\end{aligned}
$$

resulting in $D_S + \sigma_{N_2}^2 \geq \frac{(D_S^2-\sigma_Z^4)\sigma_{N_2}^4}{4D_S\sigma_Z^4}$. Thus, we know that $D_2 < D_S + \sigma_{N_2}^2$.

Based on the above, we always have $D_2 < \frac{(D_S^2-\sigma_Z^4)\sigma_{N_2}^4}{4D_S\sigma_Z^4}$ and $D_2 < D_S + \sigma_{N_2}^2$. Thus, similar to (4.C.40) and (4.C.42), we have $\sigma_{N_2}^4\left(\sigma_S^2+\sigma_{N_2}^2-D_2\right)(\sigma_S^2-D_S) - \left((\sigma_S^2+\sigma_{N_2}^2)D_S - \sigma_S^2 D_2\right)^2 > 0$, resulting in $\det(\mathbf{K_X}-\mathbf{K}_\Delta^*) \geq 0$. Thus, (4.4.3) holds because $\mathbf{K}_\Delta^* \succ \mathbf{0}$, and $\mathbf{K_X}-\mathbf{K}_\Delta^* \succeq \mathbf{0}$.

Chapter 5

Conclusions and Future Work

5.1 Conclusions

In this thesis, we first concentrated on constellation design for multiple access wireless communication and multi-hop relay-assisted networks.

For an uplink system with K single-antenna users and one base station equipped with a single antenna, the design of sum constellations belonging to the additively uniquely decomposable constellation group (AUDCG) was proposed by maximizing the minimum Euclidean distance and lattice coding, where each user utilizes a binary constellation to carry data. With such a design, the multi-access SISO channel with K users can be equivalently transformed into a virtual standard ideal SISO channel with a single user. Once the sum constellation point is determined by the detector, each user's constellation point can be directly obtained, resulting in a low latency detection technique. It was shown that our proposed NOMA scheme outperforms the existing TDMA designs for the same system in terms of the minimum distance, and a symbol error probability formula was derived. Moreover, we also developed a splitting scheme that enables us to extend the principles of our design to a system in which the k-th user employs a constellation with 2^{M_k} points. Numerical results showed that the resulting scheme provides better performance than an existing scheme based on Farey sequences.

For a multi-hop relay-assisted network, we developed a novel uniquely-factorable constellation set (UFCS) using PSK constellations to allow the source and relay nodes to transmit their own information concurrently at the symbol level, while enabling non-coherent detection. The system consists of a single-antenna source and single-antenna, amplify-and-forward relay nodes, and the destination has M antennas. The transmission was arranged in blocks of two time slots. By taking advantage of the uniquely-factorable property, fast detection can be obtained, where the optimal ML detector was equivalently reduced to a symbol-by-symbol detector. In addition, the SEP formula was also given, showing the insights that the diversity gain cannot be improved by increasing M.

Since there has been very limited analysis of the source coding subject to semantic information constraints, we also studied the rate distortion trade-offs in the presence of these constraints.

For semantic source coding, the model consists of two parts, i.e., the intrinsic state part and the extrinsic observation part, in which the intrinsic state part corresponds to the semantic feature of the source. This is not observable, and can only be inferred from extrinsic observation part. In order to characterize the rate-distortion behavior of the semantic source, we considered the case of Gaussian distributed extrinsic observation, with the assumption that there is a linear relationship between extrinsic observation part and intrinsic state part. We derived the rate-distortion function (in both centralized encoding and distributed encoding) of semantic-aware source coding under quadratic distortion structure by converting the semantic distortion constraint of the source to a surrogate distortion constraint of the observations.

5.2 Future Work

There are still some future works that can be conducted to further improve the proposed approaches.

Perfect channel state information (CSI) at the receiver, in practice, is not easily attainable. Regarding the CSI in a communication system, the receiver usually estimates the channel using a training sequence (pilot symbols) and the transmitter obtains it through a feedback channel or from previous received signals. For the accuracy of the estimation, the outdated estimation due to the channel variability has to be considered. Moreover, for the usage of the feedback channel, the quantization of the estimation and the errors in the communication through the feedback channel also should be taken into consideration. Thus, it is necessary for us to explore the sensitivity of CSI (like the tolerance of phase error) in our constellation design in Chapter 2, and to find *robust designs* that make it less sensitive to these errors by Bayesian (or stochastic) and maxi-min (or worst case) approaches.

In case that the transmitter does not have any information about the channel, the blind signal processing techniques can be applied to estimate the space-time block coded channel for the MIMO systems. Blind channel estimation involves a problem in which only observed signal is available at the receiver for processing in the identification of a channel. In future, we would like to find the condition that the signal can be uniquely distinguished from the channel in a noise-free case when only received signal is available. Moreover, based on this condition, we would like to construct a full diversity blind linear space-time block code by using the co-prime PSK constellations introduced in our second work.

In our semantic-aware source coding work, there is still space for further investigating the rate distortion for vector sources in both the case of centralized encoding and that of distributed encoding by considering other source distributions (like Laplacian distributions aiming at images and speech) and non-quadratic distortion structures. Moreover, in practice, due to complexity and delay constraints, large block lengths may not be feasible, and many communication systems benefit from designing the source-channel codes jointly. Thus, there is a great need to develop joint source-channel coding system by using machine learning and combining with typical codes, like LDPC codes or polar codes.

Bibliography

[1] 3GPP (2016a). Service requirements for next generation new services and markets.

[2] 3GPP (2016b). Study on scenarios and requirements for next generation access technologies.

[3] Arnstein, D. (1979). Power division in spread spectrum systems with limiting. *IEEE Transactions on Communications*, **27**(3), 574–582.

[4] Bao, J., Basu, P., Dean, M., Partridge, C., Swami, A., Leland, W., and Hendler, J. A. (2011). Towards a theory of semantic communication. In *IEEE Network Science Workshop*, pages 110–117.

[5] Berger, T. (1971). *Rate-distortion theory.* Englewood Cliffs, NJ, USA: Prentice-Hall.

[6] Berger, T. (1978). Multiterminal source coding. In *The Information Theory Approach to Communications (CISM International Centre for Mechanical Sciences)*, pages 171–231.

[7] Berger, T., Zhang, Z., and Viswanathan, H. (1996). The CEO problem [multiterminal source coding]. *IEEE Transactions on Information Theory*, **42**(3), 887–902.

[8] Boyd, S. P. and Vandenberghe, L. (2004). *Convex optimization.* Cambridge University Press.

[9] Carnap, R. and Bar-Hillel, Y. (1952). *An outline of a theory of semantic information.* Research Laboratory of Electronics, Massachusetts Institute of Technology.

[10] Chauhan, A. and Jaiswal, A. (2020). Non-orthogonal multiple access: A constellation domain multiplexing approach. In *IEEE Annual International Symposium on Personal, Indoor and Mobile Radio Communications*, pages 1–6.

[11] Chen, J., Zhang, X., Berger, T., and Wicker, S. B. (2004). An upper bound on the sum-rate distortion function and its corresponding rate allocation schemes for the CEO problem. *IEEE Journal on Selected Areas in Communications*, **22**(6), 977–987.

[12] Chen, J., Etezadi, F., and Khisti, A. (2017). Generalized Gaussian multiterminal source coding and probabilistic graphical models. In *IEEE International Symposium on Information Theory (ISIT)*, pages 719–723.

[13] Chen, J., Xie, L., Chang, Y., Wang, J., and Wang, Y. (2020). Generalized Gaussian multiterminal source coding: The symmetric case. *IEEE Transactions on Information Theory*, **66**(4), 2115–2128.

[14] Chevillat, P. (1981). N-user trellis coding for a class of multiple-access channels (corresp.). *IEEE Transactions on Information Theory*, **27**(1), 114–120.

[15] Chowdhury, M. Z., Shahjalal, M., Hasan, M. K., and Jang, Y. M. (2019). The role of optical wireless communication technologies in 5G/6G and IoT solutions: Prospects, directions, and challenges. *Applied Sciences*, **9**(20), 4367.

[16] Cioffi, J. M. (2008). Discrete data transmission basics. Available at `https://cioffi-group.stanford.edu/doc/book/chap1.pdf`.

[17] Courtade, T. A. and Weissman, T. (2013). Multiterminal source coding under logarithmic loss. *IEEE Transactions on Information Theory*, **60**(1), 740–761.

[18] Cover, T. M. and Joy, A. T. (2005). *Elements of information theory*. John Wiley & Sons.

[19] Da Costa, D. B. and Yang, H.-C. (2020). Grand challenges in wireless communications. *Future generation computer systems*, **1**, 1–5.

[20] Dai, L., Wang, B., Yuan, Y., Han, S., Chih-Lin, I., and Wang, Z. (2015). Non-orthogonal multiple access for 5G: Solutions, challenges, opportunities, and future research trends. *IEEE Communications Magazine*, **53**(9), 74–81.

[21] Dai, L., Wang, B., Ding, Z., Wang, Z., Chen, S., and Hanzo, L. (2018). A survey of non-orthogonal multiple access for 5G. *IEEE Communications Surveys & Tutorials*, **20**(3), 94–2323.

[22] David, K. and Berndt, H. (2018). 6G vision and requirements: Is there any need for beyond 5G? *IEEE Vehicular Technology Magazine*, **13**(3), 72–80.

[23] Ding, Z., Fan, P., and Poor, H. V. (2015). Impact of user pairing on 5G nonorthogonal multiple-access downlink transmissions. *IEEE Transactions on Vehicular Technology*, **65**(8), 6010–6023.

[24] Dobrushin, R. and Tsybakov, B. (1962). Information transmission with additional noise. *IRE Transactions on Information Theory*, **8**(5), 293–304.

[25] Dong, Z. and Zhang, J.-K. (2013a). Distributed concatenated alamouti code designs for one-way relay networks using uniquely-factorable PSK constellation. In *IEEE International Conference on Acoustics, Speech and Signal Processing*, pages 4973–4977.

[26] Dong, Z. and Zhang, J.-K. (2013b). Optimal design of distributed concatenated alamouti codes for relay networks using uniquely-factorable QAM constellations. In *IEEE China Summit and International Conference on Signal and Information Processing*, pages 575–579.

[27] Dong, Z., Chen, H., Zhang, J.-K., Huang, L., and Vucetic, B. (2018). Uplink non-orthogonal multiple access with finite-alphabet inputs. *IEEE Transactions on Wireless Communications*, **17**(9), 5743–5758.

[28] Duan, L., Liu, J., Yang, W., Huang, T., and Gao, W. (2020). Video coding for machines: A paradigm of collaborative compression and intelligent analytics. *IEEE Transactions on Image Processing*, **29**, 8680–8695.

[29] Duan, L.-Y., Lou, Y., Bai, Y., Huang, T., Gao, W., Chandrasekhar, V., Lin, J., Wang, S., and Kot, A. C. (2018). Compact descriptors for video analysis: The emerging MPEG standard. *IEEE MultiMedia*, **26**(2), 44–54.

[30] Farhadi, G. and Beaulieu, N. C. (2009). On the ergodic capacity of multi-hop wireless relaying systems. *IEEE Transactions on Wireless Communications*, **8**(5), 2286–2291.

[31] Feteiha, M. F. and Ahmed, M. H. (2018). Multihop best-relay selection for

vehicular communication over highways traffic. *IEEE Transactions on Vehicular Technology*, **67**(10), 9845–9855.

[32] Floridi, L. (2004). Outline of a theory of strongly semantic information. *Minds and machines*, **14**(2), 197–221.

[33] Floridi, L. (2009). Philosophical conceptions of information. In *Formal theories of information*, pages 13–53. Springer.

[34] Gabbard, O. (1968). Design of a satellite time-division multiple-access burst synchronizer. *IEEE Transactions on Communication Technology*, **16**(4), 589–596.

[35] Gagliardi, R. M. (1974). Optimal channelization in FDMA communications. *IEEE Transactions on Aerospace and Electronic Systems*, (6), 867–870.

[36] Ge, Y., Wen, S., Ang, Y.-H., and Liang, Y.-C. (2010). Optimal relay selection in IEEE 802.16 multihop relay vehicular networks. *IEEE Transactions on Vehicular Technology*, **59**(5), 2198–2206.

[37] Giordani, M., Polese, M., Mezzavilla, M., Rangan, S., and Zorzi, M. (2020). Toward 6G networks: Use cases and technologies. *IEEE Communications Magazine*, **58**(3), 55–61.

[38] Gündüz, D., Qin, Z., Aguerri, I. E., Dhillon, H. S., Yang, Z., Yener, A., Wong, K. K., and Chae, C.-B. (2022). Beyond transmitting bits: Context, semantics, and task-oriented communications. *IEEE Journal on Selected Areas in Communications*, **41**(1), 5–41.

[39] Guo, T., Wang, Y., Han, J., Wu, H., Bai, B., and Han, W. (2022). Semantic

compression with side information: A rate-distortion perspective. *arXiv preprint arXiv:2208.06094*.

[40] Harshan, J. and Rajan, B. S. (2011). On two-user Gaussian multiple access channels with finite input constellations. *IEEE Transactions on Information Theory*, **57**(3), 1299–1327.

[41] Harshan, J. and Rajan, B. S. (2013). A novel power allocation scheme for two-user GMAC with finite input constellations. *IEEE Transactions on Wireless Communications*, **12**(2), 818–827.

[42] Hoshyar, R., Wathan, F. P., and Tafazolli, R. (2008). Novel low-density signature for synchronous CDMA systems over AWGN channel. *IEEE Transactions on Signal Processing*, **56**(4), 1616–1626.

[43] Huang, G., Wang, Y., and Coon, J. (2011). Performance of multihop decode-and-forward and amplify-and-forward relay networks with channel estimation. In *IEEE Pacific Rim Conference on Communications, Computers and Signal Processing*, pages 352–357.

[44] Huang, J., Peng, K., Pan, C., Yang, F., and Jin, H. (2014). Scalable video broadcasting using bit division multiplexing. *IEEE Transactions on Broadcasting*, **60**(4), 701–706.

[45] Juba, B. and Sudan, M. (2008). Universal semantic communication i. In *Annual ACM Symposium on Theory of Computing*, pages 123–132.

[46] Kasami, T. and Lin, S. (1976). Coding for a multiple-access channel. *IEEE Transactions on Information Theory*, **22**, 129–137.

[47] Kasami, T. and Lin, S. (1978). Bounds on the achievable rates of block coding for a memoryless multiple-access channel. *IEEE Transactions on Information Theory*, **24**(2), 187–197.

[48] Khan, A. and Jamalipour, A. (2016). An outage performance analysis with moving relays on suburban trains for uplink. *IEEE Transactions on Vehicular Technology*, **66**(5), 3966–3975.

[49] Koike-Akino, T., Popovski, P., and Tarokh, V. (2009). Optimized constellations for two-way wireless relaying with physical network coding. *IEEE Journal on Selected Areas in Communications*, **27**(5), 773–787.

[50] Kos, A., Milutinović, V., and Umek, A. (2019). Challenges in wireless communication for connected sensors and wearable devices used in sport biofeedback applications. *Future Generation Computer Systems*, **92**, 582–592.

[51] Lapidoth, A. and Tinguely, S. (2010). Sending a bivariate Gaussian over a Gaussian MAC. *IEEE Transactions on Information Theory*, **56**(6), 2714–2752.

[52] Leung, E., Dong, Z., and Zhang, J.-K. (2016). Uniquely factorable hexagonal constellation designs for noncoherent SIMO systems. *IEEE Transactions on Vehicular Technology*, **66**(6), 5495–5501.

[53] Levin, G. and Loyka, S. (2012). Amplify-and-forward versus decode-and-forward relaying: Which is better? In *International Zurich seminar on communications (IZS)*.

[54] Li, W., Zhang, C., Duan, X., Jia, S., Liu, Y., and Zhang, L. (2012). Performance

evaluation and analysis on group mobility of mobile relay for LTE advanced system. In *IEEE Vehicular Technology Conference (VTC-Fall)*, pages 1–5.

[55] Lin, C.-H., Shieh, S.-L., Chi, T.-C., and Chen, P.-N. (2018). Optimal inter-constellation rotation based on minimum distance criterion for uplink NOMA. *IEEE Transactions on Vehicular Technology*, **68**(1), 525–539.

[56] Liu, H.-P., Shieh, S.-L., Lin, C.-H., and Chen, P.-N. (2019). A minimum distance criterion based constellation design for uplink NOMA. In *IEEE Vehicular Technology Conference (VTC-Fall)*, pages 1–5.

[57] Liu, J., Zhang, W., and Poor, H. V. (2021). A rate-distortion framework for characterizing semantic information. In *IEEE International Symposium on Information Theory (ISIT)*, pages 2894–2899.

[58] Liu, J., Shao, S., Zhang, W., and Poor, H. V. (2022). An indirect rate-distortion characterization for semantic sources: General model and the case of Gaussian observation. *IEEE Transactions on Communications*, **70**(9), 5946–5959.

[59] Liu, X. and Du, W. (2016). BER-based comparison between AF and DF in three-terminal relay cooperative communication with BPSK modulation. In *International Conference on Mobile Ad-Hoc and Sensor Networks (MSN)*, pages 296–300.

[60] Lozano, A., Tulino, A. M., and Verdú, S. (2006). Optimum power allocation for parallel Gaussian channels with arbitrary input distributions. *IEEE Transactions on Information Theory*, **52**(7), 3033–3051.

[61] Ma, S., Zhang, X., Wang, S., Zhang, X., Jia, C., and Wang, S. (2018). Joint

feature and texture coding: Toward smart video representation via front-end intelligence. *IEEE Transactions on Circuits and Systems for Video Technology*, **29**(10), 3095–3105.

[62] Marzetta, T. L. and Hochwald, B. M. (1999). Capacity of a mobile multiple-antenna communication link in Rayleigh flat fading. *IEEE Transactions on Information Theory*, **45**(1), 139–157.

[63] Navarro-Ortiz, J., Romero-Diaz, P., Sendra, S., Ameigeiras, P., Ramos-Munoz, J. J., and Lopez-Soler, J. M. (2020). A survey on 5G usage scenarios and traffic models. *IEEE Communications Surveys & Tutorials*, **22**(2), 905–929.

[64] Ng, B. K. and Lam, C.-T. (2018). Joint power and modulation optimization in two-user non-orthogonal multiple access channels: A minimum error probability approach. *IEEE Transactions on Vehicular Technology*, **67**(11), 10693–10703.

[65] Nikopour, H. and Baligh, H. (2013). Sparse code multiple access. In *IEEE Annual International Symposium on Personal, Indoor, and Mobile Radio Communications (PIMRC)*, pages 332–336.

[66] Oohama, Y. (1997). Gaussian multiterminal source coding. *IEEE Transactions on Information Theory*, **43**(6), 1912–1923.

[67] Oohama, Y. (1998). The rate-distortion function for the quadratic Gaussian CEO problem. *IEEE Transactions on Information Theory*, **44**(3), 1057–1070.

[68] Oohama, Y. (2005). Rate-distortion theory for Gaussian multiterminal source coding systems with several side informations at the decoder. *IEEE Transactions on Information Theory*, **51**(7), 2577–2593.

[69] Oohama, Y. (2014). Indirect and direct Gaussian distributed source coding problems. *IEEE Transactions on Information Theory*, **60**(12), 7506–7539.

[70] Pan, M.-S., Lin, T.-M., and Chen, W.-T. (2014). An enhanced handover scheme for mobile relays in LTE-A high-speed rail networks. *IEEE Transactions on Vehicular Technology*, **64**(2), 743–756.

[71] Petersen, K. B., Pedersen, M. S., *et al.* (2012). *The matrix cookbook*. Technical University of Denmark Press.

[72] Prabhakaran, V., Tse, D., and Ramachandran, K. (2004). Rate region of the quadratic Gaussian CEO problem. In *IEEE International Symposium on Information Theory (ISIT)*, page 119.

[73] Qian, X. and Wu, H. (2012). Mobile relay assisted handover for LTE system in high-speed railway. In *International Conference on Control Engineering and Communication Technology*, pages 632–635.

[74] Qiu, M., Huang, Y.-C., Shieh, S.-L., and Yuan, J. (2018). A lattice-partition framework of downlink non-orthogonal multiple access without SIC. *IEEE Transactions on Communications*, **66**(6), 2532–2546.

[75] Rappaport, T. S., Sun, S., Mayzus, R., Zhao, H., Azar, Y., Wang, K., Wong, G. N., Schulz, J. K., Samimi, M., and Gutierrez, F. (2013). Millimeter wave mobile communications for 5G cellular: It will work! *IEEE Access*, **1**, 335–349.

[76] Saito, Y., Kishiyama, Y., Benjebbour, A., Nakamura, T., Li, A., and Higuchi, K. (2013). Non-orthogonal multiple access (NOMA) for cellular future radio access. In *IEEE Vehicular Technology Conference (VTC-Spring)*, pages 1–5.

[77] Sari, H., Levy, Y., and Karam, G. (1997). An analysis of orthogonal frequency-division multiple access. In *IEEE Global Telecommunications Conference*, pages 1635–1639.

[78] Sekimoto, T. and Puente, J. (1968). A satellite time-division multiple-access experiment. *IEEE Transactions on Communication Technology*, **16**(4), 581–588.

[79] Shannon, C. E. (1948). A mathematical theory of communication. *The Bell System Technical Journal*, **27**(3), 379–423.

[80] Song, H., Fang, X., and Fang, Y. (2016). Millimeter-wave network architectures for future high-speed railway communications: Challenges and solutions. *IEEE Wireless Communications*, **23**(6), 114–122.

[81] Taherzadeh, M., Nikopour, H., Bayesteh, A., and Baligh, H. (2014). SCMA codebook design. In *IEEE Vehicular Technology Conference (VTC-Fall)*, pages 1–5.

[82] Tung, S.-Y. (1978). *Multiterminal source coding*. Cornell University Press.

[83] Ungerboeck, G. (1982). Channel coding with multilevel/phase signals. *IEEE Transactions on Information Theory*, **28**(1), 55–67.

[84] Van De Beek, J. and Popovic, B. M. (2009). Multiple access with low-density signatures. In *IEEE Global Telecommunications Conference*, pages 1–6.

[85] Viswanathan, H. and Berger, T. (1997). The quadratic Gaussian CEO problem. *IEEE Transactions on Information Theory*, **43**(5), 1549–1559.

[86] Wagner, A. B., Tavildar, S., and Viswanath, P. (2008). Rate region of the quadratic Gaussian two-encoder source-coding problem. *IEEE Transactions on Information Theory*, **54**(5), 1938–1961.

[87] Wang, J. and Chen, J. (2013). Vector Gaussian two-terminal source coding. *IEEE Transactions on Information Theory*, **59**(6), 3693–3708.

[88] Wang, J. and Chen, J. (2014). Vector Gaussian multiterminal source coding. *IEEE Transactions on Information Theory*, **60**(9), 5533–5552.

[89] Wang, J., Chen, J., and Wu, X. (2010). On the sum rate of Gaussian multiterminal source coding: New proofs and results. *IEEE Transactions on Information Theory*, **56**(8), 3946–3960.

[90] Wang, Y., Xie, L., Zhang, X., and Chen, J. (2018). Robust distributed compression of symmetrically correlated Gaussian sources. *IEEE Transactions on Communications*, **67**(3), 2343–2354.

[91] Wang, Y., Xie, L., Zhou, S., Wang, M., and Chen, J. (2019). Asymptotic rate-distortion analysis of symmetric remote Gaussian source coding: Centralized encoding vs. distributed encoding. *Entropy*, **21**(2), 213.

[92] Wang, Z. and Giannakis, G. B. (2000). Wireless multicarrier communications. *IEEE Signal Processing Magazine*, **17**(3), 29–48.

[93] Weaver, W. (1953). Recent contributions to the mathematical theory of communication. *ETC: A review of general semantics*, pages 261–281.

[94] Wei, Z., Guo, J., Ng, D. W. K., and Yuan, J. (2017). Fairness comparison

of uplink NOMA and OMA. In *IEEE Vehicular Technology Conference (VTC-Spring)*, pages 1–6.

[95] Wei, Z., Yang, L., Ng, D. W. K., Yuan, J., and Hanzo, L. (2019). On the performance gain of NOMA over OMA in uplink communication systems. *IEEE Transactions on Communications*, **68**(1), 536–568.

[96] Witsenhausen, H. (1980). Indirect rate distortion problems. *IEEE Transactions on Information Theory*, **26**(5), 518–521.

[97] Wolf, J. and Ziv, J. (1970). Transmission of noisy information to a noisy receiver with minimum distortion. *IEEE Transactions on Information Theory*, **16**(4), 406–411.

[98] Wu, Z., Lu, K., Jiang, C., and Shao, X. (2018). Comprehensive study and comparison on 5G NOMA schemes. *IEEE Access*, **6**, 18511–18519.

[99] Xia, D., Zhang, J.-K., and Dumitrescu, S. (2012). Energy-efficient full diversity collaborative unitary space-time block code designs via unique factorization of signals. *IEEE Transactions on Information Theory*, **59**(3), 1678–1703.

[100] Xiao, J.-J. and Luo, Z.-Q. (2005). Compression of correlated Gaussian sources under individual distortion criteria. In *Allerton Conference on Communication, Control, and Computing*, pages 438–447.

[101] Xiao, Y., Zhang, X., Li, Y., and Shi, G. (2022). Rate-distortion theory for strategic semantic communication. *arXiv preprint arXiv:2202.03711*.

[102] Xie, L., Tu, X., Zhou, S., and Chen, J. (2020). Generalized Gaussian multiterminal source coding in the high-resolution regime. *IEEE Transactions on Communications*, **68**(6), 3782–3791.

[103] Xiong, L. and Zhang, J.-K. (2012). Energy-efficient uniquely factorable constellation designs for noncoherent SIMO channels. *IEEE Transactions on Vehicular Technology*, **61**(5), 2130–2144.

[104] Yang, S., Hu, Y., Yang, W., Duan, L.-Y., and Liu, J. (2021). Towards coding for human and machine vision: Scalable face image coding. *IEEE Transactions on Multimedia*, **23**, 2957–2971.

[105] Yang, Y., Zhang, Y., and Xiong, Z. (2012). A new sufficient condition for sum-rate tightness in quadratic Gaussian multiterminal source coding. *IEEE Transactions on Information Theory*, **59**(1), 408–423.

[106] Yu, M. and Li, J. (2005). Is amplify-and-forward practically better than decode-and-forward or vice versa? In *IEEE International Conference on Acoustics, Speech, and Signal Processing*, volume 3, pages 365–368.

[107] Yuan, Z., Yu, G., Li, W., Yuan, Y., Wang, X., and Xu, J. (2016). Multi-user shared access for internet of things. In *IEEE Vehicular Technology Conference (VTC-Spring)*, pages 1–5.

[108] Zhang, J., Du, H., Zhang, P., Cheng, J., and Yang, L. (2020). Performance analysis of 5G mobile relay systems for high-speed trains. *IEEE Journal on Selected Areas in Communications*, **38**(12), 2760–2772.

[109] Zhang, X., Chen, L., Qiu, J., and Abdoli, J. (2016). On the waveform for 5G. *IEEE Communications Magazine*, **54**(11), 74–80.

[110] Zheng, L. and Tse, D. N. C. (2002). Communication on the Grassmann manifold: A geometric approach to the noncoherent multiple-antenna channel. *IEEE Transactions on Information Theory*, **48**(2), 359–383.